Characterization of *Staphylococcus aureus* antigen-specific antibodies and application of their epitopes as active vaccine against MRSA

Inaugural Dissertation

zur
Erlangung des Doktorgrades
der
Mathematisch-Naturwissenschaftlichen Fakultät
der
Rheinischen Friedrich-Wilhelms-Universität Bonn

vorgelegt von

Anne Kristin Nicolai

aus Siegen

Köln 2016

Angefertigt mit Genehmigung der Mathematisch-Naturwissenschaftlichen Fakultät
der Rheinischen Friedrich-Wilhelms-Universität Bonn

Berichterstatter: Prof. Dr. Martin Krönke
Prof. Dr. Hans-Georg Sahl

Tag der mündlichen Prüfung: 31.05.2017

Erscheinungjahr: 2017

Contents

List of Abbreviations

AAV	Adeno-Associated Virus
ab	Antibody
agr	Accessory Gene Regulator
ATCC	American Type Culture Collection
AS	Antisense Primer
BMDM	Bone Marrow-Derived macrophage
BSA	Bovine Serum Albumin
°C	Degree Celsius
CFU	Colony Forming Unit
DMEM	Dulbecco Modified Eagle Medium
DNA	Deoxyribonucleic Acid
dNTP	Desoxyribonucleotide-Triphosphate
E.coli	*Eschericha coli*
ECL	Enhanced Chemiluminescence
EGFP	Enhanced Green Fluorescent Protein
EDTA	Ethylenediaminetetraacetic acid
EtOH	Ethanol
FACS	Fluorescence Activated Cell Sorting
FAD	Flavin Adenine Dinucleotide
FCS	Fetal Calf Serum
FnBPs	Fibronectin Binding Proteins
FSC	Forward Scatter
g	Acceleration of Gravity
GFP	Green Fluorescent Protein
h	Hours
HeLa	Epithelial Cervical Cancer Cell Line
Huvec	Human Umbilical Vein Endothelial Cells
humAb	Humanized monoclonal antibody
HRP	Horseradish Peroxidase
Hp	Hypothetical Protein
i.m.	Intramuscular

i.p.	Intraperitoneal
kDa	Kilodalton
LB	Luria Bertani Medium
moAb	Monoclonal Antibody
MOI	Multiplicity of Infection
MVA	Modified Vaccinia Ankara Virus
NARSA	The Network of Antimicrobial Resistance in *S. aureus*
OD	Optical Density
ON	Overnight
PBS	Phosphate Buffered Saline
PCR	Polymerase Chain Reaction
PE	Phycoerythrin
pOxi	Protoporphyrinogen Oxidase
P/S	Penicillin / Streptomycin
RBC	Red Blood Cells
RPMI	Roswell Park Memorial Institute medium
rpm	Round per Minute
SAK	Staphylokinase
S. aureus	*Staphylococcus aureus*
s.c.	Subcutaneous
SpA	Protein A
SDS-PAGE	Sodium Dodecylphosphate Polyacrylamide Gel Electrophoresis
SP	Sense Primer
SSC	Side Scatter
Triiso	Triosephosphate Isomerase
TMB	3,3′,5,5′-Tetramethylbenzidine
TSB	Tryptic Soy Broth
U	Unit
WCL	Whole Cell Lysate
wt	Wildtype

1 Introduction

1.1 *Staphylococcus aureus*: Pathogenicity and clinical relevance

Staphylococci are eubacteria, belonging to the phylum fermicutes and to the class of bacilli. The coccal bacteria grow facultative anaerob, are catalase-positive and form grape-like clusters (Ogston, 1881). A main characteristic for a further differentiation of staphylococci is their ability to produce the enzyme coagulase, which is responsible for agglutination of blood. One of the coagulase-positive species is *Staphylococcus aureus*. *S. aureus* is a common representative of the microbial flora at mucosal surfaces, like the nasal mucosa of around 30 % of humans. A passage of the bacteria through a break in the mucosal or skin surface and subsequent entry into the blood stream may lead to severe systemic infections. As an opportunistic pathogen *S. aureus* causes a range of infections that reach from superficial skin lesions to serious life-threatening diseases, such as endocarditis, toxic-shock syndrome, pneumonia or sepsis (Lowy, 1998, Diekema *et al*., 2001).

The severity of infection often depends on the humans' immune system. Patients with a suppressed immune system are especially susceptible to *S. aureus* infections, but also healthy patients get infected, which makes *S. aureus* one of the main causative pathogens of nosocomial infections (Laupland *et al*., 2003). Beneath coagulase *S. aureus* is able to produce over 50 known virulence factors, which are differentially expressed in dependence of growth conditions (Arvidson and Tegmark 2001). This enables the bacterium to adapt to a variety of host niches and to cause a multitude of diverse symptoms. Functions of these virulence factors include adherence to host cell structures, evasion from the host immune system and active damage on host cells that allows *S. aureus* to establish the infection.

Adhesion to components of the host extracellular matrix, such as fibrinogen, fibronectin or collagen, is mediated by adhesion proteins of the MSCRAMM (microbial surface component recognizing adhesive matrix molecules) family. These are cell wall-anchored proteins (CWA), which are often covalently linked to peptidoglycan (Foster and Hook, 1998). All CWA proteins contain a secretory Sec-

dependent signal sequence at the N-terminus and a sorting signal, which comprises an LPXTG sortase cleavage motif and a stretch of positively charged residues at the C-terminus. The last two subdomains retain the protein in the membrane during secretion (Foster *et al*., 2014). Common MSCRAMMs are the fibrinogen-binding protein clumping factor A (ClfA) and the fibronectin-binding proteins (FnBP) A and B.

Another protein containing the LPXTG motif is protein A (SpA), which is multifunctional and ubiquitous in *S. aureus*. SpA is a B-cell superantigen that binds to the Fc γ region of human immunoglobulin (Ig) G1 and IgG2 with high affinity, as well as mouse IgG2a and IgG2b (Daum and Spellberg, 2012). SpA can interfere with the role of antibody in opsonization and phagocytosis, which protects *S. aureus* as a factor of the pathogen's strategy to modulate host adaptive immune response (Forsgren, 1968). SpA also binds V_H3 B-cell receptors and limits their antibody manufacturing capacity (Spellberg *et al*., 2008).

Besides the mentioned SpA, superantigens, such as enterotoxins of *S. aureus* are secreted to bind T-cell receptors and MHC class II proteins on antigen-presenting cells resulting in helper T-cell activation and the release of proinflammatory cytokines (Llewelyn and Cohen, 2002). Such secreted toxins cause food poisoning (enterotoxins A-O), the toxic shock syndrome (TSST-1) or the staphylococcal scalded skin syndrome, which is triggered by the exfoliative toxins A and B (Ladhani *et al*., 1999). Invasins, such as haemolysins (e.g. α-toxin, β-haemolysin) and leukocidins (e.g. Panton-Valentine leukocydine, PVL) are secreted cytotoxic proteins that oligomerize to form pores on the surface of host cells (Walev *et al*., 1993). Heamolysins lyse erythrocytes and parenchyma cells, whereas leukocidins destruct macrophages and leukocytes, especially neutrophils (Lina *et al*., 1999).

Other CWA proteins are the near-iron transporter motif (NEAT) proteins that are involved in iron-uptake from the iron-limited environment and help *S. aureus* to survive in the host (Foster *et al*., 2014). Here, the pathogen developed the strategy to sequester iron by synthesis of high affinity iron chelators, siderophores and corresponding membrane associated ABC-transporter systems or covalently linked iron-regulated surface determinants (Isd) for the sequestration of heme-complexed iron (Maresso and Schneewind, 2006). *S. aureus* also secretes numerous lipases and proteases that degrade host components and proteins that sequester antibodies or inactivate antibiotics (Foster, 2005).

Beside covalently-bound and secreted virulence factors, also anchorless cell wall proteins with no special signal motif or sorting signal (such as LPXTG) have been identified on the surface of *S. aureus* (Chhatwal, 2002, Gatlin *et al*., 2006, Glowalla *et al*. 2009). These intracellular or cytoplasmic membrane proteins are known to associate with the bacterial surface. Some of these non-covalently bound cell wall proteins are described in 1.5.

An overview of the best known virulence factors of *S. aureus* is shown in figure 1.1. The genetic diversity and the ability to acquire new exogenous genes allow *S. aureus* to adapt to a variety of changing environmental conditions and to modulate its pathogenicity. Humans are the primary reservoir of *S. aureus* with asymptomatic carriage from which these organisms are easily spread and cause infection. (Kluytmans *et al*., 1997; Moellering, 2012). All these facts highlight *S. aureus* as a dangerous and clinically important pathogen.

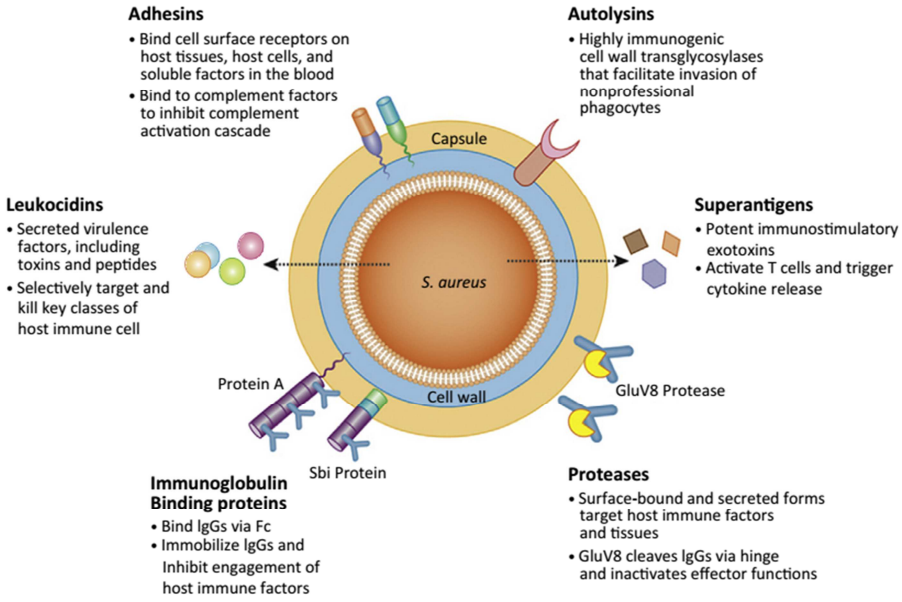

Figure 1.1: *Staphylococcus aureus* virulence factors that serve as targets for the current class of antistaphylococcal biologics being developed. These targets include surface-bound adhesins, immuno-globulin-binding proteins, surface-associated and secreted proteases, immune-stimulatory superantigens of the family of exotoxins, leukocidal toxins and immunogenic cell wall autolysins. Figure from Sause *et al*. (2016).

1.2 Acquired antibiotic resistance of *S. aureus*

Besides the tremendous amount of virulence factors, a threatening trend is the rapid emerge of *S. aureus'* resistance to several classes of antimicrobial agents. The first isolates of methicillin-resistant *Staphylococcus aureus* (MRSA) were characterized in 1961, only two years after the initial clinical use of methicillin (Jevons *et al*., 1961).

S. aureus became resistant against penicillin quickly through the acquisition of genes encoding β-lactamases, which are able to cleave β-lactam antibiotics (Murray *et al*., 1978). After the application of semisynthetic penicillins, such as methicillin and oxacillin the first MRSA strains appeared (Jevons *et al*., 1961). Methicillin-susceptible strains (MSSA) acquired the *mecA* gene that encodes an additional penicillin binding protein (PBP2a) with a low affinity to β-lactams, so that cell wall synthesis takes place in the presence of β-lactams. The *mecA* gene is located on a mobile DNA element termed staphylococcal cassette chromosome *mec (= SCCmecA).* The origin of *mecA* has been found in the coagulase-negative *Staphylococcus scuiri* group, which is not present in humans, but in animals and food products. One of the group's species *S. fleuretti* with the highest homology to MRSA strains developed the $mecA_{Sf}$ gene in an environment, where β-lactam antibiotics served as a selective pressure during the speciation process (Tsubakishita *et al*., 2010). MRSA was possibly generated under conditions where β-lactam antibiotics have been used in humans and animals. The *mecA* gene from *S. fleuretti* was combined with the *SSCmec* element in a coexistent species of MSSA and could be easily transferred to other human strains.

Since its identification, a number of MRSA clones have spread worldwide. Data from 2011 showed that MRSA accounts for more than 25 % of bloodstream infections in one-third of the European countries studied (European Centre for Disease prevention and control, EARSS).

Prior to 1990s, most MRSA were associated with hospitals or other healthcare units (Hospital-associated- (HA-) MRSA), but in the early 90s the first MRSA infections in patients without previous healthcare exposure (community-associated (CA-) MRSA) were reported (David *et al*., 2010). CA-MRSA strains developed additional virulence factors, such as the in 1.1 described PVL, which is responsible for serious infections in healthy humans. In the USA a single clone of CA-MRSA (USA-300) has become the most prevalent cause of staphylococcal soft tissue infections acquired in the community (King *et al*., 2006; Tenover *et al*., 2006) and has entered the inpatient setting, causing also invasive diseases (Davis *et al*., 2006; Gonzalez *et al*., 2006; Klevens *et al*., 2007).

The glycopeptide antibiotic vancomycin is currently the first-line treatment for severe CA- and HA-MRSA infections. However, due to the selective pressure during treatment, vancomycin intermediate resistant *S. aureus* (VISA) evolved, which was

first identified in 1997 (Hiramatsu *et al*., 1997). In 2002, the first vancomycin resistant strains (VRSA) were identified (Weigel *et al*., 2003). The *vanA* gene, conferring resistance to vancomycin was horizontally transferred from a vancomycin resistant *Enterococcus faecalis* during co-infection. Although still rare, VRSA have been reported in the USA and in some countries of Asia (Tenover *et al*., 2004; Tiwari and Sen, 2006, Askari *et al*., 2012). Another glycopeptide teicoplanin and recent antibiotics as daptomycin, linezolid and tigecyclin have been discovered and proven to be effective against MRSA (Rivera and Boucher, 2011). However, there are also already existing strains with resistance against these agents.
With this increasing propensity of *S. aureus* to develop resistance to essentially all classes of antibiotics, alternative strategies have to be pursued.

1.3 Vaccination against *S. aureus* as alternative strategy

The development of prophylactic and therapeutic vaccines as an alternative against *S. aureus* infection seems to be the most effective way to control the life-threatening infections caused by MRSA where antibiotics failed.

1.3.1 Induction of an immune response by vaccination

The adaptive immune system with its two parts, cytotoxic immune reponse (cytotoxic T-cell, $CD8^+$, CTL) and humoral immune response (B-cells) are both dependent on helper T-cells ($CD4^+$). CTLs are able to detect infected or malignant cells through recognition of MHC class I molecules that are complexed to peptides derived from proteins expressed within the cell (e.g. viral origin). Helper T-cells (Th-cells) recognize MHC class II molecules that are complexed to peptides derived from exogenous proteins. MHC II molecules are found on specialized antigen-presenting cells (APCs), such as dendritic cells or macrophages. In both cases, the T-cell receptor of T-cells binds the MHC I- or MHC II-epitope complex (see figure 1.3). These interactions are co-stimulated by CD8- or CD4-receptor recognition, respectively (Purcell *et al*., 2007).
Extracellular pathogens are opsonized by specific antibodies binding to their surface and supporting additional complement activation or phagocytosis by interaction with IgG-Fc_γ receptors on phagocytes (van Kessel *et al*., 2014). Other functions of

antibodies are the neutralization of adhesion to host cell tissue by interfering with the respective pathogen- or host cell associated binding protein and the neutralization of bacterial toxins. Immune complexes of antibodies and toxins, which are not sufficient to induce an uptake by phagocytes, are eliminated by activation of the classical pathway of complement activation. Antibodies have also been shown to amplify or suppress the inflammatory response depending on their specificity, isotype and concentration (Casadevall and Pirofski, 2003).

In the process of opsonophagocytosis, Th-cells are important for the generation of opsonizing antibodies, because T-cell help is required for antibody affinity maturation and class switch (McHeyzer-Williams *et al*., 2012; Bröker *et al*., 2016). Additionally, Th-cells promote phagocytosis. They produce different kinds of cytokines for recruiting neutrophils and macrophages from the bone marrow to the side of infection (O'Shea, 2013).

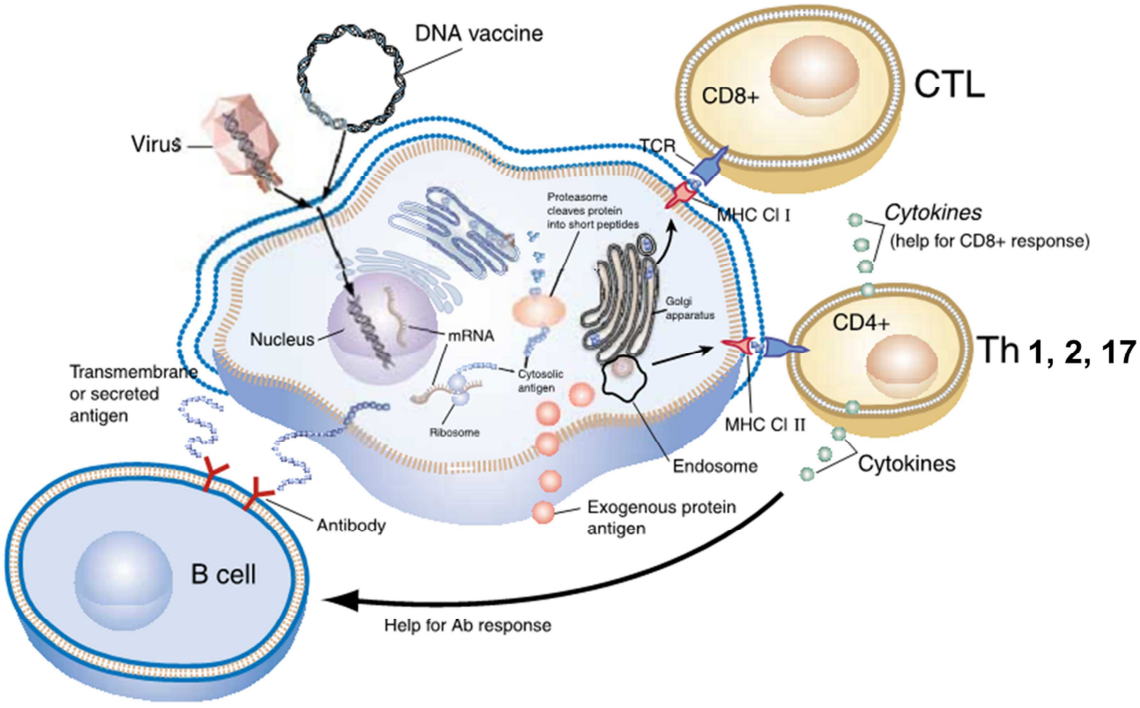

Figure 1.2: Generation of antigen-specific humoral and cellular immune responses. Exogenous antigens, such as subunit vaccines were taken up by professional antigen presenting cells (APC). The protein is degraded to peptides that are presented by MHC class II molecules (MHC Cl). Helper T-cells ($CD4^+$) recognize MHC II-peptide complexes with their T-cell receptor, are activated and provide help in the presence of cytokines. Activation of cytotoxic T-cells (CTL, $CD8^+$) is dependent on peptides that associate with MHC Cl I molecules. These peptides are degradation products of intracellular proteins encoded by foreign DNA after e.g. viral infection. For antibody response, B-cells recognize antigens that are either presented extracellularly or exposed extracellularly. Figure modified from Liu (2003).

In case of an *S. aureus* infection, the role of T-cells as the cellular arm of adaptive immunity seems to be more important than previously thought. Cytokines produced by Th cells, such as interferon-gamma (IFN-γ) released by Th1 cells and interleukin-17 (IL-17) released by different cell types (e.g. IL-17A by Th17 cells) have been proven to be important for protection from *S. aureus* (Cho *et al*., 2010; Bröker *et al*., 2016). For example, IFN-γ deficient mice were hypersusceptible to infection when *S. aureus* was injected intravenously (Lin *et al*., 2009). Cho *et al*. (2010) reported γδ-cells to be main producers of IL-17. A deficiency in γδ-cells increased the bacterial burden in skin infection in a murine wound model (Molne *et al*., 2003).

For vaccine development it is suggested that the stimulation of a $CD4^+$ T-cell response (especially Th1 and Th17) in addition to the humoral response may be advantageous. Because *S. aureus* is able to invade host cells and is persistent in these cells, the role of $CD8^+$ T-cells should also be mentioned in case of vaccination (Figure 1.3).

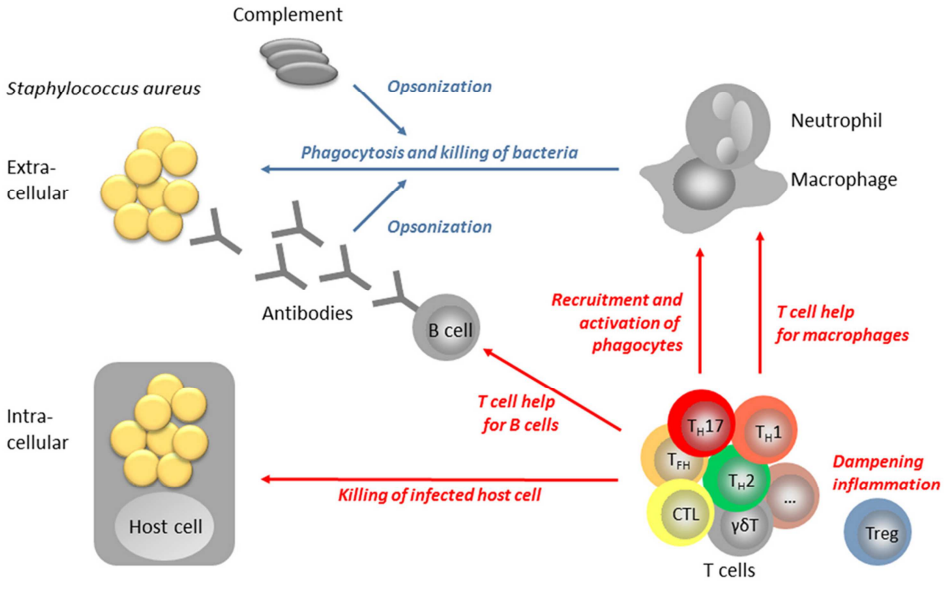

Figure 1.3: Model of B- and T-cell in anti-staphylococcal immune defense. Immune response against *S. aureus* crucially depends on the bactericidal activity of macrophages and neutrophils, facilitated by opsonization of the bacteria by B-cell generated antibodies and/or complement. T-cells can contribute by providing help for B-cells, recruiting phagocytes to the site of infection and promoting the bactericidal potential of macrophages. Cytotoxic T-cells are required to kill cells infected with *S. aureus*, which will otherwise persist in the host cell as an intracellular niche. Figure from Bröker *et al*. (2016).

1.3.2 Vaccination strategies

Immunization can be achieved in an active or passive manner. Passive immunization describes the transfer of antibodies to an organism against acute infections, but they only achieve a short-lasting effect. Active vaccines can be classified in five different types: live-attenuated and inactivated microorganisms, toxoids, subunit and genetic based vaccines induce a long-lasting immune response (Ada, 2005).

Live-attenuated pathogens induce both, humoral and cellular immune responses, but take the risk of a reversion into a virulent strain, so that they cannot be administered to immunocompromised patients. Killed microorganisms were able to induce only humoral immune responses (e.g. typhic vaccine), so that multiple boosters are inevitable. Vaccines with live-attenuated and inactivated pathogens often contain many hundreds of proteins, whereas only a few of them are responsible for a protective activity. The majority is redundant and may induce allergenic or reactogenic responses of the host.

Subunit vaccines comprise purified antigenic proteins from the pathogen (e.g. surface proteins) and can be produced in large scales in a cost effective way. They are often weakly immunogenic by themselves and require adjuvants to enhance the antigen-specific immune response (Li *et al*., 2014).

Toxoids are inactivated bacterial toxins that induce neutralizing antibodies against these virulent factors. The manufacturing issues, such as detoxification and adverse reactions are disadvantageous.

Genetic based vaccines containing a transgene that encodes the sequence of the target protein from the pathogen under control of a eukaryotic promoter for inducing long-lasting humoral and cellular immune responses without using an adjuvant (Ingolotti *et al*., 2010). DNA vaccines can also be delivered through viral, non-replicating vector systems. This is more detailed described in 1.3.4.

1.3.3 Advantages of peptide vaccination

Subunit vaccines containing novel identified target antigens have shown to be highly immunogenic and conferred protection in animal models. However, every of these candidates contain many hundreds of antigenic epitopes. Most of them are not necessary or even may be detrimental to the induction of protective immunity, because they might be very immunogenic but confer no protective effect. To avoid

this inclusion of redundant components a peptide vaccine is a safe and economical strategy. A peptide vaccine of approximately 20 amino acids can contain only epitopes capable of inducing strong, desirable B-cell and T-cell responses (Sesardic, 1993). Peptide vaccines have provided a cost effective and safe alternative. There are currently many peptide vaccines under development but mainly against viral pathogens like HIV, hepatitis C or malaria (Lui *et al*., 2007; Kolesanova *et al*., 2013; Epstein *et al*., 2007).

Immunodominant epitopes can be chosen in context of B-cells, cytotoxic or helper-T cells. Therefore, it is important to evaluate whether an epitope-based peptide immunogen can induce protective B-cell and T-cell immunity. In addition, a peptide vaccine can be designed to comprise various epitopes from different antigens of the same pathogen or multiple determinants of several pathogens in order to potentiate its efficacy.

One of the most suited approaches is the generation and selection of protective monoclonal antibodies against conserved regions in *in vivo* infection models (Li *et al*., 2014). Identification of the targeted epitopes can then be helpful in designing protective vaccine (reverse vaccinology). Due to their small size, peptides are often poorly immunogenic. In order to raise effective peptide antibodies, it is necessary to conjugate them via a bifunctional linker to a characterized carrier protein, such as bovine serum albumin (BSA) or keyhole limpet hemocyanin (KLH) being used in many preclinical studies (Hermanson, 2008). Their efficiency frequently requires repeated injections of high doses of the vaccines coupled to adjuvants. Water and mineral oil emulsions as Freund's complete adjuvant (FCA) or Freund's incomplete adjuvant (FIA) are a favored delivery method for various peptides to increase humoral and cellular immunity in animals (Awate *et al*., 2013). FCA is composed of inactivated mycobacteria, whereas FIA is devoid of this component. The process of emulsification is conducted by homogenization of antigen and adjuvant.

In summary, a peptide vaccine would be an effective way to combine protective epitopes for the design of a polyvalent vaccine against *S. aureus*. Immunization with highly purified antigens, such as B-cell-epitope-based peptides would lead to mono-specific polyclonal antibodies, which are supposedly as protective as the parental, protective, monoclonal antibodies. In addition, a combination with a suitable T-cell epitope to assure helper T-cell- ($CD4^+$) response is essential to provide long-lasting protection against *S. aureus* infection by production of memory B-cells.

1.3.4 DNA vaccines

The first evidence of immunologic use of DNA was the injection of human growth hormone (hGH) DNA into the skin of mice leading to specific anti-hGH-antibodies (Tang *et al*., 1992), which discovered that DNA may also be a suitable route for induction of an immune response against pathogenic infection.

A DNA vaccine plasmid contains the transgene and a promoter, which is often a viral one, such as cytomegalovirus (CMV) that drives the expression of the transgene in mammal cells. So, DNA immunization can mimic natural viral infection (Ingolotti *et al*., 2010). In contrast to the conventional vaccination strategy the antigen is produced endogenously (see figure 1.2).

DNA encoding the sequence of an antigen can be delivered through viral, non-replicating vector systems. Vaccination with viral vectors as heterologous antigen delivery system is primary interesting for intracellular pathogens (Lui, 2010). In this case, an induction of a humoral immune response to prevent the spread of the pathogen, as well as a $CD8^+$ T-cell response for the eradication of infected cells is induced. The humoral immune response can be increased by an additional antigen display, e.g. on the viral capsid (Rybniker *et al*., 2012). This allows recognition by B-cell receptors and the loading of MHC II molecules by antigen-presenting cells.

In contrast to subunit vaccines, viral vectors have an intrinsic adjuvant capacity. Vectors are modified to be non-replicating in mammalian cells, which allows for impaired synthesis of viral gene products (Altenburg *et al*., 2014).

DNA vaccination against *S. aureus* using viral vector systems was not investigated as yet. Induction of a humoral, as well as a cellular immune response against the extracellular pathogen that also invades host cells might be a promising alternative to subunit vaccination.

1.3.4.1 Modified Vaccinia virus Ankara (MVA)

The Modified Vaccinia virus Ankara (MVA) is an attenuated poxvirus used for vaccination against smallpox. MVA was first used licensed by the Bavarian State Vaccine Institute from 1968-1985 as a human smallpox vaccine by increasing the safety of the conventional smallpox vaccination (Stickl *et al*., 1974).

MVA was derived from Chorioallantois vaccinia virus Ankara (CVA) through serial passaging in chicken embryo fibroblasts. The serial passage of MVA resulted in

major deletions in the viral genome. During over 570 passages, MVA became host-restricted to avian cells and unable to replicate in almost all tested mammalian cell lines, including those of rodent and human origin (Sutter and Moss, 1992).

MVA holds great promise as a vaccine platform encoding one or several foreign antigens and inducing humoral and cellular immune responses (Altenburg *et al*., 2014). MVA has already been investigated as a platform for viral vaccines, such as influenza and HIV, which entered clinical trials (Kreijtz *et al*., 2014; Garcia *et al*., 2011; Volz and Sutter, 2013). The humoral immune response induced by influenza virus vaccination was mainly directed against the surface protein hemagglutinin (HA) by the production of neutralizing antibodies (Corti *et al*., 2010; Lee *et al*., 2012). Virus-specific T-cell responses ($CD4^+$ and $CD8^+$) have also been demonstrated and contributed to protective immunity (Hillaire *et al*., 2013). Preclinical studies of a new vaccine against MERS coronavirus using MVA as delivery system in mice detected a strong antibody-based immune response (Song *et al*., 2013).

In MVA vaccines the target gene sequences are transcribed under control of poxviral promotors that are only recognized and activated by virus encoded enzymes and transcription factors (Altenburg *et al*., 2014).

The target gene is cloned into an MVA shuttle vector plasmid containing flanking ends to allow recombination into the MVA genome (Sutter *et al*., 1994). The shuttle vector is then transfected into cells infected with MVA. Through homologous recombination the gene encoding the antigen is inserted into the genome. The rMVA is clonally isolated and amplified by serial passaging in chicken embryo fibroblasts.

Advantageous for MVA as vaccine delivery system is its high immune-stimulating potential by triggering rapid immigration of monocytes, neutrophils and $CD4^+$ cells to the side of inoculation (Lehmann *et al*., 2009), which makes adjuvants dispensable.

1.3.4.2 Adeno-associated virus (AAV)

Adeno-associated (AAV) vectors already have a long history in gene therapy but have also emerged in the vaccination field. AAV containing 13 serotypes is a member of the parvovirus family and is thus classed into the genus dependovirus. All serotypes contain a single-stranded DNA genome as about 5 kb within a non-enveloped protein capsid. Amino acid composition of the viral capsid proteins

determines serotype tropism as well as recognition by the host's immune system (Asokan *et al*., 2012).

AAV 2 is the most studied serotype. It contains inside of its capsid a linear single-stranded DNA genome. The wildtype genome includes the three open reading frames (ORFs) *rep*, *cap* and *aap* flanked by inverted terminal repeats (ITRs). The regulatory proteins (Rep) have several functions, which are important for the control of viral gene expression, replication and packaging of viral genomes into the preformed capsids. They also possess DNA helicase, endonuclease and ATPase functions (Pereira *et al*., 1997; Zhou *et al*., 1999; Büning *et al*., 2008). The assembly-activating protein (AAP) is required for the capsid assembly, which takes place in the nucleus. The viral capsid is built up by the three capsid proteins VP1, VP2, and VP3 (Büning *et al*., 2008). All capsid proteins are important for the generation of infectious particles, although virus-like particles can be formed without the VP1 or VP2 protein (Girod *et al*., 2002; Warrington *et al*., 2004). The ITR sides are essential *cis*-active sequences in the AAV biology. ITRs contain a Rep binding site as the origin of DNA replication. Additionally, they are essential for genome packaging, transcription, negative regulation under non-permissive conditions and site-specific integration (Daya and Berns 2008).

AAV is non-pathogenic since it cannot replicate without a helper virus. Thus, the virus is unable to multiply in unaffected cells. Recombinant AAV vectors (rAAV) have almost the entire viral genome removed for yielding a delivery vehicle with enhanced safety and transfer capacity (Choi *et al*., 2005). Except for the ITRs, all viral genes of the recombinant vector genome are substituted by the transgene expression cassette of interest.

As multiprotein complexes the viral capsids induce immune responses irrespective of viral gene expression. Rybniker *et al*. (2012) have shown that combining antigen display on a modified capsid with vector-mediated antigen overexpression resulted in a single-shot-prime-boost vaccine and an induction of a faster humoral immune response than achieved with conventional vaccine strategies.

AAV vectors require a coinfection with an unrelated virus for providing the helper functions VA, E2A, E4 for the productive life-cycle. Recombinant AAV vectors of Rybniker *et al*. (2012) are produced by a helpervirus-free method, using a helper plasmid delivering the adenoviral helper functions. E2A and VA act to enhance the viral mRNA stability and efficiency of translation, E4 is involved in facilitating the AAV

DNA replication (Xiao *et al*., 1998). A second helper plasmid is required for delivering the ORFs *rep*, *cap* and *aap* under control of the wildtype promoter but lacking the viral ITR sides. For a display on the viral surface it was shown that proteins can be incorporated into the AAV capsid via N-terminal fusion to VP2 on the viral surface without compromising viral infectivity (Lux *et al*., 2005; Münch *et al*., 2013).

1.4 Approaches in vaccine development against *S. aureus* infection

Since the detection of first MRSA strains, the definition of the risk population has changed (David *et al*., 2010). Since the epidemic occurrence of CA-MRSA, responsible for several infections of also healthy individuals in the community, not only people with suppressed immune systems, such as HIV patients, old people or neonates, patients with cystic fibrosis in hospitals are at high risk to get infected (Daum and Spellberg, 2012). Based on this fact that also healthy humans belong to the new risk population, the development of a prophylactic vaccine has become indispensable.

Currently, there is no licensed prophylactic anti-*S. aureus* vaccine available for human use. A successful vaccine has to prevent infections by *S. aureus* strains from a broad range of genetic backgrounds with a high variability of virulence factors that are known to be differently expressed. Therefore, a polyvalent vaccine that targets several different antigens would be more effective, due to the fact that targeting one single virulence factor cannot reduce the pathogenicity by its functional redundancy or the appearance of escape mutants. Stranger-Jones *et al*. (2006) analyzed the four antigens IsdA, IsdB, SdrD and SdrE as vaccine candidates and obtained significant protection with a combined vaccine in contrast to monovalent immunization. These results point towards a polyvalent vaccine as the most promising strategy to combat *S. aureus* infections.

1.4.1 Active immunization

The development of a staphylococcal vaccine is complicated because of the bacterium's complex mechanism of pathogenesis. The first studies for the establishment of an active vaccine used whole bacteria, followed by vaccination using staphylococcal phage lysate (Greenberg *et al*., 1987; Giese *et al*., 1996), but

none of them achieved protective effects. Further strategies focused on immunization with subunits, such as capsular polysaccharides or well-known virulence factors possessing LPXTG motif. To date, only two vaccines have proceeded through all clinical phases. StaphVAX (Nabi) is a bivalent polysaccharide- and protein-conjugated vaccine. It is composed of capsular polysaccharide types 5 and 8 (CP5 and CP8) conjugated to a recombinant, non-toxic variant of exotoxin A (ETA) of *Pseudomonas aeruginosa* to increase immunogenicity. By prevention of phagocytic activity the CPs represent an important factor in the pathogenicity of *S. aureus* (Kampen *et al*., 2005). With approximately 80 % serotypes 5 and 8 are the most prevalent of the 11 different serotypes among *S. aureus* isolates (Sompolinsky *et al*., 1985; Poutrel *et al*., 1988). StaphVAX was evaluated in two phase 3 studies to prevent bacteremia in renal dialysis patients and resulted in no differences between immunized patients and placebo controls (Fattom *et al*., 2004). The main reason of the second study's failure is explained by manufacturing inconsistencies between different vaccine lots used for the two trials (Fattom *et al*., 2015). The candidate V710 (Merck) describes the cell-wall-anchored protein IsdB (compare 1.1), which was evaluated in a phase 3 with patients scheduled for cardiac surgery. The clinical trial was suspended after the detection of a significantly increasing mortality rate due to *S. aureus* infection and a higher rate of other adverse events (Fowler *et al*., 2013). There are further active vaccines that entered clinical trials, such as Pfizer's SA4Ag (phase 2b), which is a polyvalent polysaccharide-protein vaccine of CP5 and CP8, manganese transport protein C (MntC) and Clumping factor A (ClfA). The purpose of this study is to evaluate the safety and efficacy of the vaccine to determine, if it prevents postoperative invasive *S. aureus* infections in patients undergoing elective spinal fusion surgery (October 2016, https://clinicaltrials.gov/ show/NCT02388165). The vaccine candidate Pentastaph (GlaxoSmithKline) is a combination of CP5 and CP8 and the two virulence factors PVL and teichoic acid and passes phase 1 (http://www.nabi.com). Another candidate named NDV-3A (NovaDigm) is based on the recombinant protein Als3p and passes phase 2a (September 2016, https://clinicaltrials.gov/show/ NCT 01926028). Als3p is an adhesion protein of *Candida albicans* and has a structural similarity to the staphylococcal ClfA, which makes the bacterium able to bind at *Candida* biofilms (Peters *et al*., 2012). Als3p showed protection against *S. aureus* skin and soft tissue and bloodstream infection in a preclinical model (Spellberg *et al*., 2008).

1.4.2 Passive immunization

As an alternative to active vaccination that often requires further booster immunizations to achieve protection, a passive vaccine is applied against acute *S. aureus* infection or as prophylaxis for patients with a suppressed immune system or for premature infants during hospital stays. Passive immunization strategies utilizing both polyclonal and monoclonal antibodies (moAbs). Several antibody candidates have been developed against different target molecules and evaluated in late stage clinical studies, but none of them demonstrated efficacy yet.

The passive vaccine candidate Altastaph (Nabi) containing polyclonal anti-CP5 and anti-CP8 IgGs obtained from patients immunized with StaphVAX (see 1.4.1) failed to prove efficacy in phase 2. Aurograb (NeuTec Pharma), a single chain variable fragment of an IgG (scFv) targeting ATP-binding cassette transporter (Burnie *et al*., 2000, Garmory *et al*., 2004), as well as Tefibazumab (Aurexis/Inhibitex) as a humanized anti-ClfA monoclonal antibody also failed in clinical trials (Weems *et al*. 2006). Aurograb combined with vancomycin did not show efficacy. Tefibazumab tested in adults with bacteremia showed decreased relapses, but no lower mortality has been shown.

The candidate Veronate (Inhibitex) is a human IgG preparation from plasma donors with naturally occurring high titers of IgG to ClfA and to the *S. epidermidis* fibrinogen binding protein (SdrG). Although protective in animal models (Vernachio *et al*., 2006), it showed only 50 % reduction in late onset *S. aureus* bacteremia in low birth weight neonates of phase 3 (DeJonge *et al*., 2007). Biosynexus has developed a humanized mouse chimeric IgG1 monoclonal antibody (Pagibaximab) with *in vitro* opsonophagocytosis activity to *S. epidermidis* lipoteichoic acid, a membrane bound glycolipid extending into the cell wall. Clinical phase 3 in low birth weight neonates for the prevention of bacteremia was completed in 2010, but no significant decrease in staphylococcal sepsis was found (Weismann *et al.*, 2011; Daum and Spellberg, 2012; https://clinicaltrials.gov/show/NCT00646399).

The described active and passive vaccine approaches that are passing through clinical trials or already failed, concentrated on well-known virulence factors, including proteins exhibiting the LPXTG sorting signal. On the contrary, Glowalla *et al*. (2009) focused on the identification of novel anchorless cell wall proteins that lack of conserved signal sequences.

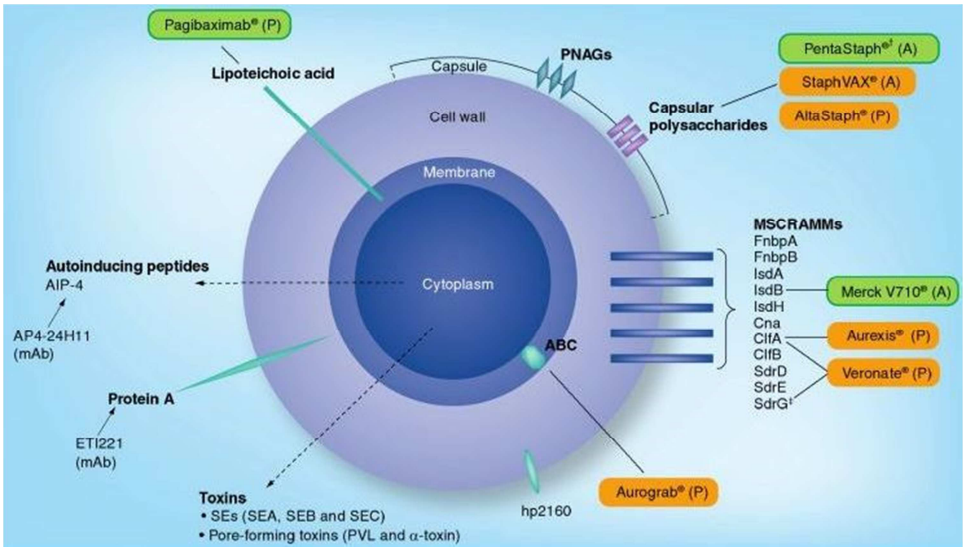

Figure 1.4: Overview of vaccine candidates targeting virulence factors that have been tested in animal and human studies. The immunization studies performed in humans are depicted in the boxes. A: Active immunization. P: Passive immunization. The protein hp2160 is explained in 1.5. Orange and green boxes indicated already analyzed vaccine candidates and status at 2011 (orange: failed vaccine candidates; green: in progress). The actual status revealed that Pagibaximab and Merck V710 also failed in clinical trials. Figure from Verkaik *et al*. (2011).

1.5 Identification of novel anchorless cell wall proteins as vaccine candidates

A large number of classical cytoplasmic proteins are described to be found on the surface of microbial pathogens. These non-covalently bound cell wall-associated proteins perform a variety of unrelated functions designated ‘moonlighting activity’ (Alderete *et al*., 2001; Pancholi 2001, Cchatwal, 2002). Moonlighting proteins are found to have two or more different functions and can occur at different locations (Jeffery, 1999). Because of their lack of typical signature sequences it is not known how they are transported to the cell surface.

Most of these proteins localized in the cytoplasm, being involved in metabolic pathways but also in adhesion or binding of e.g. blood components, which turns them into potential virulence factors (Pancholi and Chhatwal, 2003). For the development of new potential vaccine candidates Glowalla *et al*. (2009) identified several of these anchorless *S. aureus* surface proteins by a method called subtractive proteome analysis (SUPRA) using a human intravenous immunoglobulin preparation (IVIG).

IVIG is a pool of immunoglobulins from healthy humans that contains a broad spectrum of opsonizing antibodies against various pathogens. IVIG induced an

increased phagocytosis of *S. aureus* by isolated human neutrophils. Whereas, an IVIG preparation depleted of *S. aureus*-specific opsonizing antibodies (dSaIVIG) by incubation with an excess of *S. aureus* and subsequent separation showed a nearly completely abolished phagocytic activity. *S. aureus* surface proteins were isolated and separated by 2-DE gel electrophoresis, which was followed by an immunoblotting using IVIG or dSaIVIG, respectively, to identify antigenic proteins. Protein spots reacted with complete IVIG but not with dSaIVIG were considered as potential vaccine candidates, based on the assumption that those are recognized by naturally occurring *S. aureus* specific IgGs, hence representing *in vivo* expressed immunogenic proteins. Protein spots strongly reacting with both IVIG and dSaIVIG were excluded because they were thought to be recognized by IgGs that were not specific for *S. aureus* antigens.

The resulting spots were analyzed by MALDI-TOF and 39 proteins have been identified. Except for four of them, all proteins are present in the currently available completely sequenced genomes of *S. aureus*, which demonstrates their broad distribution among *S. aureus* isolates. Several of them were cloned and overexpressed in *E. coli*. Groups of mice were immunized with each of the purified proteins, respectively and challenged with *S. aureus*. Immunization with some of these proteins leads to a protection against *S. aureus* infection. The first vaccine candidates were identified as enolase, oxoacyl reductase and hypothetical protein 2160 (hp2160). The most promising candidate hp2160 is described as an esterase-like protein of unknown function and showed protection in a murine sepsis model. The more detailed function of hp2160 in the cytoplasm, as well as on the bacterial surface has to be defined.

Further investigation of the remaining recombinant proteins in the active immunization model for enlarging the pool of potential vaccine candidates lead to the proteins triosephosphate isomerase (Triiso) and protoporphyrinogen oxidase (pOxi), which showed the strongest protection after *S. aureus* infection (Tosetti, PhD thesis, 2010 and unpublished data).

1.5.1 Triosephosphate isomerase (Triiso)

In the cytoplasm, the homodimer Triiso is a metabolic enzyme that catalyzes the reversible conversion of dihydroxyacetone-phosphate into glyceraldehyde-3-phosphate in the glycolysis. Additionally, Triiso was identified on the surface of *S. aureus* as cell wall-associated protein by 2-DE gel electrophoresis of the isolated non-covalently bound cell wall protein fraction and mass spectroscopy (Gatlin *et al*., 2006; Glowalla *et al*., 2009,). Electron microscopies also detected Triiso with a low density on the surface of *S. aureus* (Yamaguchi *et al*., 2010).

This unexpected localization has also been described for other enzymes of the glycolysis, such as glyceraldehyde-3-phosphate dehydrogenase (GAPDH) and enolase (Pancholi and Fischetti, 1992, Glowalla *et al*., 2009). GAPDH has been reported to be a transferrin-, fibronectin-, laminin- and plasmin-binding protein (Modun and Williams, 1999; Modun *et al*., 2000; Gozalbo *et al*., 1998). Cell surface expression of GAPDH by erythromycin-resistant *Streptococcus pneumoniae* was increased compared to strains that are erythromycin-sensitive (Cash *et al*., 1999)

An agent of endocarditis, *Streptococcus gordonii* secretes GAPDH by increasing the pH (Nelson *et al*., 2001). Therefore, GAPDH proteins have already been investigated as potential vaccine candidates against microbial infection, including *Streptococcus uberis* in dairy cattle (Fontaine *et al*., 2002).

Pancholi and Chhatwal (2003) described the importance of housekeeping enzymes as virulence factors for a variety of pathogens. In this context Triiso was already described as a plasminogen-binding protein (Furuya and Ikeda, 2011) that is involved in the processes of blood coagulation and fibrinolysis. Coagulation is induced by the staphylococcal enzyme coagulase that activates prothrombin into thrombin, which let to polymerization of fibrin, so that *S. aureus* has enough space to proliferate in the wound, protected from the immune system (Figure 1.5). When a defined cell density is reached the expression of the enzyme staphylokinase (SAK) is increased. This process is regulated by quorum sensing. SAK activates plasminogen into plasmin, which initiates fibrinolysis. This enables *S. aureus* to proliferate in the surrounding tissue. Furuya and Ikeda described Triiso as an antagonist of staphylokinase which is therefore able to inhibit fibrinolysis as long as it is favourable for *S. aureus*. Besides Triiso, also enolase is described to be involved in these processes but as a possible inhibitor of coagulation.

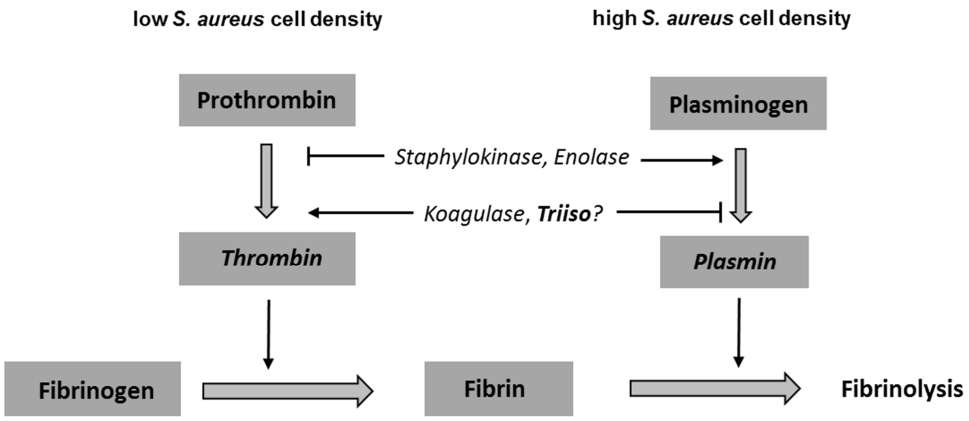

Figure 1.5: Potential moonlighting role of the glycolytic enzyme Triiso in plasminogen inhibition. Blood coagulation is initiated by the enzyme coagulase. *S. aureus* can proliferate in the wound and is protected from the host's immune system. When a defined cell density is reached expression of staphylokinase (SAK) increased. SAK activates plasminogen into plasmin, which initiates fibrinolysis allowing *S. aureus* to proliferate in the surrounding tissue. It is described that Triiso, as well as enolase influences these processes of inhibition and activation.

1.5.2 Protoporphyrinogen oxidase (pOxi)

In the cytoplasm the protein pOxi is involved in the synthesis of heme (Frankenberg *et al*., 2003). Heme is an essential cofactor for proteins involved in the transport of electrons (e.g. catalases, cytochromes). The respiratory pathways of some gram-positive pathogens rely entirely on the ability of the bacteria to scavenge exogenous heme. *S. aureus* differentially utilizes heme depending on its metabolic needs. In conditions of iron starvation, exogenously acquired heme is degraded to release free iron. When iron is abundant, heme is acquired and utilized intact to populate cytochromes of the electron transport chain. This reduces the requirement for endogenous heme synthesis and decreases the metabolic burden on the bacterium (Hammer and Skaar, 2011).

The enzyme pOxi (HemY) is O_2-dependent in *S. aureus*, whereas other prokaryotes express O_2-independent pOxi, named HemG (Panek *et al*., 2002). Hence, pOxi is only operative under aerobic conditions. For a long time it was thought that pOxi from *S. aureus* catalyzes the conversion of protoporphyrinogen IX into protoporphyrin IX by the removal of six electrons, which requires FAD as cofactor (Dailey *et al*., 1994; Hansson and Hederstedt, 1994). Then Lobo and colleagues exposed that *S. aureus* does not use the classical pathway of heme synthesis (Lobo *et al*., 2015). They discovered a transitional pathway for heme synthesis in *S. aureus*. HemY (pOxi) is

described as a coproporphyrin synthase that oxidizes coproporphyrinogen III into coproporphyrin III, whereas it is unable to oxidize protoporphyrinogen (Figure 1.6). Lobo *et al*. also showed that pOxi can be inhibited by several herbicides, highlighting pOxi as a suitable target for drug development against *S. aureus*.

Interestingly, HemY of gram-positive *Bacillus subtilis* is described as a peripheral membrane protein that is also able to oxidize both coproporphyrinogen III and protoporphyrinogen IX, whereas coproporphyrinogen III is the major substrate (Hansson and Hederstedt, 1994).

Since Glowalla *et al*. (2009) found antibodies in IVIG to be reactive against pOxi, the protein is identified to be displayed on the bacterial surface. Additionally, the fact that recombinant pOxi alone provided protection in the murine sepsis model after active immunization compared to other candidates (B. Tosetti, 2010, PhD thesis), leads to the conclusion that pOxi seems to have an important moonlighting activity on the *S. aureus* surface *in vivo*.

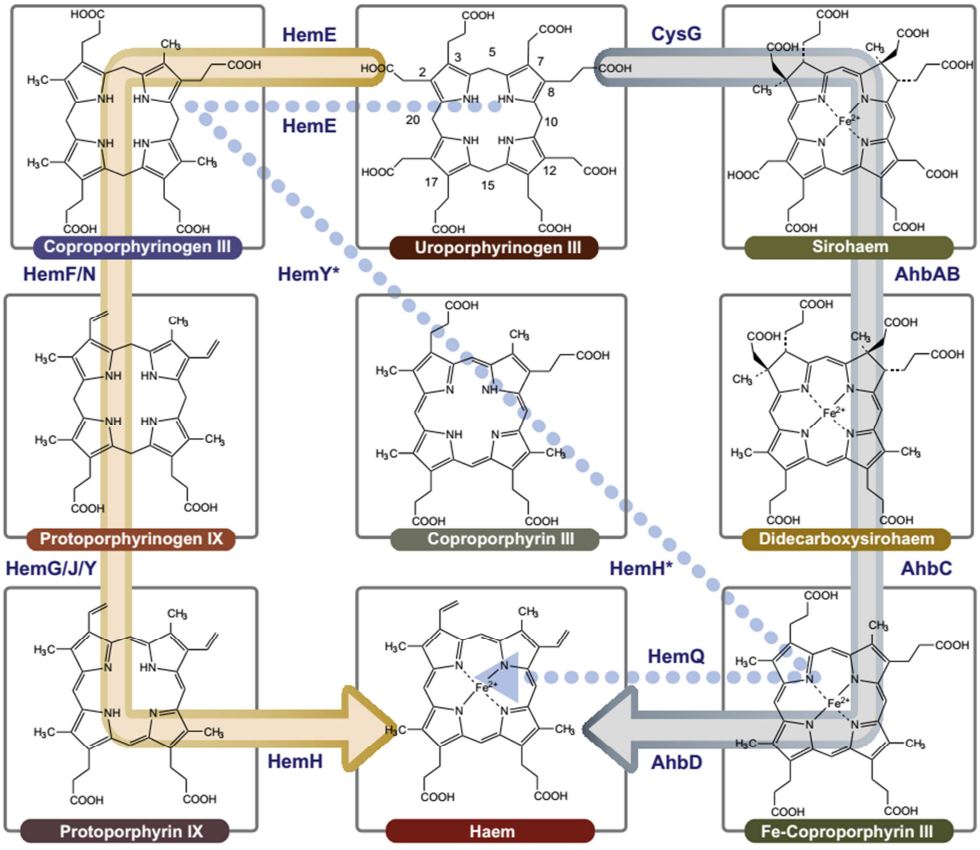

Figure 1.6: Diagrammatic representation of heme biosynthetic pathways, focusing the transitional heme pathway of *S. aureus*. The classic pathway is highlighted in in orange, the alternative pathway in grey and the transitional pathway in blue dots. Figure from Lobo *et al*. (2015).

1.5.3 Generation of monoclonal antibodies directed against the novel vaccine candidates

Encouraged by the results obtained with the *S. aureus* proteins Triiso, pOxi and hp2160 used as vaccine candidates for active immunization of mice, providing protection against a subsequent S. aureus infection, these recombinant proteins were chosen for the generation of monoclonal antibodies (moAbs) by hybridoma technology (Kohler and Milstein, 1975) to be used for passive immunization. After an infection of mice immunized with one of the recombinant proteins, respectively, the spleens of the survivors were removed. Isolated splenocytes were fused to myeloma cells to obtain hybridoma clones, which were subsequently separated from unfused myeloma cells. The hybridoma clones are immortal and have the ability to produce one particular antibody, respectively (monoclonality). The generated monoclonal antibodies (moAbs) were selected to be used as passive vaccine with the goal to provide protection in a murine sepsis model (A. Klimka, unpublished data). Out of several tested monoclonals the lead candidates anti-Triiso moAb H8, anti-pOxi moAb D3 and anti-hp2160 moAb 16-2 were selected. The three antibodies were humanized by grafting the CDRs into a human IgG backbone and also de-immunized by excluding constructed, potential human T-cell epitopes, to reduce the possibility for an adverse immune response in humans. The resulting humanized antibodies (humAbs) retained their binding specificity and their capability to protect mice against deadly *S. aureus* infection (Figure 1.7). Currently, anti-pOxi humAb D3 is chosen to be produced under GMP-conditions by the Fraunhofer institution ITEM (Braunschweig, Germany) to enter clinical trials in the near future.

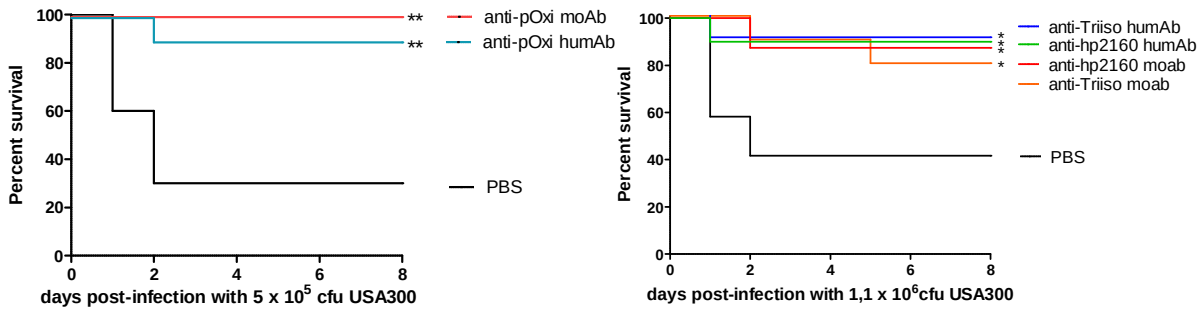

Figure 1.7: Survival upon passive immunization using monoclonal murine (moAb) or humanized (humAb) anti-pOxi, anti-Triiso and anti-hp2160 antibodies. BALB/c mice received the respective moAb or humAb before the lethal challenge with *S. aureus* MRSA strain USA300. Survival of mice was monitored for 8 days (A. Klimka, unpublished data).

1.7 Aim of this work

Multidrug resistance of the hospital- and community-associated pathogen is increasing drastically and thereby limiting therapeutic options. Vaccination as alternative strategy for treatment and prophylaxis would be important, but there is currently no vaccine against *S. aureus* infection available. All active and passive immunization approaches to date have failed at the clinical trial stage.

The aim of this study was to further characterize our previously generated *S. aureus*-specific monoclonal antibodies anti-pOxi D3, anti-Triiso H8 and anti-hp2160 16-2, which have been demonstrated to protect mice against lethal *S. aureus* infection. These antibodies should be investigated concerning their binding capacity to the *S. aureus* surface and their mode of action leading to their protective effect. This is of special interest, as Triiso and pOxi are well-known cytoplasmic proteins of metabolic pathways and it had to be analyzed, which *in vitro* conditions were necessary for the proteins' occurrence at the bacterial surface, a moonlighting activity, which was not analyzed as yet.
The mode of action of moAbs additionally included an analysis of the function of our three identified vaccine candidates as moonlighting proteins on the bacterial surface.
The aim of the second part of this thesis was the epitope identification of the three mentioned moAbs for a following application as active peptide vaccine against MRSA in a preclinical mouse model. This included an expedient combination of the epitope peptides with carriers and adjuvants and an analysis of their capacity to induce an antigen-specific humoral, as well as cellular immune response. Furthermore, the protective effect of such a vaccine should be investigated by reduction of bacterial colonization in murine tissues and by survival of mice after S. aureus challenge. With the aim to generate a polyvalent vaccine, epitope peptides should be fused to a polyepitope peptide and investigated for their protective effect. Additionally, vaccination of a polyepitope using the viral vector platforms MVA and AAV as alternative delivery systems should be investigated concerning their humoral immune response.

2 Material and Methods

2.1 Material

2.1.1 Chemicals and Enzymes

Chemicals were of research grade and purchased from Sigma-Aldrich (Steinhausen, Germany), AppliChem (Darmstadt, Germany), Merck (Darmstadt, Germany), Thermo Fisher Scientific (Dreieich, Germany) or Roth (Karlsruhe, Germany) unless stated otherwise. Buffers and solutions were prepared using bidestilled H_2O from EASYpure UV/UF H_2O purification unit (Werner Reinstwassersystem, Leverkusen), degassed and sterilized by autoclaving or filtration through a 0.2 µm filter membrane, if necessary.

Restriction enzymes, T4 ligase and polymerases were obtained from Thermo Fisher Scientific (Dreieich, Germany) and used in recommended buffers. Benzonase was obtained from Merck and recombinant lysostaphin from Sigma-Aldrich.

2.1.2 Bacteria and culture media

Strain	Genotype	Provider
E.coli		
DH5α	φ80*lac*ZΔM15 *rec*A1 *end*A1 *gyr*A96 *thi*-1 *hsd*R17 (*rK-, mK+) sup*E44 relA1 deoR Δ*lac*ZYA-*arg*F*)*U169	Invitrogen
Top 10	F- *mcr*A Δ(*mrr-hsd*RMS-*mcr*BC)φ80*lac*ZΔM15 Δ*lac*X74 *rec*A1 *ara*D139 Δ(*araleu*)7697 *gal*U *gal*K *rps*L (StrR) *end*A1 *nup*G	Invitrogen
DB3.1	F- *gyr*A462 *end*A1 Δ(sr1-recA) *mcr*B *mrr* *hsd*S20(*rB*-, *mB*-) *sup*E44 *ara*-14 *gal*K2 *lac*Y1 *pro*A2 *rps*L20(SmR) *xyl*-5 λ-*leu mtl*1	Invitrogen
BL21	F- *dcm omp*T *hsd*S (*rB-mB*-) *gal*	Stratagene

Strain	Resistance	Provider
S.aureus		
ATCC29213	MSSA	ATCC, USA
USA300	MRSA	NARSA, USA
MW2	MRSA	NARSA, USA
JE2	MRSA	NARSA, USA
JE2 Δ*spA*	Erythromycin	NARSA, USA
JE2 Δ*pOxi*	Erythromycin	NARSA, USA
JE2 Δ*hp2160*	Erythromycin	NARSA, USA
ATCC29213-GFP	Erythromycin	Inst. for Med. Microbiology, Köln, S. Leggio
MW2-Δ*agr*	Tetracycline	Inst. for Med. Microbiology, Köln, B. Tosetti

Culture Media / Antibiotics	Composition / Manufacturer
LB-Medium	1 % Tryptone, 0.5 % Yeast Extract, 0.5 % NaCl, pH 7.0
LB-Agar	LB-Medium + 15 % Agar, pH 7.0
TSB-Medium	1.7 % Tryptone, 0.5 % NaCl, 0.3 % Soytone, 0.25 % Glucose, 0.25 %, K_2HPO_4 , pH 7.3 (± 0.2)
SOC-Medium	2 % Tryptone, 0.5 % Yeast extract, 0.5 % NaCl, 100 mM $MgCl_2$, 20 mM Glucose, pH 7.0
Mueller-Hinton agar plates	Oxoid
Blood agar plates	Oxoid
Ampicillin	stock solution: 50 mg / ml in H_2O final concentration 50 µg / ml
Kanamycin	stock solution: 50 mg / ml in H_2O final concentration 50 µg / ml
Erythromycin	stock solution: 10 mg / ml in 95 % Ethanol final concentration 10 µg / ml

2.1.3 Cell lines and culture media

Cell line	Provider
HeLa ATCC (CCI-2)	ATCC, USA

Culture media / media-additives	Composition / Manufacturer
Dulbecco`s MEM (1x)	Biochrom AG
RPMI (1x)	Biochrom AG
Hanks Balanced Salt Solution (HBSS)	Life Technologies
Fetal Calf-Serum (FCS)	BioWest
Penicillin-Streptomycin (10x)	Biochrom AG
Trypsin (10x)	Biochrom AG
Na-Pyruvate	Biochrom AG
PBS (10x)	Biochrom AG

2.1.4 Buffers and solutions

Denotation	Composition / Manufacturer
Agarose gel	
TAE buffer (1x)	0.8 mM Tris, 0.4 mM Acetic acid, 0.04 mM Na_2EDTA, pH 8.5
Loading buffer (1x)	Thermo Fisher Scientific, ready to use solution
1 kb DNA-ladder	Thermo Fisher Scientific, ready to use solution
Agarose gel	1% (w/v) Agarose (Roth), 1 x TAE-buffer, 0.5 µg / ml Ethidium bromide
SDS-PAGE	
Laemmli buffer (5x)	60 mM Tris-HCl, pH 6.8, 2 % SDS, 25 % Glycerol, 0.2 % Bromphenol Blue, 10 % β-Mercaptoethanol
Protein Size Marker	Page Ruler, Thermo Fisher Scientific
Running buffer (20x)	MOPS-Buffer, Life Technologies
Coomassie staining solution	2.5 % Serva blue R250, 45 % Ethanol, 15 % Acetic acid
Destaining solution	45 % Methanol, 15 % Acetic acid
Immunoblotting	

TBST (1x)	150 mM NaCl, 50 mM Tris, 0.05 % Tween 20; pH 7.4
Blocking buffer	5 % Skim milk powder (Roth), 2 % BSA in TBST
Transfer buffer	25 mM Tris-HCl, 192 mM Glycine, 20 % Methanol

Affinity Chromatography

Recombinant Proteins

PBS (10x)	1.4 M NaCl 100 mM Na_2PO_4, 27 mM KCl, 18 mM KH_2PO_4; pH 7.4
Resuspension buffer	1 x PBS, 500 mM NaCl, 5 % Glycerol, EDTA-free complete protease inhibitor (Roche)
Binding buffer	1 x PBS, 500 mM NaCl, 40 mM Imidazole; pH 7.4
Elution buffer	1 x PBS, 500 mM NaCl, 250 mM Imidazole; pH 7.4
Dialysis buffer	1 x PBS, 10 % Glycerol; pH 7.4

Polyclonal antibody enrichment

Wash A (NHS column)	0.5 M Ethanolamine, 0.5 M NaCl; pH 8.3
Wash B (NHS column)	0.1 M NaOAc, 0.5 M NaCl; pH 4.0
PBS (1x, binding buffer)	140 mM NaCl, 2.7 mM KCl, 10 mM NaH_2PO_4, 1.8 mM KH_2PO_4; pH 7.4
Elution buffer	0.1 M Glycine-HCl; pH 2.5
Neutralization buffer	1 M Tris-HCl; pH 9.0
Storage Buffer	0.05 M Na_2HPO_4, 0.1 % NaN_3; pH 7.0

ELISA

Coating buffer	15 mM Na_2CO_3, 35 mM $NaHCO_3$; pH 9.6
Blocking buffer	StartingBlock™ T20 (PBS), Thermo Scientific
PBST (1x)	140 mM NaCl, 2.7 mM KCl, 10 mM NaH_2PO_4, 1.8 mM KH_2PO_4, 0.02 % Tween 20, pH 7.4

FACS

Blocking buffer	PBS + 1 % BSA, pH 7.5
FACS assay buffer	PBS + 1 % BSA + 0.5 mM EDTA, pH 7.5

2.1.5 Antibodies

Name	Characteristics	Provider
Primary Antibodies		
Octagam® (IVIG) 1:500	Human intravenous immunoglobulin preparation	Octapharma GmbH, Langenfeld
Anti-pOxi moAb D3 (1 mg/ml) 1:5000	Murine monoclonal IgG2a	Inst. for Med. Microbiology, Köln, A. Klimka
Anti-Triiso moAb H8 (1 mg/ml) 1:5000	Murine monoclonal IgG1	Inst. for Med. Microbiology, Köln, A. Klimka
Anti-Triiso moAb C4 (1 mg/ml) 1:5000	Murine monoclonal IgG1	Inst. for Med. Microbiology, Köln, A. Klimka
Anti-Triiso moAb C8 (1 mg/ml) 1:5000	Murine monoclonal IgG2b	Inst. for Med. Microbiology, Köln, A. Klimka
Anti-hp2160 moAb 16-2 (1 mg/ml) 1:5000	Murine monoclonal IgG1	Biogenes GmbH, Berlin
Anti-pOxi humAb D3 (1 mg/ml) 1:5000	Human monoclonal IgG1	Antitope Ltd, UK
Anti-Triiso humAb H8 (1 mg/ml) 1:5000	Human monoclonal IgG1	Antitope Ltd, UK
Anti-hp2160 humAb 16-2 (1 mg/ml) 1:5000	Human monoclonal IgG1	Antitope Ltd, UK
Secondary antibodies		
Anti-mouse IgG-HRP 1:3000	HRP-conjugated goat anti-mouse IgG	Sigma-Aldrich
Anti-mouse IgG1-HRP 1:3000	HRP-conjugated goat anti-mouse IgG	Caltag
Anti-mouse IgG2a-HRP 1:3000	HRP-conjugated goat anti-mouse IgG	Caltag
Anti-mouse IgG-PE-Cy5.5; 1:100	Goat $F(ab)_2$ anti-mouse IgG (H+L) PE-Cy®5.5 conjugate	Life Technologies
Anti-mouse IgG-AlexaFluor488 1:100	Goat $F(ab)_2$ anti-mouse IgG (H+L) Alexa Fluor® 488 conjugate	Life Technologies

Anti-human IgG-HRP 1:3000	HRP-goat anti-human IgG	BioRad
Anti-human FCγ-PE 1:100	PE-goat anti-human FC γ $F(ab)_2$	Dianova
Anti-6-His-tag-HRP	HRP-conjugate	Invitrogen
Strep-Tactin-HRP	HRP-conjugate	IBA

2.1.6 Technical equipment

Device	Specification	Manufacturer
Cell Counter	Countess™	Life Technologies
Cell Disrupter	Constant Cell Disruption Systems	IUL
Colony Counter	Countermat	IUL
Documentation Chamber	MF-ChemiBIS 3.2	Berthold Technologies
Documentation Chamber	AGFA Curix	AGFA
Electrophoresis chamber	Criterion Cell	BioRad
Flow Cytometer	FACScalibur	BD Biosciences
FPLC system	ÄKTA™ Purifier	GE Healthcare
Gel documentation	Gel Doc 2000	BioRad
High-speed centrifugation	Discovery RC26 plus	Sorvall
Incubator (bacteria)	Kelvitront	Thermo Scientific
Incubator (cells)	Hera cell 240	Thermo Scientific
Microcentrifuge	Centrifuge 5417R	Eppendorf
Microscope	Axiovert 25	Zeiss
Multimode Reader	TrisStar LB941	Berthold Technologies
PCR cycler	Thermocycler T3	Biometra
Power supply	Power Pac 3000	BioRad
Roller-mixer	CATRM5	Zipperer
Spectralphotometer	NanoVue	GE Healthcare
Spectralphotometer	Genesis 2	Thermo Scientific
Spiral platter	EddyJET	IUL
Tank Blotter	Criterion Blotter	BioRad
Thermomixer	Comfort	Eppendorf

2.1.7 Oligonucleotides

Purified oligonucleotides were obtained from Sigma-Aldrich and resuspended in TE buffer at pH 8.0 and stored at -20°C. Primers were used in a final concentration of 5 pmol/µl for cloning. The restriction sides are printed in bold.

Name	Sequence (5'- 3')
SP1 Triiso	5'-AGCGGCTCTTC**AATG**AGAACACCAATTATAGCTG-3'
MibIII-N-ASP	5'-AGCGGCTCTTC**TCCC**AGTTTGACGTACAAATGCACAC-3'
SP2-C-MibIII	5'-AGCGGCTCTTC**AATG**AAAGCACAAGGTTTAGAAATCG- 3'
ASP2 Triiso	5'-AGCGGCTCTTC**TCCC**TTTTGCACCTTCTAACAATTGTACG-3'
ASP-C-17-MibIII	5'-AGCGGCTCTTC**TCCC**GTTAGGTTTAACACTACCACC- 3'
SP2-C-19-MibIII	5'-AGCGGCTCTTC**AATG**AATGGTGCGTTCACAGGTGAAAC-3'
ASP-C-19-MibIII	5'-AGCGGCTCTTC**TCCC**ATCAATATCAGTTTGTGCCAT-3'
SP-Pep1-MibIII	5'-AGCGGCTCTTC**AATG**ACGTCTCCAGTTGCATTAG-3'
SP-Pep2-MibIII	5'-AGCGGCTCTTC**AATG**AAATACGTTGTTATCGGTC-3'
SP-Pep3-MibIII	5'-AGCGGCTCTTC**AATG**GAATTATTCCACGAAACAG-3'
SP-Pep4-MibIII	5'-AGCGGCTCTTC**AATG**GATGAAGAAATTAACAAAAAAG-3'
SP-Pep5-MibIII	5'-AGCGGCTCTTC**AATG**AAAGCGCACGCTATTTTC-3'
SP-Pep6-MibIII	5'-AGCGGCTCTTC**AATG**AAACATGGAATGACTCCA-3'
SP-Pep7-MibIII	5'-AGCGGCTCTTC**AATG**ATTATTTGTGTTGGTGAA-3'
pOxipep-TriisoN sense	5'-AGCGGCTCTTC**AATG**ACCGATAACGAACTGGTGAGC ATTGTGCGTCGCGATAAAGCGCACGCT ATTTTCAAACAT-3'
Hp2160pep-TriisoC-antisense	5'-AGCGGCTCTTC**TCCC**TTTATAGAAGAAACGTTCCACATC CTGATCGTTTTTGTTAGGTTTAACACTACCACCATA-3'
pOxi-anti-senseTriisoC	5'-AGCGGCTCTTC**TCCC**ATCGCGACGCACAATGCTCACCAG TTCGTTATCGGTGTTAGGTTTAACACTACC ACC-3'
AAV-Triepitop *Kpn*I sense	5'-TA**GGTACC**CACCGGCCACCATGGATAACGAACTGG-3'
AAV-Triepitop *Not*I AS	5'-GA**GCGGCCGC**TCTATTTATAGAAGAAACGTTCCAC-3'
AAV-Triepitop *Age*I sense	5'-TA**ACCGGT**CACCGGCCACCATGGATAACGAACTGG-3'
AAV-Triepitop *Bsr*GI AS	5'-G**TGTACA**CTTTATAGAAGAAACGTTCCAC-3'

2.1.8 Plasmids

Name	Provider
pET29b-pOxiHis	A. Klimka, Inst. for Med. Microbiology, Köln
pET29b-TriisoHis	A. Klimka, Inst. for Med. Microbiology, Köln
pET29b-hp2160His	A. Klimka, Inst. for Med. Microbiology, Köln
pENTRY-IBA51	IBA
pPSG-IBA43	IBA
IBA-Triepitop	This work
IBA-OTO	This work
IBA-pOT	This work
IBA-TpO	This work
pGFP-Anne	H. Büning, MH Hannover
pEGFP-VP2	H. Büning, MH Hannover
AAV-pTriepitop-Anne	This work
AAV-pTriepitop-VP2	This work

2.1.9 Anesthesia

Ketavet-Rompun narcotic

87.5 % physiological NaCl solution (0.9 %)
10 % Ketavet (100 mg/ml Ketaminhydrochloride)
2.5 % Rompun (2 % Xylazinhydrochloride)
intraperitoneal application (i.p.), 200 µl/20 g mouse weight

2.1.10 Kits

Designation	Manufacturer
Amersham™ ECL™ Detection Reagent	GE Healthcare
BCA Protein Assay Kit	Thermo Scientific
ECL™ Detection Reagents	GE Healthcare
Endo Free Plasmid Maxi Kit	Qiagen
LumiGLO Reserve™ Chemiluminescent Substrate Kit	KPL
PureTaq™ Ready-To-Go™ PCR beads	GE Healthcare
QIAprep Spin Miniprep	Qiagen

QIAquick PCR Purification	Qiagen
TMB Substrate Reagent Set	BD Biosciences
DuoSet ELISA Mouse IFN-γ	R & D Systems
DuoSet ELISA Mouse IL-4	R & D Systems
DuoSet ELISA Mouse IL17A	R & D Systems
BrdU Cell Proliferation ELISA Kit	Abcam

2.1.11 Consumables

Designation	Manufacturer
Amersham Hyperfilm ECL	GE Healthcare
Bottle-Top-Filter	Nalgene
Cell Culture Plastic	TPP
Centricon-Plus 70, 30 000 MWCO	Millipore
Countess™ Counter Chamber	Life Technologies
Discofix® Three-way cock	Braun
EddyJET Tips	IUL
HiTrap™ FF crude Columns	GE Healthcare
HiTrap™ NHS-activated HP Columns	GE Healthcare
Maxisorp™ flat-bottom 96-well plates	Nunc
Nitrocellulose	GE Healthcare
Novex® Midi Gel adapters	Life Technologies
NuPAGE® Novex® 10 % Bis-Tris Midi Protein	Life Technologies
Petri dishes	Sarstedt
Poly-Prep® Chromatography Columns	BioRad
Slide-A-Lyzer Dialysis Cassette 10000	Thermo Scientific
Sterifix® Injection Filter, 0.2µm	Braun
Syringes and Needles	Braun, BD Biosciences
Whatman Paper	ALBET LabScience

2.1.12 Software

Designation	Manufacturer
CellQuest™ Pro	BD Biosciences
Chromas Pro	Technelysium
GelCapture	DNR Bio Imaging Systems Ltd.
GraphPad Prism 5	GraphPad Software, Inc.
Flash & Grow Advanced Colony Counting	IUL
Image Lab	BioRad
NanoDrop 2000	ThermoScientific
MikroWin2000	Mikrotek Laborsysteme GmbH
Vector NTI	Invitrogen

2.2. Methods

2.2.1 Microbiological methods

2.2.1.1 Cultivation of E. coli

E. coli from -80 °C stocks was grown for 8-16 h at 37 °C on LB agar plates. When growing the bacteria in liquid medium, one colony was picked and grown in LB medium. An Erlenmeyer bottle was filled up to 25 % with LB medium and next day bacteria were inoculated 1:100 and incubated at 37 °C with shaking at 220 rpm.

2.2.1.2 S. aureus growth curves (planktonic)

S. aureus from ON culture was inoculated 1:100 into LB or TSB broth, supplemented with the corresponding antibiotic and cultured at 37 °C with shaking at 220 rpm. The OD was measured every hour at 600 nm.

2.2.1.3 S. aureus growth under biofilm conditions

S. aureus from ON culture was inoculated into TSB broth containing 0.5 % glucose and cultured in flat-bottom cell culture plates (usually 6-well) at 37 °C for 24-72 h without shaking.

2.2.1.4 Quantification of biofilm formation

For quantitative biofilm analysis *S. aureus* cells were stained with crystal violet. After growth of *S. aureus* in 96-well microtiter plates, biofilm was carefully washed with 1 x PBS and air-dried. Biofilm was then fixed with 100 % ethanol for 15 min, air-dried again and stained with 0.2 % crystal violet for 2 min.

After removal of crystal violet biofilm was washed 10 x with dH_2O. Bound crystal violet was extracted by extraction buffer containing 40 % ethanol and 10 % acetic acid. The absorbance was measured in a plate reader at 590 nm using extraction buffer as blank.

2.2.2 Molecular biological methods

2.2.2.1 Polymerase chain reaction (PCR)

PCR was used for the amplification of protein fragments and epitope sequences, respectively, from our vaccine candidates. Plasmids pET29b-TriisoHis, pET29b-pOxiHis and pET29-hp2160His (constructed by our AG) were used as DNA templates. The reactions were performed as follows:

10 x Buffer	5 µl
dNTPs	5 pmol
Sense Primer	10 pmol
Antisense Primer	10 pmol
DNA	100-150 ng
Pfu Polymerase	2.5 U
ddH_2O	ad 50 µl

The PCR program for *Pfu* Polymerase is used as follows:

95 °C	3 min	
95 °C	1 min	x 25
50-65 °C	0.5 min	
72 °C	2 min	
72 °C	10 min	
10 °C	forever	

Annealing temperature of primers was calculated individually. First, melting temperature (T_m) of primers was calculated with the following formula:

$$T_m = 2\ °C \times (A+T) + 4\ °C \times (G + C)$$

The starting point for the PCR annealing step is T_m – 5 °C. If too many unspecific side products appeared in subsequent gel electrophoresis, temperature was increased around 1-3 °C.

2.2.2.2 Purification of PCR products and plasmid DNA

Purification of PCR products and plasmid DNA, respectively, was performed using PCR Clean-up Kit and NucleoSpin Plasmid Kit, respectively, according to manufacturer's instructions. The methods are based on cell lysis by SDS and binding of the DNA to a silica membrane following removal of contaminations by washing with ethanolic buffer and subsequent elution of the DNA under low ionic strength conditions (Macherey-Nagel, 2015).

2.2.2.3 Quantification of nucleic acids

Concentrations of the purified DNA were determined with a NanoDrop microvolume UV/VIS spectrophotometer (Thermo Scientific). Therefore, 1 µl of DNA was applied on the device after adjusting the reference with elution buffer. The concentration was determined at a wavelength of 260 nm. Additionally, the quality of the DNA was determined by measuring the quotient of absorptions of DNA and contaminants such as proteins and phenols (A260/280). Pure DNA samples are expected to have a value ranging from 1.8 - 2.0 (Thermo Fisher Scientific, 2009).

2.2.2.4 Restriction endonuclease digest of plasmids

Digestion with restriction endonucleases was performed to ligate amplified DNA and vector or to control identity of purified plasmids. Reaction was performed using Fast digest enzymes according to manufacturer's instructions (Fermentas) in a 10-20 µl solution containing 1 U enzyme per 1 µg of DNA, 1x reaction buffer and 1 U per 1 µl Fast Alkaline Phosphatase.

2.2.2.5 Agarose gel electrophoresis

Agarose gel electrophoresis was conducted to analyze restriction enzyme reaction. Gels were prepared as 1 % agarose gels with TAE buffer and 0.0005% EtBr. A total volume of 8-10 µl of sample plus 1x loading dye was loaded per slot. Electrophoresis was performed at 100 V for 1 h and gel was analyzed under UV-light using the Gel Doc2000 with the Quantity One Software.

2.2.2.6 Ligation of amplified DNA and expression vectors

In the ligation process insert and the vector are joined to each other by hybridization of compatible ends generated by restriction endonucleases following formation of phosphodiester bonds between the 3' hydroxyl and 5' phosphate of neighboring DNA residues, which is catalyzed by ligase. Antibiotic resistance genes serve as selective markers for identification of positive clones. The amount of utilized vector and insert was calculated according to the following equation, given that the amount of used vector DNA is 100 ng and the ratio of insert and plasmid is 4:1.

$$mass_{insert\ DNA}\ [ng] = base\ pairs\ (insert) / base\ pairs\ (vector) \times 4 \times 100\ ng$$

Consistent with this formula, the utilized volume of insert DNA can be calculated according to the corresponding DNA concentration. The mixtures were prepared according to manufacturer's instructions (T4-Ligase rapid ligation, Fermentas) and incubated for 30 min at RT and then used for transformation. As a control to detect religation of the vector molecule, a sample containing 100 ng of vector (w/o insert) was prepared.

2.2.2.7 Production of heat-shock competent cells

To take up foreign plasmid DNA *E. coli* cells had to be made artificially competent. This means that the cells were exposed to a special chemical, such as calcium chloride to make the cell wall permeable by creating pores.

E. coli cells were grown ON in LB medium at 37 °C and 220 rpm. Next day ON culture was inoculated 1:100 into fresh LB medium and grown to an OD_{600} of 0.7 at 37 °C. Subsequent cooling down for 10 min on ice followed and cells were pelleted for 10 min at 4 °C and 2500 x *g*. Supernatant was discarded and pellet was resuspended in 4 ml ice-cold 0.1 M $CaCl_2$ + 15 % glycerol. The suspension was incubated for 20 min on ice and spun down for 15 min at 4 °C and 2500 x *g*. The pellet was again resuspended in 4 ml ice-cold 0.1 M $CaCl_2$ + 15 % glycerol and incubated for 10 min on ice. Aliquots of 100 µl transformation competent cells were transferred into pre-chilled tubes, shock frozen in liquid nitrogen and stored at -80 °C until further use.

2.2.2.8 Heat-shock transformation of competent cells

For transformation 100 µl of competent cells were added to each of the ligation mixes (20 µl) or to 10 ng plasmid following incubation for 30 min on ice. Subsequently the cells were heat-shocked at 42 °C for 90 sec and then incubated on ice again for 2 min. The mix was then supplemented with 800 µl SOC-medium each and incubated for 1 h at 37 °C to let the cells express antibiotic resistance. Depending on the resistance gene located on the different vectors, incubation time with shaking at 350 rpm was between 30 and 60 min. The mix was centrifuged at 13 000 x *g* for 3 min. The pellet was resuspended in 100 µl remaining supernatant, plated on LB-agar plates containing the corresponding antibiotic and incubated ON at 37 °C.

2.2.2.9 Colony PCR

Clones obtained from heat-shock transformation of the respective *E. coli* strain were picked for performing a colony PCR to screen for positive clones carrying the plasmid with insert. The picked colony was suspended in a total volume of 25 µl of the reaction mixture containing 10 pmol of sense and antisense primer.

The mixture was set up in reaction tubes supplemented with Pure*Taq*™ Ready-ToGo™ PCR beads (GE Healthcare) that contain *Taq* DNA polymerase, dNTPs, stabilizers and buffers. The *Taq*-PCR program was used as follows:

95°C	5 min	
95°C	1 min	x 25
55°C	1 min	
72°C	2 min	
72°C	10 min	
10°C	forever	

An agarose gel electrophoresis was conducted to analyze if the picked colony contains the plasmid with the cloned insert.

2.2.2.10 DNA sequencing

Purified plasmid DNA (2.2.2.2) of positive clones was enriched to a concentration of 100 ng per µl by lyophilization and a total volume of 10 µl were used for sequencing. BigDye® Terminator v3.1 Cycle Sequencing Kit (Thermo Scientific) was used according to manufacturer's instruction. 3.2 pmol of a vector-specific PCR primer was

added to each sample. The mixtures were sequenced by LGC Genomics, Berlin performing the chain-termination method of Sanger.

2.2.2.11 Preparation of glycerol stocks

The respective clones were ON cultured in LB medium supplemented with the appropriate antibiotic and incubated at 37 °C. Aliquots of 750 µl of the ON culture were mixed with 750 µl glycerol (50 %) in a Cryo.s™ tube and stored at -80 °C.

2.2.3 Protein biochemical methods

2.2.3.1 Production of S. aureus whole cell lysates (WCL)

S. aureus from ON culture was inoculated 1:100 into LB broth. Bacteria were cultured until different ODs. Bacteria were harvested by centrifugation at 10 000 x *g* and the pellet was washed in 1 x PBS and resuspended in 1 x PBS containing EDTA-free complete protease inhibitor (Roche), 5 % Glycerol and Lysonase^{TM}. 0.2 mg/ml lysostaphin was added and the pellet was incubated for 15 min at room temperature and then for 30 min on ice. After the incubation steps bacteria cells were disrupted using the Cell Disrupter (6 times at 2 bar). The cell lysate was then centrifuged for 30 min at 10 000 x *g*. The supernatant was taken for a determination of the protein concentration using the BioRad DC assay in dilutions between 1:10 and 1:30 according to the manufacturer's instructions and for a following Western blot analysis.

2.2.3.2 Isolation of S. aureus cell wall associated proteins

S. aureus from ON culture was inoculated 1:100 into LB broth. Bacteria were cultured until an OD_{600} of 0.3. Cell wall associated proteins were extracted from bacterial pellet using a modified protocol of a previously described method (Antelmann *et al*., 2002). The pellet was washed, resuspended in 1.5 M LiCl, 25 mM Tris-HCl (pH 7.2) containing complete protease inhibitors and incubated on ice for 30 min. Subsequent to centrifugation, non-enzymatic cell-wall supernatant (neCWS) was precipitated with 10 % (w/v) trichloroacetic acid ON at 4 °C. After a centrifugation at 13 000 x *g* and 4 °C the precipitate was washed twice with ice-cold ethanol and dried under vacuum. The neCWS was dissolved in 8 M urea and insoluble aggregates were removed by centrifugation. Protein concentration was determined using the BCA Protein Assay

Kit in dilutions between 1:2 and 1:20 according to the manufacturer's instructions for Western blot analysis.

2.2.3.3 Overexpression and affinity purification of vaccine candidates

The respective *E.coli* BL21 expression clone (stored at -80 °C) was plated out on Mueller-Hinton or LB agar. After ON growth one colony was inoculated into LB (+ Kanamycin). Next day the clone was inoculated 1:100 in 400 ml LB (+ Kanamycin) and cultured until an OD_{600} of 0.6. Then IPTG (final concentration 1 mM) was added and the culture was incubated for additional 4 h at 37 °C (Triiso, hp2160) or ON at 30 °C (pOxi, Diepitope- and Triepitope peptides). Bacteria were harvested at 17 000 x *g* at room temperature, washed twice in PBS and stored in 1 x PBS buffer containing EDTA-free complete protease inhibitor (Roche), 5 % Glycerol and Lysonase™ at -20 °C until lysis of the cells using the cell disrupter as described above. Upon disruption of the cells, cell debris was eliminated by centrifugation at 17 000 x *g*. Prior to loading onto equilibrated HisTrap™ FF crude column (GE Healthcare), lysates were adjusted to a final concentration of 500 mM NaCl and 40 mM Imidazole pH 7.4. Protein was loaded onto the column by ON recirculation at a flowrate of 1 ml per minute at 4 °C using a peristaltic pump. The loaded column was transferred to the pre-equilibrated FPLC system, washed with binding buffer (40 mM imidazole) and fusion protein was eluted with elution buffer (250 mM imidazole).

To eliminate imidazole, eluates were pooled and buffer was exchanged against 1 x PBS containing 10 % Glycerol by centrifugal filters (Centricon, Millipore). Protein concentration was determined using the BCA Protein Assay Kit according to the manufacturer's instructions and sterile filtered purified proteins were stored at -20 °C.

2.2.3.4 SDS-polyacrylamide-gelelectrophoresis (SDS-PAGE)

Proteins were adjusted to 5-10 µg for subsequent Coomassie staining or 1-5 µg for Western Blot analyses per lane with H_2O and 5 x Laemmli buffer and subsequently boiled at 95 °C for 5 min. WCLs and neCWS were adjusted to 40-50 µg per lane for Western blot analyses. Insoluble aggregates were removed by centrifugation at 10 000 x *g*, RT. Proteins were separated by SDS-PAGE with the Criterion gel system (Bio-Rad) in a Criterion electrophoresis chamber using a constant voltage of 120 V.

Protein gels were stained with Coomassie solution or were used for immunoblotting.

2.2.3.5 Western blot

Subsequent to protein separation by SDS-PAGE, proteins were transferred to a nitrocellulose membrane using Criterion Midi Tank-Blotsystem with a constant current of 250 mA for 70-90 min. Afterwards, the membrane was blocked with blocking solution for 1 h at room temperature to prevent non-specific binding of antibodies. Primary and HRP-conjugated secondary antibodies diluted in blocking solution were used for specific protein detection. Incubation with a primary antibody was carried out overnight at 4 °C, secondary antibody was applied for 1-1.5 h at room temperature. In order to remove unbound antibodies the membrane was washed three times for 10 min with 1x TBST buffer between incubation with antibodies. Bound proteins were detected using chemiluminescence reagent (ECL) or LumiGlo Reserve™ Chemiluminescent substrate. Chemiluminescence was imaged using the MF-ChemiBIS 3.2 Imager (Berthold Technologies) or the blot was developed with AGFA Curix (AGFA) using an X-ray film.

2.2.3.6 Interaction between Triiso and plasminogen by Far-Western blot

Detection of an interaction between human plasminogen and Triiso was performed by Far-Western blotting, according to Furuya and Ikeda (2011). With this method a protein 1 that was blotted on a membrane was then incubated with another protein 2. Protein 1 was then identified by an antibody that is specific for the protein 2 which proves the interaction between protein 1 and 2.

Recombinant Triiso was separated by SDS-PAGE and blotted onto nitrocellulose membranes. The membranes were blocked and then treated with 100 nM human plasminogen (Roche) diluted in blocking milk. Detection of Triiso by bound plasminogen was performed by goat anti-plasminogen-HRP (Abcam). For the investigation of a moAb-based inhibition of this interaction membrane was incubated with different concentrations of α-Triiso moAb H8 before plasminogen was added.

2.2.3.7 Interaction between Triiso and plasminogen by ELISA

The interaction analysis described in 2.2.3.6 was also conducted by ELISA. Plasminogen was coated in a final concentration of 5 µg/ml on a Maxisorp plate.

After blocking plate was incubated with recombinant Triiso in different concentrations that was then detected with anti-6-His-tag antibody. For the investigation of a moAb-based inhibition of the Triiso-plasminogen interaction Triiso was first incubated with α-Triiso moAb H8 for 30 min at room temperature. The mixture was then added to the plate. Incubation with anti-6-His-tag antibody followed and the change in absorbance was measured at 450 nm.

2.2.3.8 Enzymatic activity of Triiso

Enzymatic activity of native or recombinant Triiso was coupled to the oxidation of NADH by glycerol-3-phosphate dehydrogenase, according to the method of Furuya and Ikeda (2009) with some modifications in enzyme concentration.
Recombinant Triiso, *S. aureus* whole cell lysate or non-covalently bound surface protein fraction was incubated in different concentrations with 0.45 mM DL-glyceraldehyde-3-phosphate as substrate, 0.03 mg NADH and 3 mg glycerol-3-phsophate dehydrogenase in a final volume of 300 µl. The change in absorbance was measured at 340 nm.

2.2.3.9 Enzymatic activity of plasmin

Activation of plasminogen into plasmin was catalyzed by the *S. aureus* enzyme staphylokinase (SAK).
For the measurement of plasmin activity 40 µl of 500 nM human plasminogen, 40 µl of the 0.5 mM substrate S-2251 and 25 ng of human recombinant SAK in a final volume of 100 µl were mixed and the reaction was started by adding SAK. The increase in absorbance was measured at 405 nm. All reagents were diluted in 50 mM Tris-HCl buffer (pH 7.4).

2.2.3.10 Effects of native and recombinant Triiso on plasminogen activation

An influence of Triiso on plasminogen activation was proved by Furuya and Ikeda (2011). To examine an effect of recombinant Triiso on plasminogen activation the assay in 2.2.3.9 was performed in the presence of Triiso. 40 µl of 500 nM plasminogen, different dilutions of Triiso between 0 and 16 µg (10 µl volume), 40 µl of the 0.5 mM substrate S-2251 and 25 ng of human recombinant SAK (10 µl volume)

in a final volume of 100 µl were mixed and the increase in absorbance was measured at 405 nm. The reaction was started after adding SAK.
The same procedure was performed with 2-10 µg *S. aureus* cell lysate and 2-5 µg neCWS. To examine the effect of α-Triiso moAb H8 in this assay it was incubated with Triiso for 30 min at room temperature before the addition of Triiso to the reaction mixture.

2.2.3.11 Effects of intact live S. aureus on plasminogen activation

To examine the effects of intact live *S. aureus* cell were added to the plasmin activity assay system. After *S. aureus* USA300 had been cultured at 37 °C for 18 h in TSB under planktonic or biofilm conditions, respectively, cell suspensions (10 µl) at various concentrations (1×10^{10}, 5×10^{9}, 1×10^{9}, 1×10^{8}, and 1×10^{7}/ ml) were incubated with 40 µl of 500 nM plasminogen for 30 min at 37 °C in a 96-well microtiter plate. After incubation with SAK for 10 min at 37 °C, reaction was started by adding substrate S-2251 and the absorbance at 405 nm was measured.

2.2.3.12 Enrichment of specific IgGs from IVIG

For enrichment of *S. aureus* specific IgGs, 1 mg of the purified recombinant protein was covalently linked to N-hydroxysuccinimide-activated Sepharose columns (NHS; HiTrap™ NHS activated HP columns) according to manufacturer's instructions (GE Healthcare). IVIG solution was diluted 1:3 with binding buffer. Binding of IgGs was performed ON at 4 °C by slow recirculation of IVIG solution. Specifically bound IgGs were eluted from the column by pH shift using 0.1 M glycine-HCl (pH 2.7). The pH of the eluted fractions was neutralized by addition of a sufficient amount of 1 M Tris-HCl (pH 9.0). IgG-containing fractions were pooled and, after buffer exchange into PBS (pH 7.5) and concentration using Centricon Plus-70, 30 kDa cut off centrifugal filters (Millipore), stored sterile filtered at 4 °C.

2.2.3.13 Surface localization of vaccine candidates

To localize the antigens on the surface of whole *S. aureus* cells by the monoclonal antibodies (moAbs), strain JE2 or Δ*spA* was grown in LB broth at 37 °C to an OD_{600} of 0.3 or for 24-72 h under biofilm conditions (see 2.2.2.3). Bacteria were harvested,

washed and adjusted to 1 x 10^8 CFU/ml (correlates with an OD_{600} of 0.3) in PBS containing 1 % bovine serum albumin (BSA). The respective moAb was added at a concentration of 0.1-0.5 mg/ml as primary antibody, incubated for 30 min at 37 °C and washed with PBS-1 % BSA to remove free antibodies. A 1:100 dilution of a phycoerythrin-conjugated or a FITC-conjugated goat anti-mouse $F(ab')_2$ fragment (Life Technologies) was used as secondary antibody and was incubated for 30 min at 37 °C. When humanized antibodies were used the phycoerythrin-conjugated goat anti-human $F(ab')_2$ fragment (Dianova) was added as secondary antibody in a 1:100 dilution. After a washing step to remove unbound secondary antibody, samples were diluted 1:2 in FACS buffer and analyzed by flow cytometry using the FACSCalibur system and CELLQuestPro software (BD Biosciences).

2.2.4 Cell culture

2.2.4.1 Cultivation of HeLa cells

Cells were cultured in DMEM containing 10 % FCS and 1 % P/S under sterile conditions at 37 °C in a humidified atmosphere containing 5 % CO_2. Cells were passaged every 3 days. To detach cells from culture dishes, medium was removed and cells were washed once with PBS. The cells were then incubated with trypsin-EDTA at 37 °C until detachment was visible. The reaction was stopped by the addition of medium containing 10 % FCS. For long term storage, cells were suspended in FCS containing 10 % DMSO and frozen at -160 °C.

2.2.4.2 Interaction between S. aureus and HeLa cells

When cells were passaged 3 days prior to infection medium was replaced with antibiotic free DMEM medium + 10 % FCS.

For the measurement of an interaction between *S. aureus* and HeLa cells by flow cytometry, the HeLa cells were harvested, washed and adjusted to 1 x 10^7 cells per ml. *S. aureus* ATCC-GFP was grown for 48 h under biofilm conditions (see 2.2.2.3), harvested, washed in PBS (pH 5.0) and adjusted to 1 x 10^8 CFU/ml. 500 µl of 1 x 10^8 CFU/ml bacteria were incubated with 50 µg of recombinant protein (pOxi, Triiso) or moAb (anti-pOxi D3, anti-Triiso H8) or 50 µl of PBS (negative control) at 37 °C for 30 min. Bacteria were then centrifuged and washed twice in PBS (pH 5.0).

HeLa cells were infected with *S. aureus* ATCC 29213-GFP MOI of 2, 5 and 10, respectively and incubated for 15 min at 37 °C. HeLa cells were centrifuged and pellet was fixed with 3 % paraformaldehyde for 20 min. Pellet was washed thrice and resuspended in 1 ml of FACS buffer for flow cytometric measurement.

2.2.4.3 Isolation of human neutrophils

Human polymorphonuclear cells (PMNs) were isolated by dextran sedimentation and Ficoll Hypaque gradient centrifugation from 20 ml of fresh blood. Blood was collected from a healthy donor and mixed 1:1 with a solution of 2 % citrate-dextrose + 7 % Dextran 70. After sedimentation (60 min) at room temperature leucocyte rich plasma was isolated and sublayered 1:1 with Ficoll. After centrifugation at 700 x *g* without brake the lymphocyte and monocyte rich supernatant was removed and the neutrophil rich pellet was incubated for 20 sec in 0.2 % NaCl and for 20 sec in 1.6 % NaCl to lyse the red blood cells. After addition of 40-50 ml 1 x HBSS - Mg^{2+} - Ca^{2+} + 0.1 % chicken egg albumin (Sigma) and a centrifugation step the isolated human PMNs were resuspended in 1 x HBSS pH 7.3, and number of cells was determined by trypan blue exclusion in a Neubauer chamber.

2.2.4.4 Preparation of bone marrow-derived macrophages

Bone marrow derived macrophages (BMDM) were prepared from the femurs and tibias of mice. The bone marrow was flushed with plain RPMI, and subsequently erythrocytes were lysed by incubation for 5 min in RBC lysis buffer at RT. Lysis was stopped by addition of RPMI and after centrifugation at 800 x *g* at RT cells were seeded in BMDM culture medium (RPMI supplemented with 10 % FCS, 1 % P/S, 1 % HEPES and 1 % sodium-pyruvate and 20 ng/ml recombinant murine mCSF (Peprotech)), in 10 cm non-cell culture treated petri-dishes. Cells were supplemented with BMDM culture medium after 5 days of differentiation. 24 h prior to infection of BMDMs, medium was replaced with antibiotic free RPMI medium. Infections were performed on day 8-10 upon isolation.

2.2.4.5 Investigation of T-cell response in mice post immunization

Aseptically isolated spleens were mashed through a 100 µm cell strainer to dissociate splenocytes. After centrifugation the pellet was incubated for 20 sec in 0.2

% NaCl and for 20 sec in 1.6 % NaCl to lyse the red blood cells. Cells were washed three times in 5 ml of plain DMEM medium. Cells resuspended in splenocyte medium (RPMI + 1 % FCS, 1 % Pen/Strep, 1 % 50 mM β-mercaptoethanol) were counted in trypan blue solution. Cells were counted in a Neubauer cell chamber. Cell concentration was adjusted with splenocyte medium to required cell numbers. 3 x 10^6 cells per well were seeded in 96-well plates in a total volume of 100 µl. Cells were stimulated with 2 µg/ml of the respective peptide. Splenocyte medium was used as negative control and 2 µg/ml of Concanavalin A (ConA) was positive control. Cell culture supernatants were collected 72 h post stimulation and stored at -20°C until measuring of cytokine concentration in supernatant by DuoSet ELISA (R & D Systems) according to manufacturer's instructions. BrdU Cell Proliferation Assay (Abcam) was also conducted according to manufacturer's instructions.

2.2.5 Immunological methods

2.2.5.1 In vitro opsonophagocytosis of S. aureus by human neutrophils

S. aureus ATCC 29213-GFP was inoculated into LB broth and grown at 37 °C to an OD_{600} of 0.3. Bacteria were harvested, washed and adjusted to 1 x 10^9 CFU/ml. IVIG (positive control), isolated specific human IgGs (α-pOxi and α-Triiso) enriched from IVIG and human monoclonal IgGs (α-pOxi humAb D3, α-Triiso humAb H8, α-hp2160 humAb 16-2) were added at a concentration of 50 µg/ml and pre-opsonization of bacteria was allowed for 30 min at 37 °C. 2.5 x 10^6 human PMNs and bacteria at a MOI of 10 were incubated for 2-10 min at 37 °C with slow rotation upon initial synchronization of infection by centrifugation at 700 x *g* for 2 min. Phagocytosis was stopped by centrifugation for 2 min at 150 x *g* at 4 °C, and samples were washed three times, resuspended in 1 x HBSS and samples were taken for FACS analysis (1:5 dilution in PBS-0.5 % BSA (pH 7.3); kept on ice until measurement) using the FACSCalibur and Cellquest Pro Software.

2.2.5.2 In vitro opsonophagocytosis of S. aureus by BMDM's

S. aureus ATCC 29213-GFP was inoculated into LB broth and grown at 37 °C to an OD 600 of 0.3. Bacteria were harvested, washed and adjusted to 1 x 10^9 CFU/ml. Murine monoclonal IgGs (anti-pOxi moAb D3, anti-Triiso moAb H8, anti-hp2160

moAb 16-2) were added in a concentration of 50 µg/ml and pre-opsonization of bacteria was allowed for 30 min at 37 °C.
BMDM's in petri dishes were incubated in 1 x PBS + 1 mM EDTA and harvested by a cell scraper. Detached cells were diluted with plain RPMI and after centrifugation at 800 x *g* at RT cell pellets were pooled. Cells were resuspended in a defined volume of antibiotic free RPMI medium. An aliquot was stained with trypan blue and counted. Cells were infected with a MOI of 15. In order to synchronize the uptake of *S. aureus*, host cells were incubated on ice with bacteria and were subsequently centrifuged for 5 min at 800 x *g*, 4 °C. After adhesion of *S. aureus*, the temperature was increased to 37 °C for 45 min. Thereafter the supernatant containing non-internalized bacteria was removed and cells were washed twice by centrifugation at 800 x *g* and 4 °C with ice-cold PBS. For the degradation of remaining extracellular bacteria, cells were incubated with 200 µg/ml lysostaphin on ice for 20 min. Thereafter cells were washed twice with PBS in order to remove lysostaphin and dead bacteria and fresh medium supplemented with antibiotics was added. Infected cells were incubated at 37 °C until indicated time points.

2.2.5.3 Competition ELISA

To determine epitope-peptide functionality a competition ELISA was performed. For the competition of moAb binding by epitope peptides 5 µg/ml antigen was immobilized at a maxisorp plate. The competitor (peptide) was pre-diluted in a 96-well plate from 500 µg/ml to 0.8 µg/ml and the dilutions were added to the blocked ELISA plate in a total volume of 50 µl per well. MoAbs were diluted 1:500 and 50µl were added to the competitor in a total volume of 50 µl. The plate was incubated for 1 h. The secondary antibody (goat anti-mouse or goat anti-human-HRP) was diluted 1:3000. All dilutions were prepared in blocking buffer. For 3x washing between the incubation steps 1 x PBST was used. For the reaction TMB substrate reagent kit was used according to the manufacturer's instructions. The absorbance was measured at 450 nm.

2.2.5.4 Immunization of mice

Epitope peptides were conjugated to the carrier proteins KLH or BSA using a corresponding conjugation kit (Thermo Fisher) according to manufacturer's instructions.

Female BALB/c mice (6 to 10 weeks old) were purchased from ZMMK (UK Köln). Mice were injected subcutaneously with a 1:1 emulsion (total volume: 200 µl) containing 70-80 µg recombinant peptide-conjugate and complete Freund's adjuvant (Sigma) on day 0, followed by subcutaneous administration of two booster doses using an emulsion containing 50 µg antigen and incomplete Freund's adjuvant (1:1) on days 28 and 56. Mice immunized with KLH or BSA as non-specific antigen served as controls. For the bivalent immunization 40 µg of each antigen was used for initial and 25 µg for booster immunization. For immunization with rAAV or rMVA vectors mice were anesthetized by an i.p. injection with Ketamine + Rompun (10:1), diluted 1:10 with sterile 0.9 % NaCl (Ketamine/Rompun 100 mg/kg and 10 mg/kg body weight). Each vector was diluted in 0.9 % NaCl to a titer of 1x 10^{10} pfu (rAAV) or 1 x 10^8 pfu (rMVA) per mouse. Vectors were administrated by intramuscular injection into the back thighs.

2.2.5.5 Serum preparation and IgG titer determination

For the determination of the specific antibody titer, blood samples were taken on days 14, 42 and 66 by bleeding at the vena facialis and analyzing by ELISA on 5 µg/ml of the respective antigen and 500- to 1.000.000-fold serial dilution using TMB substrate reagent set. The titer is given as the dilution corresponding to the half maximal OD.

2.2.5.6 Murine model of sepsis

Two weeks after the last booster immunization BALB/c mice were challenged by i.p. injection with *S. aureus* USA300 mixed with 5 % mucin from porcine stomach (Sigma). For organ preparation mice were challenged with a sublethal dose and for survival experiments with LD_{50} of 3.3 x 10^7 CFU in 300 µl PBS. For organ preparation mice were sacrificed after 24-48 hours and for survival experiments mice were monitored daily for clinical signs of infection and mortality for 8 days.

2.2.5.7 Preparation of organs for a determination of the bacterial density

Mice were sacrificed by cervical dislocation and liver, spleen and kidneys were isolated. After preparation of all mice organs were weighted and subsequently homogenized in dH_2O containing 0.1 % Triton X-100 by OctoMACS (Miltenyi) and then centrifuged for 5 min at 300 x *g*. All samples were diluted in 0.1 % Triton X-100 and immediately plated out on Mueller-Hinton agar. After ON incubation at 37 °C colonies were counted by a colony counter (IUL) using the program Flash & Grow Advanced Colony Counting. Organ CFU was calculated as colony numbers per organ mass.

2.2.6 Statistical analysis

If not stated otherwise, results were statistically analyzed by unpaired two-tailed Student´s t-test using GraphPad Prism version 5.03 for Windows (GraphPad Software, www.praphpad.com).

3 Results

3.1 Characterization of *S. aureus* antigens and generated specific monoclonal antibodies

Anchorless cell wall proteins were identified as vaccine candidates by subtractive proteome and MALDI-TOF analysis (Glowalla *et al*., 2009). Some of them, namely protoporphyrinogen oxidase (pOxi), triosephosphate isomerase (Triiso) and the hypothetical protein 2160 (hp2160), used as vaccines achieved a repetitive protection in murine sepsis model. Monoclonal antibodies (moAbs) against these antigens were generated in our lab by hybridoma technology and some of these purified moAbs D3 (pOxi), H8 (Triiso) and 16-2 (hp2160) used as passive immunization demonstrated a repetitive protection in the murine sepsis model as well.

We were interested in the characterization of the antigens as potential virulence factors and in the mode of action of the respective moAbs. The focus was set on pOxi because it was previously decided to use first the anti-pOxi moAb D3 in clinical studies to treat MRSA-based bacteremia in the next years. The second focus was set on Triiso because its occurrence on the *S. aureus* surface was already known (Furuya *et al*., 2009). In contrast to Triiso, hp2160 is not characterized, so far and was used as a third choice.

A further aim was the identification and analysis of the epitopes of the protective moAbs to be used as a combined, polyepitope-peptide vaccine against *S. aureus* infection.

3.1.1 Identification and verification of linear epitopes

The epitopes of anti-pOxi moAb D3 and anti-hp2160 moAb 16-2 were identified by microarray analyses performed mainly by the Pepperprint GmbH, Heidelberg. The respective antigen was synthesized as peptide-fragments of 13 amino acids spotted on a chip with overlapping sequences of 12 amino acids. The array was incubated

with the respective monoclonal antibody as primary and with goat anti-mouse IgG - DyLight680 conjugate (Thermo Scientific).

Read-out was done with an Odyssey Imaging System to detect antibody interactions with the 13mer peptides of pOxi or hp2160 (Figure 3.1). A response of anti-hp2160 moAb 16-2 (A), as well as anti-pOxi moAb D3 (B) with the linear peptides *KNDQD VERFFYK* and *TDNELVSIVRRD* was identified, respectively.

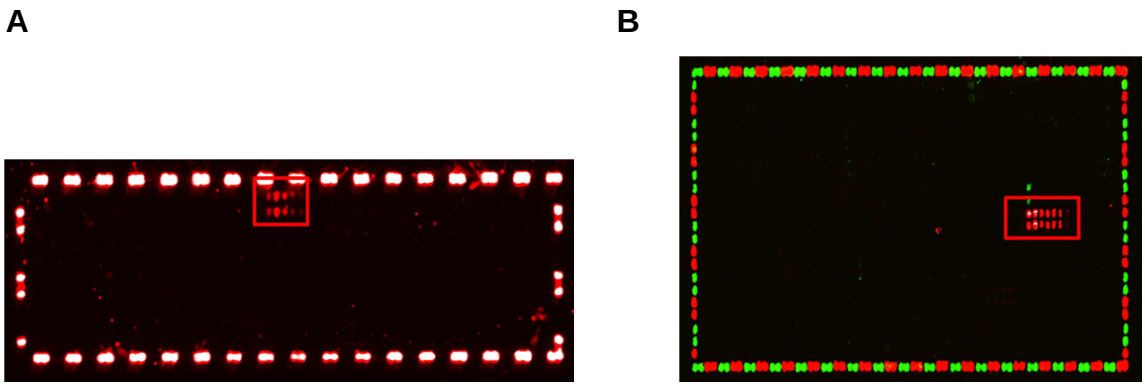

Figure 3.1: Microarray to identify the epitopes of anti-hp2160 moAb 16-2 (A) and anti-pOxi-moAb D3 (B). Respective antigen was synthesized in fragments of 13 amino acids on a chip with overlapping of 12 amino acids. Array was incubated with moAb and goat anti-mouse IgG-DyLight680 conjugate. Read-out followed with an Odyssey Imaging System.

The epitope identification of anti-Triiso moAb H8 was more complicated because three different signals were detected in the antigen Triiso (not shown).

Additionally, the linear epitope within the peptide *LADLGVKYVVIGHSERRELFHETD* of anti-Triiso moAb C4 was identified by microarrays. This anti-Triiso moAb showed only minor protection in the murine sepsis model after passive immunization, but was not tested as often as moAb H8.

The three resulting epitope peptides were synthesized by JPT Peptide Technologies GmbH, Berlin or Intavis AG, Cologne and were named hp2160 epitope-peptide (= anti-hp2160 moAb 16-2 epitope), pOxi epitope-peptide (= anti-pOxi moAb D3 epitope) and TriisoC4 epitope-peptide (= anti-Triiso moAb C4 epitope). Because of precipitation problems with the peptides synthesized by JPT Peptide Technologies GmbH, we switched later to Intavis AG.

The verification and functionality of the synthesized epitope peptides was analyzed by competition ELISA (Figure 3.2). With this method, the binding of moAbs to their respective antigen was competed by the respective peptide. The immobilized antigen was incubated with the respective moAb and different concentrations of the

anticipated epitope-peptide. Compared to the whole, recombinant protein, the hp2160 epitope-peptide showed a strong competition effect at a concentration of 0.16 µg/ml (A). At 20 µg/ml no binding of moAb 16-2 to hp2160 could be detected anymore. A stronger competition of moAb D3 by pOxi peptide in a dose-dependent manner was analyzed (B). The whole, recombinant protein pOxi showed a competition effect that didn't seem to be concentration dependent. The synthesized TriisoC4 epitope peptide also showed a competition effect that was stronger as the competition with recombinant Triiso (C).

Five different peptides of the anticipated TriisoH8 epitope were synthesized but none of them was able to compete the binding of moAb H8 (not shown). Further analysis of the moAb H8 epitope is depicted in 3.1.2.

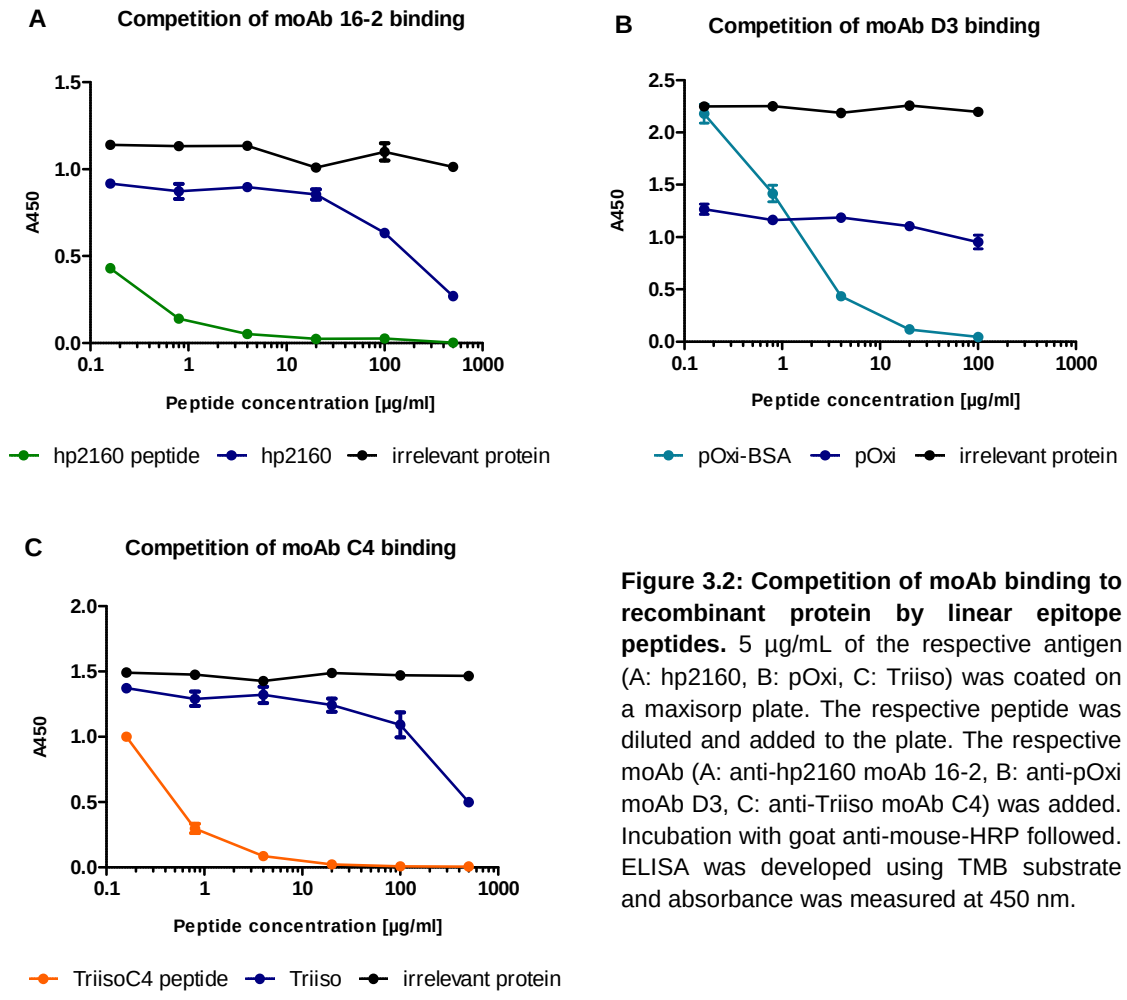

Figure 3.2: Competition of moAb binding to recombinant protein by linear epitope peptides. 5 µg/mL of the respective antigen (A: hp2160, B: pOxi, C: Triiso) was coated on a maxisorp plate. The respective peptide was diluted and added to the plate. The respective moAb (A: anti-hp2160 moAb 16-2, B: anti-pOxi moAb D3, C: anti-Triiso moAb C4) was added. Incubation with goat anti-mouse-HRP followed. ELISA was developed using TMB substrate and absorbance was measured at 450 nm.

More detailed analysis of hp2160 and pOxi epitopes followed by alanine scanning. With this systematical replacement of one amino acid by alanine, amino acids that are essential for moAb binding could be detected. 12 peptides of each epitope

sequence were synthesized (JPT GmbH, Berlin). Because these peptides were too small for coating on a maxisorp plate they were biotinylated for a binding to a streptavidin-coated 96-well plate. After incubation with anti-hp2160 moAb 16-2 and anti-mouse-HRP no binding to the hp2160 peptide without glutamic acid, which was replaced by alanine and just a weak binding without the amino acids glutamine and arginine was measured (Figure 3.3A). Binding of anti-pOxi moAb D3 to the pOxi peptide was completely inhibited, if isoleucine was replaced by alanine. A weak binding could be detected, if the second of the two arginine residues was absent (B).

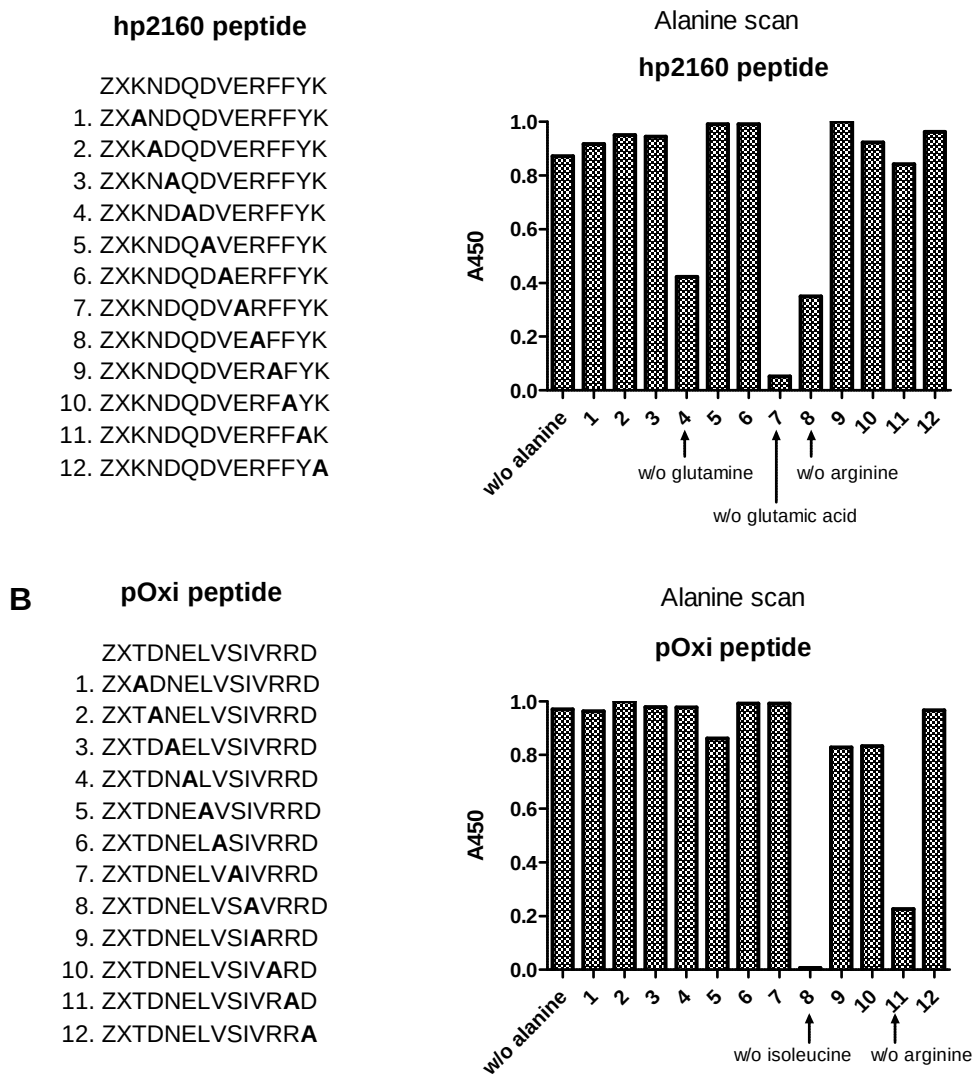

Figure 3.3: Alanine scan of epitope peptides for binding analysis of moAbs. Synthesis of 12 biotinylated peptides by JPT GmbH, where consecutively one amino acid is replaced by alanine. Maxisorp plates with immobilized streptavidin were used for ELISA. Plates were incubated first with the peptides for immobilization, then with the respective moAb and finally with goat anti-mouse-HRP. A: linear hp2160 peptide, anti-hp2160 moAb 16-2 as 1st antibody; B: linear pOxi peptide, anti-pOxi moAb D3 as 1st antibody.

The fact that no or just a weak binding was detected in absence of the mentioned amino acids indicate that these amino acids are essential for the binding of the respective antibody to its epitope peptide.

3.1.2 Analysis of discontinuous epitope of anti-Triiso moAb H8

An analysis of the synthesized peptides (shown in green in figure 3.5) of the potential H8 epitope by competition ELISA showed that none of them were able to react with moAb H8 as mentioned in 3.1.1. Neither a single nor peptide combinations were detected by moAb H8. Several signals detected by microarray analysis indicated a conformational or discontinuous epitope. For an identification of this kind of epitope a different strategy several cloning procedures of different fragments of the Triiso molecule and following binding analysis with anti-Triiso moAb H8 was pursued. After cloning (fusion to Strep-tag) and overexpression in *E. coli* BL21, bacteria cells were harvested and lysed. Equal amounts were blotted on nitrocellulose for the analysis of moAb binding. In figure 3.4 binding analysis of moAb H8 to produced fragments of Triiso is exemplary shown. After the lysis of *E. coli* cells expressing fragments 3, 4 and 5, respectively, preparations of inclusion bodies (IP) and cytoplasmic fractions (CF) were blotted. A binding of moAb H8 to fragment 5 but not to fragment 3 and 4 was detected (A). The expression of the peptides was controlled by detection with Strep-Tactin-HRP. Figure 3.5B showed an expression of all peptides that were found in the cytoplasm, as well as in inclusion bodies. Fragment 14 was the shortest analyzed Triiso fragment that was bound by moAb H8 (C).

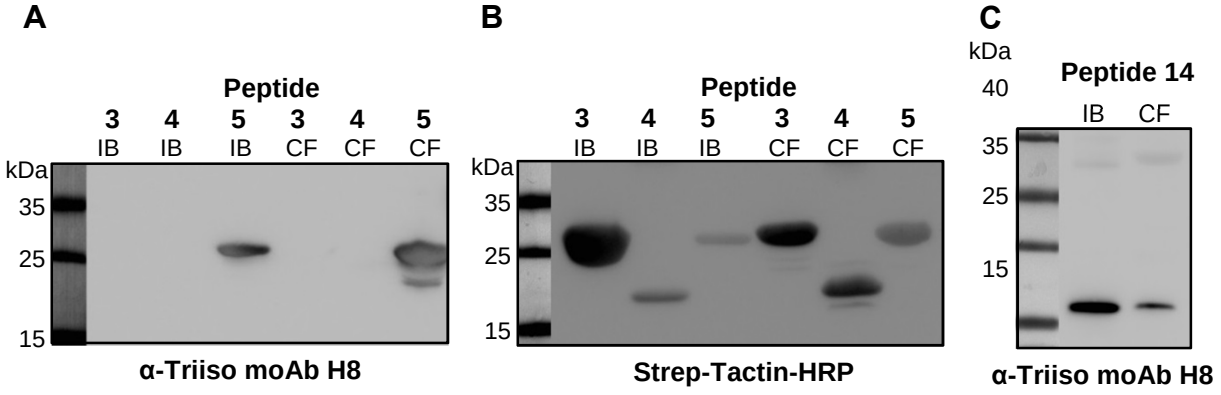

Figure 3.4: Western blot analysis of anti-Triiso moAb H8 binding to Triiso fragments. Different sections of the Triiso molecule were cloned (fused with Strep-tag) and overexpressed in *E. coli* BL21. Lysates were blotted and analyzed for antibody binding. A + B: Peptides 3, 4 and 5; C: Peptide 14. A + C: anti-Triiso moAb H8 as 1st antibody, goat anti-mouse-HRP as 2nd antibody; B: Strep-Tactin-HRP conjugate. IB: Preparation of inclusion bodies. CF: Cytoplasmic fraction.

Figure 3.5 shows a schematic overview about all binding analyses of the cloned Triiso fragments. The first analysis of fragment 1 and 2 showed that parts of both fragments are essential for binding of moAb H8. The following constructed fragments 3 to 5 showed an involvement of the C-terminus. Fragment 6 with a shorter C-terminus as fragment 5 is still able to react with the moAb, identifying the C-terminal part of the moAb H8 epitope.

Fragment 7 with a shorter N-terminus and fragment 8 with a shorter C-terminus were still detected by moAb H8. Fragment 9 was cloned with both, a shorter N- and C-terminus. In the following fragment clonings the C-terminus was left in its length to prevent problems in expression because of the small sizes of the protein fragments. With peptide 10 to 16 the N-terminus was shortened until no binding was detected anymore (see peptide 15 and 16).

With these final fragment clonings it was possible to localize the epitope of moAb H8 within an 11 kDa molecule.

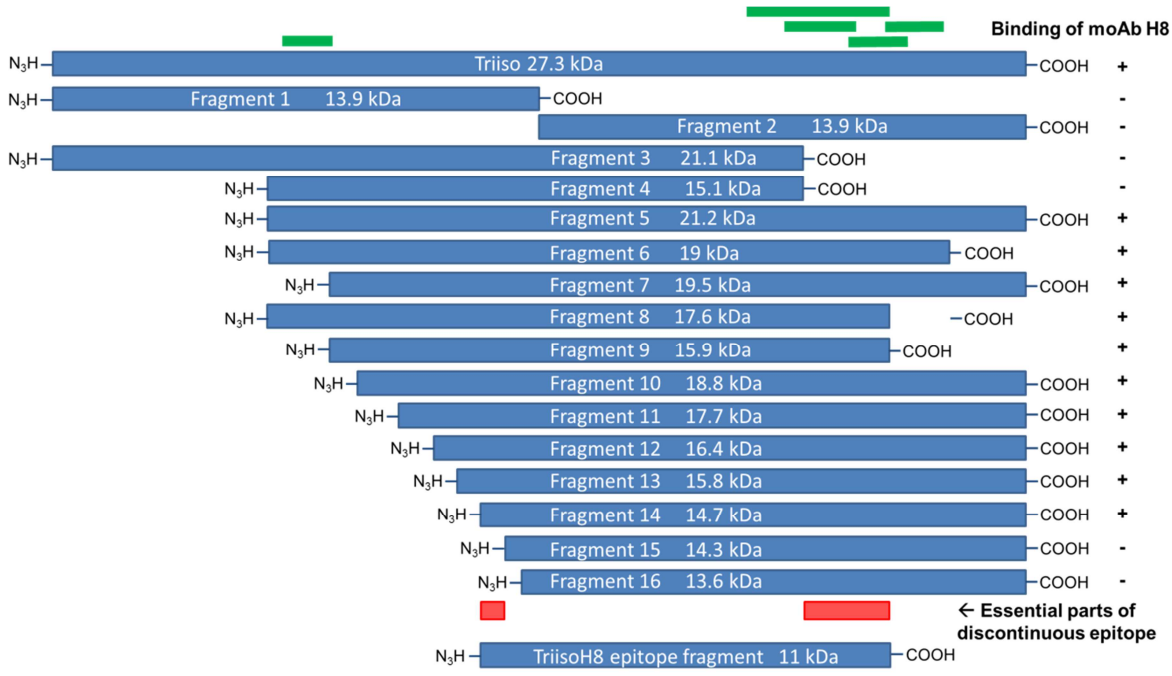

Figure 3.5: Schematic overview of Triiso fragment cloning for binding analysis of anti-Triiso moAb H8. Synthesized small peptides (green) based on microarray analysis did not show any competitive effect in competition ELISA. Fragments of different Triiso sections (blue) were cloned and overexpressed in *E.coli* BL21. Bacteria cells were harvested and lysed for binding of moAb H8 by Western blot. The essential parts for moAb binding were marked in red.

Because of the binding of moAb H8 to the different fragments in Western blot, it is certain that the moAb's binding did not depend on the conformation of the epitope within the Triiso molecule. It was confirmed that two different parts of the antigen are necessary for the binding of moAb H8 which indicates a discontinuous epitope of anti-Triiso moAb H8. A further identification of the discontinuous epitope of moAb H8 in the resulting Triiso fragment will follow by CLIPS technology of Pepscan B.V., Netherlands (Timmerman et al., 2007).

3.1.3 Binding analysis of moAb to the recombinant proteins

The genes encoding the three vaccine candidates hp2160, Triiso and pOxi identified by Glowalla *et al.* (2009) were cloned in our group and fused with a C-terminal His-tag. After an overexpression in *E. coli* the purified proteins hp2160 and Triiso led to a high amount between 20-30 mg. The overexpression of pOxi led to a red colored *E. coli* culture because of an accumulation of protoporphyrin IX. The protein pOxi is a part of the heme pathway and converts protoporphyrinogen IX to protoporphyrin IX. In contrast to the other two candidates the purification of pOxi led to a lower amount of approximately 5-8 mg. The monoclonal antibodies generated by our group were selected by their binding affinity to the respective recombinant protein. Figure 3.6 shows the detection of the overexpressed and purified proteins hp2160 (A), Triiso (B) and pOxi (C) by their respective moAb.

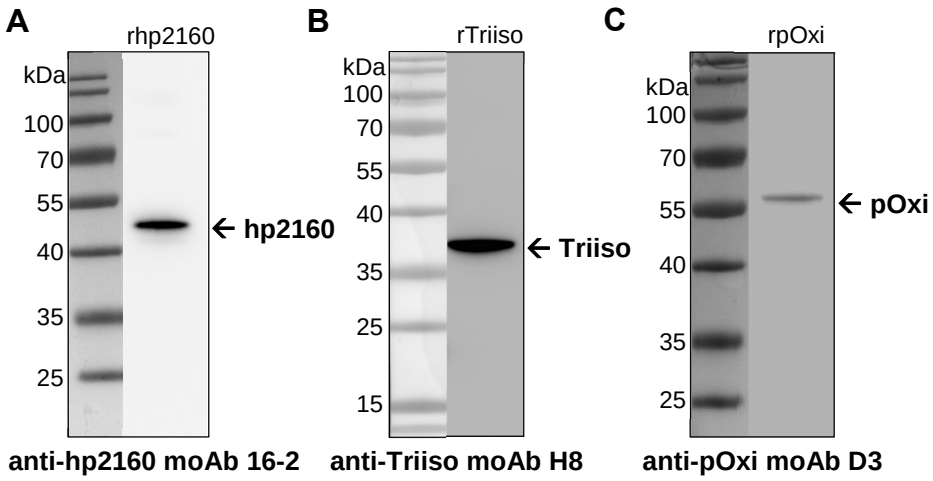

Figure 3.6: Specific binding of monoclonal antibodies to the respective recombinant protein. A-C: The gene encoding the respective *S. aureus* protein was cloned and overexpressed in *E. coli* BL21. Proteins were purified by its C-terminal His-tag. 1 µg of each protein was blotted on a nitrocellulose membrane. The membrane was first incubated with the respective moAb. A chemiluminescent detection followed after incubation with anti-mouse-HRP conjugate.

3.1.4 Binding analysis of moAbs after planktonic growth of *S. aureus*

Even though binding to the recombinant protein was proven, an analysis of the moAb binding to the native protein from *S. aureus* has to be analyzed. Therefore, the cell wall-associated protein fraction was isolated because these three proteins of cytoplasmic origin were also identified as non-covalently bound surface proteins by 2D-gel electrophoresis and MALDI-TOF analysis (Glowalla *et al*., 2009). As an additional detection method of the *S. aureus* proteins a whole cell lysate of *S. aureus* was prepared. Furthermore, binding of moAbs to the surface of whole *S. aureus* cells was analyzed under various conditions using flow cytometry.

3.1.4.1 Binding to isolated surface protein fractions and cell lysate of S. aureus

For an isolation of the non-covalently bound surface protein fraction *S. aureus* was grown in LB medium at 37 °C and 220 rpm (planktonic growth). A similar molecular weight of the protein pOxi and protein A (binds IgGs with a high affinity by their Fc region) makes it difficult to differ between these two proteins. Thus, the two *S. aureus* strains JE2 (wildtype) and a protein A deletion mutant (Δ*spA*) were used. Both strains were obtained from Network on Antimicrobial Resistance in *Staphylococcus aureus* (NARSA) data bank. Strain JE2 is an USA300 derivative and Δ*spA* was derived from JE2 by transposon mutagenesis (Fey *et al*., 2013).

The cultures were harvested at an OD_{600} of 0.6-0.8. The protein fraction was isolated by a non-enzymatic cell wall preparation containing LiCl as already described by Glowalla *et al*., 2009 and therefore used for the identification of these proteins as potential vaccine candidates. With this kind of method the anchorless surface protein fraction can be isolated without damaging the whole cell. After TCA precipitation of the isolated fraction the protein concentration of the non-enzymatic cell wall supernatant (neCWS) was measured and approximately 30 µg was blotted.

Hp2160 (35.5 kDa), as well as Triiso (27 kDa) was detected with the respective moAb in the neCWS of *S. aureus* JE2 and Δ*spA* (Figure 3.7A, B). The weak band above 55 kDa in the wildtype preparation is supposedly protein A.

It was not possible to detect the 52 kDa protein pOxi with anti-pOxi moAb D3 in the separated cell wall supernatant. In the wildtype preparation a double band between 55 and 70 kDa was detected (C). One of the bands was protein A. As an antibody of the subclass IgG2a moAb D3 has a higher affinity to bind protein A as moAb 16-2

and H8 that are both IgG1 antibodies. The second of the double band was possibly pOxi but could not be detected in the preparation of Δ*spA*.

Because the three *S. aureus* proteins usually occur in the cytoplasm cell lysates were prepared for the detection by the respective moAb. The two *S. aureus* strains and additionally pOxi and hp2160 deletion mutants obtained from NARSA were incubated with lysostaphin, followed by mechanical disruption (D-F). A deletion mutant of Triiso is not available. The four lysates were blotted and incubated with moAb 16-2 (D), moAb D3 (E) and anti-Protein A antibody (F). In figure 3.7D hp2160 was not detected anymore in the lysate of Δ*hp2160* in contrast to the remaining strains. The binding of moAb 16-2 (IgG1) to protein A was very weak. In 7E a band above 55 kDa has been detected by moAb D3 (IgG2a) in Δ*pOxi*, but not in Δ*spA*. Compared to 7F this blot looks very similar which suggests a binding of moAb D3 to protein A. Unexpectedly, the protein pOxi was not detected in the whole cell lysate of *S. aureus*.

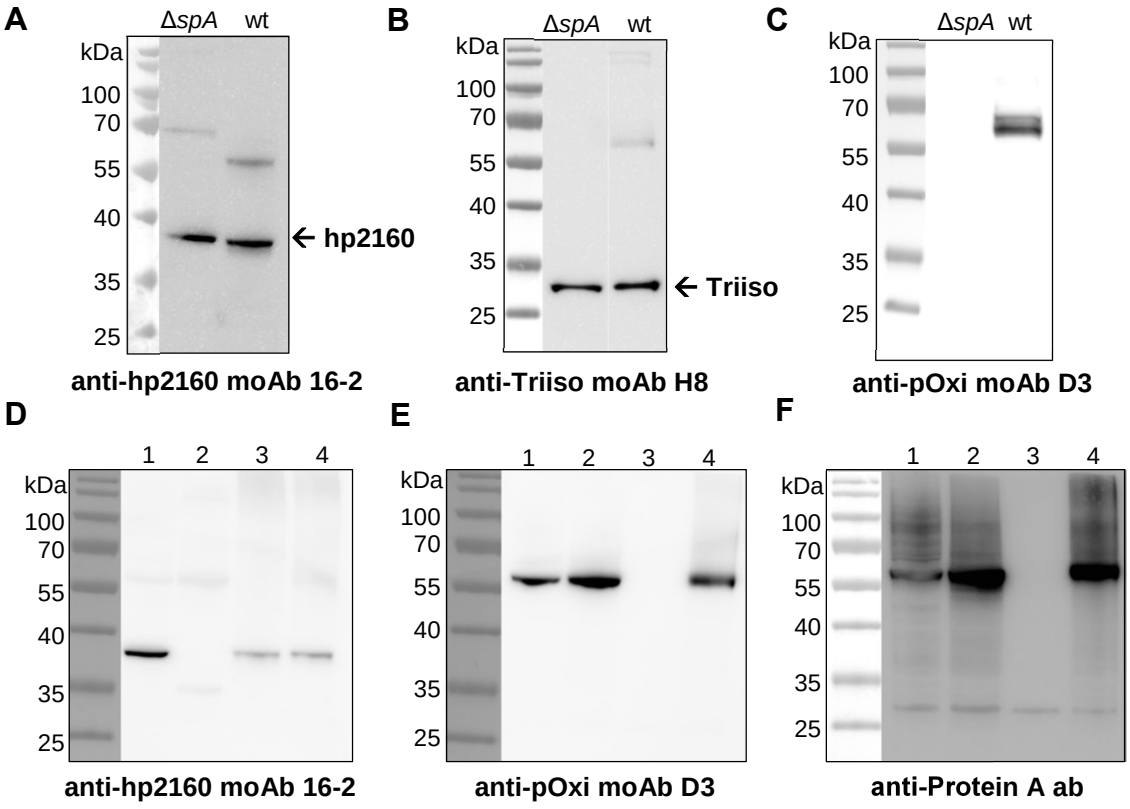

Figure 3.7: Specific binding of monoclonal antibodies to the isolated cell wall-associated protein fraction and to whole cell lysates of *S. aureus*. A-C: Cell wall-associated protein fraction was isolated from *S. aureus* JE2 (wt) and a protein A deletion mutant (Δ*spA*) by a LiCl method und was precipitated with 10 % TCA. 30 µg of non-enzymatic cell wall supernatant (neCWS) was blotted on a nitrocellulose membrane. NeCWS was incubated with anti-hp2160 moAb 16-2 (A), anti-Triiso moAb H8 (B) and anti-pOxi moAb D3 (C), respectively. D-F: Whole cell lysates (WCL) of wt and mutants were prepared by lysostaphin incubation and mechanical disruption. 30 µg of WCLs were blotted and incubated with anti-hp2160 moAb 16-2 (D), anti-pOxi moAb D3 (E) and anti-Protein A antibody (F). A chemiluminescent detection followed after incubation with anti-mouse-HRP conjugate.

3.1.4.2 Specific binding of anti-pOxi moAb D3 to the S. aureus surface

The detection of the proteins on the surface of whole *S. aureus* cells was measured by flow cytometry. *S. aureus* was grown under planktonic conditions to an OD_{600} of 0.3 (exponential growth phase). Cells were harvested and washed in PBS + 1 % BSA. To prevent an unspecific binding of antibodies to protein A the wildtype strain JE2 was blocked with a human Fc fragment. An incubation with the respective moAb and then with an anti-mouse $F(ab)_2$ fragment conjugated to phycoerythrin (PE) followed. As a negative control just the PE-conjugate was used (Figure 3.8, black line). As shown in figure 3.8A binding of anti-pOxi moAb D3 (red line) to the surface of *S. aureus* JE2 was detected. A weak competition was detectable with the pOxi epitope peptide (blue line), but not with an irrelevant peptide (here the hp2160 epitope peptide (green line)). A comparison to figure 3.8B, where *S. aureus* Δ*spA* was used, demonstrated a strong unspecific binding of moAb D3 to protein A at the surface of the wildtype, although it was incubated with the human Fc fragment for blocking this interaction. Therefore, Δ*spA* was used for the consecutive measurements. In this case the binding signal was not as strong as with the wildtype surface, but the competition with the pOxi epitope peptide resulted in a complete abolishment of the binding signal which proves again the specific binding of moAb D3 to pOxi on the bacterial surface. With the hp2160 peptide no competition of the anti-pOxi binding of moAb D3 was detectable.

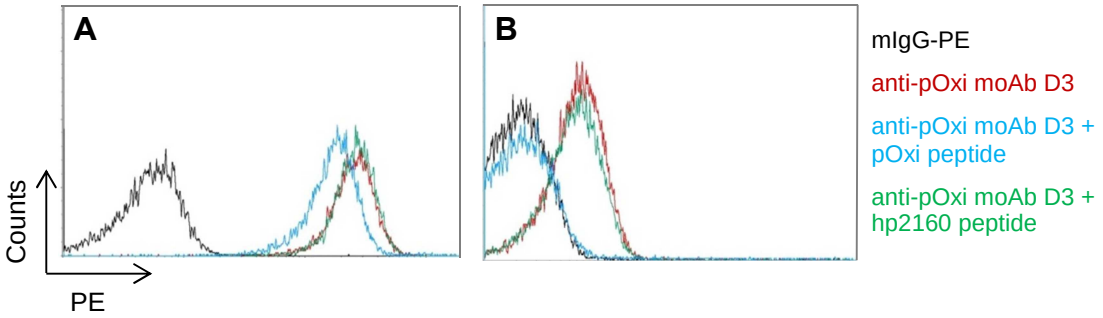

Figure 3.8: Specific binding of anti-pOxi moAb D3 to the surface of *S. aureus*. *S. aureus* Δ*spA* was grown to an OD_{600} of 0.3. Harvested and washed cells were incubated with 50 µg of anti-pOxi moAb D3 (red line), 50 µg moAb D3 + 100 µg pOxi epitope peptide as competitor (blue line), 50 µg moAb D3 + 100 µg hp2160 epitope peptide (green line) or with just an equal volume of PBS (black line) in PBS + 1 % BSA. All samples were then incubated with $F(ab)_2$ anti-mouse-IgG-PE-Cy5.5. A: *S. aureus* JE2 (wildtype), B: *S. aureus* JE2-Δ*spA*. Samples were measured by flow cytometry.

Although anti-Triiso moAb H8 showed a strong binding to wildtype, no binding to the surface of Δ*spA* was detected (data not shown). With anti-hp2160 moAb 16-2 only a weak binding to the wildtype was detected. As an IgG1 antibody moAb 16-2 has the

same subclass as moAb H8 but showed a different binding affinity to protein A. Binding to the surface of Δ*spA* was also negative.

S. aureus was harvested at different growth phases to test if it has an influence on the expression of pOxi, Triiso or hp2160 or on the epitope accessibility. The ODs 0.1, 0.3, 0.6, 1.0, 2.0, 3.0 and 6.0 were tested. The ODs 0.1, 0.3 and 3.0 were presented in figure 3.9. A binding of moAb D3 to the *S. aureus* surface (A) was measured in all growth phases but the strongest signal was detected at 0.3. Neither moAb 16-2 (B) nor moAb H8 (C) showed a binding signal at all tested growth phases.

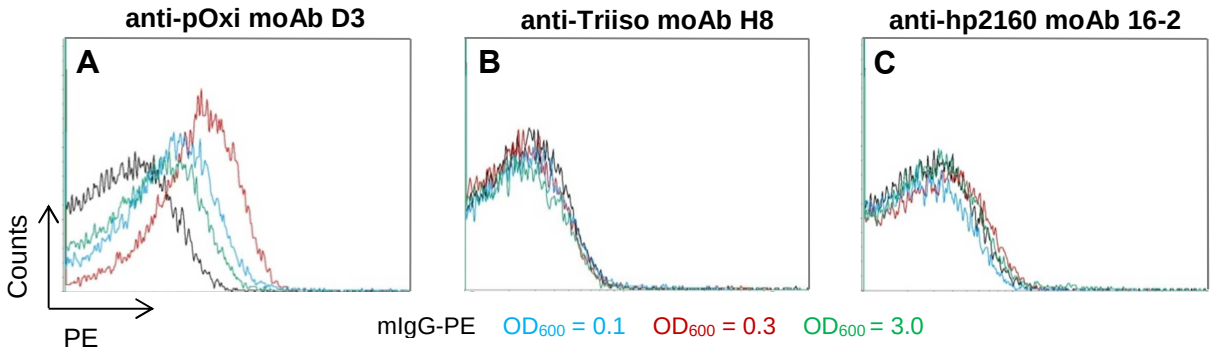

Figure 3.9: Binding analysis of moAbs to the surface of *S. aureus* harvested at different growth phases. *S. aureus* Δ*spA* was grown to the OD_{600}s 0.1 (blue line), 0.3 (red line) and 3.0 (green line). Harvested and washed cells were first incubated with 50 µg of anti-pOxi moAb D3 (A), anti-Triiso moAb H8 (B) and anti-hp2160 moAb 16-2 (C) and then with 2 µg of $F(ab)_2$ anti-mouse-IgG-PE-Cy5.5. Samples were measured by flow cytometry.

Although it was possible to extract Triiso and hp2160 from the surface a binding of moAbs H8 and 16-2 to the surface of whole *S. aureus* cells was not measured by FACS. Hereupon some other generated moAbs against Triiso were analyzed for surface binding and a comparison to the non-reactive moAb H8. In figure 3.10 binding of anti-Triiso moAbs C4 (see 3.1.2) and C8 were exemplarily shown. While the binding signal of moAb H8 (red line) was again negative, moAb C4 (IgG1, blue line), as well as C8 (IgG2b, green line) indicated a weak binding to the bacterial surface. This indicates an occurrence of Triiso on the bacterial cell surface but the epitope of moAb H8 is not accessible at these growth conditions.

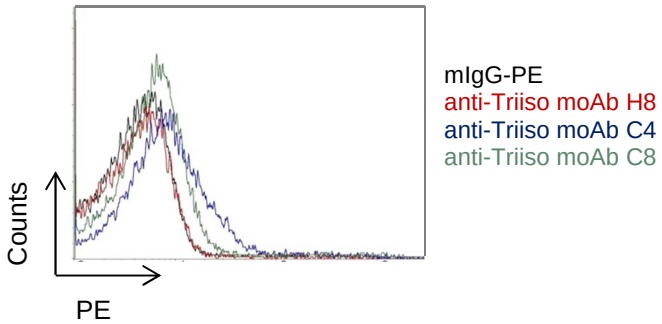

Figure 3.10: Binding analysis of anti-Triiso moAbs H8, C4 and C8 to the surface of *S. aureus*. *S. aureus* Δ*spA* was grown to an OD_{600} of 0.3. Harvested and washed cells were first incubated with 50 µg of moAb H8 (red line), 50 µg moAb C4 (blue line) or moAb C8 (green line) and then with 2 µg of $F(ab)_2$ anti-mouse-IgG-PE-Cy5.5. Samples were measured by flow cytometry.

For their influence on antigen expression or presence on the bacterial cell surface different growth media were also tested, such as TSB and the cell-culture medium RPMI which is iron-deficient and human serum as culture medium to simulate *in vivo* conditions. Because blood is a natural environment of *S. aureus* it was possible that the proteins Triiso and hp2160 as potential virulence factors were different expressed. The growth media TSB and RPMI did not influence the moAb binding on the surface (not shown). After growth of Δ*spA* in serum a strong binding of moAb 16-2 was detected compared to the negative control and other anti-*S. aureus* moAbs. However, no competition effect with the hp2160 peptide could be shown, indicating an unspecific binding event (not shown).

3.1.5 Influence of biofilm conditions and low pH on surface proteins

Foulston *et al*. (2014) describes that cytoplasmic proteins are present in the extracellular matrix of *S. aureus* biofilms and that the cell wall association is pH-dependent. Therefore, the occurrence of the proteins under biofilm conditions was analyzed. Finally, binding analysis of moAbs H8 and 16-2 to whole *S. aureus* cells after biofilm growth have been tested.

3.1.5.1 Quantitative determination of biofilm viability

First the ability to form biofilms of the different strains MW2, USA300, ATCC29213, Δ*spA* and Δ*agr* and of three clinical isolates (K180, K183 and K209) that are available in our institute was analyzed. To initiate biofilm formation *S. aureus* was grown in 96-well cell culture plates containing TSB medium and 0.5 % Glucose. The culture was incubated at 37 °C for 24 h without shaking (Figure 3.11A). The TSB medium was carefully removed after biofilm growth and a pH of 5 was measured.
Bacterial cells were fixed and stained with crystal violet. After washing the cells bound crystal violet was extracted and quantified at an absorbance of 590 nm. A similar biofilm formation was detected with the common strains of our lab. The lowest biofilm formation was detected with the clinical isolate K209 (B).

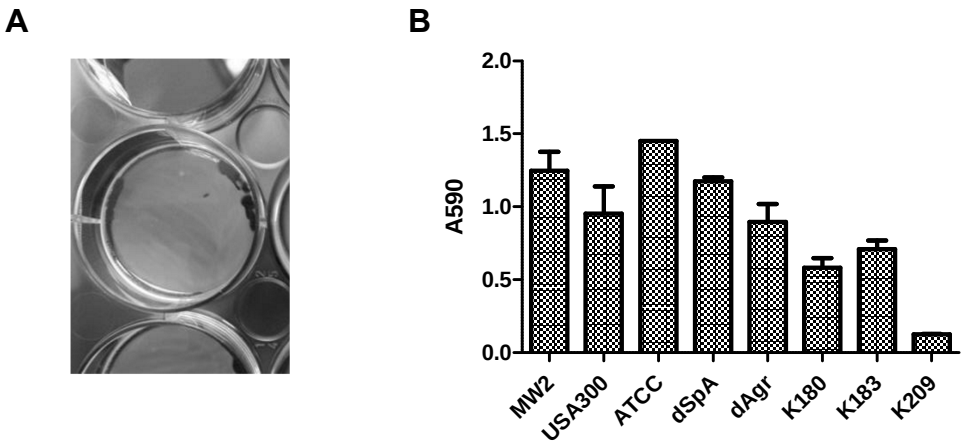

Figure 3.11: Biofilm formation by different *S. aureus* strains. *S. aureus* JE2 was grown under biofilm conditions in TSB + 0.5 % Glucose for 24 h (A). Biofilm growth was quantified by staining with 0.2 % crystal violet (B). Plates were washed 10 x after the staining and bound crystal violet was extracted with 10 % acetic acid / 40 % ethanol. The absorbance of a 1:10 dilution was measured at 590 nm. Error bars indicate mean value of triplicates ± SEM.

3.1.5.2 Biofilm growth of S. aureus influences the occurrence of Triiso and pOxi on the bacterial surface

To investigate, if the pH has an influence on the retention of the proteins on the bacterial surface, strain JE2 was grown under biofilm conditions. The detached and resuspended culture was divided into two samples and the harvested cell pellets were incubated in PBS with pH values of 5 and 7.5, respectively for one hour. After centrifugation the supernatants were collected and precipitated with TCA. Equal volumes of both resuspended precipitates were blotted on nitrocellulose.

Although both samples were treated equally, as expected a higher amount of Triiso was detected in the sample washed at neutral pH (Figure 3.12A).

With the biofilm conditions it was possible to identify pOxi with a size of 52 kDa (B). Compared to the experiments after planktonic growth described in 3.1.4.1, where neCWS was prepared (see figure 3.7C), pOxi could be detected with anti-pOxi moAb D3 in such a cell surface protein fraction for the first time. However, no differences in the two samples treated with the two different pH values were observed.

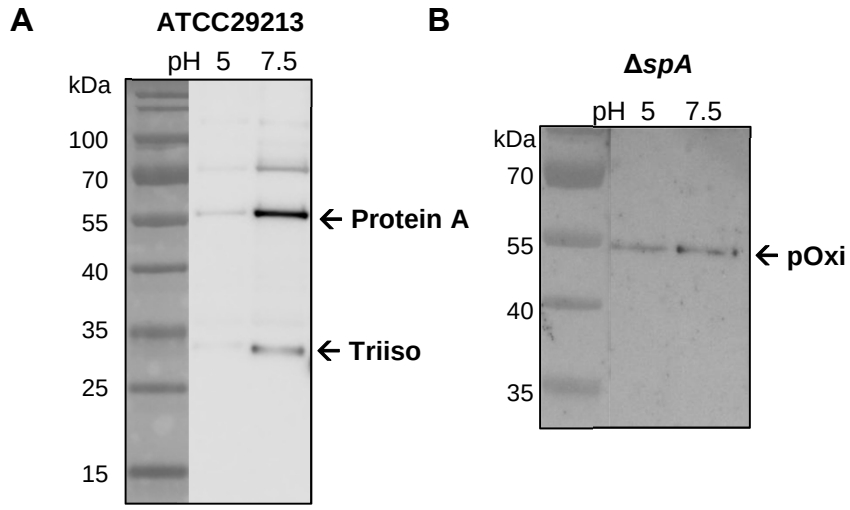

Figure 3.12: Comparison of Triiso's occurrence in the isolated cell wall-associated protein fraction at low and neutral pH after biofilm growth of *S. aureus.* *S. aureus* was grown under biofilm conditions in TSB + 0.5 % Glucose for 24 h. The harvested cell pellet was resuspended in PBS of a pH of 5 and 7.5, respectively for 1 h. After centrifugation the supernatants were collected and precipitated with 10 % TCA. The precipitates were washed and dissolved in 8 M Urea. 30 µl of each sample was blotted on nitrocellulose and incubated with first the respective moAb and then anti-mouse-HRP conjugate. The blot was developed by chemiluminescence. A: *S. aureus* ATCC29213, anti-Triiso moAb H8; B: *S. aureus* Δ*spA*, anti-pOxi moAb D3.

In summary, biofilm conditions have an influence on the occurrence of the cell wall-associated proteins Triiso and pOxi. At low pH conditions that are present in the medium after biofilm growth, a higher amount of Triiso remains on the *S. aureus* surface, compared to the conditions at neutral pH.

In contrast, changes in the pH have no influence on the occurrence of pOxi, whereas biofilm conditions are required for its detection by Western blot.

3.1.5.3 Binding of moAbs H8 and 16-2 to the S. aureus surface after biofilm growth

It was not possible to detect a binding of anti-Triiso moAb H8 and anti-hp2160 moAb 16-2 to the surface of whole *S. aureus* cells after planktonic growth. For further binding analyses of moAbs H8 and 16-2 by flow cytometry, strain Δ*spA* was grown for 40 h under biofilm conditions. Additionally, binding of anti-pOxi moAb D3 and anti-Triiso moAb C4 were also analyzed after biofilm growth, although these moAbs already showed a surface binding after planktonic growth (compare figures 3.8, 3.10). The detached biofilm cells were harvested and washed at a pH of 5.0 for a few times. The cell pellet was then fixed with 3 % paraformaldehyde and then incubated with the respective moAb and the PE-conjugated secondary antibody.

Compared to negative control (black line) a strong binding was detected with anti-Triiso moAb H8 (red line in figure 3.13A), as well as with anti-hp2160 moAb 16-2 (red line in B). Because the moAb H8 epitope peptide was not characterized yet, a competition experiment of moAb H8 binding was excluded. To prove a specific binding of the moAbs a monoclonal antibody against 6 x histidine produced in mouse was used as a negative control (green line). The signal was as negative as the sample with just the secondary antibody, which demonstrates the specific binding of moAbs H8 and 16-2 to the *S. aureus* cell surface grown under biofilm conditions.

A binding of anti-Triiso moAb C4 (orange line) and anti-pOxi moAb D3 (blue line) to the *S. aureus* surface was presented in figures C-D. To prove a specific binding to biofilm grown *S. aureus* a competition with the available pOxi and TriisoC4 epitope peptides (green lines) was done. The respective antibody was preincubated with the epitope peptide and then added to the bacterial cells. In comparison to the bacteria where just the moAb was added the fluorescent signal was decreased.

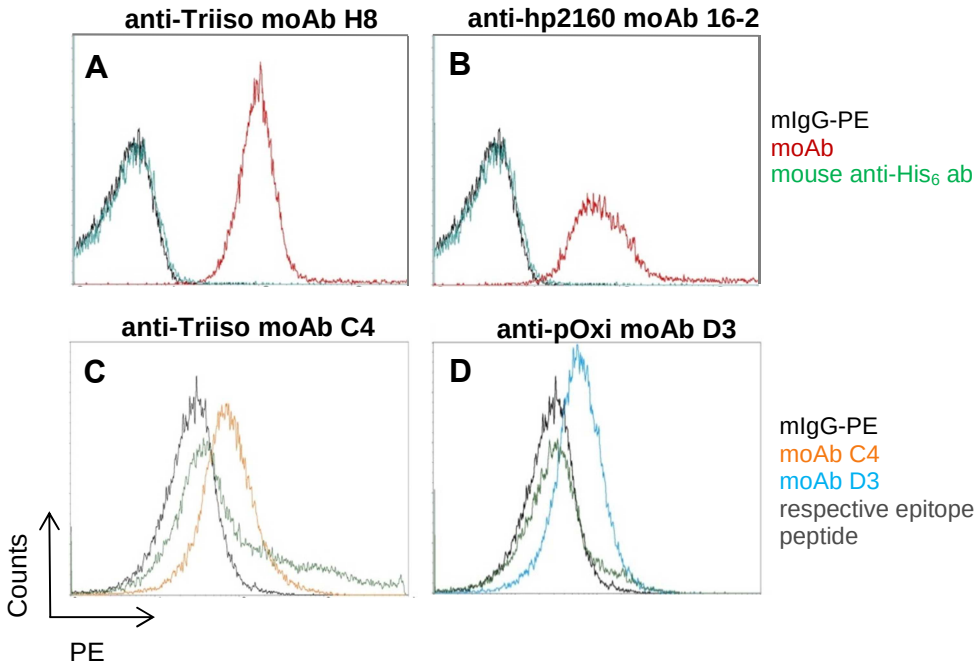

Figure 3.13: Specific binding of moAbs to the surface of *S. aureus* Δ*spA* after biofilm growth. *S. aureus* Δ*spA* was grown for 24 h under biofilm conditions. A-B: Detached and washed cells (pH 5.0) were fixed and incubated with the respective anti-*S. aureus* moAb (red line), mouse anti-His-tag moAb (green line) or the same volume of PBS (black line) for 30 min at 37 °C. C-D: Cells were incubated with anti-Triiso moAb C4 (orange line) or anti-pOxi-moAb D3 (blue line). For a competition of moAb binding they were incubated by the respective epitope peptide (green line). An incubation with 2 µg of $F(ab)_2$ anti-mouse-IgG-PE-Cy5.5 followed. Samples were measured by flow cytometry.

3.1.6 Antigen function on surface and mode of action of monoclonal antibodies

The three moAbs D3 (pOxi), H8 (Triiso) and 16-2 (hp2160) were selected because of their protective function in the murine sepsis models after passive immunization.
The binding of the three moAbs have been detected on the *S. aureus* surface, so a further *in vitro* characterization of the potential antigen function and the influence of the moAbs towards these functions was started. This included an analysis, if moAbs trigger opsonophagocytosis by phagocytic cells isolated from eukaryotes. Additionally, an investigation of the moonlighting function of the respective antigen as a kind of virulence factor and a possible inhibition by its moAb was performed.

3.1.6.1 MoAbs do not promote opsonophagocytosis by human neutrophils

The three humanized moAb candidates (humAbs) were first analyzed regarding their potential to induce an opsonophagocytosis by human neutrophils.
Additionally, anti-pOxi and anti-Triiso IgGs were enriched from polyclonal human intravenous IgG preparation (IVIG) for a comparison to the monoclonal antibodies. The enrichment was executed by affinity chromatography using a NHS-column coupled with the respective recombinant proteins pOxi or Triiso. Bound IgGs from IVIG were eluted by a low pH and buffered to neutral pH. IVIG was used as a positive control because it was already proven that it contains opsonizing antibodies to *S. aureus* (Glowalla *et al*., 2009). Human PMNs were isolated from whole blood of a volunteer using a Ficoll gradient. *S. aureus* ATCC 29213-GFP (MOI 10) was incubated with the neutrophils without addition of any antibody source, as a negative control. The investigated antibodies were pre-incubated with ATCC 29213-GFP in a concentration of 100 µg/ml for opsonization. Neutrophils were analyzed by flow cytometry. A positive signal describes the fraction of cells with internalized ATCC 29213-GFP. The percentage of fluorescent particles was calculated (subtraction of negative control from the respective GFP-positive sample), as shown in the histograms of figure 3.14. IVIG preparation (A) efficiently triggered opsonophagocytosis, resulting in 54 % GFP-positive neutrophils. A similar result was detected with anti-Triiso IgGs (C) isolated from IVIG preparation (55 % GFP-positive neutrophils). With specific IgGs for pOxi (B) opsonophagocytosis was increased (66 % GFP-positive neutrophils).

Although polyclonal IgGs clearly promote phagocytosis no enhanced uptake of GFP-positive *S. aureus* in neutrophils was detected with the humanized monoclonal antibodies against hp2160, pOxi and Triiso (D-F).

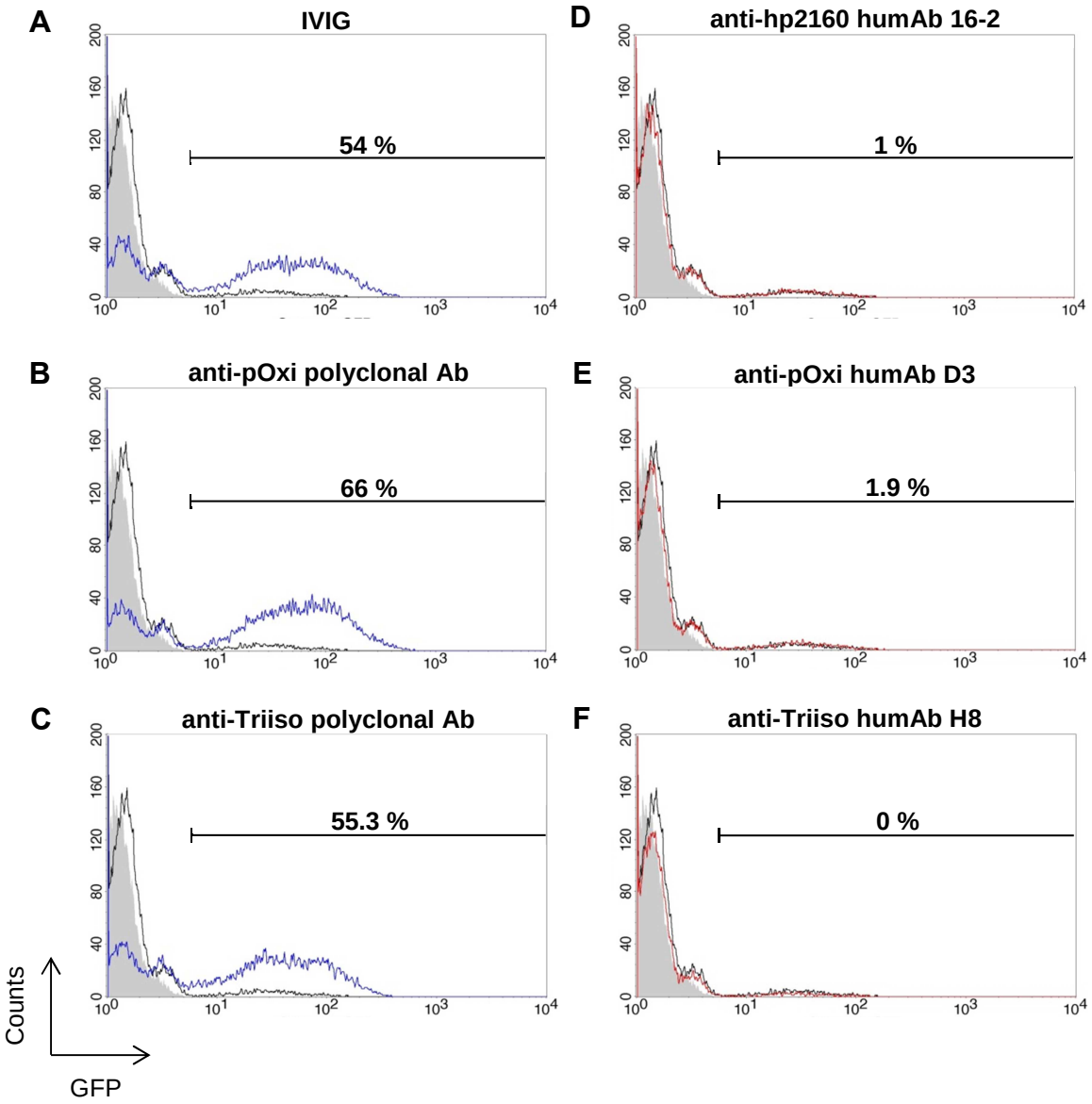

Figure 3.14: Opsonophagocytosis of *S. aureus* ATCC 29213-GFP by human neutrophils. Bacteria were grown to an OD_{600} of 0.3 and opsonized with 100 µg/ml of human intravenous immunoglobulin preparation (IVIG), polyclonal antibody enriched from IVIG (blue line), humanized monoclonal antibody (red line) or without antibody as negative control (black line) for 30 min at 37 °C. Opsonized bacteria (MOI 10) were incubated with human PMNs three times for 2 min at 37 °C. Before every incubation step they were centrifuged at 300 x *g* for 2 min. Grey filled lines represent just human PMNs. Green fluorescence was measured by flow cytometry. Given percentages of GFP-positive human PMNs (marked region) represent the fraction of cells with internalized *S. aureus.*

3.1.6.2 MoAbs do not promote opsonophagocytosis by murine BMDM's

The potential of the three moAbs to induce the opsonophagocytic activity by murine bone marrow-derived macrophages was also investigated.

Tibia and femur of BALB/c mice were prepared for the isolation of bone marrow. Monocytes were differentiated by recombinant macrophage colony-stimulating factor (mCSF). *S. aureus* ATCC 29213-GFP was opsonized for 30 min with the moAbs, respectively. ATCC-GFP (MOI 15) was then incubated with the macrophages for 90 min at 37 °C. Samples were measured every 15 min by flow cytometry.

As shown in figure 3.15 an uptake of GFP-expressing bacteria in macrophages was measured after 30 min (A). This uptake was stronger after 90 min (B). The grey filled line respresents BMDM's that were not incubated with bacteria. No differences between the negative control where non-opsonized bacteria were incubated with BMDM's and the samples opsonized with moAb D3 (blue), moAb H8 (red) or moAb 16-2 (green) were detected, which proves that the generated moAbs do not trigger the uptake of *S. aureus* by phagocytic cells.

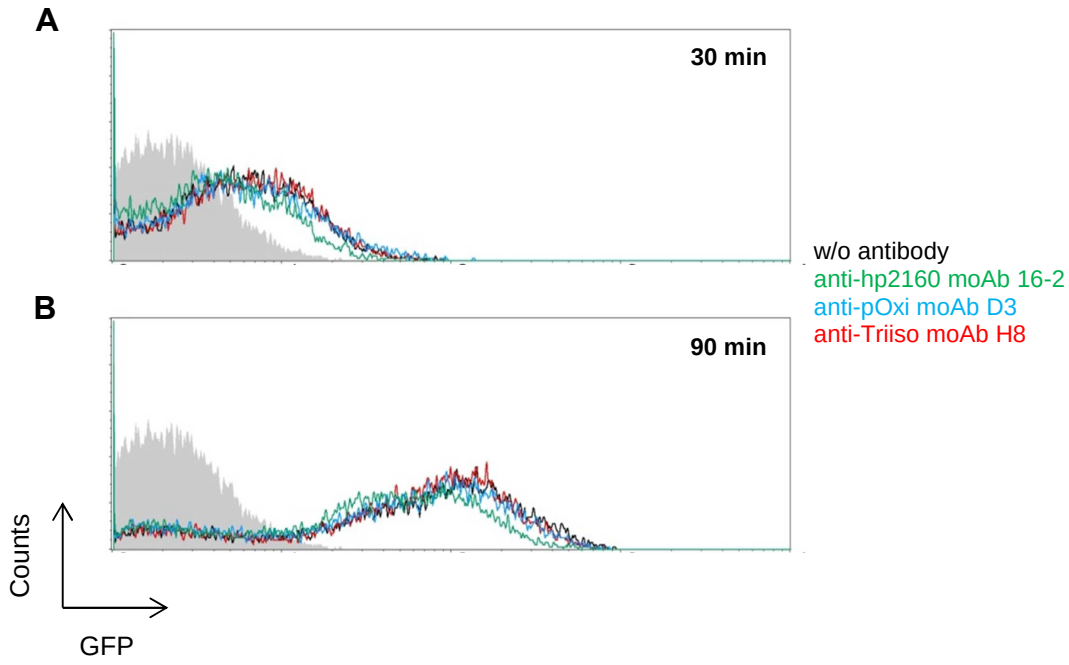

Figure 3.15: Opsonophagocytosis of *S. aureus* ATCC 29213-GFP by murine BMDM's. Bacteria were grown to an OD_{600} of 0.3 and opsonized with 100 µg/ml of a murine antibody or without an antibody as negative control (black line) for 30 min at 37 °C. Opsonized bacteria (MOI 15) were incubated with BMDM's for 30-90 min at 37 °C. Grey filled line represents BMDM's without bacteria. Green fluorescence was measured by flow cytometry. A: 30 min incubation; B: 90 min incubation. Green line: anti-hp2160 moAb16-2; red line: anti-Triiso moAb 16-2; blue line: anti-pOxi moAb D3.

3.1.6.3 Enzymatic activity of Triiso

For a further characterization, the enzymatic activity of Triiso was analyzed. Triiso catalyzes the reversible conversion of dihydroxyacetone-phosphate into glycerinaldhyde-3-phosphate as a part of the glycolysis. Although Triiso usually acts as a cytoplasmic protein, it was identified on the cell surface of *S. aureus* (Furuya *et al*., 2009; compare to 3.1.5.1). Besides Triiso, several enzymes of the glycolysis were detected on the surface, such as GAPDH and enolase. According to Henderson and Martin (2011), glycolysis might also happen on the cell surface for ATP generation. After the determination of an enzymatic activity it should be proven, if anti-Triiso moAb H8 influences Triiso's activity by a possible binding at the active site of the enzyme.

The *in vitro* activity assay was coupled to the oxidation of NADH by glycerin-3-phosphate dehydrogenase and measured as change in absorbance at 340 nm. The activity of recombinant Triiso as well as in whole cell lysate (WCL) and cell wall associated protein fraction (neCWS) of strain USA300 was measured as demonstrated in figure 3.16A. An enzymatic activity was measured in all samples, which proved enzymatically the occurrence of Triiso in WCL and neCWS.

In figure 3.16B the enzymatic activity of recombinant Triiso was analyzed after a preincubation of 30 ng Triiso with 1.25 - 40 µg of moAb H8. As shown in the graph moAb H8 was not able to inhibit the enzymatic activity of recombinant Triiso.

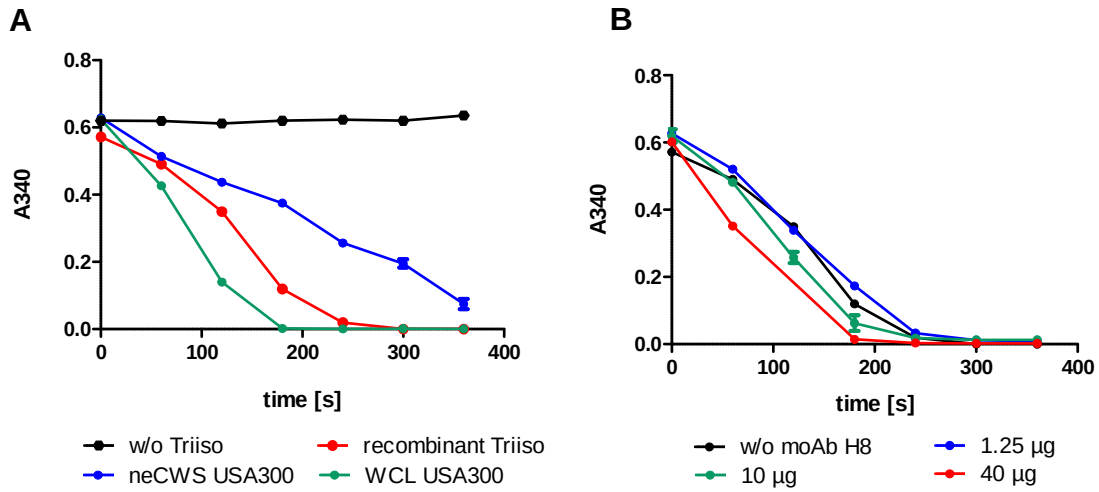

Figure 3.16: Enzymatic activity of Triiso. A: 0.9 mM glycerinaldehyde-3-phosphate, 25 µg NADH and 4 ng recombinant Triiso or 4 µg non-enzymatic cell wall supernatant (neCWS) or whole cell lysate (WCL) were incubated in a final volume of 250 µl in a 96-well-plate (duplicates). Reaction was started after adding 2.5 mg glycerin-3-phosphate dehydrogenase. B: 30 ng of recombinant Triiso was incubated with 1.25-40 µg of anti-Triiso moAb H8. Then the same reaction as described in A was started. The absorbance was measured at 340 nm.

3.1.6.4 Secretion of Triiso

For a further characterization of *S. aureus'* Triiso it was analyzed if the protein is secreted from the bacterial cell. Triiso's sequence does not contain any known signal motif, which is responsible for a secretion, such as LPXTG.

While preparing the extracts of the cell wall-associated protein fraction in 3.1.4.1 after planktonic growth, the medium supernatant was collected, sterile filtrated and precipitated over night with 10 % TCA. The resulting pellet was washed and resuspended in 8 M urea. The medium supernatant containing the secreted protein fraction (sPF) was blotted together with neCWS on a membrane, followed by an incubation with one of the moAbs. In contrast to hp2160 and pOxi (not shown), Triiso was detected as a secreted exoenzyme in the medium (Figure 3.17).

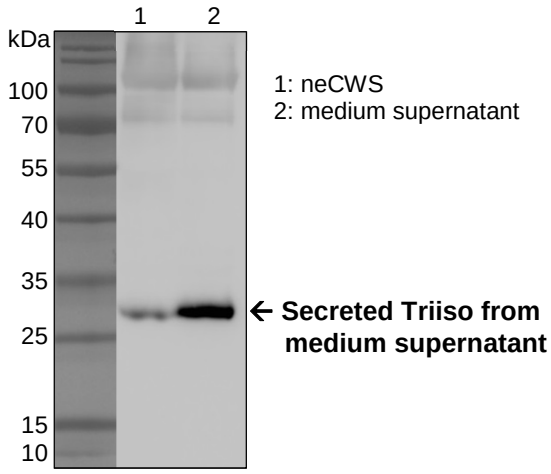

Figure 3.17: Extracellular Triiso from *S. aureus*. *S. aureus* Δ*spA* was grown to an OD_{600} of 0.6. The harvested cell pellet was resuspended and prepared with LiCl. The medium supernatant was precipitated with 10 % TCA. The precipitates were washed and dissolved in 8 M Urea. 30 µl of each sample was blotted on nitrocellulose and incubated with moAb H8 as primary and anti-mouse-HRP conjugate as secondary antibody. The blot was developed by chemiluminescence. 1: non-enzymatic cell wall supernatant; 2: Secreted protein fraction derived from medium supernatant.

3.1.6.5 Interaction between Triiso and plasminogen

According to Furuya and Ikeda (2011) Triiso from *S. aureus* is able to bind plasminogen from human blood. Plasminogen can be activated to plasmin by the staphylococcal enzyme staphylokinase (SAK), which initiates fibrinolysis. Together with the process of blood coagulation by the enzyme coagulase, the initiation of fibrinolysis is important for the proliferation of *S. aureus* in human blood and tissues. Because of its moonlighting function of plasminogen binding at the bacterial cell surface Triiso seems to interact in the process of plasminogen activation. In this case, Triiso would be a virulence factor, which possibly can be inhibited by anti-Triiso moAb H8.

The binding of plasminogen to Triiso had to be confirmed before a possible inhibition of this interaction by anti-Triiso moAb H8 was investigated. Figure 3.18 shows a Far Western blot, where 0.5 and 2 µg of recombinant Triiso were blotted. In figure 3.18B the blot was incubated with 500 nM of human plasminogen. An interaction between Triiso and plasminogen was proved, because bound plasminogen could be detected by anti-plasminogen-HRP conjugate. The blotted amount of 0.5 µg of Triiso was the lowest amount where an interaction with plasminogen was detected.
In 18A the blot was incubated with anti-Triiso moAb H8 before the same amount of plasminogen was added while the blot on the right side remained in blocking milk without antibody. Although both blots were developed together a lower signal was measured in figure 3.18A. This result was a positive hint for an inhibition of plasminogen binding by moAb H8, but a quantification and a titration with different dilutions was easier in ELISA.

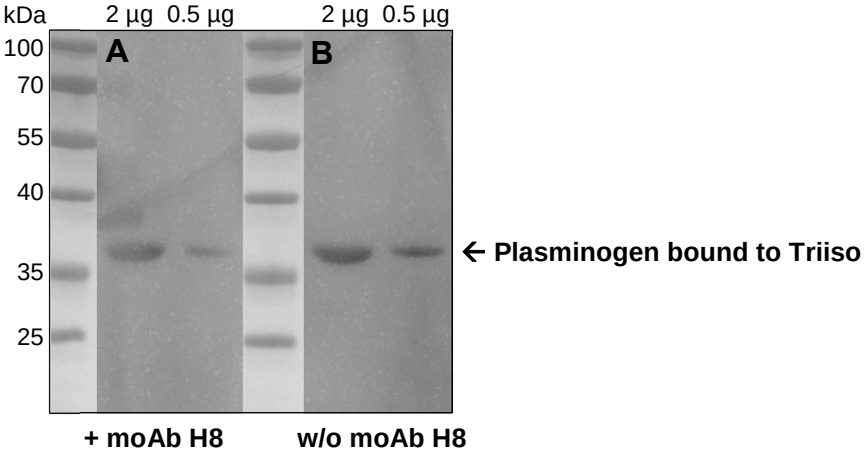

Figure 3.18: Interaction between Triiso and plasminogen in Far Western blot analysis. 2 µg and 0.5 µg of recombinant Triiso were blotted on nitrocellulose. The membrane was blocked and incubated with 500 nM of human plasminogen. A: The blot was incubated with anti-Triiso moAb H8. B: Incubation in blocking milk w/o antibody. Both blots were then incubates with human plasminogen. Detection of bound plasminogen was performed with anti-plasminogen-HRP. For a comparison both blots were developed together under exactly same conditions.

For an analysis of an interaction between plasminogen and Triiso by ELISA plasminogen was immobilized in different concentrations between 0 and 10 µ/ml to a maxisorp 96-well plate. The plate was incubated with different dilutions of Triiso to titrate the best conditions for the plasminogen interaction. A detection followed by anti-His-tag-HRP conjugate that binds to recombinant His-tagged Triiso. As shown in figure 3.19A, binding of Triiso to coated plasminogen was weak but increased in a

dose-dependent manner with rising the Triiso concentration. The binding signal was not dependent on the plasminogen concentrations used. The different concentrations of Triiso did not show any binding signals without plasminogen.

In a further experiment a concentration of 5 µg/ml plasminogen for coating and a concentration of 150 µg/ml Triiso was used for the incubation. Before Triiso was added the coated plasminogen was preincubated with different dilutions of moAb H8 (0 and 150 µg/ml). As shown in figure 3.19B, a decrease in absorbance in presence of moAb H8 was not detected.

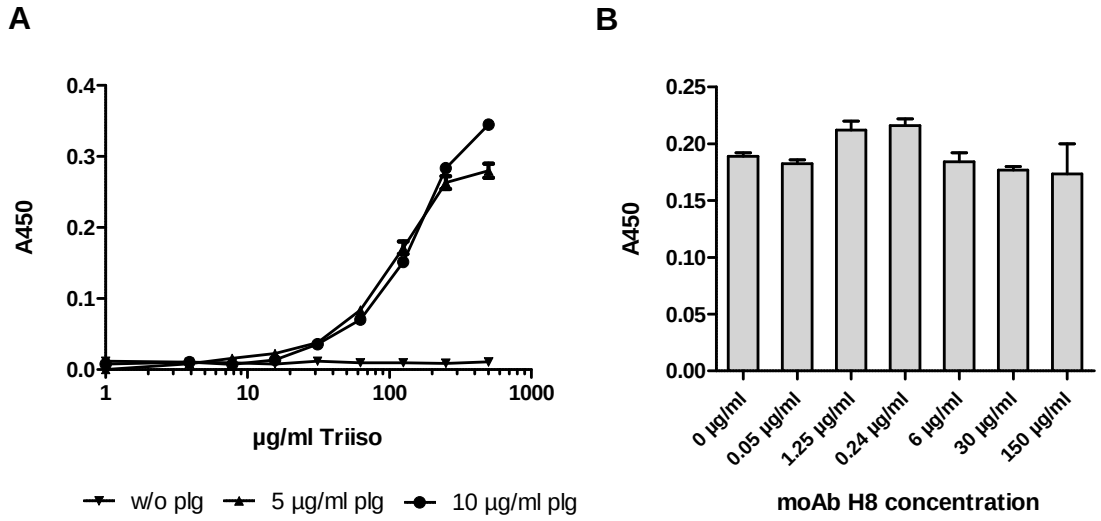

Figure 3.19: Interaction between Triiso and Plasminogen in ELISA. A: 0, 5 or 10 µg/ml of human plasminogen was immobilized to a maxisorp plate. After blocking, the plate was incubated with different concentrations of recombinant Triiso. For a detection of bound Triiso anti-His-tag-HRP was used. B: The same protocol as in A in the presence of anti-Triiso moAb H8. A Triiso concentration of 150 µg/ml was used. Before Triiso was added to the plate it was supplemented with different concentrations of moAb H8 for 30 °C at room temperature.

The experiment presented in figure 3.19B showed a binding of Triiso to human plasminogen but no inhibition of this binding with moAb H8 was detected. Therefore, moAb H8 does not seem to interfere with the plasminogen binding site. If the activation of plasminogen was nevertheless impaired needs to be further examined. Furuya and Ikeda (2011) already showed an inhibition of the plasminogen activation in presence of Triiso from *S. aureus*.

To investigate the effects of recombinant Triiso on the activation of plasminogen, an enzymatic activity assay was performed according to Furuya and Ikeda (2011) with modifications. Plasminogen was activated by SAK into plasmin that hydrolyses the substrate S-2251. This could be measured as a change in absorbance at 405 nm. An

increase in absorbance indicated plasmin activity. In figure 3.20A the amount of SAK that is necessary for an activation of plasminogen was titrated. With a final concentration between 250-500 ng/ml a plasmin activity was measurable. Below 250 ng/ml of SAK the plasmin activity would be too low to see an effect of recombinant Triiso in the following assay. So, 300 ng/ml of SAK was used for further tests. Therefore, Triiso was preincubated with plasminogen for 30 min at room temperature. Then 300 ng/ml of SAK were added.

In the presence of Triiso no changes in plasmin activity were measured, compared to the sample without Triiso (B). Different amounts of Triiso were tested up to a final concentration of 160 µg/ml. In contradiction to Furuya and Ikeda (2011), Triiso does not influence plasminogen activation in this set-up. Because of the results further investigations of the influence of moAb H8 could not be performed. The activation of plasminogen was also not affected by different concentrations of whole *S. aureus* ATCC29213 cells (planktonic growth) that were pre-incubated with plasminogen (C).

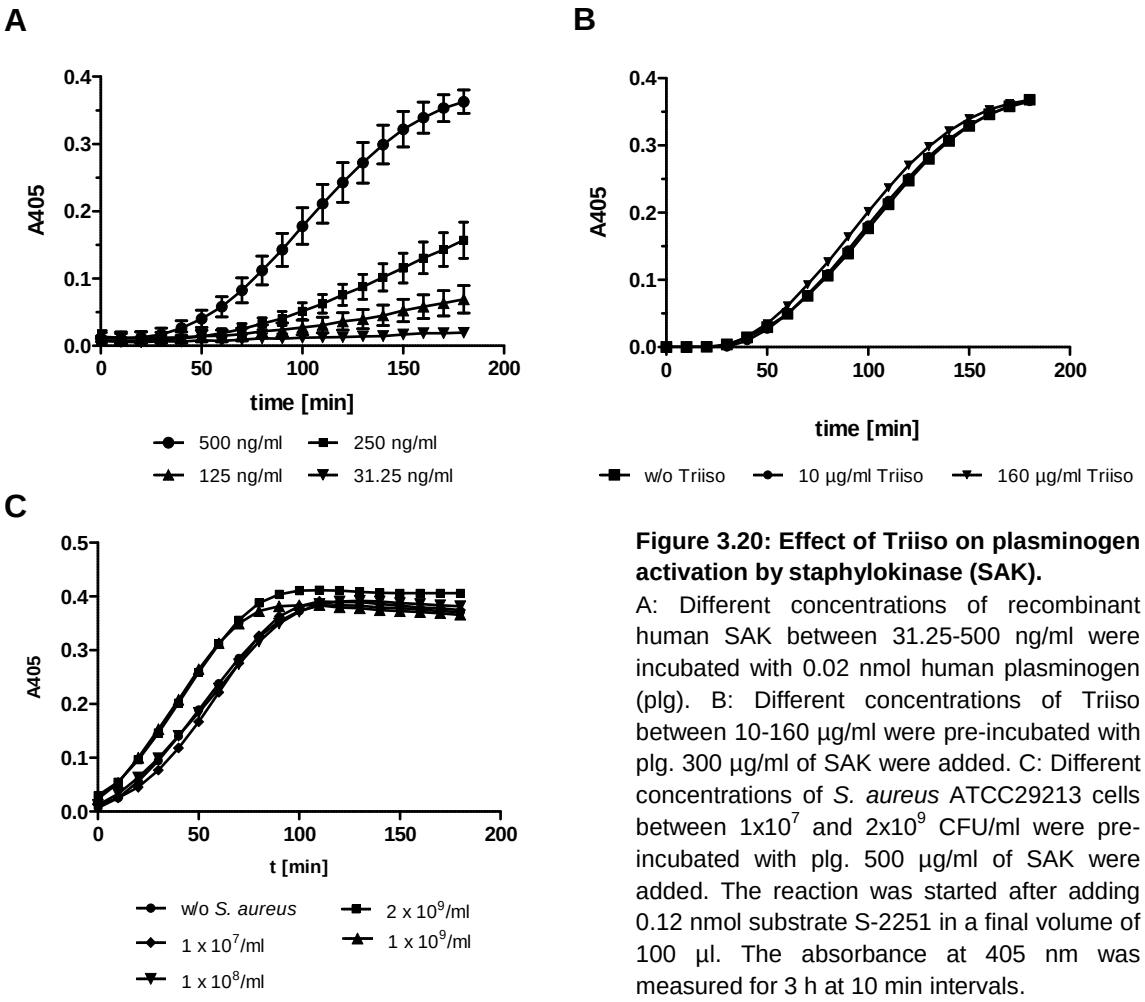

Figure 3.20: Effect of Triiso on plasminogen activation by staphylokinase (SAK).
A: Different concentrations of recombinant human SAK between 31.25-500 ng/ml were incubated with 0.02 nmol human plasminogen (plg). B: Different concentrations of Triiso between 10-160 µg/ml were pre-incubated with plg. 300 µg/ml of SAK were added. C: Different concentrations of *S. aureus* ATCC29213 cells between $1x10^7$ and $2x10^9$ CFU/ml were pre-incubated with plg. 500 µg/ml of SAK were added. The reaction was started after adding 0.12 nmol substrate S-2251 in a final volume of 100 µl. The absorbance at 405 nm was measured for 3 h at 10 min intervals.

3.1.6.6 Deletion of pOxi leads to an impaired growth and virulence of S. aureus

Because of the existence of the deletion mutants Δ*pOxi* and *Δhp2160* the two antigens did not seem to be essential, whereas a Triiso deletion mutant was not found. The exponential growth rate of the two deletion mutants Δ*pOxi* and Δ*hp2160* compared to the wildtype strain JE2 (Figure 3.21A) was analyzed by measuring the OD at 600 nm. Compared to the wildtype, Δ*hp2160* showed a similar growth rate, whereas the growth rate of Δ*pOxi* was strongly retarded but not completely inhibited. The protein pOxi converts protoporphyrinogen to XI protoporphyrin XI that is the precursor of protoheme, also called hemin. Hemin is the precursor of heme, an important cofactor of several proteins, such as cytochrome or catalase, which are required for the aerobic growth of *S. aureus*.

The Δ*pOxi* mutant also showed a slow growth on agar plates. After 2-3 days of growth at 37 °C small colony variants were detected on the plate.

In figure 3.21B different concentrations of hemin were added to the medium before inoculation with Δ*pOxi* and wildtype. Whereas hemin does not influence the growth rate of the wildtype, Δ*pOxi*'s growth rate picked up by increasing the hemin concentration.

Because of the negative influence of the pOxi deletion on *S. aureus* growth the protein seems to be important for the vitality of the organism. In a further experiment it was tested *in vivo,* if the pOxi deletion also influences the virulence of *S. aureus*.

Therefore, BALB/c mice (n = 6) were challenged i.p. with 6 x 10^6 CFU of *S. aureus* JE2. A second group received an equal dose of Δ*pOxi*. Mice were monitored for two days. After the first day 50 % of mice challenged with wildtype died, whereas every mouse of the Δ*pOxi* group survived (Figure 3.22). Even inocula of 1.2 x 10^7 Δ*pOxi* did not lead to a lethal effect (data not shown). This proved an influence of pOxi on the virulence of *S. aureus*.

A

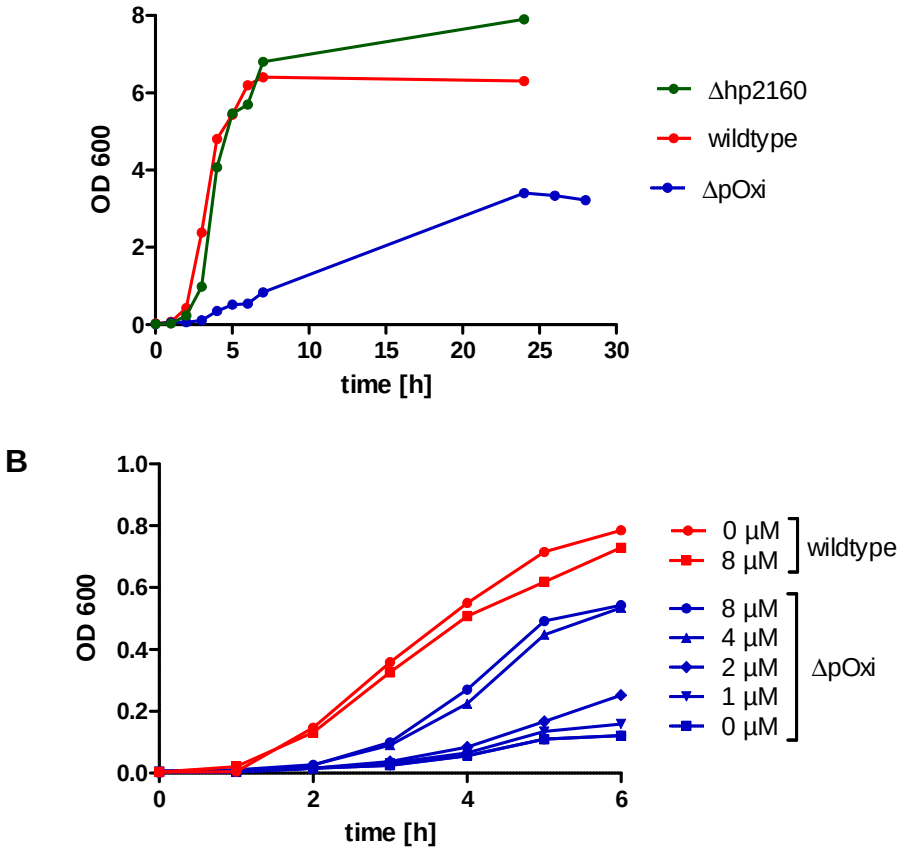

Figure 3.21: Comparison between exponential growth of *S. aureus* wildtype and deletion mutants. A: Overnight cultures of *S. aureus* JE2 and Δ*pOxi* and Δ*hp2160* were inoculated 1:100 into LB medium and incubated at 37 °C and 220 rpm. Optical density was measured every hour at 600 nm. The samples were diluted 1:10 for the measurement. B: Same procedure as described in A, but hemin was added in different concentrations to a respective culture of JE2 and Δ*pOxi* before inoculation.

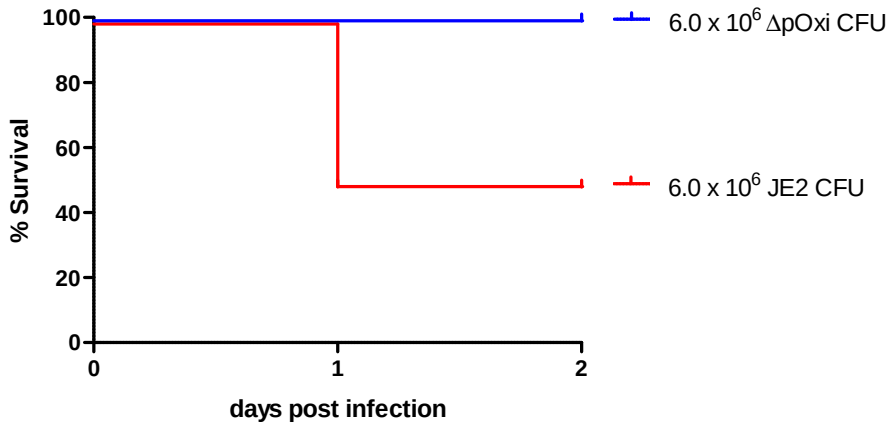

Figure 3.22: Survival of mice challenged with *S. aureus* Δ*pOxi* and wildtype. BALB/c mice (n = 6) were challenged i.p. with 6 x 10^6 CFU of *S. aureus* JE2 (red line) or Δ*pOxi* (blue line). Survival was monitored for 2 days. *P*-value was determined by Mantel-Cox test: $p = 0.055$.

3.1.6.7 Binding of recombinant proteins to the surface of S. aureus upon biofilm growth

In 3.1.5.3 it was shown that binding of moAbs to the cell surface of biofilm grown *S. aureus* was competed by the available epitope peptides. For a competition of anti-Triiso moAb H8 binding the whole protein should be used as a competitor.

The recombinant protein Triiso was preincubated with moAb H8 and then added to biofilm grown *S. aureus* Δ*spA*. For a comparison moAb H8 was incubated with Δ*spA* on its own. Unexpectedly, compared to the moAb H8 binding at the bacterial surface as presented in figure 3.23A (orange line), the fluorescence signal in presence of Triiso (red) was slightly increased. A similar result was also shown with pOxi, which was preincubated with moAb D3 (B). Compared to moAb D3 on its own (green), the binding to the *S. aureus* surface was strongly increased upon preincubation of moAb D3 with recombinant pOxi (light blue). The binding of the recombinant proteins to the bacterial surface was also detected with a murine anti-His_6-tag antibody as shown in figures C-D. Instead of moAbs H8 and D3, this antibody can only bind to the recombinant proteins, but it is not able to bind to the surface on its own (dark blue line in C and D). An increased fluorescence signal in presence of Triiso (red), as well as pOxi (light blue) incubated with anti-His_6-tag antibody was measured. These results are a clear hint that the recombinant proteins are both able to bind to the *S. aureus* surface after adding them from outside.

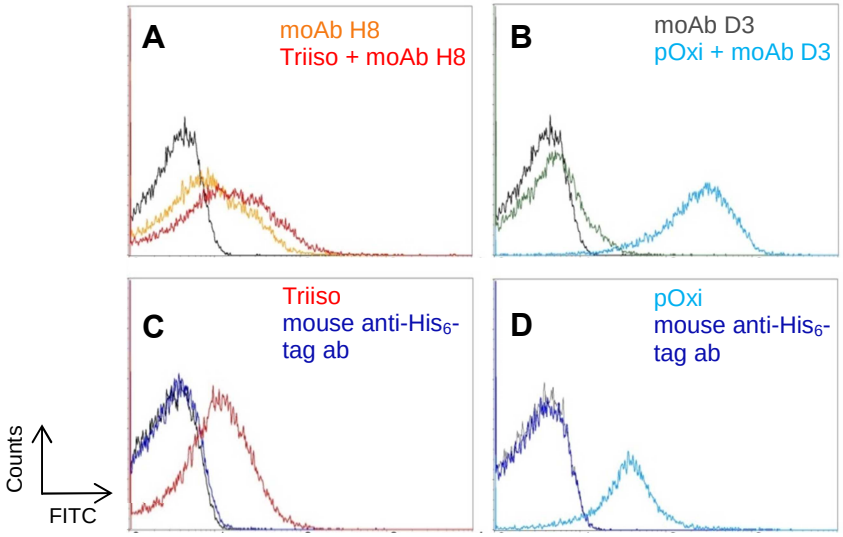

Figure 3.23: Specific binding of recombinant Triiso and pOxi to the *S. aureus* surface upon biofilm growth. Strain Δ*spA* was grown for 24 h under biofilm conditions. Bacteria were detached and washed. A-B: Bacterial cells were incubated with moAb H8 (orange) or D3 (green). Triiso or pOxi was preincubated with moAb H8 (red) or D3 (light blue). C-D: Bacteria were first incubated with Triiso (red) or pOxi (light blue) and then with 2 µg of anti-His-tag moAb or just with murine anti-His-tag moAb alone (dark blue). An incubation with anti-mouse-IgG-AlexaFluor488 followed for a detection by flow cytometry. Black line: anti-ms-IgG-AlexaFluor488.

3.1.6.8 Adherence of pOxi to eukaryotic cells

Recombinant pOxi showed a strong binding to the surface of *S. aureus* after biofilm growth. A specific binding of pOxi to HeLa cells as shown in figure 3.24 was already proven in our lab by Dr. Sonja Mertins. A monolayer of HeLa cells was incubated with different amounts of recombinant pOxi and washed then three times. The cells were detached and lysed. Equal amounts of the lysate were blotted on a nitrocellulose membrane. The membrane was then incubated with anti-His-tag-HRP conjugate for the detection of pOxi and with anti-β-Actin-HRP conjugate to ensure that equal amounts of the cell lysate were used. The binding of pOxi was inhibited after the addition of 10 µg of anti-pOxi moAb D3, whereas the addition of an irrelevant IgG2a antibody does not influence the binding of pOxi to the cells. The same experiment was done with Huvec cells (endothelial). Triiso did not show any or just a very weak binding to eukaryotic cells.

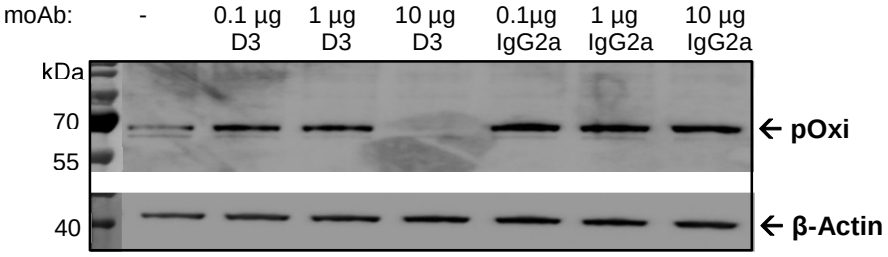

Figure 3.24: Specific binding of recombinant pOxi to the surface of HeLa cells and inhibition by anti-pOxi moAb D3. 100 µg/ml of recombinant pOxiHis_6 was preincubated for 15 min at 37 °C with different concentrations of moAb D3, an irrelevant IgG2a antibody or just PBS. A monolayer of HeLa cells was then incubated with this mix for 5h and washed 3x. Cells were detached and lysed. Equal amounts of the lysates were blotted on a nitrocellulose membrane. The membrane was then incubated with anti-His-tag HRP conjugate. The same membrane was stripped and incubated with anti-β-Actin-HRP. Data from S. Mertins.

To investigate the binding of *S. aureus* to eukaryotic cells, both were mixed, incubated and then analyzed by flow cytometry as shown in figure 3.25. In 3.25A the gated population of HeLa cells is shown as a control. Strain ATCC 29213-GFP was grown under biofilm conditions. The detached and washed bacteria were added to the HeLa cells at different MOI's. Figure 3.25B shows ATCC 29213-GFP incubated with the cells at a MOI of 5. The percentage of fluorescent bacteria bound to HeLa cells was shown by dot plots. By increasing the MOI a higher percentage of positive particles was measured in the HeLa population. Pretests showed that no binding could be measured anymore with a MOI below 5 (data not shown). Therefore, MOI 5 was chosen to demonstrate a competition effect after adding the moAbs to *S. aureus*.

In presence of anti-pOxi moAb D3, binding of GFP-expressing *S. aureus* to HeLa cells was reduced from 21.2 % to 13.7 % (C) and with anti-Triiso moAb H8 to 17.6 % (F). To analyze an influence of the proteins on host cell adherence the bacteria were incubated with recombinant Triiso or pOxi, respectively. An increase to from 21.2 % to 44.4 % of *S. aureus* binding to HeLa cells after the incubation with pOxi (D) was shown, in contrast to Triiso (G), where no increase was measured. A preincubation of pOxi with moAb D3 (before added to *S. aureus*) lead to a reduced binding from 44.4 % to 2.1 % (E). This proves the specific interaction of recombinant pOxi between *S. aureus* and HeLa cells, which can be inhibited by moAb D3. A pre-incubation of Triiso with moAb H8 does not show any changes in binding of *S. aureus* to HeLa cells (H). In summary, the protein pOxi showed an influence on the adhesion of *S. aureus* to eukaryotic cell lines, whereas Triiso does not seem to influence an interaction with the host. After addition of anti-pOxi moAb D3 the binding to HeLa cells was strongly decreased.

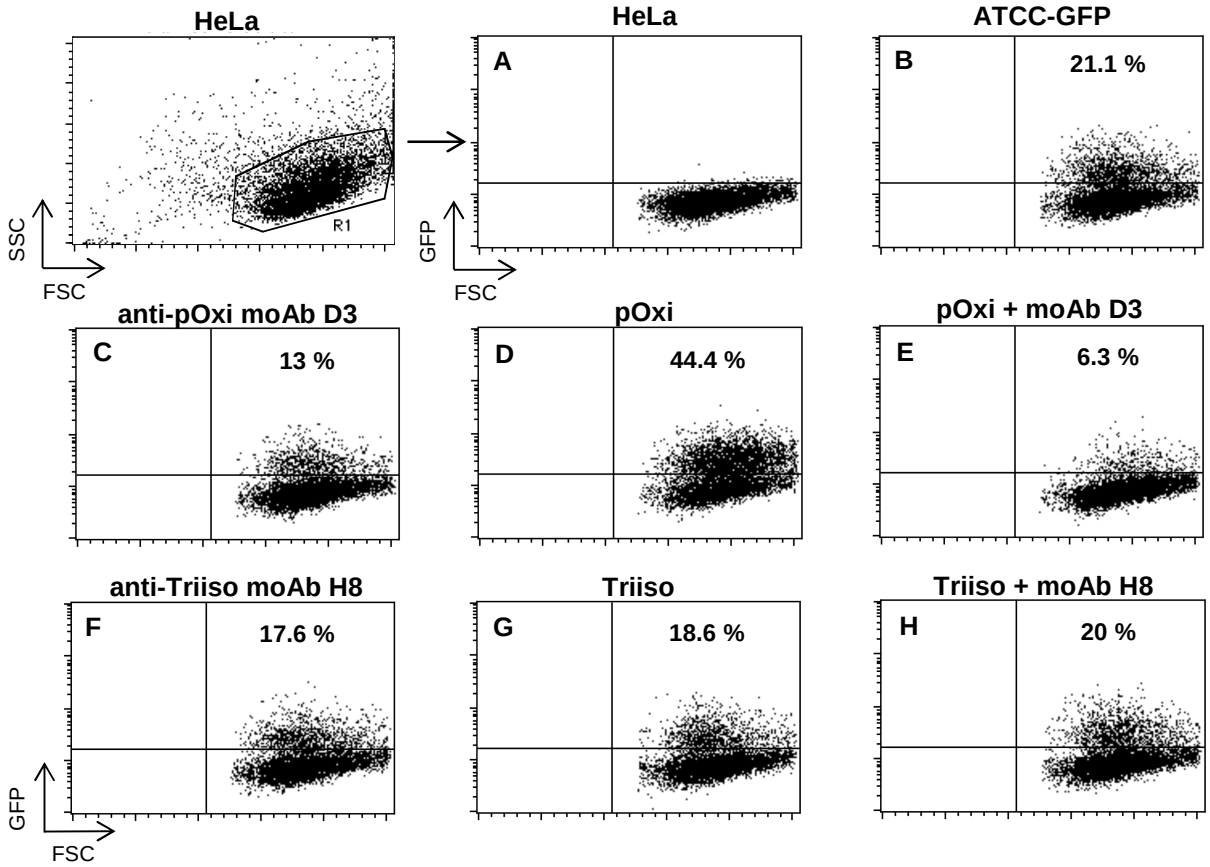

Figure 3.25: Influence of the interaction between *S. aureus* and HeLa cells in presence of moAbs and recombinant proteins. *S. aureus* ATCC29213-GFP was grown under biofilm conditions. The bacteria were preincubated with PBS (B) moAb D3 (C) or H8 (F), the recombinant protein pOxi (D) or Triiso (G) or a mix of preincubated pOxi with moAb D3 (E) or Triiso with moAb H8 (H). The bacteria were then incubated with HeLa cells (MOI 5). The HeLa cells were fixed and analyzed by flow cytometry. The percentage of fluorescent bacteria bound to HeLa cells was shown in the dot plots. HeLa cells w/o bacteria served as control for analysis set-up (A).

3.2 Active immunization with epitope peptides

3.2.1 Immunization with epitope peptides induces an antigen-specific immune response

The strategy described here, is an active immunization with the epitopes of our already investigated monoclonal antibodies (moAbs) that showed protection in our murine sepsis model after passive immunization. Vaccination with the synthesized epitope peptides shown in chapter 3.1 should induce the production of the same protective IgGs by the organism's immune system itself.

Synthesized pOxi-, hp2160- and TriisoC4-peptides were either conjugated to the carrier protein bovine serum albumin (BSA) or the protein keyhole limpet hemocyanin (KLH) isolated from *Megathura crenulata* because the peptides themselves were too small for the generation of an immune response.

Groups of BALB/c mice (n = 2) were initial immunized with 80 µg of the respective peptide-conjugate using Freund's complete adjuvant (FCA) and boosted twice after four weeks with 50 µg of peptide-conjugate using Freund's incomplete adjuvant (FIA).

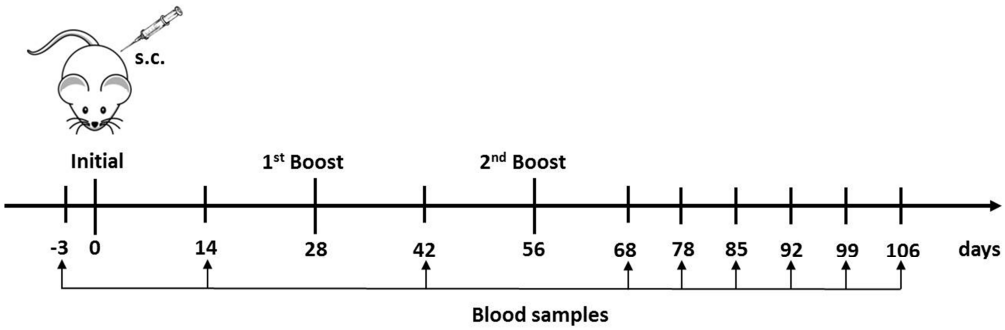

Figure 3.26: Schematic overview of the immunization model to investigate IgG humoral immune response. BALB/c mice (n = 2) received s.c. an initial and two booster immunizations every four weeks. Blood samples were collected two weeks post immunization and every week until 50 days post last boost for an analysis of serum IgG titer.

Blood samples from mice were collected at *vena facialis* prior to immunization (negative control) and at indicated time points post immunization until 50 days post last boost (Figure 3.26). Serum IgG titer against the whole respective antigen was quantified by serial dilutions in ELISA. Therefore, recombinant hp2160, pOxi or Triiso was immobilized on a 96-well maxisorp plate, which was then incubated with the different serum dilutions. Anti-mouse-HRP was used as detection antibody.

The titer is given as the dilution corresponding to the half maximal absorbance at 450 nm. The serum titer of mice treated with BSA as a control group remained non-reactive for the proteins hp2160, pOxi and Triiso. An induction of an antigen-specific IgG production by vaccination with peptide-conjugates pOxi-BSA, hp2160-BSA and TriisoC4-BSA was already detected after the initial immunization (Figure 3.27). A rapid increase after the first boost was measured with all peptides followed by a moderate increase of half a log after the second boost. The antigen-specific IgG titer in murine blood still remained at the same level 50 days after the last booster immunization.

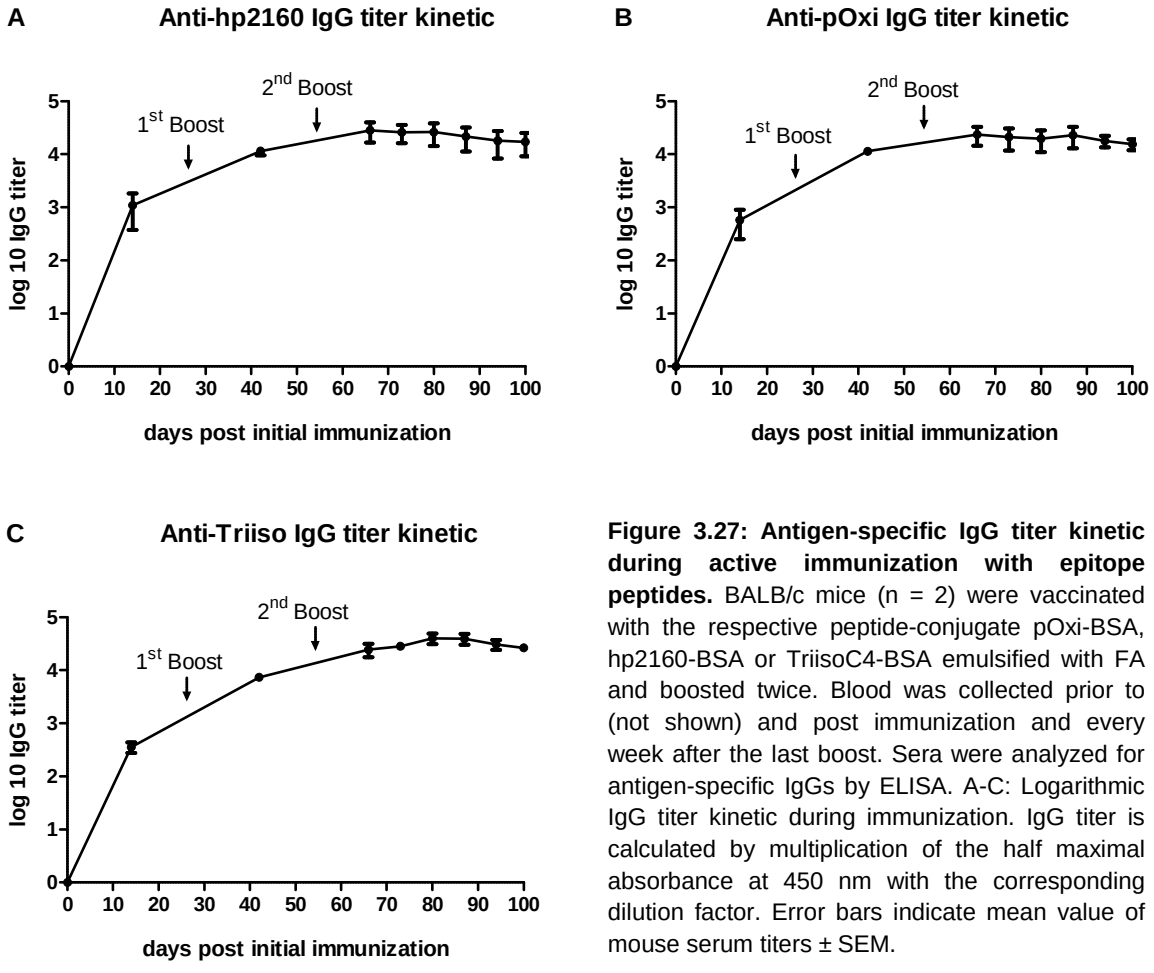

Figure 3.27: Antigen-specific IgG titer kinetic during active immunization with epitope peptides. BALB/c mice (n = 2) were vaccinated with the respective peptide-conjugate pOxi-BSA, hp2160-BSA or TriisoC4-BSA emulsified with FA and boosted twice. Blood was collected prior to (not shown) and post immunization and every week after the last boost. Sera were analyzed for antigen-specific IgGs by ELISA. A-C: Logarithmic IgG titer kinetic during immunization. IgG titer is calculated by multiplication of the half maximal absorbance at 450 nm with the corresponding dilution factor. Error bars indicate mean value of mouse serum titers ± SEM.

3.2.2 Mono- and bivalent immunization with epitope peptides leads to significant higher bacterial clearance in organs after *S. aureus* infection

Larger groups of mice (n = 10-12) were immunized with the respective epitope peptide conjugated to BSA or KLH emulsified with Freund's adjuvant (FA). The number of mice in one experiment was conformed to the availability of mice at the ZMMK. 80 µg of antigen for the initial and 50 µg for the booster immunizations were used. After determination of an antigen-specific immune response of every mouse, all groups were challenged i.p. with a sublethal dose of the clinically relevant community-acquired (CA) MRSA strain USA300. The bacterial titer was calculated by Casy Cell Counter and mixed with 5 % mucin from porcine stomach. This method is based on our already established infection model after passive immunization, where mucin was used to increase bacterial virulence allowing application of a lower *S. aureus* CFU-titer. Mice were sacrificed after 24 h, organs were prepared and homogenized. Several dilutions were plated out to determine bacterial density the following day (Figure 3.28).

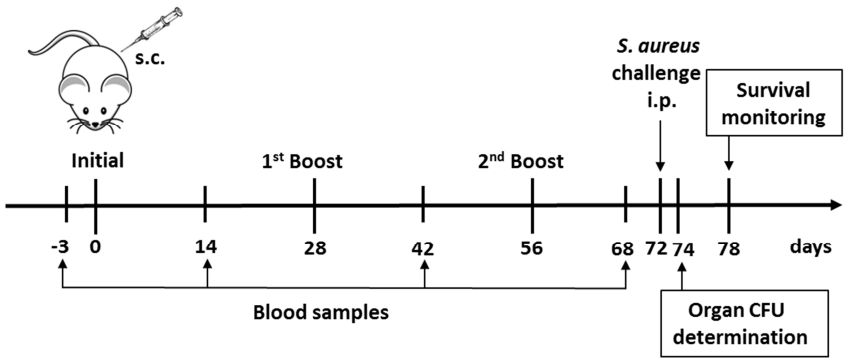

Figure 3.28: Schematic overview of the immunization model to investigate the bacterial load in organs or survival of mice after *S. aureus* infection. BALB/c mice (n = 10-12) received s.c. an initial and two booster immunizations every four weeks. Blood samples were collected two weeks post immunization. After the last boost mice were challenged i.p. with a sublethal dose of *S. aureus* USA300. After 24 h mice were sacrificed and organs were prepared for a determination of the bacterial density. In case of a survival experiment mice were infected with a lethal dose and they were monitored for 6 days.

3.2.2.1 Vaccination with hp2160 peptide

Mice were vaccinated with the corresponding epitope of anti-hp2160 moAb 16-2. The synthesized peptide was conjugated to KLH, and therefore the control group was immunized solely with the protein KLH. Serum of every mouse was analyzed two weeks after the last booster immunization to determine a specific IgG titer against the whole protein hp2160 (Figure 3.29A). Every hp2160-KLH immunized mouse showed

an antigen-specific immune response. The control mice sera showed specific IgGs against KLH (not shown), but they were non-reactive for hp2160 (hp2160-KLH vs. KLH, $p = 0.0002$). The sera of mice were pooled and used for detection of hp2160 in the cell wall-associated protein fraction (neCWS) of *S. aureus* Δ*spA*, as well as in the whole cell lysate (WCL) of *S. aureus* JE2, as presented in figure 3.29B. The serum IgGs showed an unspecific binding to protein A in WCL of the wildtype strain JE2 but also a specific binding to staphylococcal hp2160.

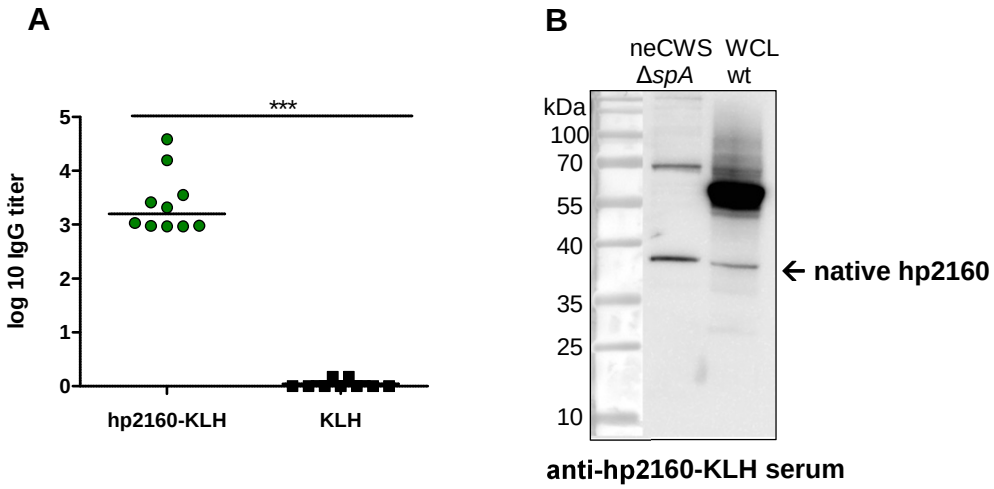

Figure 3.29: Immune response after immunization with hp2160-KLH. BALB/c mice (n = 10) were vaccinated with hp2160 epitope peptide conjugated to KLH or with KLH as a control emulsified with FA. Serum of every mouse was collected after the last boost and analyzed for hp2160-specific IgGs by ELISA and Western blot. A: Logarithmic antigen-specific IgG titer. The titer is given as the dilution corresponding to the half maximal absorbance at 450 nm. *P*-value was analyzed by Mann-Whitney test: $p \leq 0.001$ = ***. Each data point represents an individual animal. B: neCWS and whole cell lysate (WCL) of *S. aureus* Δ*spA* or wt, respectively, were blotted on a nitrocellulose membrane. Serum was pooled and incubated with the membrane, followed by detection with anti-mouse-HRP.

After the last booster immunization mice were challenged i.p. with 4.5 x 10^6 CFU of *S. aureus* USA300. After infection with this sublethal dose, mice were monitored for 24 h and then sacrificed for preparation of liver, spleen and kidneys.

The quantification of the CFU presented in individual organs of immunized mice post *S. aureus* infection demonstrated that immunization with hp2160 epitope peptide resulted in lower bacterial densities in all prepared organs (Figure 3.30). Compared to spleen ($p = 0.0892$) and kidneys ($p = 0.2176$) these reductions were statistically significant in liver ($p = 0.0355$).

Two following experiments with a comparable set up (BSA as conjugate, different amounts of antigen) revealed the same trend, but with a significance just once in the spleen (p = 0.0422, not shown).

In order to achieve a clearer difference between peptide and control group after challenge we also prepared organs after 48 hours in further *in vivo* experiments, compared to the preparation after 24 hours. The bacterial load was lower in liver and spleen and higher in kidneys. The results between peptide and control group looked very similar, but the colony counting after 24 h was more exactly. With these conclusions, we went on with organ preparation after 24 h.

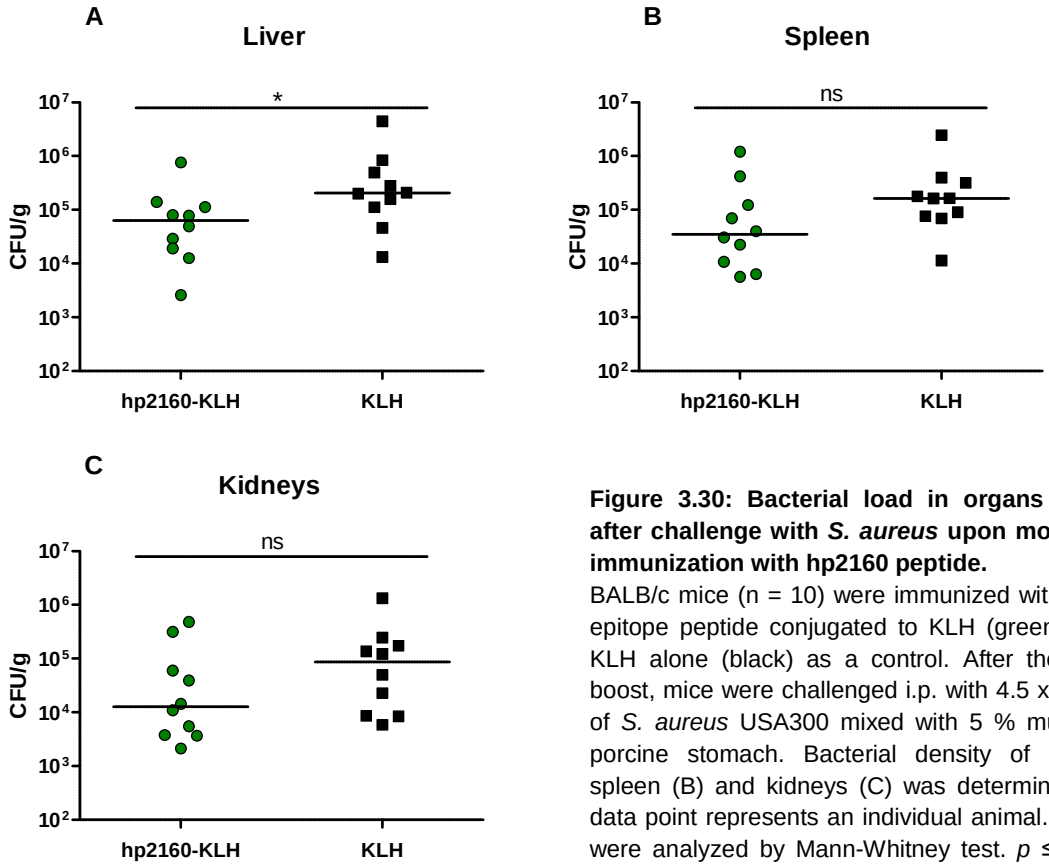

Figure 3.30: Bacterial load in organs of mice after challenge with *S. aureus* upon monovalent immunization with hp2160 peptide.
BALB/c mice (n = 10) were immunized with hp2160 epitope peptide conjugated to KLH (green) or with KLH alone (black) as a control. After the second boost, mice were challenged i.p. with 4.5 x 10^6 CFU of *S. aureus* USA300 mixed with 5 % mucin from porcine stomach. Bacterial density of liver (A), spleen (B) and kidneys (C) was determined. Each data point represents an individual animal. *P*-values were analyzed by Mann-Whitney test. $p \leq 0.001$ = ***; $p = 0.01$ = **; $p \leq 0.05$ = *; ns = not significant.

3.2.2.2 Vaccination with pOxi peptide

The pOxi epitope peptide conjugated to KLH produced by JPT Peptide Technologies arrived our lab already precipitated, so we assumed that the actual concentration of peptide-conjugate and therefore the available amount of peptide-conjugate per immunization was lower as expected.

Groups of mice (n = 10) were vaccinated with pOxi-KLH and KLH, respectively. Initial and first booster immunization with pOxi-KLH resulted in a low anti-pOxi IgG titer (data not shown) but it was increased after the last boost (Figure 3.31A). Mice immunized with KLH did not show an immune response against pOxi.

As a further analysis recombinant pOxi and KLH were blotted on a nitrocellulose membrane that was then incubated with the pooled serum of the mice immunized with pOxi-KLH. As shown in 3.31B the serum IgGs showed a specific binding to recombinant pOxi. A binding to KLH was also detected. Binding of serum antibodies to WCL and neCWS was not detected, as already described for anti-pOxi moAb D3 (see 3.1.4.1)

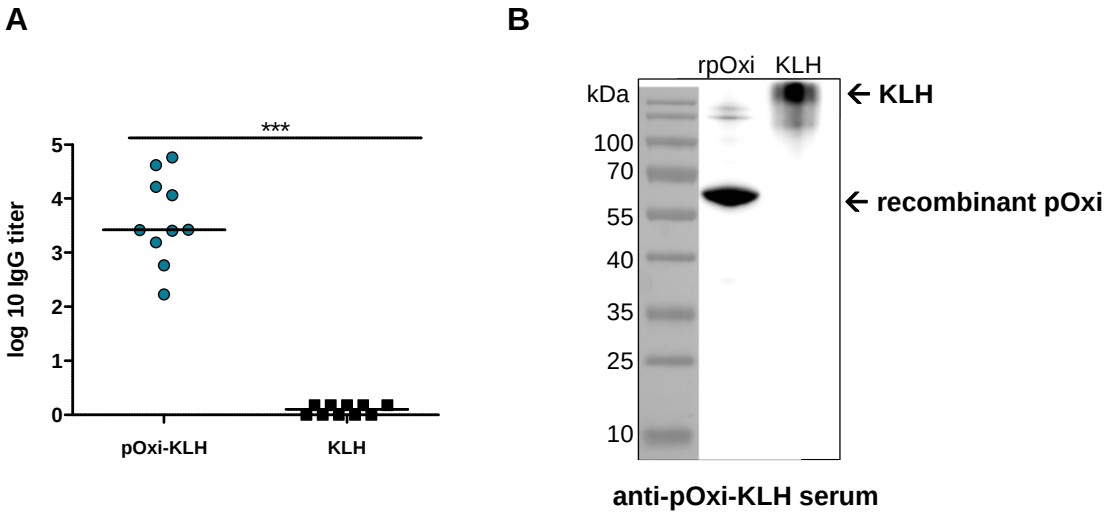

Figure 3.31: Immune response after immunization with pOxi-KLH. BALB/c mice (n = 10) were vaccinated with pOxi epitope peptide conjugated to KLH or with KLH as a control. Serum of every mouse was collected after the last booster immunization and analyzed for pOxi-specific IgGs by ELISA and Western blot. A: Logarithmic antigen-specific IgG titer. The titer is given as the dilution corresponding to the half maximal absorbance at 450 nm. Each data point represents an individual animal. *P*-value was analyzed by Mann-Whitney test: $p \leq 0.001$ = ***. B: Recombinant pOxi and KLH protein were blotted on a nitrocellulose membrane. Serum was pooled and incubated with the membrane, followed by detection with anti-mouse-HRP.

After infection with 4.2 x 10^6 CFU of *S. aureus* USA300 a significant higher bacterial clearance in liver (p = 0.0029), spleen (p = 0.0005) and kidneys (p < 0.0001) of mice vaccinated with pOxi-KLH was determined, compared to the control group (Figure 3.32). Additionally mentionable is that all mice of the pOxi-KLH group showed a much healthier phenotype before organ preparation compared to the mice immunized with KLH, which showed ruffled fur, hunched posture, loss of movement and weight loss.

Comparable vaccination experiments with divergent antigen amounts and conjugates often demonstrated a trend for a lower bacterial load in organs of the pOxi-KLH group after infection but statistical significance was not reached every time (not shown).

In conclusion, *in vivo* experiments using pOxi-KLH as vaccine resulted in a stronger protective effect after infection with the MRSA strain compared to hp2160-KLH immunization studies (see 3.2.2.1).

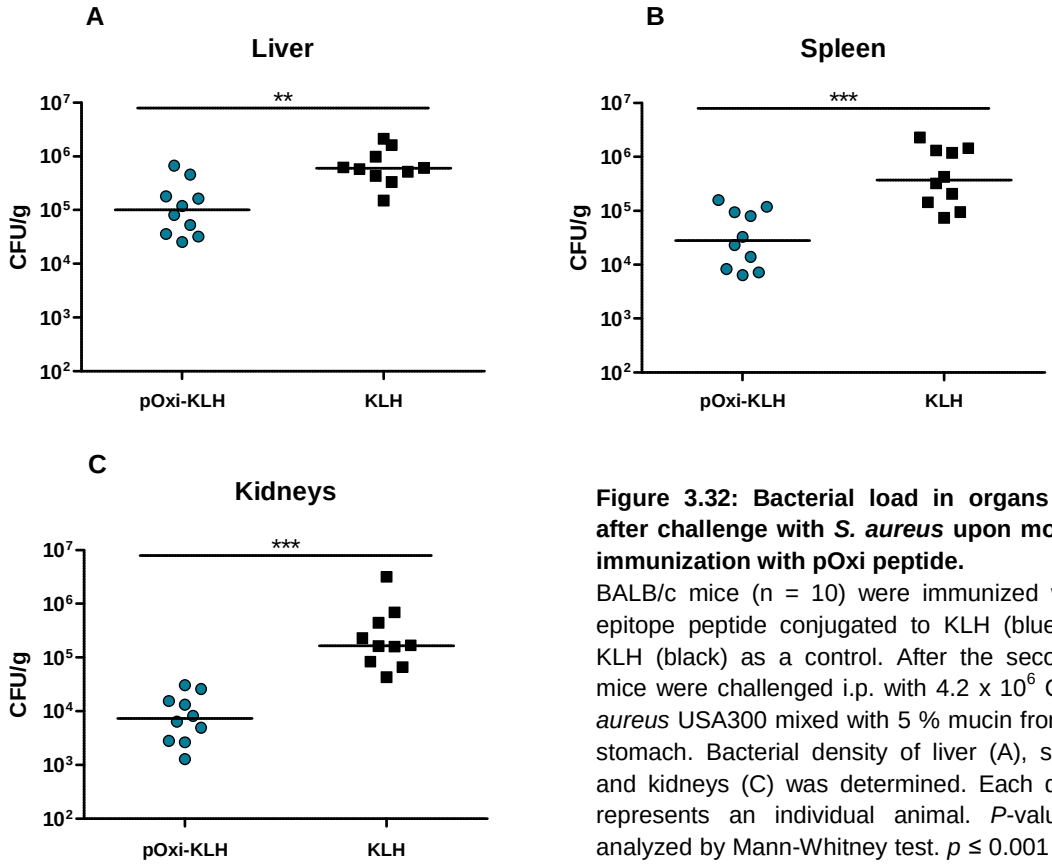

Figure 3.32: Bacterial load in organs of mice after challenge with *S. aureus* upon monovalent immunization with pOxi peptide.
BALB/c mice (n = 10) were immunized with pOxi epitope peptide conjugated to KLH (blue) or with KLH (black) as a control. After the second boost mice were challenged i.p. with 4.2 x 10^6 CFU of *S. aureus* USA300 mixed with 5 % mucin from porcine stomach. Bacterial density of liver (A), spleen (B) and kidneys (C) was determined. Each data point represents an individual animal. *P*-values were analyzed by Mann-Whitney test. $p \leq 0.001$ = ***; p = 0.01 = **; $p \leq 0.05$ = *; ns = not significant.

3.2.2.3 Vaccination with hp2160 and pOxi peptides

Comparable to the animal experiment in 3.2.2.2 a third group was vaccinated with a combination of hp2160-KLH and pOxi-KLH to observe, whether immunization with both peptides potentiate the bacterial clearance in the murine tissues.

The group was immunized with a mixture of both peptide-conjugates. Compared to 3.2.2.2 a higher spread of the anti-pOxi IgG serum titer within the group was measured (Figure 3.33).

For a comparison of serum IgG titer and CFU after infection, the same KLH control group as in 3.2.2.2 was used because these groups were vaccinated at the same time. Serum of the control group was non-reactive against hp2160 and pOxi, respectively (hp2160-KLH vs. KLH, $p = 0.0002$; pOxi-KLH vs. KLH, $p = 0.0001$).

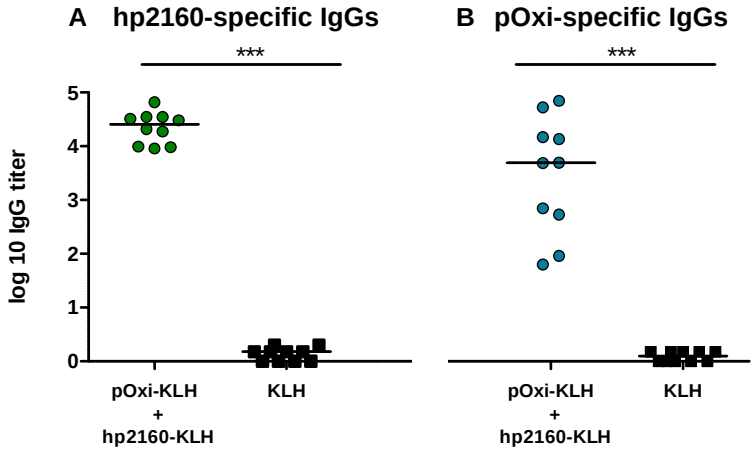

Figure 3.33: Antigen-specific IgG titer after immunization with hp2160-KLH + pOxi-KLH. BALB/c mice (n = 10) were vaccinated with a combination of hp2160 and pOxi epitope peptide conjugated to KLH or with KLH as a control. Serum of every mouse was collected after the last booster immunization and analyzed for hp2160- (A) and pOxi-specific IgGs (B) by ELISA. The IgG titer is given as the dilution corresponding to the half maximal absorbance at 450 nm. Each data point represents an individual animal. *P*-value was analyzed by Mann-Whitney test: $p \leq 0.001$ = ***.

Mice were challenged with 4.2 x 10^6 CFU of *S. aureus* USA300 as already described in 3.2.2.2. Compared to the control group a significant lower bacterial density was measured in all prepared organs of bivalently immunized mice. Statistical analysis of *p*-values ($p = 0.0039$ in liver, $p = 0.0015$ in spleen and $p = 0.0468$ in kidneys) indicates in this experiment that monovalent immunization from 3.2.2.2 with only pOxi-KLH (same control group) resulted in a higher significance than bivalent immunization (Figure 3.34). Because of a more protective effect of the pOxi peptide

compared to the hp2160 peptide in several experiments, pOxi was chosen to be used later in 3.2.2.6 (diepitope-peptide).

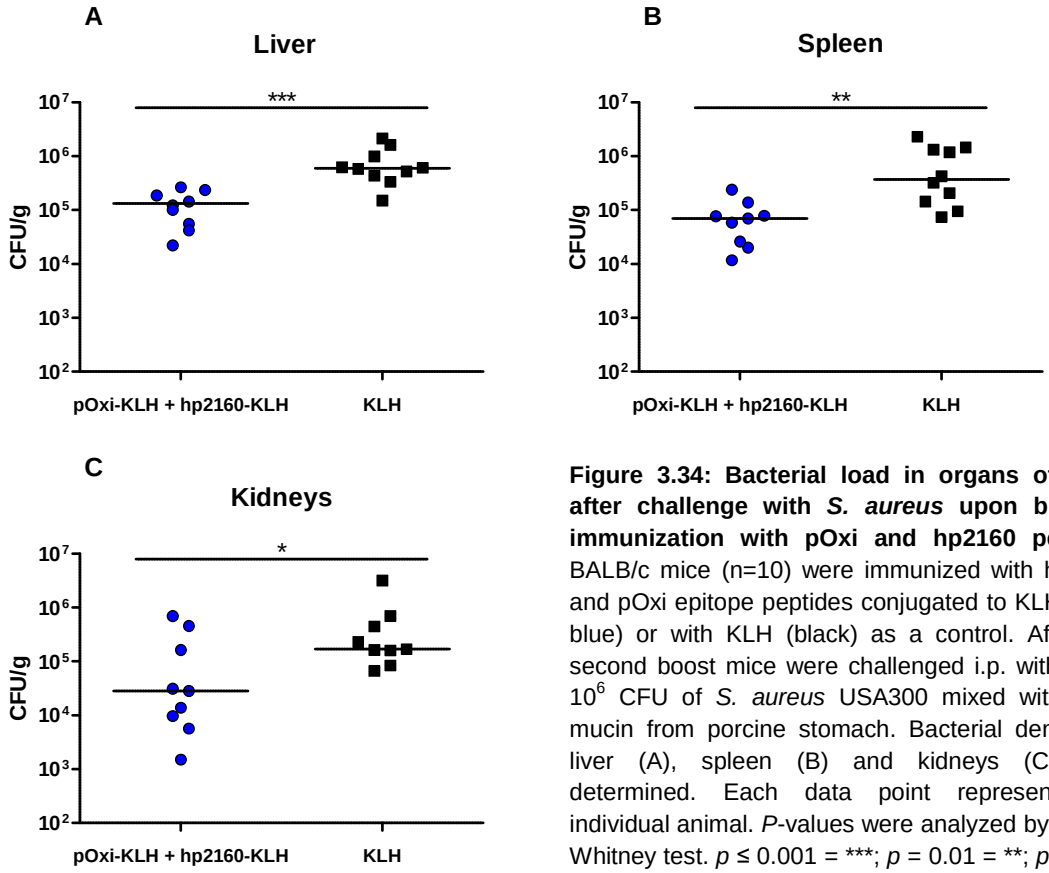

Figure 3.34: Bacterial load in organs of mice after challenge with *S. aureus* upon bivalent immunization with pOxi and hp2160 peptide. BALB/c mice (n=10) were immunized with hp2160 and pOxi epitope peptides conjugated to KLH (dark blue) or with KLH (black) as a control. After the second boost mice were challenged i.p. with 4.2 x 10^6 CFU of *S. aureus* USA300 mixed with 5 % mucin from porcine stomach. Bacterial density of liver (A), spleen (B) and kidneys (C) was determined. Each data point represents an individual animal. *P*-values were analyzed by Mann-Whitney test. $p \leq 0.001$ = ***; $p = 0.01$ = **; $p \leq 0.05$ = *; ns = not significant.

3.2.2.4 Vaccination with TriisoC4 peptide

Immunization with the linear epitope of anti-Triiso moAb C4 was tested as a further candidate for an active peptide vaccine because the discontinuous epitope of anti-Triiso moAb H8 was not determined at this time. Anti-Triiso moAb C4 achieved only a minor or no protective effect in the sepsis model after passive immunization but was not tested as often as the most protective candidate moAb H8 (unpublished data).

The synthesized epitope peptide was conjugated to BSA and stable at 4 °C, compared to pOxi-KLH. Vaccination of BALB/c mice (n = 11) resulted in a strong and consistent IgG titer in all mouse sera against recombinant Triiso (Figure 3.35A). Two mice of the control group vaccinated with BSA showed a very low immune response against Triiso that is probably unspecific.

In figure 3.35B recombinant Triiso as well as neCWS of *S. aureus* Δ*spA* was blotted on nitrocellulose, followed by incubation with the pooled serum of the TriisoC4-BSA immunized mice. Both, recombinant and native Triiso of *S. aureus* were detected by the serum.

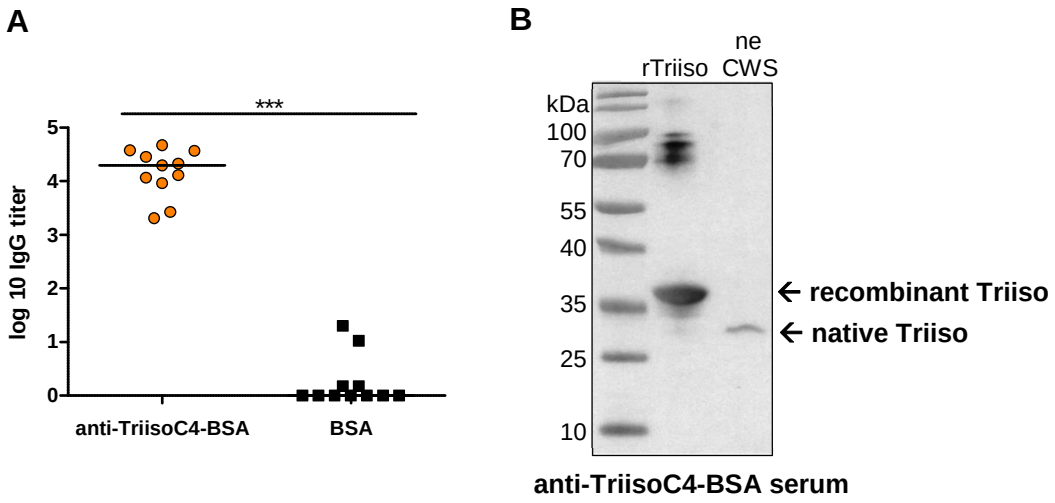

Figure 3.35: Immune response after immunization with TriisoC4-BSA. BALB/c mice (n = 11) were vaccinated with TriisoC4 epitope peptide conjugated to BSA or with BSA as a control. Serum of every mouse was collected after the last booster immunization and analyzed for Triiso-specific IgGs by ELISA and Western blot. A: Logarithmic antigen-specific IgG titer. The titer is given as the dilution corresponding to the half maximal absorbance at 450 nm. Each data point represents an individual animal. *P*-value was analyzed by Mann-Whitney test: $p \leq 0.001$ = ***. B: Recombinant Triiso and neCWS were blotted on a nitrocellulose membrane. Serum after the 1st boost was pooled and incubated with the membrane, followed by detection with anti-mouse-HRP.

Infection with 4.75 x 10^6 CFU of *S. aureus* USA300 resulted in a lower bacterial density in the kidneys of TriisoC4-BSA immunized mice without any statistical significance as shown in figure 3.36 ($p = 0.29$). Bacterial load in liver and spleens of both groups look very similar. A possible reason is the moderate total bacterial load of the control group of between 1 x 10^3 and 1 x 10^5 CFU/g in liver, 1 x 10^2 and 5 x 10^4 CFU/g in spleen and between 1 x 10^2 and 1 x 10^5 CFU/g in kidneys whereas bacterial loads of former experiments were showed a minimum of 5 x 10^4 and a maximum of 1 x 10^7 CFU/g. Although a higher bacterial titer was used for challenge as in the former infections, the mice showed a much healthier phenotype here.
Altogether, vaccination with TriisoC4 peptide resulted in a very strong immune response it does not seem to have a protective effect after *S. aureus* infection.

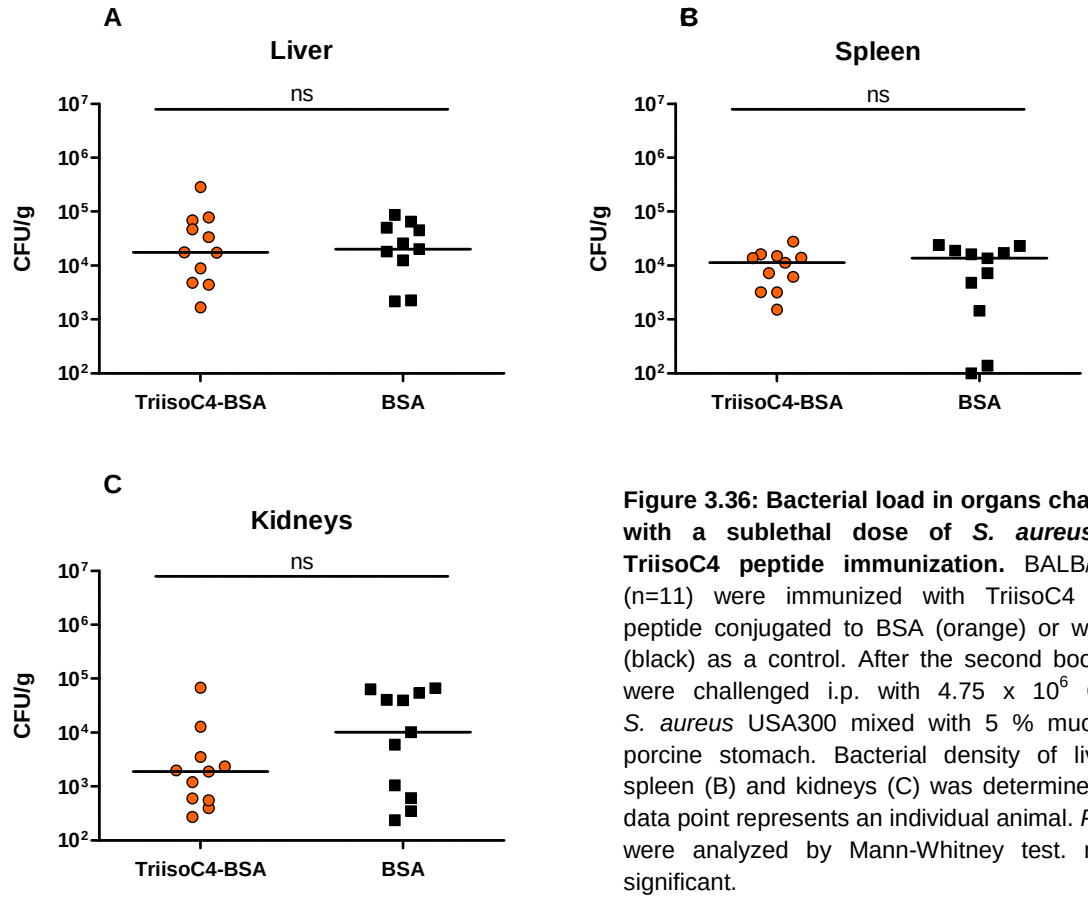

Figure 3.36: Bacterial load in organs challenged with a sublethal dose of *S. aureus* upon TriisoC4 peptide immunization. BALB/c mice (n=11) were immunized with TriisoC4 epitope peptide conjugated to BSA (orange) or with BSA (black) as a control. After the second boost mice were challenged i.p. with 4.75 x 10^6 CFU of *S. aureus* USA300 mixed with 5 % mucin from porcine stomach. Bacterial density of liver (A), spleen (B) and kidneys (C) was determined. Each data point represents an individual animal. *P*-values were analyzed by Mann-Whitney test. ns= not significant.

3.2.3 Construction of a recombinant triepitope fusion peptide

Using fragment-cloning, the epitope of anti-Triiso moAb H8 could be localized within an 11.3 kDa Triiso fragment (3.1.2), but it was still too large for a chemical peptide synthesis. While single hp2160 and pOxi epitope peptides were still tested *in vivo*, the genetic information encoding a triepitope peptide containing pOxi and hp2160 epitope peptides and the Triiso fragment that includes the epitope of moAb H8 was cloned for expression in *E. coli*. With this strategy the protective effect using a trivalent peptide vaccine should be investigated. Furthermore, the epitope of moAb H8 could be tested for the first time in active immunization.

3.2.3.1 Cloning, overexpression and purification of triepitope peptide

As shown in figure 3.37 the sequences encoding the three epitopes were cloned consecutively in the expression vector pPSG-IBA43 containing a T7 promoter, N-terminal Strep-tag and C-terminal His-tag. As primers pOxipep-TriisoN sense containing the sequence encoding the pOxi epitope and Hp2160pepTriisoC

antisense containing the sequence encoding the hp2160 epitope were used. With peptide 14 (compare 3.1.2) as template, the triepitope peptide coding sequence was amplified and cloned into the donor vector pENTRY-IBA51 followed by homologue recombination into the destination vector pPSG-IBA43 using the StarGate cloning system according to manufacturer's instructions (IBA, Göttingen, Germany). The resulting plasmid was sequenced and did not show any mutations.

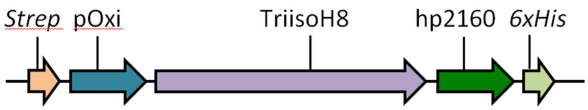

Figure 3.37: Cloning strategy of triepitope fusion-peptide. Sequences encoding the epitopes of anti-pOxi moAb D3, anti-hp2160 moAb 16-2 and Triiso fragment where epitope of anti-Triiso moAb H8 is located were cloned consecutively and N-terminal fused to Strep-tag and C-terminal fused to His-tag.

After the cloning procedure was finished the plasmid IBA-Triepitop was transformed into the expression strain *E. coli* BL21. Overexpression of triepitope peptide was induced by IPTG at an OD_{600} of 0.6. Bacteria were cultured ON at 30 °C. The highest amount of peptide was found in inclusion bodies, which were prepared for affinity purification. While Strep-tag purification leads to a peptide yield of only 3 mg, His-tag purification yielded to 9 mg of triepitope peptide (14.3 kDa) (Figure 3.38). Elution fractions were pooled, adjusted to a concentration of 2.5 mg/ml, sterile filtrated and stored at 4 °C in 1 x PBS, pH = 7.5.

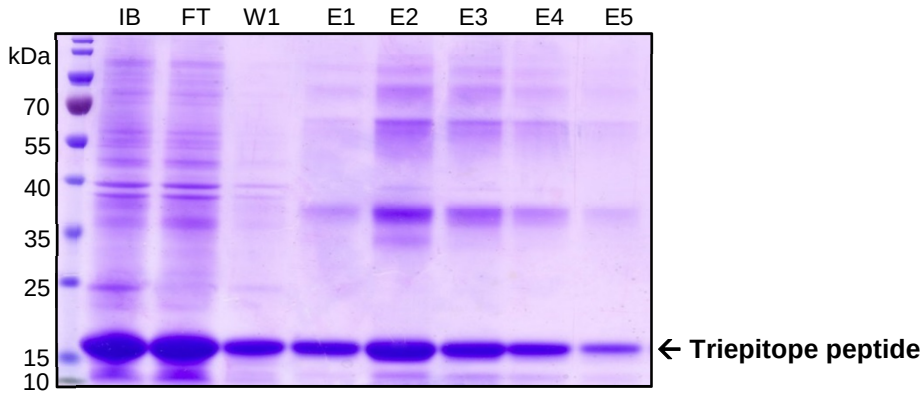

Figure 3.38: Purification of triepitope peptide via His-tag. Coomassie stained SDS-PAGE of triepitope purification via His-tag after heterologous overexpression and preparation of inclusion bodies. 15 µl of each sample was used for the protein gel. IB: inclusion body preparation, FT: flow through, W: wash fraction, E: elution fraction.

3.2.3.2 Binding analysis of moAbs to triepitope peptide

Before vaccinating groups of mice with the purified triepitope peptide, the quality had to be analyzed. It had to be clarified that just this kind of specific antibodies would be produced in the organism that formerly provided protection against *S. aureus* by passive immunization. First, binding of the three moAbs to the triepitope peptide was analyzed (Figure 3.39). The peptide was blotted onto nitrocellulose and incubated with the respective moAb as first and with anti-mouse-HRP as secondary antibody.
Anti-pOxi moAb D3 (A), anti-hp2160 moAb 16-2 (B) and anti-Triiso moAb H8 (C) are able to bind the triepitope peptide (below 25 kDa). There were also some strong binding signals detected with proteins of 40 kDa and above 55 kDa. All moAbs showed these signals that were not unspecific signals of the secondary antibody (D).

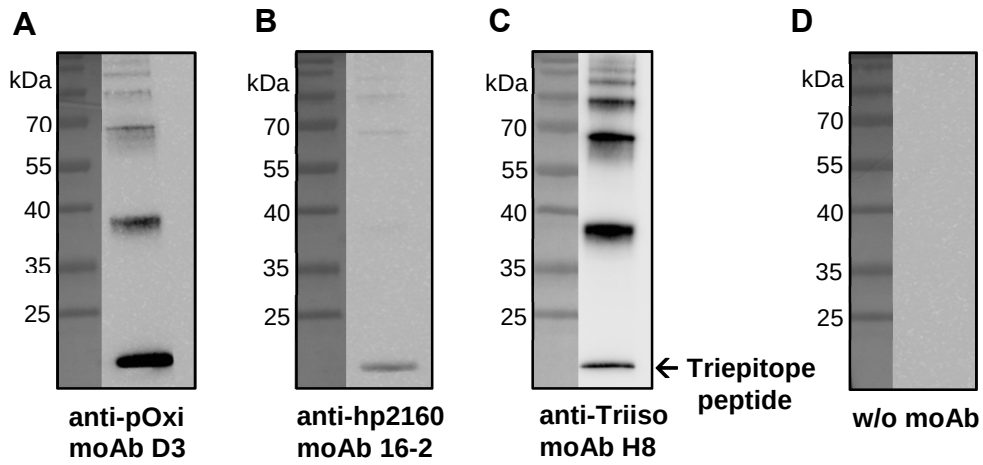

Figure 3.39: Binding of monoclonal antibodies to triepitope peptide. 10 µg of purified triepitope peptide was blotted on a nitrocellulose membrane. Membrane was incubated with anti-pOxi moAb D3 (A), anti-hp2160 moAb 16-2 (B), anti-Triiso moAb H8 (C) and without a moAb (D). Incubation with goat anti-mouse-HRP membrane followed. Membrane was developed using chemiluminescence reagent (ECL).

3.2.3.3 Competition of moAb binding to the antigen by triepitope peptide

The verification and functionality of the constructed triepitope peptides was further analyzed by its binding specificity to the respective moAbs anti-pOxi D3, anti-Triiso H8 and anti-hp2160 16-2 in competitive ELISA (Figure 3.40). The three recombinant proteins hp2160, pOxi and Triiso were immobilized on a maxisorp plate that was incubated with their respective moAb and different concentrations of triepitope peptide as competitor (compare to single peptides in 3.1.1, Figure 3.2).

A strong competition of moAb-binding to hp2160 as well as to pOxi by triepitope peptide was detected. The competitive ELISA also worked with Triiso, but just a moderate competition of moAb H8 binding was caused by the triepitope.

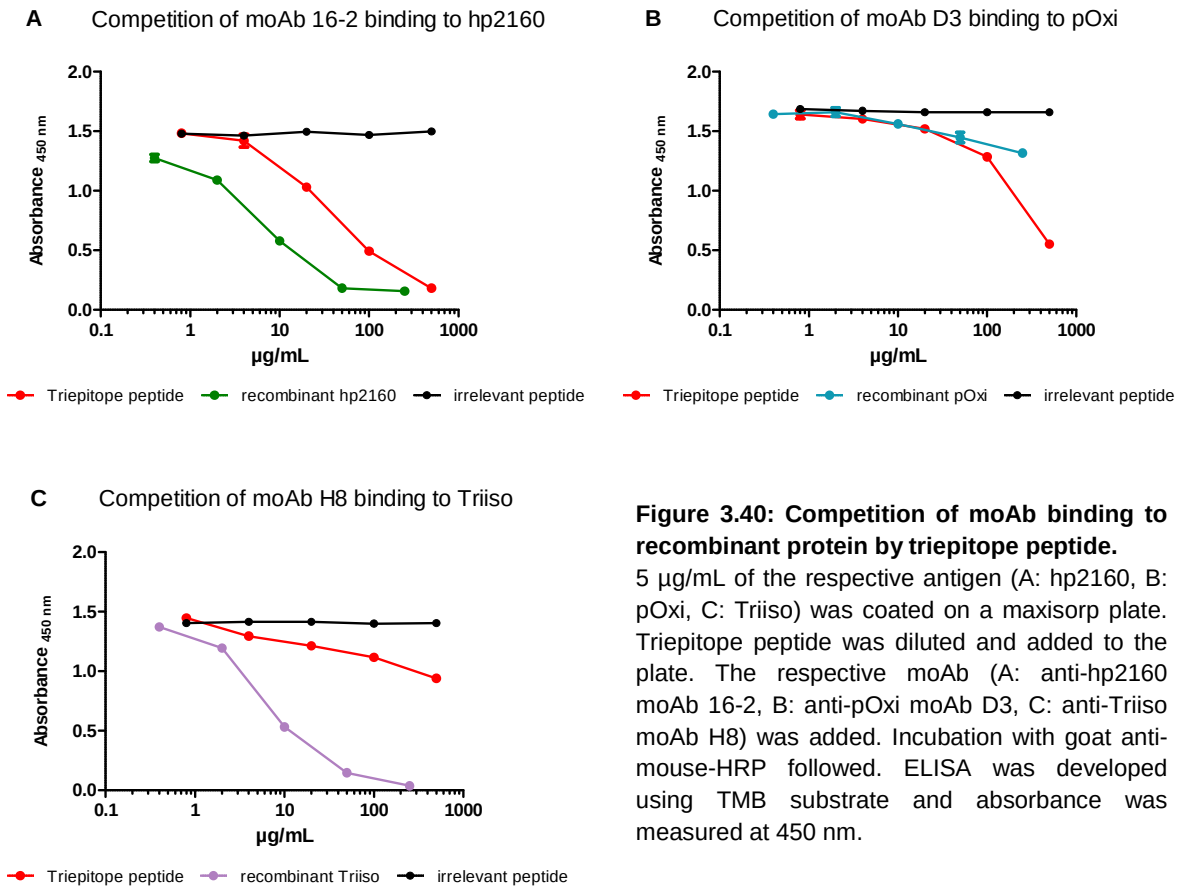

Figure 3.40: Competition of moAb binding to recombinant protein by triepitope peptide.
5 µg/mL of the respective antigen (A: hp2160, B: pOxi, C: Triiso) was coated on a maxisorp plate. Triepitope peptide was diluted and added to the plate. The respective moAb (A: anti-hp2160 moAb 16-2, B: anti-pOxi moAb D3, C: anti-Triiso moAb H8) was added. Incubation with goat anti-mouse-HRP followed. ELISA was developed using TMB substrate and absorbance was measured at 450 nm.

3.2.3.4 Specific IgG titer against recombinant hp2160, pOxi and Triiso after immunization with triepitope peptide

Recombinant triepitope peptide was conjugated to KLH for active immunization.
The peptide was large enough to generate an immune response by itself. This was first analyzed in a small test immunization with two mice (not shown). However, the high immunogenicity of KLH additionally triggers the humoral as well as cellular immune response. For an IgG titer kinetic as already explained in 3.2.1 a group of mice (n = 2) was immunized with the triepitope-peptide-KLH conjugate and serum samples were collected for a following analysis by ELISA (Figure 3.41). It was possible to detect a specific IgG titer against all three antigens by immunization with the conjugated triepitope peptide. As presented previously for synthetic single peptides (see 3.2.1), serum titer also achieved the highest peak after the second

boost and remained high for at least 45 days. Compared to hp2160 and pOxi Triiso-specific titer was much higher during whole immunization procedure.

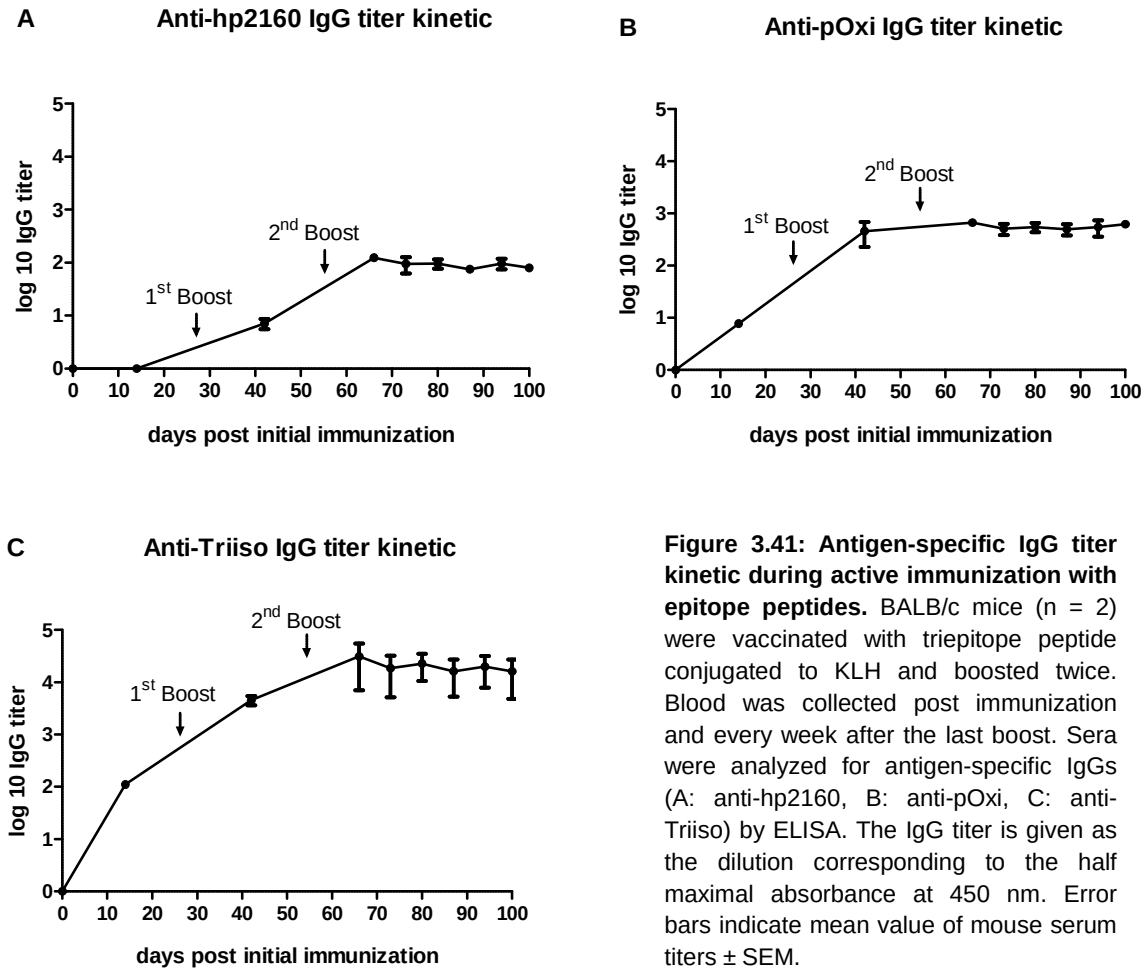

Figure 3.41: Antigen-specific IgG titer kinetic during active immunization with epitope peptides. BALB/c mice (n = 2) were vaccinated with triepitope peptide conjugated to KLH and boosted twice. Blood was collected post immunization and every week after the last boost. Sera were analyzed for antigen-specific IgGs (A: anti-hp2160, B: anti-pOxi, C: anti-Triiso) by ELISA. The IgG titer is given as the dilution corresponding to the half maximal absorbance at 450 nm. Error bars indicate mean value of mouse serum titers ± SEM.

3.2.3.5 Significant lower bacterial load in organs of mice challenged with S. aureus upon immunization with triepitope peptide

Larger groups of mice were immunized with triepitope-KLH (n = 11) and KLH (n = 12) as a control group. Total anti-pOxi-, anti-Triiso and anti-hp2160-IgG titer of every mouse was determined after the last boost (Figure 3.42). As already described in 3.2.3.4 IgG titer against hp210 and pOxi was lower in contrast to Triiso. The serum IgG titer against pOxi showed a high spread between 10 and 10^5. Sera of KLH immunized mice were non-reactive for the three antigens.

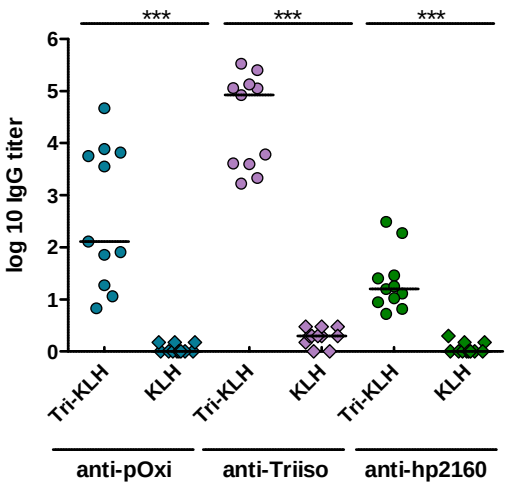

Figure 3.42: Antigen-specific IgG titer after immunization with triepitope-KLH. BALB/c mice were vaccinated with triepitope peptide (n = 11) conjugated to KLH (Tri-KLH) or with KLH (n = 12) as a control. Serum of every mouse was collected after the last booster immunization and analyzed for pOxi-, Triiso and hp2160-specific IgGs by ELISA. The IgG titer is given as the dilution corresponding to the half maximal absorbance at 450 nm. *P*-values were analyzed by Mann-Whitney test. $p \leq 0.001$ = ***.

Three days after the last blood collection, mice were i.p. challenged with 5.19 x 10^6 CFU of *S. aureus* USA300. Organs were prepared after 24 hours. The bacterial colonization was significantly lower in liver and spleen, as well as in kidneys of mice vaccinated with triepitope peptide (Figure 3.43) compared to the KLH-immunized control group. In this animal experiment a third group immunized with hp2160-KLH was also challenged with *S. aureus*, which showed a higher bacterial load in the prepared organs, compared to the triepitope peptide (hp2160-KLH vs. KLH: $p = 0{,}218$ in liver, $p = 0{,}073$ in spleen and $p = 0{,}062$ in kidneys, data not shown).

In following experiments, triepitope concentration and protein carrier were changed. Immunization with the triepitope peptide always resulted in a significant higher bacterial clearance in the mouse organs, compared to control groups and a higher clearance compared to the groups immunized with pOxi or hp2160 peptide conjugates which demonstrates a more protective effect of the triepitope peptide. In one experiment the triepitope group just could be compared with one of these two groups because of the capacity of materials and executing persons in the lab.

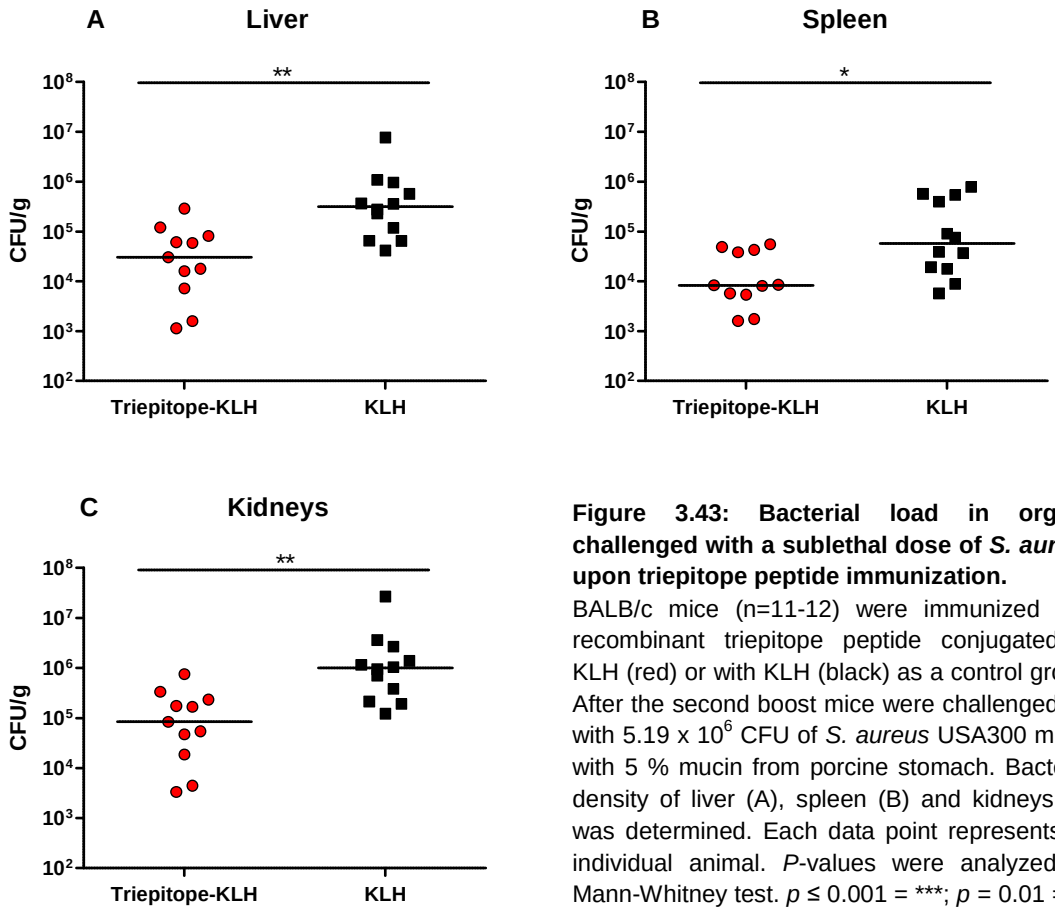

Figure 3.43: Bacterial load in organs challenged with a sublethal dose of *S. aureus* upon triepitope peptide immunization.
BALB/c mice (n=11-12) were immunized with recombinant triepitope peptide conjugated to KLH (red) or with KLH (black) as a control group. After the second boost mice were challenged i.p. with 5.19 x 10^6 CFU of *S. aureus* USA300 mixed with 5 % mucin from porcine stomach. Bacterial density of liver (A), spleen (B) and kidneys (C) was determined. Each data point represents an individual animal. *P*-values were analyzed by Mann-Whitney test. $p \leq 0.001$ = ***; $p = 0.01$ = **; $p \leq 0.05$ = *; ns = not significant.

3.2.4 Construction of recombinant diepitope fusion peptides

3.2.4.1 Cloning, overexpression and purification of diepitope peptides

Because of the reduced protective effect in the sublethal mouse model concerning the hp2160 peptide shown in 3.2.2.1, new fusion peptides were cloned that only included the pOxi epitope- and the Triiso fragment-encoding sequence in different orders. The construct OTO contains pOxi both at the C-terminus and the N-terminus. In the pOT construct pOxi is located at the N-terminus and in TpO at the C-terminus (Figure 3.44). Primers pOxipep senseTriisoN, ASP-C-17-MibIII (pOT), pOxipep senseTriisoN, pOxi-antisenseTriisoC (OTO), SP-Pep5-MibIII, pOxi-antisenseTriisoC (TpO) and peptide 14 as template were used to amplify diepitope sequences.
These diepitope sequences were cloned into pPSG-IBA45 from IBA StarGate fusion cloning system as described in 3.2.3.1 and fused to Strep- and His-tag. The resulting

plasmids were sequenced. One clone without any mutations was chosen, respectively, and transformed in *E. coli* BL21 for expression.

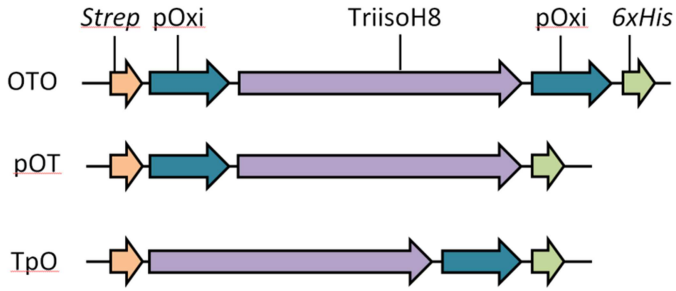

Figure 3.44: Cloning strategy of diepitope fusion-peptides OTO, pOT and TpO. Sequences encoding the epitopes of anti-pOxi moAb D3 and of anti-Triiso moAb H8 (Triiso fragment) were cloned consecutively into pPSG-IBA43 resulting in N-terminal fusion to Strep-tag and C-terminal fusion to His-tag. OTO: Triiso fragment surrounded by C- and N-terminal pOxi epitope; pOT: N-terminal pOxi epitope; TpO: N-terminal pOxi epitope.

Western blot analysis of the bacteria cell lysates after expression ON at 30 °C showed that OTO (14.1 kDa) as well as pOT (12.7 kDa) were overexpressed, but not TpO (12.7 kDa) (Figure 3.45, 3 and 6 in A-C).

Additionally, binding of anti-pOxi moAb D3 (B) and anti-Triiso moAb H8 (C) to overexpressed OTO and pOT was proven by Western blot analysis.

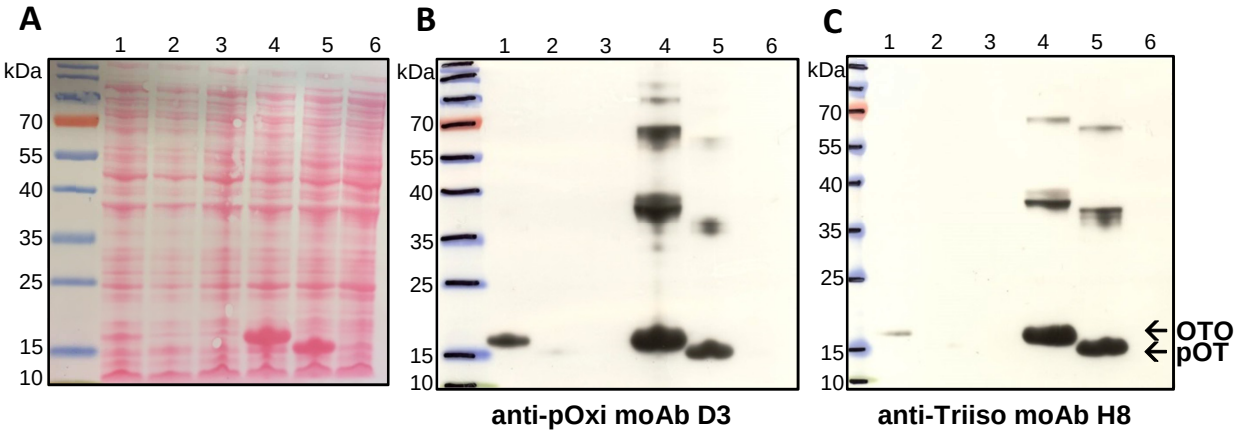

Figure 3.45: Expression of diepitope peptides prior to and post induction. *E. coli* BL21 containing respective plasmid was grown to an OD600 = 0.6 and induced with 1 mM IPTG for an overexpression ON at 30 °C. Lysates were blotted on nitrocellulose. 1 and 4: OTO, 2 and 5: pOT, 3 and 6: TpO. 1-3: prior to induction, 4-6: post induction. A: Ponceau staining, B: anti-pOxi moAb D3, C: anti-Triiso moAb H8. Incubation with goat anti-mouse HRP and development by ECL reagent followed.

The highest amount of OTO as well as pOT was detected in the soluble fraction, in contrast to triepitope overexpression in 3.2.3. So purification via His-tag was performed. Elution fractions were pooled and concentrated (Figure 3.46). A high yield of 25 mg of pOT peptide and 13 mg of OTO peptide was produced (800 ml culture volume). After buffer exchange and sterile filtration peptides were ready for *in vivo* use and stored at 4 °C.

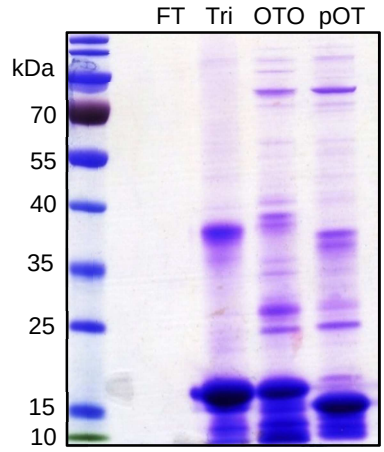

Figure 3.46: Purification of diepitope peptides via His-tag. Coomassie stained SDS-PAGE of purification of OTO and pOT peptides via His-tag after heterologous overexpression. 15 µl of each sample and 7 µl of PAGE Ruler prestained protein ladder was pipetted on the protein gel. IB: inclusion body preparation. FT: flow through. Tri: final triepitope peptide (see 3.2.3) used for immunization. OTO: final OTO peptide. pOT: final pOT peptide.

3.2.4.2 Competition of moAb binding to the antigen by diepitope peptide

To prove the binding specificity of anti-pOxi moAb D3 and anti-Triiso moAb H8 to bind the different diepitope peptides, a competition ELISA was performed (Figure 3.47). Recombinant pOxi as well as Triiso were immobilized to a maxisorp plate. The respective moAb together with different concentrations of one of the diepitope peptides as a competitor (compare to single peptides in 3.1.1, figure 3.2) was added.
As shown in figure 3.47A, the absorbance decreased by increasing the concentration of OTO, as well as pOT. A competition effect of moAb D3 binding to pOxi with both peptides has been proven. With regard to the two curves of OTO and pOT, both peptides showed a similar affinity to moAb D3. At a peptide concentration of 1 mg/ml no binding of moAb D3 to the coated protein was detected anymore. The competition effect of OTO and pOT was even stronger than the competition with the whole protein pOxi.
A competition of the moAb H8 binding to Triiso with both, OTO and pOT was also measured in a dose-dependent manner. However, the competition with the diepitope peptides was not as strong as with the whole protein Triiso (B). With competitor concentrations between 350 and 600 µg/ml, the decrease in absorbance in presence of recombinant Triiso was stronger.

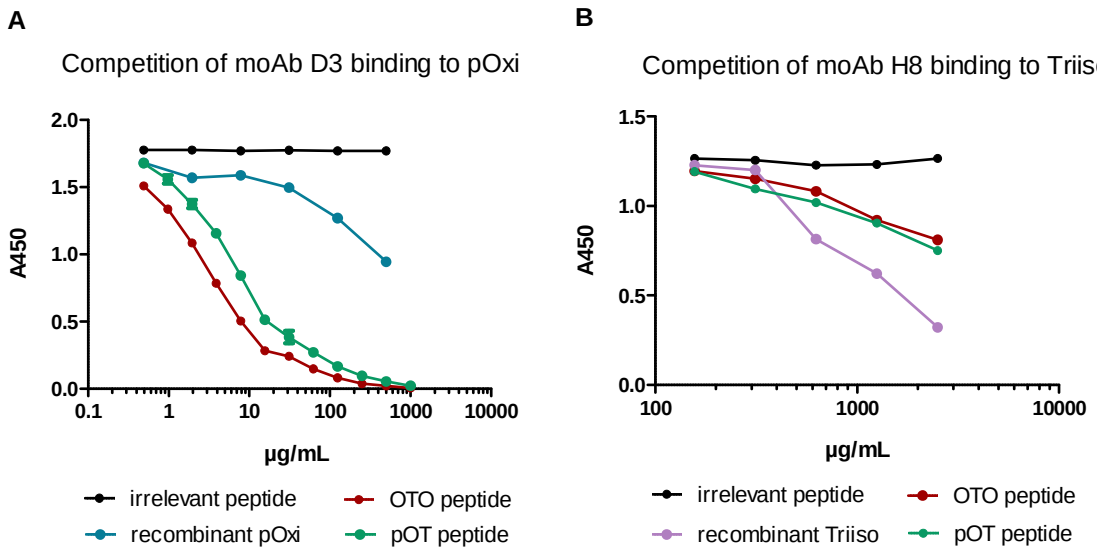

Figure 3.47: Competition of moAb binding to recombinant protein by diepitope peptides. 5 µg/mL of the respective antigen (A: pOxi, B: Triiso) was coated on a maxisorp plate. Respective diepitope peptide was diluted and added to the plate. The respective moAb (A: anti-pOxi moAb D3, B: anti-Triiso moAb H8) was added. Incubation with goat anti-mouse-HRP followed. ELISA was developed using TMB substrate and absorbance was measured at 450 nm.

3.2.4.3 Antigen-specific immune response and significant lower bacterial load in organs of mice immunized with diepitope peptide pOT

After binding and competition analysis of the two unconjugated diepitope peptides using moAbs D3 and H8, an immunization with groups of 10 mice, each following the standard protocol, was performed. The control group was vaccinated with PBS and Freund's adjuvant. The IgG serum titer against recombinant Triiso protein was equal for both constructs. Anti-pOxi IgG titer was slightly lower in the pOT group (Figure 3.48). The serum of the control group was non-reactive for both recombinant proteins (not shown).

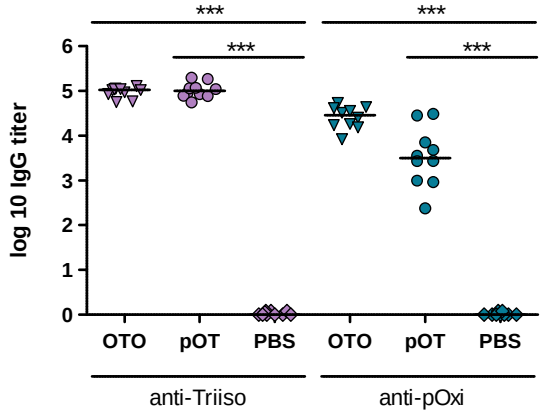

Figure 3.48: Antigen-specific IgG titer after immunization with diepitopes. BALB/c mice (n = 11) were vaccinated with unconjugated diepitope peptides OTO and pOT. Serum of every mouse was collected after the last booster immunization and analyzed for pOxi-, Triiso and hp2160-specific IgGs by ELISA. The IgG titer is given as the dilution corresponding to the half maximal absorbance at 450 nm. Each data point represents an individual animal. *P*-values were analyzed by Mann-Whitney test.

For the i.p. infection of mice 5.4 x 10^6 CFU of *S. aureus* USA300 was used, which was higher as in the former animal experiments. It was observed that the mice tolerated the last used infection doses better and looked healthier as in the previous experiments, without any relieving postures, ruffled fur or diminished activity. The mice were purchased from the ZMMK as in the former *in vivo* experiments. The usage of new infection aliquots of strain USA300 in this experiment did not change these observations.

By CFU determination a higher bacterial clearance was determined in every organ in mice of pOT group in comparison to the control group (Figure 3.49). *P*-values of pOT vs. control group showed significance in all prepared organs (liver: $p = 0.0068$, spleen: $p = 0.0185$, kidneys: $p = 0.0015$). Whereas immunization with OTO peptide did not improve bacterial clearance compared to infected control mice. Therefore, we decided to focus on pOT peptide in the following experiments.

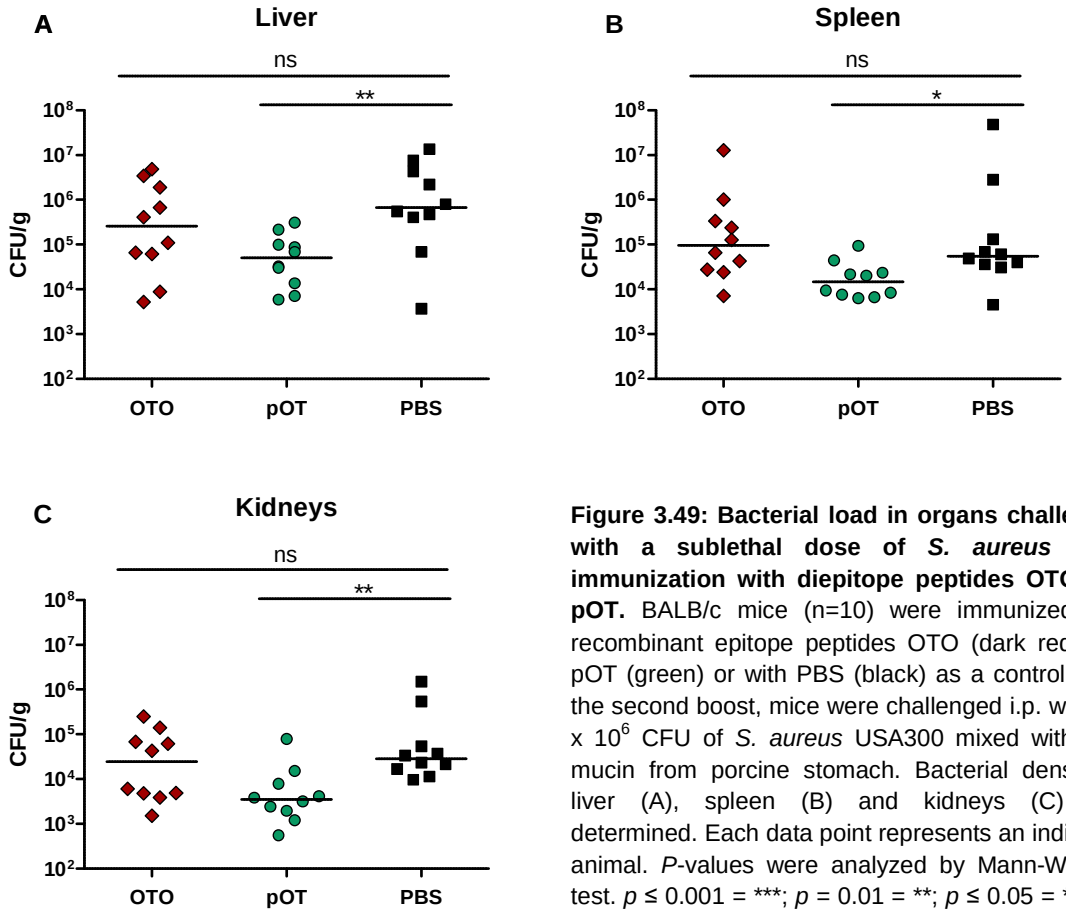

Figure 3.49: Bacterial load in organs challenged with a sublethal dose of *S. aureus* upon immunization with diepitope peptides OTO and pOT. BALB/c mice (n=10) were immunized with recombinant epitope peptides OTO (dark red) and pOT (green) or with PBS (black) as a control. After the second boost, mice were challenged i.p. with 5.4 x 10^6 CFU of *S. aureus* USA300 mixed with 5 % mucin from porcine stomach. Bacterial density of liver (A), spleen (B) and kidneys (C) was determined. Each data point represents an individual animal. *P*-values were analyzed by Mann-Whitney test. $p \leq 0.001$ = ***; $p = 0.01$ = **; $p \leq 0.05$ = *; ns = not significant.

3.2.5 Efficacy of immunization upon sublethal *S. aureus* infection

Table 3.1 presents the results of the described organ-CFU experiments in summary. Except TriisoC4 peptide-conjugate and OTO diepitope, all peptide immunizations led to a lower bacterial load in the prepared organs after *S. aureus* infection. Immunization with the pOxi peptide resulted in the highest significance. The combination of hp2160- and pOxi-conjugate, as well as the triepitope-conjugate and pOT diepitope showed a significant reduced colonization of *S. aureus* with a lower *p*-value in every organ.

Table 3.1: Efficacy of immunization upon sublethal challenge with *S. aureus.* The significance of the analyzed organs of the former described experiments was tabulated for a comparison of the peptide vaccine candidates.

Peptide	Liver	Spleen	Kidneys
Hp2160-KLH	*	Ns	ns
pOxi-KLH	**	***	***
Hp2160-KLH + pOxi-KLH	***	**	*
TriisoC4-BSA	ns	Ns	ns
Triepitope-KLH	**	*	**
Diepitope pOT	**	*	**
Diepitope OTO	ns	Ns	ns

3.2.6 Survival of mice upon lethal challenge with *S. aureus* USA300

In further experiments the survival of mice immunized with peptides of table 3.1 upon lethal challenge with *S. aureus* have been analyzed. Therefore, the inoculum of infection was determined. Groups of mice (n = 10) were immunized with KLH and then i.p. challenged with different doses of strain USA300 + 5 % mucin (Figure 3.50). The infected mice were monitored for six days. After infection with 1.5×10^7 CFU four of ten mice survived. 20 % survived after a challenge with 1.78×10^7 CFU and only 10 % survived after a challenge with 1.6×10^7 CFU.

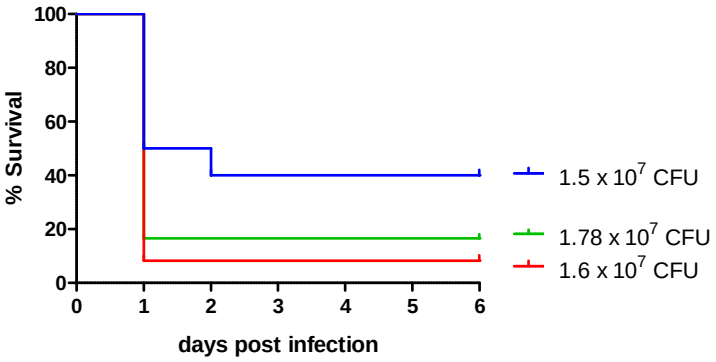

Figure 3.50: Survival of mice challenged with different doses of *S. aureus* upon KLH immunization. BALB/c mice (n=10) immunized with KLH were infected i.p. with 1.5 x 10^7 CFU (blue), 1.78 x 10^7 CFU (green) and 1.6 x 10^7 CFU (red) of *S. aureus* USA300 mixed with 5 % mucin from porcine stomach. Survival was monitored for 6 days.

The titer of 1.5 x 10^7 CFU approaches an LD_{50} and was chosen to be used for following experiments. Except in 3.2.7.1, mice used in following experiments better coped with the chosen titer. Hence, the LD_{50} after an infection with higher doses of strain USA300 was titrated again as shown in figure 3.51 (n = 6). The results showed that four of six mice of the group challenged with 2.9 x 10^7 CFU survived, as well as with 3.01 x 10^7 CFU and only one of six mice survived after a challenge with 3.27 x 10^7 CFU. The highest titer of 3.27 x 10^7 CFU was used for further challenges (see 3.2.7.2).

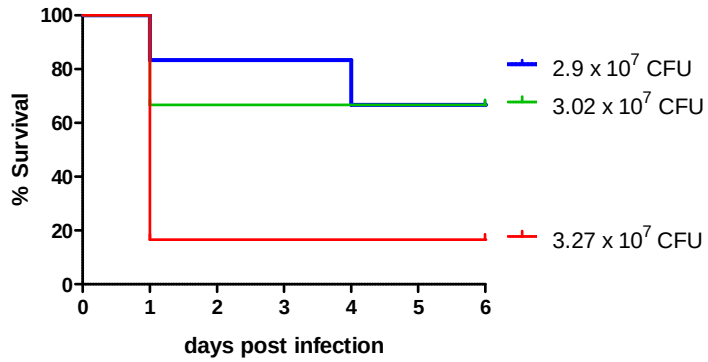

Figure 3.51: Survival of mice challenged with different doses of *S. aureus* upon KLH immunization. BALB/c mice (n=6) immunized with KLH were infected i.p. with 2.9 x 10^7 CFU (blue), 3.02 x 10^7 CFU (green) and 3.27 x 10^7 CFU (red) of *S. aureus* USA300 mixed with 5 % mucin from porcine stomach. Survival was monitored for 6 days.

3.2.7 pOxi epitope and pOT diepitope protect mice from death upon lethal challenge with *S. aureus*

3.2.7.1 Significant protection of mice immunized with pOT-KLH

In 3.2.4 it was determined that immunization with recombinant diepitope-peptide pOT leads to a reduced bacterial colonization in organs of mice after infection with a sublethal dose of *S. aureus*. Compared to OTO it led to statistical better results. The triepitope peptide showed comparable results, but it contains the hp2160 epitope that

was less significant in organ-CFU experiments. So, it was decided to work on first with pOT as a candidate of a higher priority.

In the next step it should be examined, if a pOT immunization also protects mice against a lethal challenge of *S. aureus*. The immunization procedure followed the protocol as explained in figure 3.28.

In order to achieve a stronger immune response, pOT was conjugated to KLH and control group was immunized with KLH alone as unspecific antigen. Compared to 3.2.4, the immune response after the last boost was slightly increased in every mouse serum and constantly distributed.

To reach an LD_{50} the mice immunized with pOT-KLH and KLH were i.p. challenged with 1.2 x 10^7 CFU of strain USA300 + 5 % mucin and monitored for six days.

As shown in figure 3.52, immunization with pOT peptide leads to a survival of 100 % in contrast to only 45.5 % surviving mice in the control group. The experiment also showed significance with a *p*-value of 0.005 determined by Gehan-Breslow test.

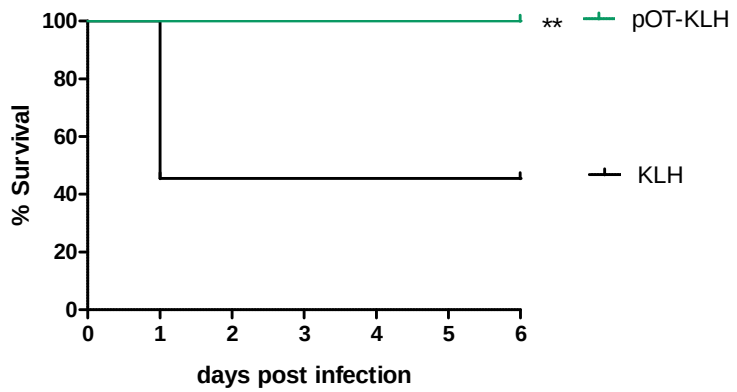

Figure 3.52: Survival of mice challenged with an LD_{50} of *S. aureus* upon diepitope peptide immunization. BALB/c mice (n=11) immunized with pOT-KLH (green) or KLH (black) as a control were infected i.p. with 1.2 x 10^7 CFU *S. aureus* USA300 mixed with 5 % mucin from porcine stomach. Survival was monitored for 6 days. *P*-value was determined by Gehan-Breslow test (p = 0.005).

3.2.7.2 Significant protection of mice immunized with pOxi-BSA compared to pOT-KLH upon lethal challenge with S. aureus

It was proven that the generated diepitope peptide pOT containing pOxi and Triiso epitopes protected mice from death although they received a lethal dose of *S. aureus*. In further survival experiments also the single peptide was tested for a protection effect after immunization. Therefore, a group of mice (n = 11) was immunized with pOxi-BSA and a second group received pOT-KLH. Because of the

different carriers the control group was immunized with a combination of both carrier proteins BSA and KLH.

The initial immunization and the two boosts resulted in a strong immune response: The pOxi peptide achieved a high IgG titer against recombinant pOxi and pOT against both antigens, Triiso and pOxi. The control group showed an immune response against BSA and KLH but was not reactive against the vaccine candidates.

The mice immunized with pOT-KLH, pOxi-BSA and KLH/BSA were then challenged with 3.3 x 10^7 CFU *S. aureus* USA300.

After one day the bacterial burden for the control group was very high, so that 8 mice from 11 died (Figure 3.53). A further mouse died at the second day, so that the control group resulted in a survival of 18 %. In comparison to the control group 90 % of the mice immunized with pOT (p = 0.0017) and 100 % of the pOxi group (p = 0.0001) survived. At the first day after challenge the surviving mice showed an affected phenotype with scrubby fur and weight loss but on the second day they fully recovered.

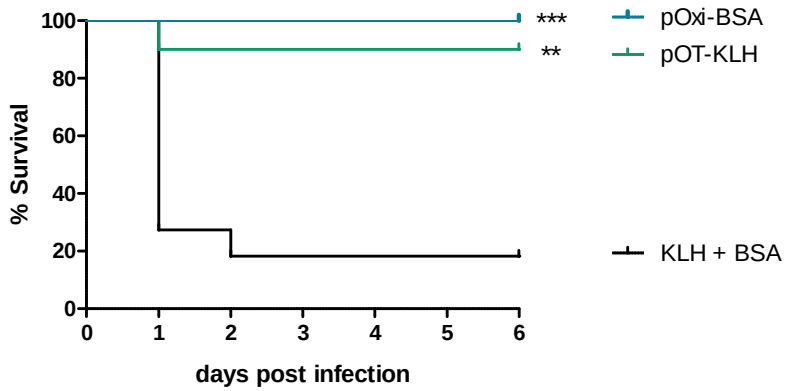

Figure 3.53: Survival of mice challenged with *S. aureus* upon immunization with pOxi-BSA or pOT-KLH. BALB/c mice (n=11) immunized with pOxi-BSA (blue), pOT-KLH (green) or a combination of BSA and KLH (black) as a control group, were infected i.p. with 3.3 x 10^7 CFU *S. aureus* USA300 mixed with 5 % mucin from porcine stomach. Survival was monitored for 6 days. *P*-values were determined by Gehan-Breslow test.

Once again, this experiment underlines the importance of the pOxi epitope as vaccine candidate to achieve a protection against MRSA infection. The diepitope pOT also showed a repetitive protection and will be a good candidate for active immunization. The two peptide candidates will now be tested with alternative adjuvants, which are approved for humans. Once, the epitope of anti-Triiso moAb H8 is determined for a synthesis as single peptide. Mice will be immunized with TriisoH8 peptide for a comparison with the diepitope pOT.

3.2.7.3 Survival of mice immunized with hp2160-BSA and Triepitope-BSA upon lethal challenge with *S. aureus*

In further *in vivo* experiments groups of mice were immunized with hp2160-BSA (n = 10) and BSA (n = 11) as a control. After a challenge with a lethal dose of *S. aureus* only three mice of the control group died, whereas all mice of the hp2160 group survived. This resulted in a non-significant experiment. In a comparable experiment groups of mice (n = 11) were immunized with Triepitope-BSA, pOxi-BSA, hp2160-BSA and BSA, respectively. However, only two of eleven control mice died. One mice of hp2160 group and none of the mice of Triepitope and pOxi groups died which also led to a non-significant result.

3.2.8 Immunization with Modified Vaccinia virus Ankara (MVA) encoding triepitope peptide

With the aim to develop a different and above all established strategy of vaccine-delivery in humans against *S. aureus* we focused on Modified Vaccinia virus Ankara (MVA) encoding our triepitope construct. MVA is a vaccinia virus strain that was generated thirty years ago and used very successful as a vaccine against smallpox (Mayr *et al*., 1964). Our construct was generated by cooperation with the laboratory of Prof. Gerd Sutter (LMU München).

In case of vaccination against *S. aureus* by using MVA as a vector, a recombinant MVA encoding the DNA sequence of the triepitope peptide was generated (MVA-SA-Triepitope). The triepitope peptide was cloned into an MVA shuttle plasmid containing flanking ends to allow recombination into the genome of MVA. Cloning and recombinant MVA generation was performed by the laboratory of G. Sutter according to the strategy of Kremer *et al*. (2012). A second recombinant MVA encoding the triepitope fused with Vaccinia Virus Hemagglutinin (HA) that leads to the presentation of the triepitope on the outer cell membrane of host cells was additionally constructed (MVA-HA-SA-Triepitope). The shuttle vector was then transfected into cells infected with MVA. Through homologous recombination the gene encoding the antigen was inserted into the genome of MVA. MVA-HA-SA-Triepitope was clonally isolated and amplified in chicken embryo fibroblasts.

To verify whether the generated viral vectors are able to express the triepitope peptide, baby hamster kidney (BHK) cells were infected. Cells were lysed and equal amounts of cell lysates were run on a 4-20% polyacrylamide SDS gel. Then proteins were blotted on a nitrocellulose membrane. As a control for equal protein loading, the membrane was incubated with an anti-GAPDH antibody as shown in figure 3.54 (Data provided by M.H.Lehmann and G. Sutter). The triepitope (14.3 kDa) and the HA-SA-triepitope fusion protein (~80 kDa) were detected by Western blot using our anti-pOxi moAb D3 in the cell lysate upon infection of BHK cells with recombinant MVA-SA-Triepitope or MVA-HA-SA-Triepitope, respectively. This confirmed the antigen expression after infection of eukaryotic cells.

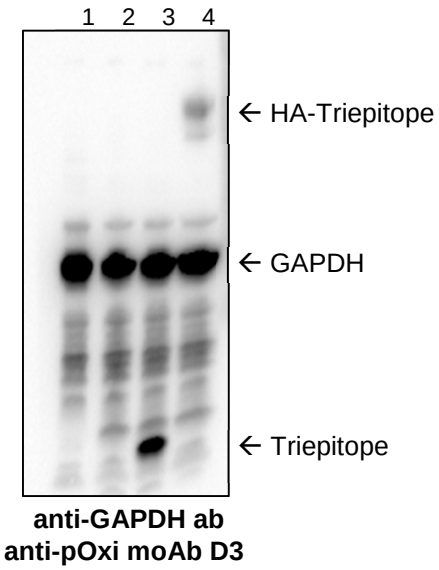

Figure 3.54: Expression of triepitope peptide in eukaryotic cells infected with recombinant MVA viruses. BHK cells were infected with MVA viruses. Cells were lysed and equal protein amounts were blotted on nitrocellulose, followed by incubation with anti-GAPDH and anti-pOxi moAb D3. Detection followed by anti-mouse-HRP. 1: Mock; 2: MVA; 3: MVA-SA-Triepitope; 4: MVA-HA-SA-Triepitope. Data provided by M.H.Lehmann and G. Sutter, LMU München.

To investigate an immune response *in vivo*, groups of mice (n = 3) were immunized intramuscularly with 1 x 10^8 plaque forming units (pfu) of one of the two recombinant MVA constructs, respectively. An adjuvant was not used. According to our conventional immunization model, the mice received an initial immunization and two following boosts with equal amounts of recombinant virus particles.

Serum samples were collected between boosts and IgG titer against the three antigen pOxi, hp2160 and Triiso, as well as against the triepitope peptide were analyzed by ELISA. As shown in figure 3.55A the immunization with MVA-SA-Triepitope resulted in a very weak immune response. The first clear signal was detected after the first boost against Triiso and the triepitope peptide. A very weak signal against pOxi and hp2160 was measured after the second boost.

Immunization with MVA-HA-SA-Triepitope led to a much stronger immune response as shown in figure 3.55B. A first booster immunization is necessary because an IgG titer against the recombinant proteins as well as the triepitope peptide was not detected after the initial vaccination. After the second boost, the titer was only slightly increased compared to the first boost.

In summary, MVA-HA-SA-Triepitope should be used for the following immunizations that will include a challenge with *S. aureus* to look for a protective effect, although the antigen-specific humoral immune response was not as strong as with the triepitope-peptide itself (see 3.2.3.4).

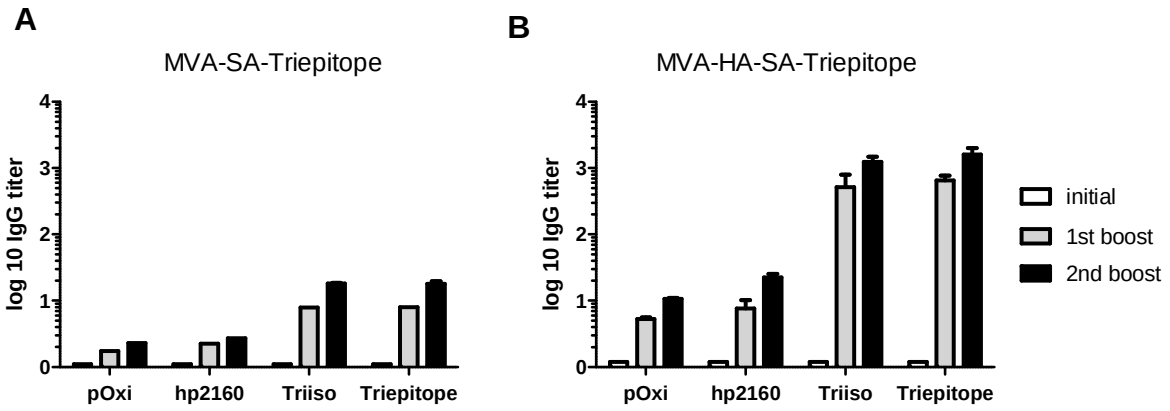

Figure 3.55: Antigen-specific IgG titer after immunization with recombinant MVA vectors encoding triepitope BALB/c mice (n = 3) were vaccinated with 1 x 10^8 pfu of MVA-SA-Triepitope (A) and MVA-HA-SA-Triepitope (B), respectively. Serum of both mice was collected between the immunizations and analyzed for pOxi-, hp2160-, Triiso- and triepitope-specific IgGs by ELISA. The IgG titer is given as the dilution corresponding to the half maximal absorbance at 450 nm.

3.2.9 Immunization with Adeno-Associated-Virus (AAV) encoding the triepitope peptide

In cooperation with the laboratory of Prof. Hildegard Büning (Medizinische Hochschule Hannover) we focused on vector constructs based on Adeno-Associated-Virus encoding the triepitope peptide with the aim to use an additional vaccine platform against *S. aureus*. Two vector constructs were generated: The conventional recombinant AAV (rAAV) containing an expression cassette encoding the triepitope and a capsid-modified rAAV containing the triepitope expression cassette and additionally displays the triepitope on the vector capsid by fusion with the VP2 capsid protein.

In this work AAV serotype 2 (AAV2) was used. A triepitope peptide expression plasmid and a plasmid for expression of the fusion construct of triepitope peptide and viral capsid protein VP2 were cloned using the primers AAV-Triepitop-*Kpn*I Sense and AAV-Triepitop-*Not*I AS and the plasmid IBA-Triepitop (see 3.2.3.1) as template. The restriction sides *Kpn*I and *Not*I were used to insert the triepitope in the plasmid pGFP-Anne. In order to generate the fusion construct of triepitope and VP2 the primers AAV-Triepitop-*Age*I Sense and AAV-Triepitop-*Bsr*GI AS were used introducing *Age*I and *Bsr*GI restriction sides. The amplified triepitope was inserted in the plasmid pEGFP-VP2. Both plasmids were transformed in *E. coli*. Positive clones were picked from agar plates for a colony PCR and plasmids were isolated for a control digest. Figure 3.56 shows the restriction digest of the generated plasmids AAV-pTriepitop-Anne and AAV-pTriepitop-VP2 with *Kpn*I and *Not*I for the detection of the insert (392 bp).

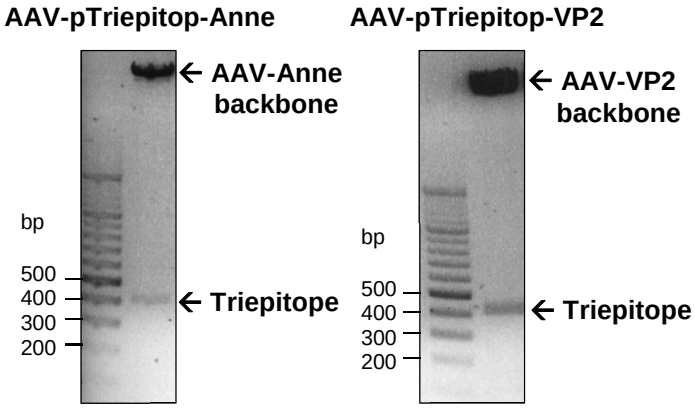

Figure 3.56: Restriction digest of cloned plasmids AAV-pTriepitop-Anne and AAV-pTriepitop-VP2 200 ng of AAV-pTriepitop-Anne was digested with *Kpn*I and *Not*I and 200 ng of AAV-pTriepitop-VP2 was digested with *Age*I and *Bsp*140171. Both are loaded on an 1 % agarose gel. 100 + 500 bp marker was used.

After sequencing the plasmid-DNA was prepared by an endotoxin-free purification kit (Qiagen, Hilden) and the plasmids were sent to AG Büning for AAV packaging and purification. AAV particles were produced in HEK293 cells transfected with either AAV-pTriepitop-Anne or both, AAV-pTriepitop-Anne and AAV-pTriepitop-VP2 and additionally, with the helper plasmids encoding the adenoviral helper functions (helper-virus-free method of Rybniker et al., 2012, see 1.7.3). Cells were lysed and the recombinant AAV's were purified by an iodixanol gradient. The resulting vaccine vectors arrived our lab and were called rAAV2:Tri (unmodified capsid) and rAAV2:TriTri (vector with modified capsid). Genomic and capsid titers of the vector preparations were determined (Table 3.2). The genomic titer determined by RT-PCR

using a primer specific for CMV promotor reveals the number of vector genome containing viral particles per microliter vector solution (data of AG Büning).

The packaging efficiency for the capsid-modified vector rAAV2:TriTri was quantified by calculating the ratio of capsids to genomes and was compared to that of vector rAAV2:Tri containing wild type capsids. The capsid titer, determined by ELISA using an anti-capsid-specific antibody, reveals the amount of capsid (DNA containing as well as empty) per microliter vector solution. The two very similar capsid to genomic particle ratios indicate that incorporation of triepitope peptide into the AAV capsid by fusion to VP2 did not affect the vector packaging efficacy.

Table 3.2: Determination of genomic and capsid titer of generated rAAV vectors All titers refer to the volume of 1 µl. Capsid to genomic particle ratio enables judgement on the quality of the vector preparation in a volume independent manner

Vector	genomic titer (RT-PCR)	capsid titer (ELISA)	capsid titer / genomic Titer
AAV2:TriTri	1.97×10^9	2.73×10^9	1,39
AAV2:Tri	1.93×10^9	2.17×10^9	1,12

To investigate, if the generated vectors are able to express the triepitope peptide, human monocytic cells were transduced with the constructs. Equal amounts of the cell lysates were blotted (Figure 3.57). Anti-β-Actin antibody bound to the housekeeping protein actin was used as a loading control of cell lysates and their blot transfer. With anti-pOxi moAb D3 the triepitope (14.3 kDa) was identified in the lysate of cells transduced with recombinant rAAV2: Tri and rAAV2:Tri:Tri. This verified the antigen expression after transduction of eukaryotic cells.

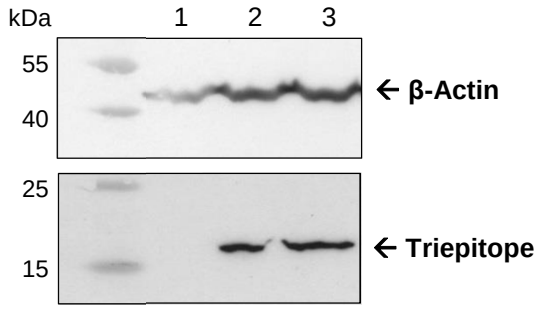

Figure 3.57: Expression of triepitope peptide in eukaryotic cells transduced with recombinant AAV2 viruses. Human monocytic cells were transduced with rAAV viruses. Cells were lysed and blotted on nitrocellulose, followed by incubation with anti-pOxi moAb D3 and anti-β-Actin antibody. Detection with anti-mouse-HRP. 1: cells not transduced; 2: transduced with rAAV2:Tri; 3: transduced with rAAV2:TriTri.

To investigate the capsid protein composition, denatured capsids of the vector AAV2:TriTri containing the VP2-triepitope fusion and the conventional vector AAV2:Tri containing the wildtype capsid denatured capsids of both virus-constructs

were blotted and immunostained with one of the three respective moAbs anti-Triiso H8, anti-pOxi D3, anti-hp2160 16-2 and with mouse anti-AAV capsid protein antibody B1 that binds a sequence located at the C' terminus of all AAV capsid proteins (Figure 3.58), respectively. The triepitope-VP2 fusion protein with a size of nearly 86.3 kDa was detected with all three moAbs. As expected, AAV2:Tri with the wildtype capsid did not show any binding signals with the anti-triepitope antibodies. The capsid proteins VP1 (90 kDa), VP2 (72 kDa), VP3 (60 kDa) of AAV2:Tri were detected by B1 antibody. The VP2 protein showed a different molecular weight because of the fusion with triepitope peptide

72 kDa in the preparation of vectors with wild type capsid was ablated and a band with a size of about 100 kDa corresponding to the fusion of triepitope and VP2 protein was detected. As expected, detection of the fusion protein by B1 antibody was unclear because of similar molecular weights of VP1 (90 kDa) and the fusion protein (86.3 kDa).

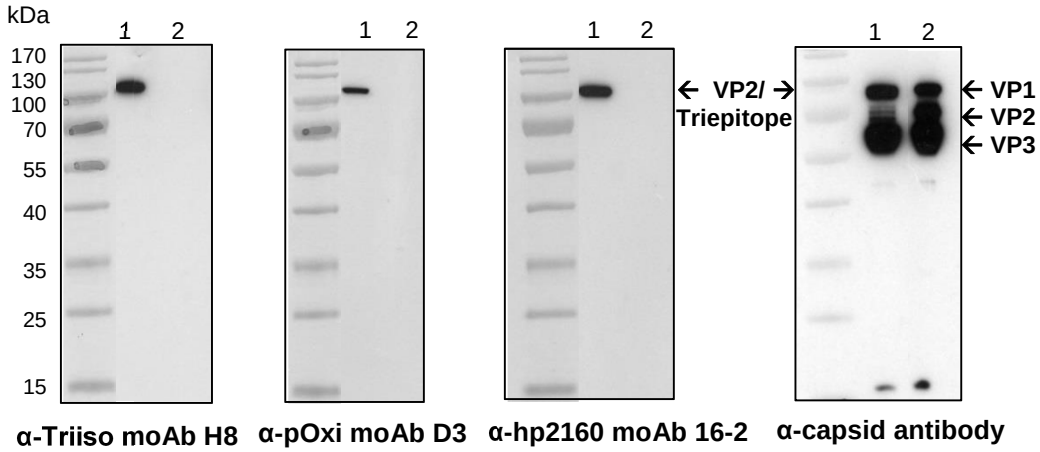

Figure 3.58: Western Blot of recombinant AAV2 vector preparations encoding triepitope peptide
1 x 10^9 of denatured vector capsids per preparation were blotted on a nitrocellulose membrane in order to analyze capsid composition and a possible incorporation of the VP2-triepitope fusion protein. The blots were incubated with the respective moAb and with capsid-specific B1 antibody. The band with a size of 83.3 kDa corresponds to the fusion protein. 1: rAAV2:TriTri (capsid modified vector); 2: rAAV2:Tri (conventional vector).

To investigate the potency of the generated AAV2 vectors to induce an antigen-specific immune response, groups of mice (n = 2) were initial vaccinated intramuscularly with 1 x 10^{10} pfu of AAV2:Tri and AAV2:TriTri, respectively, followed by a two booster immunizations. Unfortunately, no antigen-specific immune response was detected in the group immunized with AAV2:Tri (data not shown). With AAV2:TriTri a very weak immune response after the 2nd boost against Triiso and the

triepitope was measured as shown in figure 3.59. A pOxi- or hp2160-specific IgG titer was not measureable.

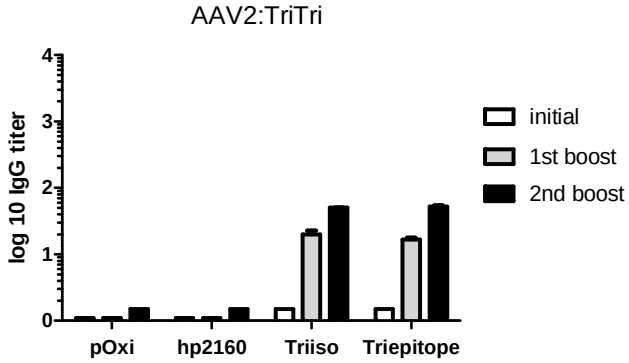

Figure 3.59: Antigen-specific IgG titer after immunization with recombinant AAV vectors encoding triepitope BALB/c mice (n = 2) were vaccinated i.m. with 1 x 10^{10} pfu of AAV2:TriTri. Serum of both mice was collected between the immunizations and analyzed for pOxi-, hp2160, Triiso- and triepitope-specific IgGs by ELISA. The IgG titer is given as the dilution corresponding to the half maximal absorbance at 450 nm.

3.2.10 Analysis of T-cell response upon vaccination with pOT-KLH and triepitope-KLH

Vaccination with triepitope-KLH resulted in a higher bacterial clearance upon sublethal *S. aureus* challenge and pOT vaccination protected mice from dead upon lethal challenge. Both peptides resulted in a high antibody production. In the following experiment we were interested in the T-cell response upon active immunization with triepitope- and pOT-KLH (n = 5). At this time, the single peptides were not available as KLH conjugates in our lab. Immunization with BSA conjugates resulted in a re-stimulation of splenocytes with medium containing fetal calf serum alone. Hence, these conjugates were excluded from these experiments.

Before T-cell response was investigated, the antigen-specific titer of IgG subclasses in sera of mice and the IgG1 / IgG2a ratio was analyzed first because it gave a hint to the dominant class of helper T-cells. In this case, a higher IgG1/IgG2a ratio reveals a Th2 response and a lower ratio reveals a Th1 response.

Twelve days after the last boost blood was collected, the specific IgG1 and IgG2a titer were determined by ELISA and the ratio between IgG1 and IgG2a titers was calculated. The respective proteins hp2160, pOxi and Triiso were immobilized, as well as triepitope and pOT peptides. The respective subclass was detected by anti-mouse IgG1- or IgG2a-HRP. As presented in figure 3.60, the ratio of pOT-KLH immunized mice was lower, in contrast to triepitope-KLH immunized group.

Triepitope-KLH immunization resulted in a higher IgG1/IgG2a ratio, but also in a higher spread within the group.

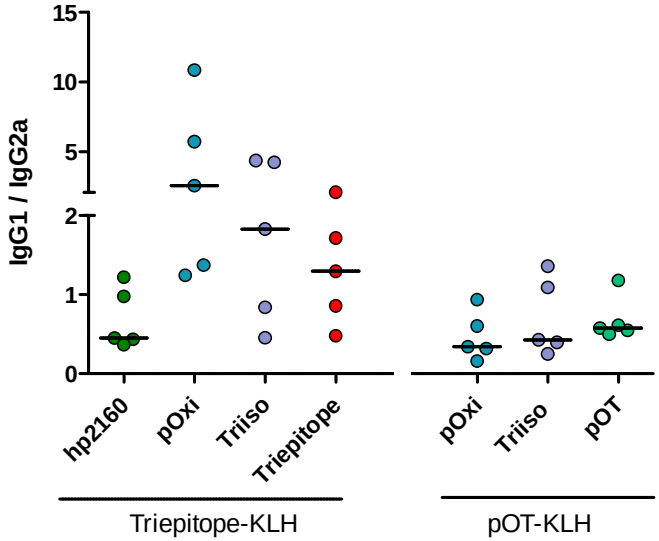

Figure 3.60: Ratio of antigen-specific IgG1 and IgG2a titer upon immunization with triepitope-KLH and pOT-KLH. BALB/c mice (n = 6) were immunized with triepitope-KLH and pOT-KLH, respectively. IgG subclasses in serum were determined by ELISA. Recombinant proteins or polyepitope peptides were immobilized. After incubation with serum detection with anti-mouse IgG1- and IgG2a-HRP followed.

Two weeks after the last boost, splenocytes were isolated aseptically, cultivated and re-stimulated with unconjugated pOT, triepitope, pOxi and hp2160 epitope peptides, respectively. Because both pOT and triepitope contain the pOxi and the discontinuous Triiso epitope, both of them were used for re-stimulation of splenocytes derived from mice immunized with triepitope-KLH, pOT-KLH and KLH. Splenocytes from KLH immunized mice function as a negative control. Cell culture medium without any stimulus was used as a second negative control. The protein concavalin A (ConA) that functions as a mitogen was used as positive control for the stimulation of splenocytes.

Cell proliferation was measured using BrdU cell proliferation assay kit. The synthetic nucleoside bromodeoxyuridine (BrdU) is thereby incorporated into newly synthesized DNA of replicating cells by substitution of thymidine. With an antibody specific for BrdU the incorporated chemical was detected, thus indicating cells that were replicating their DNA and therefore proliferating. Immunization with triepitope-KLH resulted in a significantly increased proliferation of splenocytes stimulated with triepitope, pOT- and pOxi peptide, respectively, compared to the same group of splenocytes stimulated with medium and compared to triepitope stimulated cells isolated from KLH immunized mice (Figure 3.61). Immunization with pOT-KLH

resulted in a stronger cell proliferation of splenocytes after stimulation with pOT, triepitope and pOxi peptide. Compared to medium stimulated cells these results were not significant because of an unexpected increased cell proliferation in medium control. Compared to pOT stimulated cells from KLH immunized mice, cell proliferation was significantly increased.

Altogether, a re-stimulation with the respective unconjugated epitope peptides induced a proliferation of splenocytes derived from mice immunized with triepitope-KLH and pOT-KLH. Splenocyte proliferation from mice immunized with KLH alone was not induced after addition of epitope peptides.

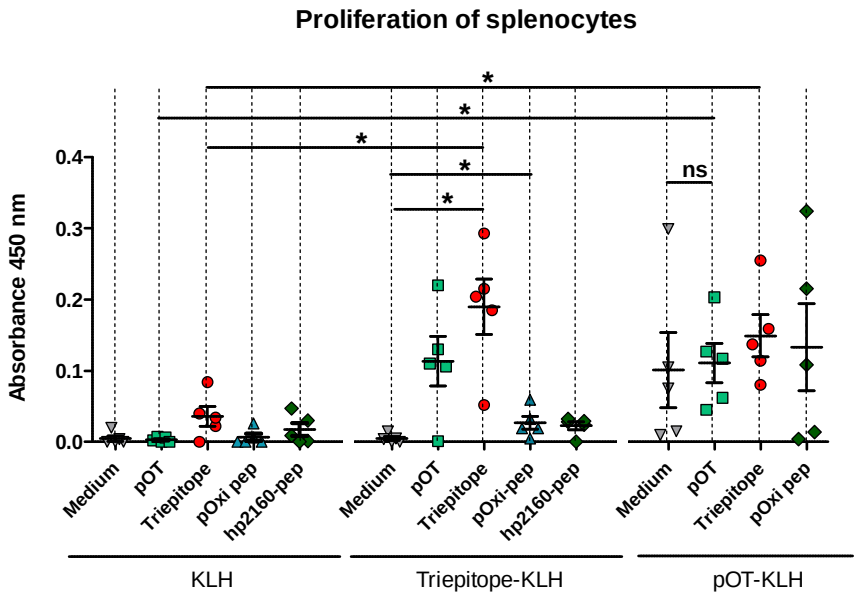

Figure 3.61: Proliferation of splenocytes derived from triepitope-KLH, pOT-KLH and KLH vaccinated mice (n = 5). Cell proliferation after 72 h stimulated by triepitope-, pOT-, pOxi- and hp2160-peptides, respectively, was used as readout for cellular immune activation. Proliferation of splenocytes was quantified by BrdU cell proliferation assay kit. Unpaired two-tailed t-test: ***, $p \leq 0.001$; **, $p \leq 0.01$; *, $p \leq 0.05$.

The cytokines Interferon-gamma (IFN-γ), IL-4 and IL17A secreted in the supernatant of the stimulated splenocytes were quantified by DuoSet ELISA. Cellular immune activation was assessed as epitope peptide-stimulated cytokine release. As presented in figure 3.62, splenocytes from those mice immunized with triepitope-KLH, as well as pOT-KLH revealed a significantly higher cytokine secretion after re-stimulation with the respective unconjugated epitope peptides, compared to the KLH immunized control group.

Unconjugated pOT and triepitope, as well as unconjugated pOxi and hp2160 peptides were used as stimuli. The latter was not used for re-stimulation of splenocytes from pOT-KLH immunized mice because pOT does not contain the hp2160 epitope.

A strong release of IFN-γ was measured after 72 h indicating Th1-cell or/and $CD8^+$ T-cell proliferation (A). Unexpectedly, both unconjugated triepitope and pOT peptides stimulated IFN-γ release of splenocytes from KLH immunized mice. However, splenocytes of mice immunized with triepitope-KLH, as well as pOT-KLH induced a significantly stronger IFN-γ release post triepitope and pOT stimulation. The smaller unconjugated pOxi epitope and hp2160 epitope peptides were also able to induce an IFN-γ release. With pOxi peptide the production of IFN-γ was significantly increased compared to IFN-γ production of splenocytes from the KLH control group.

A moderate release of IL-4 was measureable upon stimulation indicating a Th2-cell response. Compared to IFN-γ, the detection of an IL-4 concentration in the medium supernatant upon re-stimulation was more difficult (B). However, a significantly higher IL-4 secretion of splenocytes derived from triepitope-KLH and pOT-KLH immunized mice after re-stimulation with both unconjugated peptides was measured. Splenocytes from KLH immunized mice were non-reactive to re-stimulation. The unconjugated single pOxi- and hp2160 peptides were not able to induce a strong Th2 response. The unconjugated single pOxi- and hp2160 peptides were not able to induce strong IL-4, as well as IL-17A releases (B-C).

Re-stimulation with triepitope and pOT resulted in a strong IL-17A production (C). IL-17A is produced by Th17- and γδ-cells. Splenocytes of KLH immunized mice only showed a moderate IL-17A level post stimulation with triepitope and pOT, respectively. IL17-A release of splenocytes from triepitope-KLH immunized mice was stronger post stimulation with triepitope and significantly stronger with pOT. Splenocytes of one mouse did not release IL-17A post stimulation with triepitope peptide, which led to the non-significance.

A significantly higher IL-17A level was measured after re-stimulation of splenocytes derived from mice immunized with pOT-KLH in contrast to KLH.

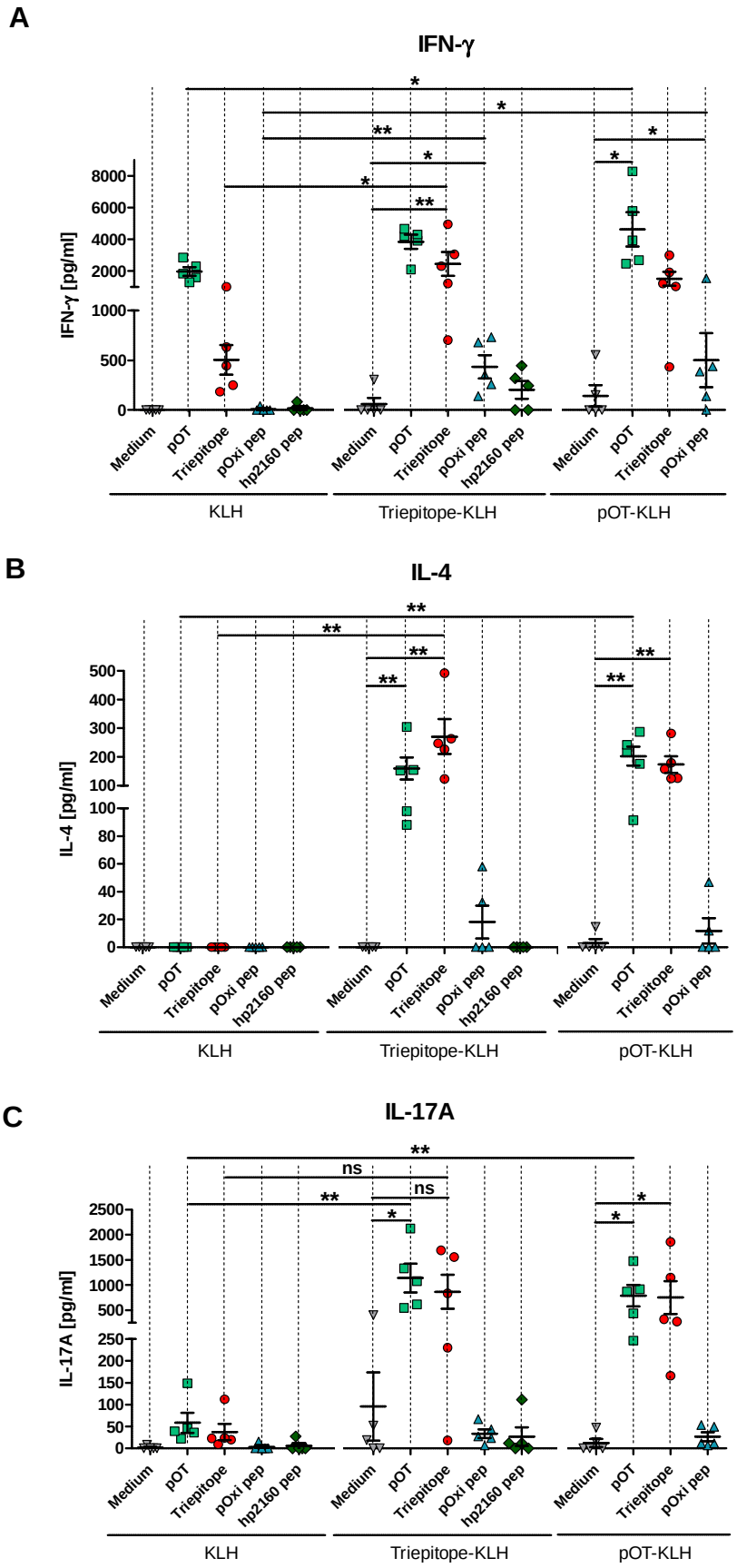

Figure 3.62: Cytokine levels measured in cell culture supernatants of splenocytes derived from Triepitope-KLH, pOT-KLH and KLH vaccinated mice (n = 5). Cytokine release after 72 h stimulated by Triepitope-, pOT-, pOxi- and hp2160-peptides (pep), respectively, was used as readout for cellular immune activation. Cytokines were quantified by ELISADuoSet. A: IFN-gamma release; B: IL-4 release; C: IL-17A release. Unpaired two-tailed t-test: ***, $p \leq 0.001$; **, $p \leq 0.01$; *, $p \leq 0.05$.

In summary, immunization with triepitope-KLH resulted in higher IgG1/IgG2a ratios detected in mouse sera, whereupon a higher spread within the groups was detected. In contrast IgG1/IgG2a ratio was much lower.

Immunization with triepitope-KLH, as well as pOT-KLH led to a strong proliferation of splenocytes after re-stimulation with epitope peptides. The Th ($CD4^+$) -cell directed immune response is predominantly Th1-directed (cellular) as represented by high concentrations of IFN-γ. However, IL-4 (Th2-directed response) and IL-17A releases (Th17-directed response) have also been detected.

4 Discussion

The genetic diversity and the ability to acquire new exogenous genes allow *S. aureus* to adapt to a variety of changing environmental conditions and to modulate its pathogenicity. *S. aureus* causes a broad spectrum of diseases, reaching from minor skin infection to life-threatening blood stream infections (Lowy, 1998, Diekema *et al*., 2001). Multidrug resistance of the hospital- and community-associated strains of this pathogen is increasing and thereby limiting therapeutic options, up to the point where none of the antibiotics will work and alternative strategies are indispensable. Vaccination as therapy and prophylaxis would be an expedient alternative, but there is currently no vaccine available. All active and passive immunization approaches to date have failed at the clinical trial stage. These approaches or those, who are currently passing through clinical trials, concentrated on well-known virulence factors, including proteins exhibiting the LPXTG sorting signal. LPXTG proteins are cell wall-anchored and often covalently linked to peptidoglycan (Foster and Hook, 1998), such as clumping factor A (ClfA) or iron-regulated surface determinants (Isd) (DeJonge *et al*., 2007; Fowler *et al*., 2013).

Alternatively, a growing number of classical cytoplasmic proteins are described to be found on the surface of microbial pathogens. These non-covalently bound cell wall-associated proteins are involved in metabolic pathways but also in adhesion or binding of e.g. blood components, which turns them into virulence factors (Pancholi and Chhatwal, 2003). Glowalla *et al*. (2009) identified novel anchorless cell wall proteins that lack the conserved LPXTG signal sequence. They were identified in the cell wall-associated protein extract by performing a subtractive proteome analysis with human IgG solution (IVIG) of healthy donors, which contains antibodies against these candidates (see 1.5). Several of them were produced as recombinant proteins and tested in a murine active immunization model with a consecutive *S. aureus* challenge. This resulted in the discovery of the lead vaccine candidates Triiso, pOxi and hp2160 that showed the strongest protection against *S. aureus* infection. Monoclonal antibodies against the lead candidates were generated by hybridoma technology of which anti-pOxi moAb D3, anti-Triiso moAb H8 and anti-hp2160 moAb 16-2 revealed protection in a murine sepsis model upon passive immunization (A. Klimka, unpublished data; see 1.5.3).

The present work focused on the characterization of these generated antigen-specific monoclonal antibodies, their epitope identification and application as active vaccine. MoAb binding to the respective antigen has been shown by varying the *in vitro* growth conditions. The mode of action of anti-pOxi moAb D3 and anti-Triiso moAb H8 leading to their protective effect has been investigated together with the function of the identified vaccine candidates as moonlighting proteins. Triiso and pOxi are well-known cytoplasmic proteins. Beside their cytoplasmic function, moonlighting proteins are described to have one or more different functions on the bacterial surface (Jeffery, 1999). A contribution of pOxi to host cell adhesion and an inhibition of this by anti-pOxi moAb D3 was demonstrated.

Furthermore, the moAb epitopes have been identified and verified. The epitope application as active peptide vaccine in the preclinical mouse model induced strong antigen-specific humoral and T-cell mediated immune responses and gave a protective effect against MRSA. The epitope of anti-pOxi moAb D3, as well as a diepitope fusion (bivalent vaccine) of anti-pOxi moAb D3 and anti-Triiso moAb H8 epitopes were identified as candidates with the strongest protective potential. A humoral immune response with the viral vector platforms MVA and AAV as alternative vaccination strategy has been detected and will be followed as these are encouraging results to proceed with the development of an efficient vaccine to prevent MRSA infection in human risk patients.

4.1 Epitope characterization of protective monoclonal antibodies

After identification of the novel cell wall-associated proteins Glowalla *et al*. (2009) started to use the whole, recombinant proteins as active vaccines, of which some already achieved protection against *S. aureus* infection. In this work the principle of peptide immunization was demonstrated. Whereas only a few immunodominant epitopes are sufficient to induce a protective effect, whole antigens contain many epitopes that are not necessary or even may be detrimental because they are immunodominant but not protective, which makes the antigen less potent as a peptide vaccine (Otto, 2010; Correia *et al*., 2014).

B-cell epitopes have already been used as vaccine candidates against *S. aureus* infection. In recent studies Zhao and colleagues (2015) designed a polyepitope vaccine composed of B-cell epitopes of enterotoxin B (SEB) and showed protection

against MRSA with some of them. For B-cell epitope mapping of SEB they used an overlapping 18-mer peptide ELISA, which was incubated with sera of mice immunized with recombinant SEB and infected with strain MRSA 252. The same procedure was used by Yang *et al*. (2016), who identified some immunodominant B-cell epitopes of manganese transport protein C, which provided protection against *S. aureus* infection.

In the present work a “reverse immunology” approach was described using the protective monoclonal antibodies as a “pathfinder” towards potentially highly efficient peptide vaccines in terms of their respective epitopes. Active immunization with correctly identified epitopes of these lead candidates of passive immunization should provide a stronger protection as obtained with the whole antigen.

The epitopes of moAb D3, as well as moAb 16-2 have been clearly identified by microarrays as the linear sequences *KND**Q**DV**ER**FFYK* (hp2160 epitope peptide, essential amino acids in bold) and *TDNELVS**I**VR**R**D* [(pOxi epitope peptide, essential amino acids in bold) Fig. 3.1]. Both epitopes have been verified by competitive ELISA using the synthesized peptides, which was a relevant result for the upcoming animal trials (Fig. 3.2). With an alanine scan we got a closer look to the amino acids that are essential for binding of the respective moAb (Fig. 3.3). In addition, the linear epitope of anti-Triiso moAb C4 was identified and verified within the peptide *LADLGVKYVVIGHSERRELFHETD*. Compared to anti-Triiso moAb H8, anti-Triiso moAb C4 was identified as a candidate with a lower protective effect in the passive immunization model. It has been used to investigate, if its epitope would be an alternative to the unidentified discontinuous epitope of the lead candidate moAb H8. The three identified epitopes are conserved in different *S. aureus* strains, but not found in different species like *S. epidermidis* or in other gram-positives as *B. subtilis* (data not shown). These findings indicate that our moAbs and antibodies generated by active immunization with the identified epitopes are acting against different strains of *S. aureus*, but not against different species. In humans three isoforms of Triiso are found that completely differ to *S. aureus* Triiso concerning their amino acid sequences (data not shown). In humans pOxi has only 21 % similarity to *S. aureus* pOxi. The pOxi epitope was not identified. Both findings exclude a cross-reaction of anti-Triiso moAbs, as well as anti-pOxi moAb D3 to the human proteins. The fact that the three antigens were identified by using a preparation of naturally occurring IgGs derived from healthy humans also ensures that we do not expect a cross-reaction to

human tissues. During clonal selection of B-cells autoreactive lymphocyte clones are deleted before they develop into fully immunocompetent cells (Burnet, 1962).
The indistinct microarray analyses of anti-Triiso moAb H8 supported a discontinuous epitope. A discontinuity is characterized by a cluster of residues that are brought together by the folding of a polypeptide chain (Arnon and van Regenmortel, 1992).
The discontinuity of the epitope of moAb H8 has been proven by our first fragment cloning experiments, where moAb H8 was not able to bind neither a C-terminal nor N-terminal fragment of Triiso (Fig. 3.5). However, with the following fragment constructions of Triiso the epitope of moAb H8 has been verified within a smaller protein fragment of 11 kDa. According to Sharon *et al*. (2014) a B-cell epitope can contain between two up to 34 residues. Because the generated Triiso fragment is with 105 residues too large for an economical synthesis, a closer verification of the epitope of moAb H8 has been initiated. The identification of the amino acids, which are essential for the moAb's binding could reduce production costs and would be advantageous for our further experiments. Further binding analyses of moAb H8 with the remaining Triiso fragment will follow by CLIPS technology of Pepscan, where peptides structurally fixed into defined three-dimensional structures (Timmerman *et al*., 2007).

4.2 Binding of anti-pOxi moAb D3 to staphylococcal pOxi

Binding analysis of anti-pOxi moAb D3 to pOxi showed some unexpected results. In contrast to the binding of moAb D3 to recombinant pOxi (Fig. 3.6), it was not possible to detect binding to pOxi from both, surface-associated protein fractions (neCWS) and whole cell lysate (WCL) in Western blot analyses (Fig. 3.7). Different growth phases in LB medium were tested because we assumed a dependence of the expression rate of pOxi as surface protein, but this did not improve the results. Obviously, the problem with this kind of measurement was that *in vitro* growth conditions of *S. aureus* are different to *in vivo* growth conditions. For example, the expression of several virulence factors, such as hemolysins, enterotoxins, proteases, and iron acquisition factors in growth media, such as LB or TSB is quite different from the expression in an *in vivo* situation (Oogai *et al*., 2011). Thus, all performed measurements using *in vitro* grown *S. aureus* are very likely to differ from *S. aureus*' activities *in vivo*. This seems to be crucial for the conclusions drawn from our

experiments and it is therefore important to simulate *in vitro* the *in vivo* conditions as well as possible. For further analyses flow cytometric analyses were conducted, which confirmed a strong binding of moAb D3 to the surface (Fig. 3.8A). These binding analyses were done with *S. aureus* wildtype strain, with the addition of a human Fc fragment to block IgG-binding of protein A.

Binding analyses using wildtype strains were already described for moAbs generated by other groups. For example, surface expression of the protein IsdB was identified by the strong binding of an anti-IsdB moAb to a *S. aureus* wildtype strain (Kuklin *et al*., 2006). However, our following flow cytometric binding analyses using a *S. aureus* protein A deletion mutant (Δ*spA*) showed that a huge part of moAb binding to wildtype was non-specific. Obviously, only a small part of protein A was blocked by using human Fc fragment. This was shown by a competition with the pOxi epitope peptide, which only moderately decreased the strong binding of moAb D3 to the wildtype. Especially, anti-pOxi moAb D3, which was identified as antibody of IgG2a subclass shows high affinity to protein A.

Further FACS analysis with moAb D3 and whole *S. aureus* Δ*spA* cells showed a moderate binding signal. This weak signal was completely competed by pOxi epitope peptide, suggesting the specific binding of moAb D3 to pOxi on the surface of Δ*spA* (Fig. 3.8B). This notion is supported by the identification of pOxi as a surface protein with polyclonal pOxi-specific antibodies existing in a human immunoglobulin solution (IVIG). The strongest binding of moAb D3 to surface localized pOxi was shown at an OD of 0.3, but lower binding was also detected in early and late-exponential growth phases, indicating that pOxi is mainly required at the surface during exponential growth. A possible reason for the non-detection of pOxi in neCWS and WCL (described above) would be the amount of pOxi in these fractions and the method's sensitivity. Flow cytometry is known to be a more sensitive way compared to Western Blotting allowing the identification of low amounts of pOxi at the *S. aureus* surface. A look at subtractive proteome analysis of anchorless cell wall proteins performed by Glowalla *et al*. (2009) shows also only a very weak spot for pOxi.

It is important to emphasize that pOxi could be detected with moAb D3 in the isolated and precipitated cell wall associated protein fraction blotted on nitrocellulose when *S. aureus* was grown under biofilm conditions, (Fig. 3.12B). Biofilm conditions imply a longer growth of approximately 24 hours without shaking (Cramton *et al*., 1999). Hence, the bacteria are in a late stationary phase with highly produced amounts of

biomass (Foulston *et al*., 2014), which obviously increases the amount of pOxi and making it therefore amenable for Western blot analysis.
In flow cytometric measurements binding of moAb D3 to *S. aureus* surface after biofilm growth and competition by pOxi epitope peptide does not differ from those results that were obtained after planktonic growth (Fig. 3.13D).
Altogether, these investigations established specific binding of anti-pOxi moAb D3 to the cell-wall associated protein fraction, as well as to the surface of whole *S. aureus* cells.

4.3 Binding of anti-Triiso moAb H8 and anti-hp2160 moAb 16-2

Both Triiso and hp2160 from *S. aureus* have been identified with their respective moAb in the non-enzymatically isolated cell wall protein fraction (neCWS), as well as in the cell lysate (Fig. 3.7). Concerning Triiso, an occurrence at the surface of *S. aureus* has already been proven by proteome analysis (Gatlin *et al*., 2006). Additionally, further glycolytic enzymes were identified on the *S. aureus* surface, such as GAPDH and enolase (Pancholi and Fischetti, 1992).
In contrast to pOxi, both Triiso and hp2160 were not detectable with their respective moAb at the surface of *S. aureus* Δ*spA* by flow cytometry after planktonic growth (Fig. 3.9). Although both antibodies belong to subclass IgG1, different binding affinities to protein A were detected. Whereas anti-Triiso moAb H8 showed high affinity to protein A, no binding of anti-hp2160 moAb 16-2 to the wildtype was detected. Some other generated moAbs were also tested. Two anti-Triiso moAbs C4 (lower protective efficacy as moAb H8) and C8 (non-protective) showed a weak binding to *S. aureus* (Fig. 3.10). Compared to moAb H8, the two epitopes recognized by moAb C4 and C8, respectively, are located at a different site of the Triiso molecule. A quite similar affinity to Triiso with moAb C4 was observed, compared to moAb H8 (data not shown). For this reason and because Triiso is a well-known surface associated protein, the only explanation for the non-binding of moAb H8 after planktonic growth was that its epitope or a part of its eptiope is not accessible at the bacterial surface under these growth conditions. The same was assumed for the epitope of anti-hp2160 moAb 16-2. In Western blot analyses Triiso and hp2160 are detached from the surface and denatured, which would explain the binding signals under these conditions.

In comprehensive flow cytometric analyses different growth conditions of *S. aureus* were analyzed. It was not possible to improve the binding of moAb H8 and 16-2 to *S. aureus* harvested at different growth phases (Fig. 3.9B-C), although it is known that many virulence factors are differently expressed at exponential and stationary growth phase (Loughman *et al*., 2009; Matsuo *et al*., 2011). Different culture media as TSB and RPMI have also been tested, as well as human serum to simulate *in vivo* conditions. Kuklin *et al*. (2006) showed that the surface expression of the protein IsdB is regulated by iron and therefore used different media, such as RPMI as iron deficient medium. Oogai *et al*. (2011) described an increased expression of surface occurring virulence factors after growth in serum. However, we did not detect any differences in binding intensity of moAbs, when serum grown *S. aureus* was used for FACS analysis. We conclude that these diverse planktonic growth conditions do not improve *in vitro* binding of our moAbs.

Foulston *et al*. (2014) described that the matrix of biofilms comprises cytoplasmic proteins that are released from *S. aureus* cells and associate with the bacterial surface in a pH-dependent manner. They determined that biofilm matrix formation is triggered by a decrease in pH during mid-exponential phase in biofilm-inducing medium. This assembly process is reversible after manual disruption of the biofilm and increasing the pH.

An upregulation of gene expression of *tpiA* encoding Triiso under biofilm growth conditions in contrast to planktonic growth has already been demonstrated by Becker *et al*., 2001. Therefore, we also tried biofilm conditions (TSB medium supplemented with glucose, growth without shaking) in our *in vitro* experiments. First, biofilm viability was measured by crystal violet staining according to the protocol of O'Toole (2011). In addition to the strains available in our lab, three clinical isolates were tested. For USA300 and MW2 the ability to biofilm formation was already known (Periasamy *et al*., 2012). Besides one of the clinical isolates, all strains were competent to form biofilms under these conditions (Fig. 3.11). A protein A deletion mutant derived from *S. aureus* HG003 was proven to be unaffected in its ability to form biofilms (Foulston *et al*., 2014), which matches the results obtained with our Δ*spA* mutant. The pH measured in biofilm cultures after 24 hours was acidic (pH 5), which also concurs with the findings of Foulston and colleagues.

After biofilm growth of *S. aureus* Δ*spA* a surface binding of anti-Triiso moAb H8, as well as anti-hp2160 moAb 16-2 have been detected by flow cytometry (Fig. 3.13).

After biofilm growth bacteria cells were fixed to prevent the protein detachment from the surface (described by Foulston *et al*., 2014) and to enable moAb incubations at neutral pH. An irrelevant antibody was used as non-binding control to biofilm grown *S. aureus*. The detected fluorescence signal with and without the secondary antibody was equally negative, which demonstrates the specific binding of moAbs H8 and 16-2 to the *S. aureus* cell surface grown under these biofilm conditions.

We also grew *S. aureus* under biofilm conditions in the presence of moAbs, but no impaired growth or biofilm formation was measured after crystal violet staining (data not shown). This leads to the assumption that our antibodies do not have an impact on the bacterial growth but presumably on the S. aureus – host interaction *in vivo*.

To analyze the effect of pH after biofilm growth, harvested biofilm cells were incubated at pHs 5 and 7.5. The supernatant was precipitated, separated by SDS-PAGE and blotted. Although both samples were treated equally (despite the pH), a higher amount of Triiso was detected in the sample washed at neutral pH (Fig. 3.12A), leading to the conclusion that the cell associated proteins detach from the surface under neutral pH. Thus, a higher amount of Triiso remained at the cell surface under acidic conditions. These results agree with Foulston *et al*. (2014), who detected the same for other glycolytic enzymes (GAPDH, enolase). This pH influence has also been described for enolase and GAPDH of gram-positive *Lactobacillus crispatus* (Antikainen *et al.,* 2007). At pH 5 no release of the proteins from the surface was detected. A stepwise increase of the pH from 4.4 to 7 revealed that the release of these proteins became detectable at pH 5.2, which is close to the isoelectric point (pI) of enolase (4.8) and GAPDH (5.2). Both proteins are positively charged at lower pH values and thus bind to negatively charged cell wall components, such as lipoteichoic acid (LTA). This suggests that negatively charged LTA may be involved in the surface anchoring of these proteins. The same can be assumed for *S. aureus* Triiso with a pI of 4.8.

In summary, both the increased expression of Triiso and the acidic growth conditions (< pH 5) after biofilm growth lead to an increased presentation of the protein at the *S. aureus* surface and obviously to a better accessibility of the epitope for anti-Triiso moAb H8. On the contrary, the pH does not seem to influence the occurrence of pOxi because no differences were detected in this case (Fig. 3.12B; see 4.1). In contrast to Triiso the pI of pOxi (6.3) is much higher. These results would also explain the

binding signals of anti-pOxi moAb D3 in flow cytometric analyses after planktonic growth conditions, compared to the non-binding of anti-Triiso moAb H8.

4.4 Extracellular matrix proteins associate with the *S. aureus* cell surface

Our vaccine candidates do not contain any signal motives so that it is possible that they do not reach the surface from the intracellular space but from the outside, where lysed bacterial cells act as a donor. In addition to its occurrence on the bacterial surface, native Triiso from *S. aureus* was detected by moAb H8 in the extracellular medium after planktonic growth to the mid-exponential phase (Fig. 3.17). In contrast, hp2160 and pOxi were verified at the bacterial surface, but they were not detectable in the medium supernatant under these conditions.

It has previously been reported that a variety of species of gram-positive bacteria, including *S. aureus*, release cytoplasmic proteins into the external environment during stationary phase. It is likely that these released proteins produced by gram-positive pathogens are an important component of an enhanced virulence (Foster *et al.,* 2005). Using the CA-MRSA strains MW2 and USA300, Burlak and colleagues (2007) identified a range of extracellular proteins that are known to be associated with the virulence of *S. aureus*. In accordance to our results they also identified Triiso as an exoenzyme, as well as the glycolytic enzyme enolase. Enolase mediates binding to host tissues (Carneiro *et al.,* 2004) and it is known to activate the clotting cascade in conjunction with the main actor coagulase, which was also identified in medium supernatant (Molkanen *et al.,* 2002; Panizzi *et al.,* 2006; see Fig.1.5).

After biofilm growth, which creates an acidic pH, a larger amount of Triiso was found at the surface of *S. aureus.* After increasing the pH most of the protein was detected in the supernatant (Fig. 3.12A). *In vivo* the same might happen: After activation of the clotting-cascade by coagulase *S. aureus* proliferates, which decreases the pH by production of metabolic waste products. By an undefined way (from lysed cells or by secretion) Triiso reaches the surface and is anchored to surface compounds, such as LTA (compare 4.2). When fibrinolysis is initiated by staphylokinase at a defined bacterial cell density (quorum sensing), *S. aureus* singularizes and can reach the surrounding tissue through the blood, which results in an increase of the surface pH and the detachment of Triiso. It is likely that anti-Triiso moAb H8 binds *in vivo* only to the secreted, but not cell wall-associated form of Triiso for inhibiting its moonlighting

role, which needs to be further characterized. This would also explain the non-binding of moAb H8 to Triiso at the *S. aureus* surface after planktonic growth, where we hypothesized that the epitope of moAb H8 is not accessible (compare 4.2).

In further experiments, we demonstrated that exogenously added *S. aureus* proteins are able to attach to the cell surface of biofilm grown *S. aureus*. The principle aim of this experiment was the detachment of bound moAbs from the surface of biofilm grown *S. aureus* by their respective epitope peptides. Performing competition experiments to verify specificity of moAb binding to *S. aureus* surface, we showed in contrast to pOxi- and TriisoC4 peptides that competed with binding of the respective moAbs to the *S. aureus* surface, an addition of the protein Triiso increased the binding of anti-Triiso moAb H8. The same was shown after trying to compete anti-pOxi moAb D3 binding with whole pOxi protein (Fig. 3.23). Moreover, it was possible to spike biofilm grown *S. aureus* with the exogenous, recombinant proteins pOxi and Triiso. While it was assumed that the proteins bind non-specifically at the *S. aureus* surface, anti-His_6-tag antibody by itself was not able to bind.

In *Δica* mutants it has been shown that protein A (SpA) is essential for biofilm formation. The *ica* operon is important in mediating biofilm formation (Cramton *et al.,* 1999). Biofilm growth in *ΔspA* mutants was recovered by addition of exogenous SpA indicating that it is not necessary for SpA to be covalently anchored to the cell wall, but it is also functional as an added exogenous form (Merino *et al.,* 2009).

The mechanism by which proteins lacking signal peptides are exported from cells is unclear and both mechanisms, specific by e.g. protein secretion or non-specific by e.g. cell lysis, are possible (Pasztor *et al.,* 2010; Yang *et al*., 2011; Boel *et al.,* 2005).

A conceivable mechanism is also a regulated autolysis as basis of extracellular presence of moonlighting cytoplasmic proteins (Foulston *et al.,* 2014).

Because binding of anti-Triiso moAb H8 and anti-hp2160 moAb 16-2 to *S. aureus* was only detected under biofilm conditions we assume that endogenous Triiso and hp2160 were released from the cytoplasm after cell lysis during biofilm formation and associated with the surface from the extracellular space, which would explain the positive binding after biofilm growth.

However, it has been described for some bacteria including *S. aureus* that DNA and signal motif lacking proteins found extracellularly are independent of cell lysis and instead a secretion of small lipid-bilayer vesicles is involved in this process (Brown *et al.,* 2015). A clarification of the pathway and natural conditions necessary for cell wall

association of vaccine candidates, would give a better understanding of the mode of action of our protective moAbs.

4.5 Analysis of opsonophagocytosis mediated by moAbs

The main function of immunoglobulins is opsonization of pathogens and mediating the increased uptake by phagocytic cells, which bind IgGs via the Fc region. Therefore, we wanted to analyze whether our murine or humanized monoclonal antibodies are able to promote phagocytosis of murine macrophages or human neutrophils.

With IVIG, as well as with anti-Triiso and anti-pOxi polyclonal antibodies purified from IVIG, opsonophagocytosis by neutrophils was measured via flow cytometry. The results matched with those, obtained by Glowalla *et al*. (2009) and Bettina Tosetti (PhD thesis, 2010). Polyclonal antibodies were enriched by affinity chromatography using Triiso or pOxi immobilized to a column medium.

In contrast, with our monoclonal antibodies, we were not able to show an enhanced phagocytosis by human neutrophils, as well as by murine macrophages upon opsonization of *S. aureus*, which was an unexpected finding (Fig. 3.14, 3.15). At a later point of time we discovered in flow cytometric analyses by changing wildtype against protein A deletion mutant, a specific binding to the *S. aureus* surface was only detectable with anti-pOxi moAb D3. Especially anti-Triiso moAb or humAb H8 showed high affinity to protein A. Thus, non-opsonization of anti-Triiso moAb/humAb H8 and anti-hp2160 moAb/humAb 16-2 was not surprising, while anti-pOxi moAb/humAb D3 should have been able to opsonize. Clearly, additional factors, such as complement are necessary to trigger *in vitro* opsonophagocytosis. Phagocytosis is typically promoted by complement and antibodies binding to receptors on the cell surface (Lee *et al.*, 2003). However, an enhanced uptake of *S. aureus* by neutrophils was even shown without opsonins after adding baby-rabbit complement in previous experiments (data not shown). Because the complement itself was able to trigger *in vitro* phagocytosis it was not used in following trials, missing probably important factors to demonstrate phagocytic efficacy of our moAbs.

Non-binders anti-Triiso H8 and anti-hp2160 16-2 under planktonic growth conditions showed a binding activity upon *in vitro* biofilm growth of *S. aureus* Δ*spA*. To perform flow cytometric analyses with biofilm grown *S. aureus* remains difficult, as for these

analyses bacteria have to be treated under acidic pH conditions and were fixed with paraformaldehyde. These assay conditions are quite inappropriate for phagocytosis analysis.

Binding analyses of anti-Triiso moAb H8 to whole *S. aureus* cells and extracellular occurrence of Triiso at mid-exponential phase of planktonic growth have shown that it is possible that moAb/humAb H8 does not bind *in vivo* to the surface-associated but to the secreted form of Triiso. In this case, it would not be possible to show an opsonophagocytosis *in vitro*.

Lu *et al*. (2014) proved that *in vitro* assay conditions have a significant influence on phagocytosis and killing of *S. aureus* by neutrophils. They found out that phagocytosis by adherent neutrophils is comparable for serum opsonized and unopsonized *S. aureus*. *In vivo* it is possible that human serum may provide adequate opsonization because of high levels of naturally occurring antibodies directed to *S. aureus* and that increasing the amount makes no appreciable difference for *S. aureus* killing (Dryla *et al*., 2005; Sause *et al*., 2016). Although neutrophils are essential for host defense against *S. aureus* infection it is known that all vaccine approaches that showed an opsonophagocytic activity *in vitro* have failed to demonstrate protection in human trials (Giersing *et al*., 2016). Therefore, opsonophagocytosis is not a biomarker for antibodies to be successful in clinical trials. Hence, we investigated the moonlighting activities of the antigens and how the moAbs can interfere. It is possible that our generated monoclonal antibodies do not promote phagocytosis but neutralize the respective protein by inactivation or inhibition of the antigen's moonlighting function. To go on with opsonophagocytic or killing analyses, optimal *in vitro* assay conditions have to be found, which remains problematic. However, it is obvious that *in vivo* conditions for *S. aureus* and the interplay of phagocytic cells with additional factors occurring in blood and tissue completely differ from the artificially created conditions in shaking flasks using broths.

4.6 Triiso's moonlighting role and mode of action of anti-Triiso moAb H8

Moonlighting proteins are described to have two or more different functions (Jeffery, 1999). Because we have not identified an opsonophagocytic activity with neutrophils and macrophages we focused on other possible functions of anti-Triiso moAb H8. Therefore, the moonlighting role of Triiso had to be determined. In this context

Pancholi and Chhatwal (2003) described the importance of housekeeping enzymes as virulence factors for a variety of pathogens.

One possible approach was the analysis of Triiso's enzymatic activity that might be inhibited by moAb H8 because of a binding at the active site. The enzyme Triiso is part of the glycolysis, which happens in the cytoplasm. Henderson and Martin (2011) hypothesized that glycolysis can also happen at the pathogen's cell surface. In human cells the glucose concentration of the extracellular medium is 5 mM. This indicates sufficient glucose to allow glycolysis on the surface of bacteria that are infecting or colonizing humans. The generation of ATP can be used for as yet undefined processes or the generated substrates of glycolysis have signaling actions to other bacteria.

We measured an enzymatic activity with recombinant Triiso, as well as in cell lysate and in the isolated cell wall associated protein fraction (fig. 3.16A) and therefore, we went on with activity assays in presence of anti-Triiso moAb H8. We were able to demonstrate that surface occurring Triiso is enzymatically active, but could not detect an inhibition of its activity by moAb H8 (Fig. 3.16B). This result indicates that binding of moAb H8 to Triiso does not influence its active site. Therefore, inhibition of Triiso's enzymatic activity does not seem to be the mode of action of moAb H8.

It was described that the rate of nosocomial infection is higher in patients with an increased glucose concentration in blood (Pomposelli *et al*., 1998). Glycolysis and ATP generation increased acidification of the medium due to fermentation of glucose. Interestingly, acidification leads to an increased expression of a range of extracellular virulence factors for optimal performance in the acidic milieu. Other virulence factors are down-regulated allowing *S. aureus* to adapt to the changing environment conditions (Weinrick *et al*., 2004). We measured an acidification after biofilm growth. The biofilm growth medium contains a higher amount of glucose than media used for planktonic growth. In Fig. 4.2 it is shown that binding of moAb H8 to Triiso was only detected after biofilm growth. Although it does not inhibit the enzymatic activity of Triiso it is possible that moAb H8 is only able to act under *in vivo* conditions, where a high amount of glucose is available (such as in biofilm culture medium). Because Triiso is up-regulated under biofilm conditions (Becker *et al*., 2001), increased surface presentation and secretion into the extracellular space is obvious, which may change the binding conditions or epitope availability for moAb H8 and reveals its mode of action.

A range of *S. aureus* surface proteins play important roles in adherence to host cells and cell invasion. A moonlighting function of Triiso was identified as a host plasminogen binder and inhibitor (Furuya and Ikeda, 2011). Other glycolytic enzymes are described to have similar functions. GAPDH has been reported to be a transferrin-, fibronectin-, laminin- and plasmin-binding protein (Modun and Williams, 1999; Modun *et al*., 2000; Gozalbo *et al*., 1998). Enolase of *S. aureus* binds host plasminogen and enhances the conversion to plasmin (Molkanen *et al*., 2002), which would be the antagonistic function to Triiso. The function of the activated form plasmin is fibrinolysis (Hekman and Loskutoff, 1987), in contrast to blood coagulation. The main actors of these processes are staphylokinase and coagulase (compare to 1.5.1).

Concerning our results, we detected an interaction between Triiso and human plasminogen (Fig. 3.18, 3.19A). Binding of plasminogen to Triiso detected by ELISA and Far Western blot was weak, but detectable and matches to those signals, detected by Furuya and Ikeda (2011). An inhibition of the interaction between Triiso and plasminogen by moAb H8 was not measured indicating that the plasminogen binding site of the Triiso molecule was not blocked by moAb H8 (Fig. 3.19B). Enolase of Streptococci possesses two C-terminal lysine residues that were found to be important for plasminogen binding (Derbise *et al*., 2004). Two lysine residues also occur at the C-terminus of both *S. aureus* enolase and Triiso. Our anti-Triiso moAb H8 does not bind in this area and can therefore not directly interfere with this interaction.

Furthermore, we were interested in investigating the influence of moAb H8 on Triiso's inhibition of plasminogen activation. An inhibition of plasminogen activation by staphylococcal Triiso was described by Furuya and Ikeda (2011). Unexpectedly, we did not observe initially an inhibition of the conversion of plasminogen to plasmin in presence of recombinant Triiso (Fig. 3.20B). Therefore, we were not able to demonstrate any influence of our moAb to this effect. Triiso from *S. aureus* was used in the experiments of Furuya and Ikeda, whereas we used the recombinant one. However, when we used whole *S. aureus* cells, no effects of influencing plasminogen activation were measured (Fig. 3.20C). Although an interaction between Triiso and plasminogen was detected, our results did not confirm the findings of Furuya and Ikeda.

In addition to its plasmin- and plasminogen-binding, the enzyme enolase is also described to bind the extracellular matrix protein laminin (Carneiro *et al*., 2004). GAPDH is known to bind transferrin, a glycoprotein that transports iron from serum to cells (Modun and Williams, 1999; Modun *et al*., 2000). The glycolytic enzymes like GAPDH, enolase and Triiso are localized in an operon, which is conserved in Staphylococci (Becker *et al*., 2001). Hence, we suggest that further binding analyses are necessary. For future experiments we want to analyze the binding of Triiso to other blood components like transferrin, laminin, fibronectin and fibrinogen.

Triiso is also described as a lectin that binds to the fungus *Cryptococcus neoformans* via a capsular polysaccharide and induces apoptose-like cell death of this yeast species by recognizing and binding to mannose residues (Furuya and Ikeda, 2009). We supposed that Triiso is engaged in direct adhesion to host cells. Unexpectedly, only detect a very weak binding of recombinant Triiso to endothelial and epithelial cell lines could be detected in contrast to the protein pOxi (see 4.7). This may indicate that Triiso plays a different role in infection of the host.

4.7 Identification of pOxi as adhesion protein and mode of action of anti-pOxi moAb D3

The existence of the *S. aureus* deletion mutants Δ*pOxi* and Δ*hp2160* proved that both proteins are not essential for the bacterium. A mutant with a Triiso deletion was not available in the data bank of NARSA (Network on Antimicrobial Resistance in *S. aureus*), which indicates that Triiso is an essential enzyme. As a part of the glycolysis this seems obvious.

We analyzed the exponential growth of the two deletion mutants compared to wildtype under planktonic conditions. In contrast to wildtype and Δ*hp2160* an interesting result was the impaired *in vitro* growth of Δ*pOxi* representing pOxi as an important protein for *S. aureus* (Fig. 3.21A).

Compared to *Bacillus subtilis*, where pOxi is a peripheral membrane protein (Hansson and Hederstedt, 1994), pOxi occurs in the cytoplasm, and according to our experiments also on the *S. aureus* surface as a non-covalently bound protein. In the cytoplasm pOxi (= HemY) is involved in heme synthesis (Frankenberg *et al*., 2003). It is an O_2-dependent protein in *S. aureus* and was recently described as a coproporphyrin synthase that oxidizes coproporphyrinogen III into coproporphyrin III

in heme pathway and does not oxidize protoporphyrinogen into protoporphyrin as thought before (Panek *et al*., 2002; Lobo *et al*., 2015). Like Lobo and colleagues, we also tried to measure the enzymatic activity of recombinant pOxi by using protoporphyrinogen as substrate. We reduced protoporphyrin, but did not measure any oxidation after adding pOxi to the reaction mixture. The new findings of Lobo *et al*. now explain the outcome of our experiments.

Heme is essential for the respiratory electron transport chain as a cofactor of cytochromes and catalase. With the lack of pOxi, *S. aureus* is not able to produce heme endogenously. The organism is auxotrophic to hemin, the precursor of heme. After adding hemin to the medium Δ*pOxi* returned to a similar growth as the wildtype (Fig. 3.21B). When heme or hemin is not extracellular available *S. aureus* has to switch to fermentation, which obviously slows down the rate of expansion.

Growth of Δ*pOxi* on agar plates was also decelerated. After two or three days of growth, small colony variants (SCV) were detected. SCVs are a subpopulation, which was detected to be well adapted to the intracellular milieu and described for many clinical isolates (Sendi *et al*., 2006; Proctor *et al*., 1995). The two subpopulations with different phenotypes allow *S. aureus* the option of both extracellular and intracellular survival and persistence in the host (Sendi and Proctor, 2009). Heme auxotrophy has an influence on colony size and doubling time because the bacteria require large quantities of ATP for cell wall synthesis. In accordance to our results the same phenotypes were obtained after deletion of *hemB* and *hemQ*, other members of the heme biosynthetic pathway (von Eiff *et al*., 1997; Mayfield *et al*., 2013).

In previous experiments we looked for growth inhibition of wildtype strain JE2 in presence of anti-pOxi moAb D3. A neutralization of surface-associated pOxi by moAb D3 would have been influenced the normal growth of the wildtype strain, but we did not detect any specific differences in growth (data not shown). We were also interested in an *in vivo* investigation using the pOxi deletion mutant and detected that Δ*pOxi* is less virulent as the wildtype (Fig. 3.22). Although it is supposed that the main amount of pOxi occurs intracellular, these observations might also influence the moonlighting role of surface-associated pOxi.

It is known that *S. aureus* is able to adhere to and invade in many different cell types, such as epithelial and endothelial cells (Lowy, 2000). In further analyses we demonstrated that recombinant pOxi is able to adhere to epithelial, as well as endothelial cells. This adhesion can be inhibited by our moAb D3 indicating its

possible mode of action (Fig. 3.24). We went on with flow cytometric analyses using whole *S. aureus* cells and showed a decrease in *S. aureus* adhesion upon addition of moAb D3 (Fig. 3.25). In 4.4 it was already explained that the *S. aureus* cell surface can be spiked with exogenously added pOxi. We proved that an addition of exogenous pOxi to biofilm grown *S. aureus* increased the binding of the bacterium to epithelial cells by two fold (from 21 % to 44 %). After addition of moAb D3, binding was decreased from 44 % to only 6 % indicating an inhibition of host cell adhesion by our moAb D3.

Besides the anchorless cell wall protein pOxi, several *S. aureus* surface proteins are described to contribute to host cell adherence. Beneath cell wall-anchored adhesion proteins of the MSCRAMM family, *S. aureus* also comprises non-covalently bound proteins, such as the autolysins AtlA and AtlE or secreted proteins, such as Eap of the SERAM (= secretable expanded repertoire adhesive molecules) family that are involved in adhesion (Paharik and Horswill, 2016; Chavakis *et al*., 2005). Additionally, there are many structurally uncharacterized proteins, such as surface protein SasX that promotes aggregation on cell surfaces for biofilm formation (Foster *et al*., 2014).

To clarify the function of the surface-associated pOxi to contribute to host cell adhesion, a deletion mutant of the major adhesion factors fibronectin-binding proteins (FnBPs) would be important. Many further adhesins of the MSCRAMM family are able to adhere directly to host cells. Previous data showed that *S. aureus* is able to bind to host cells in absence of FnBPs, but adherence as well as invasion properties are much reduced (Sinha *et al*., 2000). Thus, an inhibition of pOxi might have an influence on preventing host adhesion.

We propose that pOxi plays several moonlighting roles as observed for Triiso. To promote adhesion to host cells is obviously one of these functions. For example, Isd proteins adhere to hemoglobin with the ability to capture heme, which helps the bacteria to survive in the iron limited environment in the host (Foster *et al*., 2014). The contribution of pOxi to host cell adherence might also support an additional major moonlighting function, providing a benefit for *S. aureus*.

4.8 Antibody-mediated immunity and protection against MRSA mediated by vaccination with synthetic epitope peptides

The second part of this thesis highlighted the development of an active vaccine against *S. aureus* infection. We suggested that a peptide vaccine combining the analyzed protective epitopes of our generated monoclonal antibodies would result in an effective polyvalent vaccine. Peptide vaccines under current development target mainly viral pathogens, such as malaria, HIV or HCV (Liu *et al*., 2007; Epstein *et al*., 2007; Kolesanova *et al*., 2013). But also peptide vaccines against *S. aureus* were already described and achieved protective effects (Chen *et al*., 2011; Zhao *et al*., 2015; Yang *et al*., 2016). All these approaches based on the identification of immunogenic epitopes with serum containing polyclonal antibodies after active immunization with a whole antigen. The application of epitopes derived from protective monoclonal antibodies was not applied so far.

All used synthetic peptides based on the identified linear epitopes (hp2160-, pOxi- and TriisoC4 peptide) and conjugated to carrier proteins, a high and specific serum IgG titer against the whole antigen was achieved by vaccination of mice (Fig. 3.27). These results point out that the constructed peptide-conjugates are together with Freund's adjuvant effective immunogens for the generation of antibodies. With the different conjugates KLH and BSA we did not observe any differences concerning the IgG titer in serum, although KLH is known to be more immunogenic. The only detected differences concerning IgG titer were related to precipitation problems with KLH conjugates, which is a larger and more hydrophobic protein than BSA. The precipitation problems led presumably to a higher spread and a lower IgG response within the group, which was observed with pOxi-KLH. The precipitated synthetic peptides only induced a moderate serum IgG level after the first boost. Therefore, we decided to set a second boost and measured an increase in IgG level.

In general, we showed that IgG titers of initially immunized mice increased to 10-15-fold after the second boost. An increase from first to second boost was especially measured during immunization with recombinant triepitope, where the titer has been increased around 1-1.5 logs after the second boost (Fig. 3.41).

The aim for further immunization studies would be to consider setting only one boost, which would be advantageous for patients later on. Instead of three times patients would only exposed two times to the vaccine and its containing adjuvant.

Additionally, one boost instead of two would reduce vaccine production costs. Possibly, a protective effect can also be achieved with the humoral immune response detected after the first boost because we verified that the IgG level does not correlate with protection of mice.

The IgG titers were still detectable in the serum 50 days after the last boost, indicating the existence of a memory response. Upon later exposure to the same epitope long-lived plasma cells are able to secrete large amounts of specific antibodies. Manz *et al*. (1997) determined that plasma cells in the bone marrow after a booster immunization survived for more than 90 days without proliferation. The second type of memory response describes memory B-cells that are unable to produce antibodies, but differentiate rapidly into antibody-secreting cells following re-exposure to antigen (Nutt *et al*., 2015). Memory B-cells are generated during primary humoral responses to antigens and requires the help of Th-cells. T-cell epitopes are presented in the sequences of the protein conjugates KLH or BSA. For this reason our results are a first hint of a $CD4^+$ T-cell dependent immune response achieved by our peptide-conjugates, which is important for our peptide vaccination model.

The infection of mice was performed by intraperitoneal infection. Although started with intravenous infection we realized that intraperitoneal administering is more precise. Concerning our *in vivo* trials an application of exactly the same volume of the pathogen to every mouse is of great importance for comparing the protective effects of our vaccines. The i.p. infection of lethal doses was already used in active immunization trials (Stranger-Jones *et al*., 2006; Rauch *et al*., 2012). The infection requires a very large inoculum to develop lethal disease of peritonitis/sepsis in mice. The animals typically succumb within 12-24 hours of challenge (Kim *et al*., 2014). We add 5 % mucin to the bacterial preparation because mucin from porcine stomach was already used for the mouse model of passive immunization. This increases the bacterial virulence and therefore, a lower dose of *S. aureus* can be applied (A. Klimka, unpublished data). Fattom *et al*. (1996) also used 5 % hog mucin in their mouse lethal challenge model and proved that mucin alone did not induce mortality in mice. The lethal inoculums of 1.1 to 3.3 x 10^7 CFU we used are approximately three logs lower compared to those of Stranger-Jones and colleagues, who did not use mucin. Rauch *et al*. used doses between 5 x 10^8 and 6 x 10^9 CFU, which are also much higher as our inoculums.

For sublethal challenge we started with half of the determined lethal dose, but detected in every new *in vivo* trial that the virulence of the used *S. aureus* inoculum decreased. To exclude a pre-immunization of mice within the breed, mice were ordered at the ZMMK (Uniklinik Köln). In contrast to e.g. Charles River as an animal provider, the ZMMK animal facility is extremely cautious and tests against *S. aureus* directly after birth.

Immunization with the single peptides hp2160 and pOxi led to a reduction of bacterial colonization in all prepared organs after sublethal infection. Whereas hp2160-KLH conferred only statistically significant reduction of *S. aureus* CFU in the liver, the reduction was highly significant in all organs upon immunization with pOxi-KLH (Fig. 3.30, 3.32). Bivalent immunization with both hp2160-KLH and pOxi-KLH also reduced the bacterial load in organs significantly (Fig. 3.34), but compared to pOxi-KLH alone the bivalent vaccination was less significant after statistical analysis by Mann-Whitney test, demonstrating no synergistic effect. One reason could be that only half the amount of each peptide-conjugate was used for bivalent vaccination. However, the mean concentration of anti-pOxi IgGs in mouse sera is similar in both cases (Fig 3.31, 3.33). Further reasons might be a stronger protective effect of pOxi epitope peptide or less protection efficacy of hp2160 peptide that restrained the efficacy of pOxi peptide in the bivalent immunization approach. These results are similar to those, obtained by Bettina Tosetti (PhD thesis, 2010), who demonstrated that the whole antigen pOxi alone still conferred statistically significant protection against *S. aureus*, whereas bivalent immunization with pOxi and Triiso did not achieve significant results in protection.

Immunization with the synthesized epitope peptide of anti-Triiso moAb C4 did not achieve any significant results concerning a reduction of bacterial colonization in organs (Fig. 3.36). Compared to synthetic pOxi- and hp2160 peptide an equal concentration of antigen-specific IgG titer in serum of mice was determined and also still remained in serum 50 days after the last boost (Fig. 3.35A). Additionally, anti-Triiso IgGs of the pooled mouse serum were able to bind to *S. aureus* Triiso of isolated cell wall-associated protein fraction (Fig. 3.35B). In contrast to the other challenges (Fig. 3.30, 3.32, 3.34) the bacterial burden detected in organs of the control group was lower in this experiment. After analyzing and comparing the IgG titers of the different mouse sera we determined that a strong IgG titer does not

correlate with a reduced bacterial colonization. This was also determined in animal trials with hp2160- and pOxi peptide.

It is obvious that the moAb C4 epitope does not reveal such a robust protection against MRSA as our other identified epitopes do. Interestingly, a recent passive immunization trial using anti-Triiso moAb C4 did not show protection in the murine model. These findings demonstrate that the epitope peptide of non- or low-protective moAb C4 is not capable of inducing a protective immune response as a vaccine and supports our hypothesis that a successful vaccine is epitope- rather than antigen-specific.

4.9 Polyepitope peptides as multivalent active vaccine against MRSA

We went on with cloning of a triepitope fusion peptide containing the linear pOxi and hp2160 epitopes, as well as the discontinuous epitope of anti-Triiso moAb H8 within the analyzed Triiso fragment (N'-pOxi-Triiso fragment-hp2160-C'). As one of the leading candidates for passive immunization we were interested in an inclusion of the moAb H8 epitope for a generation of a multivalent construct. The cloning procedure was followed by a successful heterologous overexpression in *E. coli* and purification via its His_6-tag. After expression the highest amount of the peptide was found in inclusion bodies, which are insoluble aggregates of non-native peptide/protein (Baneyx and Mujacic, 2004). A protein gel of triepitope peptide showed several bands above 35 kDa, in addition to the 14.3 kDa band of the fusion peptide (Fig. 3.38). The same bands were detected with anti-pOxi moAb D3, anti-Triiso moAb H8 and anti-hp2160 moAb 16-2 (Fig. 3.39), demonstrating that they are aggregates of the purified peptide.

A strong competition of moAb-binding to hp2160, as well as to pOxi by the triepitope peptide was detected, indicating a successful cloning and recognition of the two small moAb epitopes (Fig. 3.40). The triepitope peptide also competed with moAb H8 binding to Triiso but only moderately. A possible reason for this might be a stronger binding affinity of anti-Triiso moAb H8 to Triiso as to the triepitope.

Another reason for the moderate competition effect might be that the epitope of moAb H8 is localized within a long amino acid sequence. This indicates that possibly some other kinds of anti-Triiso antibodies are produced besides moAb H8-like

antibodies by the immune system *in vivo*, because we detected a strong humoral immune response against recombinant Triiso.

We achieved specific serum IgG titers against the three recombinant proteins pOxi, hp2160 and Triiso with the triepitope vaccination (Fig. 4.41). As already observed with single epitope peptides the serum IgG titer still remained at the same level 50 days after the last booster immunization, which is a relevant result for our infection model. Compared to pOxi and Triiso the immune response to hp2160 was moderate. A reason might be that the fusion and the C'terminal His_6-tag altered the structural properties of the hp2160 epitope peptide part in such a way that binding of anti-hp2160 moAb 16-2 is disturbed to some extent.

Mice immunized with the triepitope peptide that were challenged with MRSA showed a significantly increased bacterial clearance in the examined organs (Fig. 3.43). The KLH-conjugated triepitope peptide was analyzed within the same animal trial as hp2160-KLH. Compared to hp2160 conjugate, triepitope revealed an expected more protective effect. These results were the reason for cloning of diepitope peptides without the hp2160 epitope. The diepitopes OTO (N'-pOxi epitope-Triiso fragment-pOxi epitope-C') and pOT (N'-pOxi epitope -Triiso fragment-C') were successfully overexpressed in *E. coli,* whereas TpO (N'-Triiso fragment-pOxi epitope-C') was not (Fig. 3.45). All peptides are very small so that we anticipated some problems with overexpression and therefore designed different constructs. Small peptides undergo degradation by proteinases easily, which might have happened to TpO (Baneyx and Mujacic, 2004). The highest amount of the two other peptides was detected in the soluble fraction. Binding of anti-pOxi moAb D3 and anti-Triiso moAb H8 and competition experiments proved both diepitope peptides to contain the correct epitope sequences and functionality. Compared to triepitope, competition of moAb H8 binding to Triiso was stronger with both diepitope peptides (Fig. 3.47). Possibly, the relative binding affinity of OTO as well as pOT to moAb H8 is higher, which has not been determined.

Immunization with the diepitope pOT was more successful in the sublethal animal model than with OTO, although OTO led to a stronger humoral immune response against recombinant pOxi (Fig. 3.48, 3.49). This difference was expected because OTO contains two pOxi epitopes within one molecule. Due to the high serum IgG titer achieved by OTO immunization, a conformational problem of OTO compared to pOT was excluded. The difference between the two diepitopes concerning their protective

effects might stem from different T-cell responses. OTO immunization possibly led to a T-cell independent B-cell activation, but a comparison was not further investigated in this work. We went on with the most promising candidate pOT. Compared to triepitope immunization, pOT achieved very similar results in organ-CFU trials with the same significance in all examined organs. Nevertheless, diepitope pOT was preferred for the first survival experiments. The reason was that hp2160 epitope peptide did not work as well as pOxi epitope in former organ CFU experiments and was therefore omitted in the diepitope peptides. We conclude that the hp2160 epitope is negligible in providing protection compared to the other examined peptides and has instead a detrimental effect on protection efficiency.

The diepitope peptide pOT was able to significantly protect mice from lethal challenge with MRSA (Fig. 3.52). A further comparison of pOT with single pOxi peptide resulted in 100 % protection after immunization with pOxi-BSA conjugate and 90 % protection using pOT-KLH conjugate, which demonstrates their great protective effect (Fig. 3.53).

A synergistic effect of pOT, compared to pOxi was not detected, highlighting pOxi epitope peptide as the most promising candidate for peptide vaccination. However, the development of a polyvalent vaccine is of greatest interest. This is the reason why we want to go on in analyzing the epitope of anti-Triiso moAb H8, reducing its size but retaining its specificity. We suppose that a pure and synthesized TriisoH8 epitope peptide would provide more effective protection against MRSA and in combination with pOxi peptide would result in a stronger synergistic effect. A di- or polyepitope would also be necessary to target escape mutants. With the single TriisoH8 peptide it would also be possible to investigate the efficacy of monovalent vaccination compared to the diepitope peptide.

Although we identified the pOxi epitope and pOT diepitope as promising candidates for the development of an active vaccine, the remaining epitopes hp2160 and triepitope should not be disregarded and additionally still further investigated. If they are not protective against lethal challenge, they might attenuate the infection by making *S. aureus* more sensible to antibiotics, so that patients can be treated more easily (adjunctive therapy).

4.10 Induction of T-cell-mediated immune response with polyepitope peptides

We have determined that the IgG level detected in sera of mice upon vaccination does not correlate with the protection of mice against *S. aureus* infection. It has been described that the cellular immune response, with particular attention to Th1 and Th17 cells becomes more important in case of *S. aureus* infection (Moyle and Toth, 2013; Cho *et al*., 2010; Brown *et al*., 2015; Bröker *et al*., 2016). We proposed that not only the epitope-specific antibody level supported by Th2 response, but also the outcome of the cellular immune response influences the obtained protection and therefore we were interested in analyzing the T-cell response upon vaccination with epitope peptides, in addition to humoral immune response. In a study, where immunization with IsdB revealed the generation of specific antibodies, protection against *S. aureus* was only achieved in T-cell competent but not in deficient mice, which additionally underlines the importance of T-cell response (Joshi *et al*., 2012).

For an investigation of the T-cell response triepitope-KLH and the promising diepitope pOT-KLH were used. The single epitope peptides were only available as BSA conjugates in our lab because of precipitation problems with KLH conjugates. An immunization with BSA conjugates would result in an undesired re-stimulation with the medium supplemented with fetal calf serum (FCS) during culturing of the dissected splenocytes. BSA is an integral part of FCS that cannot be omitted. Due to this fact, our analyses could only be done upon vaccination with KLH-conjugates.

Before analyzing the cytokine profile, we were interested in a determination of IgG subclasses after the second boost. The IgG subclass is a result of the subtype of $CD4^+$ T-cell response (Stevens *et al*., 1988). It is known that the Th1 cytokine interferon-γ (IFN-γ) stimulates the secretion of IgG2a, whereas the Th2 cytokine interleukin-(IL)-4 regulates the class switch to IgG1 in activated B-cells (Snapper and Paul, 1987; Petit-Frere *et al*., 1993). A high serum IgG1 level is a hint for a Th2 mediated response, whereas a high IgG2a level is a hint for a Th1 response.

The analysis of IgG subclasses upon vaccination suggested a stronger Th1 response in pOT-immunized mice because of a lower ratio of IgG1 to IgG2a than obtained with triepitope-KLH immunization. A stronger Th2 response in triepitope-KLH immunized mice was suggested because triepitope-KLH immunization was associated with an increased ratio of IgG1 to IgG2a (Fig. 3.60).

Both triepitope and pOT immunization resulted in a significant proliferation of splenocytes upon re-stimulation measured by BrdU incorporation, which consist of a variety of T-and B-lymphocytes (Fig. 3.61). This result indicates an immune response upon antigen exposure and highlights vaccine efficacy.

We further investigated the secretion of certain cytokines. A strong release of IFN-γ was measured after exposure of splenocytes to the relevant antigens indicating $CD4^+$ (Th1) and $CD8^+$ cell proliferation (Fig. 3.62A). A difference between triepitope- and pOT immunization could not be detected. Both synthesized unconjugated pOxi and hp2160 peptides were able to induce IFN-γ release, which indicates a T-cell epitope within their peptide composition. Both did not stimulate KLH-specific splenocytes excluding an unspecific stimulation. pOT stimulates the IFN-γ production of KLH-immunized mice stronger that the triepitope. This is obviously related to the purification grade of pOT that can contain endotoxin (lipopolysaccharide, LPS) derived from heterologous overexpression in *E. coli*. Endotoxin is known to induce IFN-γ production (Varma *et al*., 2002). However, compared to pOT-immunization, KLH-specific splenocytes were significantly less stimulated. The same was occurred by comparison of triepitope- and KLH-specific splenocytes.

Previous studies proved the essentiality of IFN-γ competent $CD4^+$ T-cells for survival in blood stream infections caused by *S. aureus* (Lin *et al*., 2009). Studies of Brown et al. (2015) demonstrated a significantly increased IFN-γ production in the peritoneal cavity soon after *S. aureus* i.p. challenge. After comparison with $CD8^+$ T-cells they detected that $CD4^+$ T-cells (Th1) were the primary source of IFN-γ in the infected mice. They also showed that human *S. aureus* blood stream infection induces *S. aureus* antigen-specific memory Th1 cells and developed a vaccine comprising ClfA, combined with the Th1-driving adjuvant CpG. This Th1-inducing vaccine candidate conferred significant reduced bacterial colonization in peritoneal cavity and examined organs of mice upon *S. aureus* infection. In comparison to our findings we already achieved a protective effect with our tri- and diepitope (pOT) vaccines and also demonstrated here a strong IFN-γ release after subsequent antigen exposure. We did not differentiate between $CD8^+$- and $CD4^+$ T-cells that both produce IFN-γ, so far. The role of $CD8^+$ mediated T-cell response would also be interesting because *S. aureus* is able to persist inside host cells, such as epithelial and endothelial cells and professional phagocytes (Lowy, 2000; Löffler *et al*., 2014; Grosz et al., 2014) as small colony variants that were already described in 4.7.

IFN-γ secreted by T-cells is a potent activator of monocytes. It was detected that pre-treatment of monocytes with IFN-γ increased their potential to eradicate intracellular *S. aureus* (Kubica *et al*., 2008; Smith *et al*., 2010).

In addition to IFN-γ and IL-4 release, we were interested in IL-17 production by Th17 and γδ-cells, which are known to be important for host defense against *S. aureus* (Bröker *et al*., 2016; Cho *et al*., 2010).

Concerning vaccination approaches, a peptide construct mimicking peptidoglycan was described to provide partial protection from *S. aureus* challenge (Wang *et al*., 2015). Compared to our peptide immunization model, they applied inactivated *S. aureus* cells as booster immunization. Their results showed that protection was associated with increased amounts of Th1 and Th17 cells in the spleen.

In our studies a significant IL-17A production was measured upon re-stimulation with antigens from pOT- and triepitope-specific splenocytes, while KLH-specific splenocytes were non-reactive upon antigen exposure (Fig. 3.62C). IL-17 is produced by $CD4^+$ Th17 cells and γδ- cells and important for neutrophil recruitment and priming them for bactericidal activity (Iwakura *et al*., 2008). It was found that mice deficient in epidermal γδ- but not αβ-T cells had larger skin lesions with higher *S. aureus* colonization and impaired neutrophil recruitment than wildtype mice (Cho *et al*., 2010). In γδ-deficient mice infected with *S. aureus*, the treatment with recombinant IL-17 restored the impaired immunity of these animals. In human skin, γδ-T cells have been reported to be recruited to a site of infection and a large amount of αβ-Th17-cells are found on inflamed skin (Modlin *et al*., 1989; Pene *et al*., 2008). All these findings underline the importance of cytokine IL-17 for host defense against *S. aureus* and a vaccine development directed to IL-17 elicitation. We detected that especially splenocytes of pOT-KLH immunized mice generated a significant increased IL-17A rate and suppose a correlation between the protective efficacy of pOT and IL-17 production.

Compared to IL-17, pOT and triepitope vaccination resulted in a moderate release of the Th2 cytokine IL-4 upon re-exposure of all antigens, except hp2160 peptide, while KLH-specific splenocytes were non-reactive upon stimulation (Fig. 3.62B). These results indicate a weak Th2 response that was not as strong as IFN-γ and IL-17A mediated T-cell response. It is described that *S. aureus* infection induced a Th2 response and that IL-4 plays a role in regulation of IFN-γ in *S. aureus* infection together with IL-10 (Sasaki *et al*., 2000). Compared to these findings, Brown *et al*.

(2015) were not able to detect IL-4 in the peritoneal cavity after *S. aureus* infection of mice.

Compared to our results Joshi *et al*. (2012) were not able to detect IL-4 upon immunization with IsdB. They mention that the level of IFN-γ is negligible, whereas a large level of IL-17A was detected. Their results suggest that IL-17A producing Th17 cells play an essential role in IsdB mediated protection after *S. aureus* challenge in mice. It has also been shown that the lack of T-cells in IsdB immunized mice impairs protection upon *S. aureus* challenge, while the lack of B-cells does not.

Concerning our data, we conclude that the increased level of IFN-γ and IL-17A upon peptide immunization together with the strong antigen-specific IgG titer confers the protective effect against *S. aureus*. Especially the lead protective vaccine candidate pOT achieved these high levels, measured as an elevated IgG2a titer and high releases of both IFN-γ and IL-17A.

For a comparison of T-cell responses of the remaining epitope peptides upon vaccination, a different conjugation method is necessary. We will switch again to KLH conjugates by limiting precipitation through slight changes of the epitope's amino acid sequence. Additionally, branched peptides of B-cell epitopes might be constructed by addition of a potent T-cell epitope derived from the respective antigen. These multiple antigenic peptides (MAP) peptides would be advantageous for an application of our vaccines in humans. However, the construction of MAP peptides is a very expensive method and the search for a qualitative relevant T-cell epitope for achieving a strong and long-lasting immune response possibly needs several attempts.

Furthermore, it was shown that in combination with a Th1-driving adjuvant CpG the vaccine antigen ClfA conferred protection in an *S. aureus* peritonitis model (Brown *et al*., 2015). In ongoing studies we will compare the adjuvant alum in addition to CpG that are both admitted to humans, with the previous applied Freund's adjuvant as the next step of our vaccine development.

4.11 Recombinant viral vectors as vaccine platform against *S. aureus*

In addition to peptide immunization we focused on alternative vaccination strategies. We used the two non-replicating viral vector systems MVA and AAV encoding the triepitope peptide as DNA vaccine platform.

Modified Vaccinia virus Ankara (MVA) was already used as viral vaccine platforms, such as influenza and HIV, which entered clinical trials (Kreijtz *et al*., 2014; Garcia *et al*., 2011; Volz and Sutter, 2013). Although developed for vaccination against intracellular pathogens, antibody-based immune responses have often been demonstrated. In recent studies it has been shown that DNA vaccination against MERS coronavirus using recombinant MVA as delivery system in mice achieved a strong antibody titer in mice (Song *et al*., 2013). Additionally, specific $CD4^+$ and $CD8^+$ T-cell responses upon DNA vaccination with recombinant MVA have been detected (Hillaire *et al*, 2013). *S. aureus* is not only an extracellular pathogen, but also able to persist intracellular upon adhesion at and invasion into host cells. This emphasizes the importance of the host's cellular immune response, as already described in 4.10.

In addition to the conventional vector expressing the triepitope peptide (rMVA-SA-Triepitope), a fusion protein of triepitope peptide and the vaccinia virus protein hemagglutinin (HA) was designed, which is transported and integrated into the host's cell membrane after viral infection and expression in host cells (Lehmann and Sutter, unpublished data). Vaccinia virus HA is not comparable to other hemagglutinins of e.g. influenza virus. Because of lacking hemagglutinic functions it is not essential for the infection of host's cells. The HA-triepitope fusion protein is constructed by presenting the triepitope peptide to the extracellular space.

After infection of cells the triepitope peptide was expressed as conventional and as HA-fusion protein, respectively, indicating that immunization with these vectors should work (Fig. 3.54).

Immunization with rMVA-HA-SA-Triepitope induced a strong serum IgG titer against the respective whole antigens Triiso, pOxi, hp2160 and against the triepitope peptide, while the conventional vector rMVA-SA-Triepitope only achieved a moderate titer (Fig. 3.55). We already assumed that the titer of the conventional method would be lower because the triepitope was only endogenously expressed. After expression of the triepitope peptide in host cells it should be degraded and presented on MHC class I complex that activates cytotoxic T-cells ($CD8^+$) for lysing the infected cells. For

the generation of an antibody-mediated immune response the released triepitope can be endocytosed by antigen presenting cells (APCs) for MHC class II presentation after cell lysis. Additionally, endogenous antigens can be presented by MHC class II when they are degraded through autophagy. Macroautophagy delivers intracellular proteins to lysosomal degradation and contributes to the pool of MHC class II displayed peptides. For this process, produced autophagosomes have to fuse with MHC class II containing compartments (Crotzer and Blum, 2009; Münz 2012). The explained possibilities were obviously not performed to a great extent because the virus is not able to replicate. This would explain the weak humoral immune response obtained by rMVA-SA-Triepitope. The second vector is additionally encoding the fusion protein of HA and triepitope, which is integrated in the membrane of the host cell upon expression. Thus, it can be directly endocytosed by professional APCs for MHC class II presentation, which additionally triggers antibody generation. Naturally occurring antibodies that recognize foreign residues on the host cell surface can opsonize the cell and bind to the Fc receptor of macrophages, which may additionally enhance the uptake. Compared to our established conventional peptide vaccination the humoral immune response we obtained in this animal trial was less strong. Nevertheless, in case of rMVA-HA vaccination there was no need of an adjuvant, which is very advantageous. The high immune-stimulating potential by triggering rapid immigration of monocytes, neutrophils and $CD4^+$ cells to the side of inoculation has already been described (Lehmann *et al*., 2009).

According to previous animal trials we set two booster immunizations. The second boost revealed as not necessary because the titer did not significantly rose. The first boost was essential because an IgG titer was not measureable upon initial immunization. For analyses of its protective effect in animal trials we will go on with rMVA-HA-SA-Triepitope vaccination, which revealed as a promising alternative strategy.

In a second vaccination strategy we analyzed two vector constructs of Adeno Associated Virus (AAV). Cloning of the two plasmids encoding the triepitope and the triepitope-VP2 fusion protein was successful and necessary for vector packaging, which was performed by our cooperation group (Fig. 3.56). With the conventional vector AAV2:Tri expressing the triepitope peptide we expected a similar result in vaccine-induced humoral immune response as observed with MVA-SA-Triepitope.

Compared to MVA vaccination an IgG titer in mouse sera was not detected (Fig. 3.59). The titer of capsid and genomic particles was analyzed. The similar capsid-to-genomic-particle ratios indicate that the incorporation of the triepitope peptide into the AAV capsid by fusion to VP2 did not affect the vector packaging efficacy (Tab. 3.2). The transduction of eukaryotic cells demonstrated the expression of intracellular triepitope peptide (Fig. 3.57). The western blot of modified capsid proved the successful incorporation of the triepitope peptide in contrast to the wildtype capsid (Fig. 3.58). These results indicate a successful generation of recombinant AAVs. Based on these results the non-reactive antibody response suggests that no or too less expressed triepitope has been presented on MHC class II. Obviously, the transduced cells were not lysed by cytotoxic T-cells for releasing the triepitope peptide and allowing an uptake by APCs. Rybniker *et al*. (2012) fused their antigen to human tissue plasminogen activator leader peptide that induced a continuous release of the expressed protein to the extracellular milieu. Compared to our results they obtained a humoral immune response because their protein functioned as an exogenous antigen, which was taken up from APCs for a MHC II presentation.

The capsid-modified vector expressing the triepitope and additionally displays the triepitope on the vector capsid by VP2 fusion induced a moderate humoral immune response after the second boost. Because the conventional vector did not reveal as immunogenic it is evident that the capsid incorporation of the triepitope induced the detected antibody-mediated immune response. The occurrence of triepitope on the viral surface leads to an uptake of APCs and presentation by MHC class II.

We conclude that AAV vaccination under the demonstrated conditions was not useful for following experiments. As a further strategy, we cloned a new plasmid and fused the sequence encoding the triepitope to a an IgG-kappa signal sequence, similar to the method of Rybniker *et al*. (2012). The additional signal motif will allow the triepitope’s release from the host cell into the extracellular milieu, where it can act as an antigen, while it will be continuously expressed and exported.

5 Summary

Patients infected with the life-threatening, methicillin-resistant, human pathogen *Staphylococcus aureus* (MRSA) can be treated only with antibiotics of last resort. The development of a vaccine as an alternative to antibiotics is therefore of great clinical importance to fight MRSA.

Based on a *S. aureus* proteome screen with *S. aureus* specific human antiserum, novel surface-associated proteins were identified as vaccine candidates. Proto-porphyrinogen oxidase (pOxi), Triosephosphate isomerase (Triiso) and the hypothetical protein 2160 (hp2160) provided protection in a murine sepsis model upon active immunization. Monoclonal antibodies (moAbs) against these target proteins were generated of which three demonstrated significant, repetitive, epitope-specific protection against *S. aureus* infection in mice.

The present work focused on the characterization of these protective moAbs and their epitopes. Binding of these moAbs to a preparation of cell wall-associated proteins as well as to the *S. aureus* surface depended on *in vitro* growth conditions. For binding of anti-Triiso moAb H8 and anti-hp2160 moAb 16-2 to the bacterial surface, biofilm growth of *S. aureus* was essential. Anti-pOxi moAb D3 showed a surface binding also after planktonic growth. In addition to biofilm conditions it was detected that the pH of the surrounding medium influences the occurrence of Triiso and the epitope accessibility for moAb H8 on the cell surface whereas it does not influence the pOxi presence. Triiso was also identified as exoenzyme in the medium supernatant and it was shown that the surface of *S. aureus* can be spiked with exogenous Triiso and pOxi.

The moAbs' mode of action was investigated first with regard to *in vitro* opsonophagocytosis but we did not observe this. An enzymatic activity of recombinant Triiso was measured, as well as an enzymatic activity of native Triiso in the cell wall-associated protein fraction and cell lysate. Furthermore, an interaction between Triiso and human plasminogen was demonstrated. These measurements were not influenced by moAb H8. Additional experiments with other blood compounds have to be performed to investigate this further.

Using deletion mutants, an impaired *in vitro* growth of Δ*pOxi*, but not Δ*hp2160*, compared to wildtype was demonstrated. In the mouse infection model the virulence

of Δ*pOxi* was also impaired, highlighting pOxi as a potential virulence factor for *S. aureus*. Moreover, we succeeded to show that the protein pOxi contributes to host cell adherence. This unexpected moonlighting function was identified using epithelial and endothelial cells and demonstrated that the addition of moAb D3 leads to a detachment of pOxi from these cells. Furthermore, it was detected that exogenous pOxi increases the binding of *S. aureus* to HeLa cells and that this increased binding was inhibited by our moAb D3.

The identified epitopes of the three moAbs were further characterized and used in different approaches for active immunization of mice. Using the pOxi- and hp2160-epitope-peptides for immunization, an antigen-specific IgG response and a significant higher bacterial clearance of organs after *S. aureus* challenge was measured. It was also demonstrated that the protection is epitope-specific because another epitope of Triiso, derived from a non-protective anti-Triiso antibody, triggered an IgG-response in immunized mice but failed to show protective efficacy after *S. aureus* challenge. Out of several mono- and multivalent epitope fusion peptides the pOxi epitope peptide and a pOxi and Triiso diepitope fusion peptide demonstrated to be the best candidates, providing significant protection upon lethal MRSA challenge. Additionally, the T-cell response was analyzed upon immunization with the fusion epitope peptides. The exposure of isolated splenocytes to unconjugated fusion peptides led to an increased cell proliferation and to a strong IFN-γ (Th1 response) and IL-17 release (Th17), described to be important to combat *S. aureus* infection.

The triepitope construct was also used as part of MVA and AAV vaccine vectors. Vaccination with rMVA-HA-Triepitope resulted in a strong humoral immune response. In addition to the viral genome encoding the triepitope peptide, the triepitope was also fused to a viral protein, which supports the integration into the membrane of the host cell. Vaccination with rAAV encoding the triepitope peptide in addition to a triepitope fusion with a viral capsid protein induced just a moderate IgG titer.

The achieved results gave new insights in the moonlighting functions and surface occurrence of our vaccine candidates and in the mode of action of the generated, protective antibodies. The successful peptide vaccination underlines the feasibility of such a “reverse immunology”-approach and therefore the importance of differentiating between protective and non-protective epitopes.

6 Zusammenfassung

Patienten, die mit dem lebensbedrohlichen, Methicillin-resistenten, humanen Pathogen *Staphylococcus aureus* (MRSA) infiziert sind, können nur noch mit Reserveantibiotika behandelt werden. Die Entwicklung eines Impfstoffes als Alternative zu Antibiotika ist daher von großer klinischer Bedeutung für die Bekämpfung von MRSA.

Basierend auf einer Proteomanalyse mit einem *S. aureus*-spezifischen, humanen Antiserum, wurden neue Zellwand-assoziierte Proteine als Vakzinekandidaten identifiziert. Die Proteine Protoporphyrinogen Oxidase (pOxi), Triosephosphat Isomerase (Triiso) und das hypothetische Protein 2160 (hp2160) zeigten nach Immunisierung eine Protektion im Sepsis-Mausmodell. Gegen diese Zielproteine wurden monoklonale Antikörper (moAbs) generiert, von denen drei eine signifikante, wiederholbare, Epitop-spezifische Protektion gegen eine *S. aureus* Infektion im Mausmodell aufwiesen.

Die vorliegende Arbeit war auf die Charakterisierung dieser protektiven moAbs und ihrer Epitope fokussiert. Die Bindung der moAbs, sowohl an die Zellwand-assoziierte Proteinfraktion als auch an die Oberfläche von *S. aureus*, war abhängig von bestimmten *in vitro* Bedingungen. Für die Bindung von anti-Triiso moAb H8 und anti-hp2160 moAb 16-2 an die Bakterienoberfläche war ein Wachstum von *S. aureus* unter Biofilm-Bedingungen essenziell. Anti-pOxi moAb D3 hingegen zeigte auch unter planktonischen Wachstumsbedingungen eine Bindung an die Oberfläche.

Zusätzlich zu den Biofilm-Bedingungen war nachweisbar, dass der pH des Kulturmediums das Vorhandensein von Triiso und die Epitop-Erreichbarkeit für moAb H8 auf der Zelloberfläche beeinflusst. Triiso wurde außerdem als Exoenzym im Medium-Überstand identifiziert. Darüber hinaus zeigte von außen hinzu gegebenes Triiso oder pOxi eine Bindung an die Oberfläche von *S. aureus*.

Die Wirkungsweise unserer Antikörper wurde zunächst im Hinblick auf eine *in vitro* Opsonophagozytose untersucht, welche jedoch nicht verifizierbar war. Eine enzymatische Aktivität des rekombinanten Triiso war nachweisbar, die außerdem sowohl in der Zellwand-assoziierten Proteinfraktion als auch im Zelllysat detektiert wurde. Des Weiteren war eine Interaktion von Triiso und humanem Plasminogen

nachweisbar. Es ließ sich bei diesen Messungen jedoch kein Einfluss von moAb H8 feststellen. Weitere Untersuchungen mit anderen Blut-Komponenten werden hier noch durchgeführt.

Die Analyse von Deletionsmutanten zeigte im Vergleich zum Wildtyp ein vermindertes *in vitro* Wachstum von Δ*pOxi*, jedoch nicht von Δ*hp2160*. Im Maus-Infektionsmodell war eine verminderte Virulenz von Δ*pOxi* nachweisbar, die pOxi als einen potenziellen Virulenzfaktor von *S. aureus* hervorhebt. Weiterhin konnte erfolgreich dargestellt werden, dass pOxi zur Adhäsion an Wirtszellen beiträgt. Diese unerwartete Nebenfunktion wurde mit Epithel- und Endothelzellen identifiziert und bewiesen, dass die Zugabe von moAb D3 zur Ablösung von pOxi von diesen Zellen beiträgt. Darüber hinaus konnte gezeigt werden, dass exogenes pOxi die Bindung von *S. aureus* an HeLa Zellen steigert, und dass diese Steigerung durch moAb D3 inhibiert werden kann.

Die identifizierten Epitope der drei moAbs wurden weiter charakterisiert und für die aktive Immunisierung von Mäusen eingesetzt. Nach Immunisierung mit den jeweiligen pOxi- und hp2160-Epitop-Peptiden war eine spezifische, gegen das Antigen gerichtete IgG-Antwort und nach einer *S. aureus* Infektion eine signifikant geringere Bakterienbelastung in den Organen nachweisbar. Es wurde belegt, dass diese Protektion Epitop-spezifisch ist, da ein weiteres Triiso-Epitop, das von einem nicht-protektiven anti-Triiso moAb stammte, zwar eine IgG-Antwort, jedoch keine protektive Wirksamkeit zeigte. Von mehreren mono- und multivalenten Epitop-Fusionspeptiden stellten sich das pOxi Epitop-Peptid und ein Fusionspeptid aus den pOxi und Triiso Epitopen als beste Kandidaten heraus, die einen signifikanten Schutz gegen letale MRSA Infektionen boten. Zusätzlich wurde die T-Zell-Antwort nach Immunisierung mit den Fusionspeptiden untersucht. Eine Restimulation der isolierten Milzzellen mit den jeweiligen Fusionspeptiden führte zu einer erhöhten Zell-Proliferation und zu einem vermehrten Ausschüttung von IFN-γ (Th1-Antwort) und IL-17 (Th17), die als äußerst wichtig für die Bekämpfung einer *S. aureus* Infektion beschrieben wurden.

Das Triepitop-Konstrukt wurde als Teil einer MVA- bzw. AAV-Vakzine eingesetzt. Die Impfung mit rMVA-HA-Triepitop führte zu einer starken humoralen Immunantwort. Zusätzlich zu dem viralen Genom, das für das Triepitop-Peptid kodiert, wurde das Triepitop hier mit einem viralen Protein fusioniert, das nach der Expression in der Wirtszelle in deren Zellmembran eingebaut wird. Die Impfung mit einem für das

Triepitop kodierenden AAV, bei dem das Triepitop zusätzlich mit einem viralen Kapsidprotein fusioniert wurde, induzierte nur einen moderaten IgG-Titer.
Die erzielten Ergebnisse ergaben neue Einblicke in die Oberflächenfunktion unserer Vakzinekandidaten, ihr Vorkommen auf der Zelloberfläche und in die Wirkungsweise unserer generierten, protektiven Antikörper. Die erfolgreiche Peptid-Impfung unterstreicht die Umsetzbarkeit dieses Ansatzes der „reversen Immunologie“ und die damit verbundene Wichtigkeit der Differenzierung von protektiven und nicht protektiven Epitopen.

7 Bibliography

Ada G. 2005. Overview of vaccines and vaccination. *Mol Biotechnol* 29: 255-72

Alderete JF, Millsap KW, Lehker MW, Benchimol M. 2001. Enzymes on microbial pathogens and *Trichomonas vaginalis*: molecular mimicry and functional diversity. *Cell Microbiol* 3: 359-70

Altenburg AF, Kreijtz JH, de Vries RD, Song F, Fux R, et al. 2014. Modified vaccinia virus ankara (MVA) as production platform for vaccines against influenza and other viral respiratory diseases. *Viruses* 6: 2735-61

Antikainen J, Kuparinen V, Lahteenmaki K, Korhonen TK. 2007. pH-dependent association of enolase and glyceraldehyde-3-phosphate dehydrogenase of *Lactobacillus crispatus* with the cell wall and lipoteichoic acids. *J Bacteriol* 189: 4539-43

Arnon R, Van Regenmortel MH. 1992. Structural basis of antigenic specificity and design of new vaccines. *FASEB J* 6: 3265-74

Arvidson S, Tegmark K. 2001. Regulation of virulence determinants in *Staphylococcus aureus*. *Int J Med Microbiol* 291: 159-70

Askari, E, Zarifian A, Pourmand MR, Naderi-Nasab, M. 2012. High-Level Vancomycin-Resistant *Staphylococcus aureus* (VRSA) in Iran: A Systematic Review. *J Med Bacteriol.* 1 (2): 53-61

Asokan A, Schaffer DV, Samulski RJ. 2012. The AAV vector toolkit: poised at the clinical crossroads. *Mol Ther* 20: 699-708

Awate S, Babiuk LA, Mutwiri G. 2013. Mechanisms of action of adjuvants. *Front Immunol* 4: 114

Baneyx F, Mujacic M. 2004. Recombinant protein folding and misfolding in Escherichia coli. *Nat Biotechnol* 22: 1399-408

Bartlett JS, Kleinschmidt J, Boucher RC, Samulski RJ. 1999. Targeted adeno-associated virus vector transduction of nonpermissive cells mediated by a bispecific F(ab'gamma)2 antibody. *Nat Biotechnol* 17: 181-6

Becker P, Hufnagle W, Peters G, Herrmann M. 2001. Detection of differential gene expression in biofilm-forming versus planktonic populations of *Staphylococcus aureus* using micro-representational-difference analysis. *Appl Environ Microbiol* 67: 2958-65

Boel G, Jin H, Pancholi V. 2005. Inhibition of cell surface export of group A streptococcal anchorless surface dehydrogenase affects bacterial adherence and antiphagocytic properties. *Infect Immun* 73: 6237-48

Broker BM, Mrochen D, Peton V. 2016. The T Cell Response to *Staphylococcus aureus*. *Pathogens* 5

Brown AF, Murphy AG, Lalor SJ, Leech JM, O'Keeffe KM, et al. 2015a. Memory Th1 Cells Are Protective in Invasive *Staphylococcus aureus* Infection. *PLoS Pathog* 11: e1005226

Brown L, Wolf JM, Prados-Rosales R, Casadevall A. 2015b. Through the wall: extracellular vesicles in Gram-positive bacteria, mycobacteria and fungi. *Nat Rev Microbiol* 13: 620-30

Buning H, Perabo L, Coutelle O, Quadt-Humme S, Hallek M. 2008. Recent developments in adeno-associated virus vector technology. *J Gene Med* 10: 717-33

Burlak C, Hammer CH, Robinson MA, Whitney AR, McGavin MJ, et al. 2007. Global analysis of community-associated methicillin-resistant *Staphylococcus aureus* exoproteins reveals molecules produced in vitro and during infection. *Cell Microbiol* 9: 1172-90

Burnet FM. 1962. The immunological significance of the thymus: an extension of the clonal selection theory of immunity. *Australas Ann Med* 11: 79-91

Burnie JP, Matthews RC, Carter T, Beaulieu E, Donohoe M, et al. 2000. Identification of an immunodominant ABC transporter in methicillin-resistant *Staphylococcus aureus* infections. *Infect Immun* 68: 3200-9

Carneiro CR, Postol E, Nomizo R, Reis LF, Brentani RR. 2004. Identification of enolase as a laminin-binding protein on the surface of *Staphylococcus aureus*. *Microbes Infect* 6: 604-8

Casadevall A, Pirofski LA. 2003. The damage-response framework of microbial pathogenesis. *Nat Rev Microbiol* 1: 17-24

Cash P, Argo E, Ford L, Lawrie L, McKenzie H. 1999. A proteomic analysis of erythromycin resistance in *Streptococcus pneumoniae*. *Electrophoresis* 20: 2259-68

Chavakis T, Wiechmann K, Preissner KT, Herrmann M. 2005. *Staphylococcus aureus* interaction with the endothelium: the role of bacterial "secretable expanded repertoire adhesive molecules" (SERAM) in disturbing host defense systems. *Thromb Haemost* 94: 278-85

Chen Y, Liu B, Yang D, Li X, Wen L, et al. 2011. Peptide mimics of peptidoglycan are vaccine candidates and protect mice from infection with *S. aureus*. *J Med Microbiol* 60: 995-1002

Chhatwal GS. 2002. Anchorless adhesins and invasins of Gram-positive bacteria: a new class of virulence factors. *Trends Microbiol* 10: 205-8

Cho JS, Pietras EM, Garcia NC, Ramos RI, Farzam DM, et al. 2010. IL-17 is essential for host defense against cutaneous *Staphylococcus aureus* infection in mice. *J Clin Invest* 120: 1762-73

Choi VW, McCarty DM, Samulski RJ. 2005. AAV hybrid serotypes: improved vectors for gene delivery. *Curr Gene Ther* 5: 299-310

Correia BE, Bates JT, Loomis RJ, Baneyx G, Carrico C, et al. 2014. Proof of principle for epitope-focused vaccine design. *Nature* 507: 201-6

Corti D, Suguitan AL, Jr., Pinna D, Silacci C, Fernandez-Rodriguez BM, et al. 2010. Heterosubtypic neutralizing antibodies are produced by individuals immunized with a seasonal influenza vaccine. *J Clin Invest* 120: 1663-73

Cramton SE, Gerke C, Schnell NF, Nichols WW, Gotz F. 1999. The intercellular adhesion (ica) locus is present in *Staphylococcus aureus* and is required for biofilm formation. *Infect Immun* 67: 5427-33

Crotzer VL, Blum JS. 2009. Autophagy and its role in MHC-mediated antigen presentation. *J Immunol* 182: 3335-41

Dailey TA, Meissner P, Dailey HA. 1994. Expression of a cloned protoporphyrinogen oxidase. *J Biol Chem* 269: 813-5

Daum RS, Spellberg B. 2012. Progress toward a *S. aureus* vaccine. *Clin Infect Dis* 54: 560-7

David MZ, Daum RS. 2010. Community-associated methicillin-resistant *Staphylococcus aureus*: epidemiology and clinical consequences of an emerging epidemic. *Clin Microbiol Rev* 23: 616-87

Davis SL, Rybak MJ, Amjad M, Kaatz GW, McKinnon PS. 2006. Characteristics of patients with healthcare-associated infection due to SCCmec type IV methicillin-resistant *Staphylococcus aureus*. *Infect Control Hosp Epidemiol* 27: 1025-31

Daya S, Berns KI. 2008. Gene therapy using adeno-associated virus vectors. *Clin Microbiol Rev* 21: 583-93

DeJonge M, Burchfield D, Bloom B, Duenas M, Walker W, et al. 2007. Clinical trial of safety and efficacy of INH-A21 for the prevention of nosocomial staphylococcal bloodstream infection in premature infants. *J Pediatr* 151: 260-5, 65 e1

Derbise A, Song YP, Parikh S, Fischetti VA, Pancholi V. 2004. Role of the C-terminal lysine residues of streptococcal surface enolase in Glu- and Lys-plasminogen-binding activities of group A streptococci. *Infect Immun* 72: 94-105

Diekema DJ, Pfaller MA, Schmitz FJ, Smayevsky J, Bell J, et al. 2001. Survey of infections due to *Staphylococcus* species: frequency of occurrence and antimicrobial susceptibility of isolates collected in the United States, Canada, Latin America, Europe, and the Western Pacific region for the SENTRY Antimicrobial Surveillance Program, 1997-1999. *Clin Infect Dis* 32 Suppl 2: S114-32

Dryla A, Prustomersky S, Gelbmann D, Hanner M, Bettinger E, et al. 2005. Comparison of antibody repertoires against *Staphylococcus aureus* in healthy individuals and in acutely infected patients. *Clin Diagn Lab Immunol* 12: 387-98

Epstein JE, Giersing B, Mullen G, Moorthy V, Richie TL. 2007. Malaria vaccines: are we getting closer? *Curr Opin Mol Ther* 9: 12-24

Fattom A, Matalon A, Buerkert J, Taylor K, Damaso S, Boutriau D. 2015. Efficacy profile of a bivalent *Staphylococcus aureus* glycoconjugated vaccine in adults on hemodialysis: Phase III randomized study. *Hum Vaccin Immunother* 11: 632-41

Fattom AI, Horwith G, Fuller S, Propst M, Naso R. 2004. Development of StaphVAX, a polysaccharide conjugate vaccine against *S. aureus* infection: from the lab bench to phase III clinical trials. *Vaccine* 22: 880-7

Fattom AI, Sarwar J, Ortiz A, Naso R. 1996. A *Staphylococcus aureus* capsular polysaccharide (CP) vaccine and CP-specific antibodies protect mice against bacterial challenge. *Infect Immun* 64: 1659-65

Fontaine MC, Perez-Casal J, Song XM, Shelford J, Willson PJ, Potter AA. 2002. Immunisation of dairy cattle with recombinant *Streptococcus uberis* GapC or a chimeric CAMP antigen confers protection against heterologous bacterial challenge. *Vaccine* 20: 2278-86

Forsgren A. 1968. Protein A from *Staphylococcus aureus*. VI. Reaction with subunits from guinea pig gamma-1- and gamma-2-globulin. *J Immunol* 100: 927-30

Foster TJ. 2005. Immune evasion by staphylococci. *Nat Rev Microbiol* 3: 948-58

Foster TJ, Geoghegan JA, Ganesh VK, Hook M. 2014. Adhesion, invasion and evasion: the many functions of the surface proteins of *Staphylococcus aureus*. *Nat Rev Microbiol* 12: 49-62

Foster TJ, Hook M. 1998. Surface protein adhesins of *Staphylococcus aureus*. *Trends Microbiol* 6: 484-8

Foulston L, Elsholz AK, DeFrancesco AS, Losick R. 2014. The extracellular matrix of *Staphylococcus aureus* biofilms comprises cytoplasmic proteins that associate with the cell surface in response to decreasing pH. *MBio* 5: e01667-14

Fowler VG, Allen KB, Moreira ED, Moustafa M, Isgro F, et al. 2013. Effect of an investigational vaccine for preventing *Staphylococcus aureus* infections after cardiothoracic surgery: a randomized trial. *JAMA* 309: 1368-78

Frankenberg N, Moser J, Jahn D. 2003. Bacterial heme biosynthesis and its biotechnological application. *Appl Microbiol Biotechnol* 63: 115-27

Furuya H, Ikeda R. 2009. Interaction of triosephosphate isomerase from the cell surface of *Staphylococcus aureus* and alpha-(1->3)-mannooligosaccharides derived from glucuronoxylomannan of *Cryptococcus neoformans*. *Microbiology* 155: 2707-13

Furuya H, Ikeda R. 2011. Interaction of triosephosphate isomerase from *Staphylococcus aureus* with plasminogen. *Microbiol Immunol* 55: 855-62

Garcia F, Bernaldo de Quiros JC, Gomez CE, Perdiguero B, Najera JL, et al. 2011. Safety and immunogenicity of a modified pox vector-based HIV/AIDS vaccine candidate expressing Env, Gag, Pol and Nef proteins of HIV-1 subtype B (MVA-B) in healthy HIV-1-uninfected volunteers: A phase I clinical trial (RISVAC02). *Vaccine* 29: 8309-16

Garmory HS, Titball RW. 2004. ATP-binding cassette transporters are targets for the development of antibacterial vaccines and therapies. *Infect Immun* 72: 6757-63

Gatlin CL, Pieper R, Huang ST, Mongodin E, Gebregeorgis E, et al. 2006. Proteomic profiling of cell envelope-associated proteins from *Staphylococcus aureus*. *Proteomics* 6: 1530-49

Giersing BK, Dastgheyb SS, Modjarrad K, Moorthy V. 2016. Status of vaccine research and development of vaccines for *Staphylococcus aureus*. *Vaccine* 34: 2962-6

Giese MJ, Adamu SA, Pitchekian-Halabi H, Ravindranath RM, Mondino BJ. 1996. The effect of *Staphylococcus aureus* phage lysate vaccine on a rabbit model of staphylococcal blepharitis, phlyctenulosis, and catarrhal infiltrates. *Am J Ophthalmol* 122: 245-54

Girod A, Wobus CE, Zadori Z, Ried M, Leike K, et al. 2002. The VP1 capsid protein of adeno-associated virus type 2 is carrying a phospholipase A2 domain required for virus infectivity. *J Gen Virol* 83: 973-8

Glowalla E, Tosetti B, Kronke M, Krut O. 2009. Proteomics-based identification of anchorless cell wall proteins as vaccine candidates against *Staphylococcus aureus*. *Infect Immun* 77: 2719-29

Gonzalez BE, Rueda AM, Shelburne SA, 3rd, Musher DM, Hamill RJ, Hulten KG. 2006. Community-associated strains of methicillin-resistant *Staphylococccus aureus* as the cause of healthcare-associated infection. *Infect Control Hosp Epidemiol* 27: 1051-6

Gozalbo D, Gil-Navarro I, Azorin I, Renau-Piqueras J, Martinez JP, Gil ML. 1998. The cell wall-associated glyceraldehyde-3-phosphate dehydrogenase of *Candida albicans* is also a fibronectin and laminin binding protein. *Infect Immun* 66: 2052-9

Greenberg DP, Ward JI, Bayer AS. 1987. Influence of *Staphylococcus aureus* antibody on experimental endocarditis in rabbits. *Infect Immun* 55: 3030-4

Grosz M, Kolter J, Paprotka K, Winkler AC, Schafer D, et al. 2014. Cytoplasmic replication of *Staphylococcus aureus* upon phagosomal escape triggered by phenol-soluble modulin alpha. *Cell Microbiol* 16: 451-65

Hammer ND, Skaar EP. 2011. Molecular mechanisms of *Staphylococcus aureus* iron acquisition. *Annu Rev Microbiol* 65: 129-47

Hansson M, Hederstedt L. 1994. *Bacillus subtilis* HemY is a peripheral membrane protein essential for protoheme IX synthesis which can oxidize coproporphyrinogen III and protoporphyrinogen IX. *J Bacteriol* 176: 5962-70

Hekman CM, Loskutoff DJ. 1987. Fibrinolytic pathways and the endothelium. *Semin Thromb Hemost* 13: 514-27

Henderson B, Martin A. 2011. Bacterial virulence in the moonlight: multitasking bacterial moonlighting proteins are virulence determinants in infectious disease. *Infect Immun* 79: 3476-91

Hermanson, GT. 2008. Bioconjugate Techniques. 2nd edition, Academic Press, New York. (Part No. 20036). Chapter 19 discusses carrier protein uses and immunogen preparation.

Hillaire ML, Rimmelzwaan GF, Kreijtz JH. 2013. Clearance of influenza virus infections by T cells: risk of collateral damage? *Curr Opin Virol* 3: 430-7

Hiramatsu K, Hanaki H, Ino T, Yabuta K, Oguri T, Tenover FC. 1997. Methicillin-resistant *Staphylococcus aureus* clinical strain with reduced vancomycin susceptibility. *J Antimicrob Chemother* 40: 135-6

Ingolotti M, Kawalekar O, Shedlock DJ, Muthumani K, Weiner DB. 2010. DNA vaccines for targeting bacterial infections. *Expert Rev Vaccines* 9: 747-63

Isakson PC, Pure E, Vitetta ES, Krammer PH. 1982. T cell-derived B cell differentiation factor(s). Effect on the isotype switch of murine B cells. *J Exp Med* 155: 734-48

Ito Y. 1960. A tumor-producing factor extracted by phenol from papillomatous tissue (Shope) of cottontail rabbits. *Virology* 12: 596-601

Iwakura Y, Nakae S, Saijo S, Ishigame H. 2008. The roles of IL-17A in inflammatory immune responses and host defense against pathogens. *Immunol Rev* 226: 57-79

Jeffery CJ. 1999. Moonlighting proteins. *Trends Biochem Sci* 24: 8-11

Jevons MP. 1961. Celbenin-resistant staphylococci. *Br Med J* 1: 124–5.

Joshi A, Pancari G, Cope L, Bowman EP, Cua D, et al. 2012. Immunization with *Staphylococcus aureus* iron regulated surface determinant B (IsdB) confers protection via Th17/IL17 pathway in a murine sepsis model. *Hum Vaccin Immunother* 8: 336-46

Kampen AH, Tollersrud T, Lund A. 2005. *Staphylococcus aureus* capsular polysaccharide types 5 and 8 reduce killing by bovine neutrophils in vitro. *Infect Immun* 73: 1578-83

Kim HK, Missiakas D, Schneewind O. 2014. Mouse models for infectious diseases caused by *Staphylococcus aureus*. *J Immunol Methods* 410: 88-99

King MD, Humphrey BJ, Wang YF, Kourbatova EV, Ray SM, Blumberg HM. 2006. Emergence of community-acquired methicillin-resistant *Staphylococcus aureus* USA 300 clone as the predominant cause of skin and soft-tissue infections. *Ann Intern Med* 144: 309-17

King NP, Sakinc T, Ben Zakour NL, Totsika M, Heras B, et al. 2012. Characterisation of a cell wall-anchored protein of *Staphylococcus saprophyticus* associated with linoleic acid resistance. *BMC Microbiol* 12: 8

Klevens RM, Morrison MA, Nadle J, Petit S, Gershman K, et al. 2007. Invasive methicillin-resistant *Staphylococcus aureus* infections in the United States. *JAMA* 298: 1763-71

Kluytmans J, van Belkum A, Verbrugh H. 1997. Nasal carriage of *Staphylococcus aureus*: epidemiology, underlying mechanisms, and associated risks. *Clin Microbiol Rev* 10: 505-20

Kohler G, Milstein C. 1975. Continuous cultures of fused cells secreting antibody of predefined specificity. *Nature* 256: 495-7

Kolesanova EF, Sanzhakov MA, Kharybin ON. 2013. Development of the schedule for multiple parallel "difficult" Peptide synthesis on pins. *Int J Pept* 2013: 197317

Kreijtz JH, Goeijenbier M, Moesker FM, van den Dries L, Goeijenbier S, et al. 2014. Safety and immunogenicity of a modified-vaccinia-virus-Ankara-based influenza A H5N1 vaccine: a randomised, double-blind phase 1/2a clinical trial. *Lancet Infect Dis* 14: 1196-207

Kremer M, Volz A, Kreijtz JH, Fux R, Lehmann MH, Sutter G. 2012. Easy and efficient protocols for working with recombinant vaccinia virus MVA. *Methods Mol Biol* 890: 59-92

Kubica M, Guzik K, Koziel J, Zarebski M, Richter W, et al. 2008. A potential new pathway for *Staphylococcus aureus* dissemination: the silent survival of S. aureus phagocytosed by human monocyte-derived macrophages. *PLoS One* 3: e1409

Kuklin NA, Clark DJ, Secore S, Cook J, Cope LD, et al. 2006. A novel *Staphylococcus aureus* vaccine: iron surface determinant B induces rapid antibody responses in rhesus macaques and specific increased survival in a murine S. aureus sepsis model. *Infect Immun* 74: 2215-23

Kwon I, Schaffer DV. 2008. Designer gene delivery vectors: molecular engineering and evolution of adeno-associated viral vectors for enhanced gene transfer. *Pharm Res* 25: 489-99

Ladhani S, Poston SM, Joannou CL, Evans RW. 1999. Staphylococcal scalded skin syndrome: exfoliative toxin A (ETA) induces serine protease activity when combined with A431 cells. *Acta Paediatr* 88: 776-9

Laupland KB, Church DL, Mucenski M, Sutherland LR, Davies HD. 2003. Population-based study of the epidemiology of and the risk factors for invasive *Staphylococcus aureus* infections. *J Infect Dis* 187: 1452-9

Lee BS, Huang JS, Jayathilaka GD, Lateef SS, Gupta S. 2010. Production of antipeptide antibodies. *Methods Mol Biol* 657: 93-108

Lee PS, Yoshida R, Ekiert DC, Sakai N, Suzuki Y, et al. 2012. Heterosubtypic antibody recognition of the influenza virus hemagglutinin receptor binding site enhanced by avidity. *Proc Natl Acad Sci U S A* 109: 17040-5

Lee WL, Harrison RE, Grinstein S. 2003. Phagocytosis by neutrophils. *Microbes Infect* 5: 1299-306

Lehmann MH, Kastenmuller W, Kandemir JD, Brandt F, Suezer Y, Sutter G. 2009. Modified vaccinia virus ankara triggers chemotaxis of monocytes and early respiratory immigration of leukocytes by induction of CCL2 expression. *J Virol* 83: 2540-52

Li W, Joshi MD, Singhania S, Ramsey KH, Murthy AK. 2014. Peptide Vaccine: Progress and Challenges. *Vaccines (Basel)* 2: 515-36

Lin L, Ibrahim AS, Xu X, Farber JM, Avanesian V, et al. 2009. Th1-Th17 cells mediate protective adaptive immunity against *Staphylococcus aureus* and *Candida albicans* infection in mice. *PLoS Pathog* 5: e1000703

Lina G, Piemont Y, Godail-Gamot F, Bes M, Peter MO, et al. 1999. Involvement of Panton-Valentine leukocidin-producing *Staphylococcus aureus* in primary skin infections and pneumonia. *Clin Infect Dis* 29: 1128-32

Liu MA. 2003. DNA vaccines: a review. *J Intern Med* 253: 402-10

Liu MA. 2010. Immunologic basis of vaccine vectors. *Immunity* 33: 504-15

Liu Y, McNevin J, Zhao H, Tebit DM, Troyer RM, et al. 2007. Evolution of human immunodeficiency virus type 1 cytotoxic T-lymphocyte epitopes: fitness-balanced escape. *J Virol* 81: 12179-88

Llewelyn M, Cohen J. 2002. Superantigens: microbial agents that corrupt immunity. *Lancet Infect Dis* 2: 156-62

Lobo SA, Scott A, Videira MA, Winpenny D, Gardner M, et al. 2015. *Staphylococcus aureus* haem biosynthesis: characterisation of the enzymes involved in final steps of the pathway. *Mol Microbiol* 97: 472-87

Loffler B, Tuchscherr L, Niemann S, Peters G. 2014. *Staphylococcus aureus* persistence in non-professional phagocytes. *Int J Med Microbiol* 304: 170-6

Loughman JA, Fritz SA, Storch GA, Hunstad DA. 2009. Virulence gene expression in human community-acquired *Staphylococcus aureus* infection. *J Infect Dis* 199: 294-301

Lowy FD. 1998. *Staphylococcus aureus* infections. *N Engl J Med* 339: 520-32

Lowy FD. 2000. Is *Staphylococcus aureus* an intracellular pathogen? *Trends Microbiol* 8: 341-3

Lu T, Porter AR, Kennedy AD, Kobayashi SD, DeLeo FR. 2014. Phagocytosis and killing of *Staphylococcus aureus* by human neutrophils. *J Innate Immun* 6: 639-49

Lux K, Goerlitz N, Schlemminger S, Perabo L, Goldnau D, et al. 2005. Green fluorescent protein-tagged adeno-associated virus particles allow the study of cytosolic and nuclear trafficking. *J Virol* 79: 11776-87

Manz RA, Thiel A, Radbruch A. 1997. Lifetime of plasma cells in the bone marrow. *Nature* 388: 133-4

Maresso AW, Schneewind O. 2006. Iron acquisition and transport in *Staphylococcus aureus*. *Biometals* 19: 193-203

Matsuo M, Oogai Y, Kato F, Sugai M, Komatsuzawa H. 2011. Growth-phase dependence of susceptibility to antimicrobial peptides in *Staphylococcus aureus*. *Microbiology* 157: 1786-97

Mayr A, Munz E. 1964. [Changes in the vaccinia virus through continuing passages in chick embryo fibroblast cultures]. *Zentralbl Bakteriol Orig* 195: 24-35

Mayfield JA, Hammer ND, Kurker RC, Chen TK, Ojha S, et al. 2013. The chlorite dismutase (HemQ) from *Staphylococcus aureus* has a redox-sensitive heme and is associated with the small colony variant phenotype. *J Biol Chem* 288: 23488-504

McHeyzer-Williams M, Okitsu S, Wang N, McHeyzer-Williams L. 2011. Molecular programming of B cell memory. *Nat Rev Immunol* 12: 24-34

Merino N, Toledo-Arana A, Vergara-Irigaray M, Valle J, Solano C, et al. 2009. Protein A-mediated multicellular behavior in *Staphylococcus aureus*. *J Bacteriol* 191: 832-43

Modlin RL, Pirmez C, Hofman FM, Torigian V, Uyemura K, et al. 1989. Lymphocytes bearing antigen-specific gamma delta T-cell receptors accumulate in human infectious disease lesions. *Nature* 339: 544-8

Modun B, Morrissey J, Williams P. 2000. The staphylococcal transferrin receptor: a glycolytic enzyme with novel functions. *Trends Microbiol* 8: 231-7

Modun B, Williams P. 1999. The staphylococcal transferrin-binding protein is a cell wall glyceraldehyde-3-phosphate dehydrogenase. *Infect Immun* 67: 1086-92

Moellering RC, Jr. 2012. MRSA: the first half century. *J Antimicrob Chemother* 67: 4-11

Molkanen T, Tyynela J, Helin J, Kalkkinen N, Kuusela P. 2002. Enhanced activation of bound plasminogen on *Staphylococcus aureus* by staphylokinase. *FEBS Lett* 517: 72-8

Molne L, Corthay A, Holmdahl R, Tarkowski A. 2003. Role of gamma/delta T cell receptor-expressing lymphocytes in cutaneous infection caused by *Staphylococcus aureus. Clin Exp Immunol* 132: 209-15

Moyle PM, Toth I. 2013. Modern subunit vaccines: development, components, and research opportunities. *ChemMedChem* 8: 360-76

Munch RC, Janicki H, Volker I, Rasbach A, Hallek M, et al. 2013. Displaying high-affinity ligands on adeno-associated viral vectors enables tumor cell-specific and safe gene transfer. *Mol Ther* 21: 109-18

Munz C. 2012. Antigen Processing for MHC Class II Presentation via Autophagy. *Front Immunol* 3: 9
Murray BE, Moellering RC, Jr. 1978. Patterns and mechanisms of antibiotic resistance. *Med Clin North Am* 62: 899-923

Nelson D, Goldstein JM, Boatright K, Harty DW, Cook SL, et al. 2001. pH-regulated secretion of a glyceraldehyde-3-phosphate dehydrogenase from *Streptococcus gordonii* FSS2: purification, characterization, and cloning of the gene encoding this enzyme. *J Dent Res* 80: 371-7

Nieto K, Salvetti A. 2014. AAV Vectors Vaccines Against Infectious Diseases. *Front Immunol* 5: 5

Nutt SL, Hodgkin PD, Tarlinton DM, Corcoran LM. 2015. The generation of antibody-secreting plasma cells. *Nat Rev Immunol* 15: 160-71

O'Toole GA. 2011. Microtiter dish biofilm formation assay. *J Vis Exp*

Ogston A. 1881. Report upon Micro-Organisms in Surgical Diseases. *Br Med J* 1: 369 b2-75

Oogai Y, Matsuo M, Hashimoto M, Kato F, Sugai M, Komatsuzawa H. 2011. Expression of virulence factors by *Staphylococcus aureus* grown in serum. *Appl Environ Microbiol* 77: 8097-105

Oscherwitz J, Yu F, Cease KB. 2009. A heterologous helper T-cell epitope enhances the immunogenicity of a multiple-antigenic-peptide vaccine targeting the cryptic loop-neutralizing determinant of *Bacillus anthracis* protective antigen. *Infect Immun* 77: 5509-18

Otto M. 2010. Novel targeted immunotherapy approaches for staphylococcal infection. *Expert Opin Biol Ther* 10: 1049-59

Paharik AE, Horswill AR. 2016. The Staphylococcal Biofilm: Adhesins, Regulation, and Host Response. *Microbiol Spectr* 4

Pancholi V. 2001. Multifunctional alpha-enolase: its role in diseases. *Cell Mol Life Sci* 58: 902-20

Pancholi V, Chhatwal GS. 2003. Housekeeping enzymes as virulence factors for pathogens. *Int J Med Microbiol* 293: 391-401

Pancholi V, Fischetti VA. 1992. A major surface protein on group A streptococci is a glyceraldehyde-3-phosphate-dehydrogenase with multiple binding activity. *J Exp Med* 176: 415-26

Panek H, O'Brian MR. 2002. A whole genome view of prokaryotic haem biosynthesis. *Microbiology* 148: 2273-82

Panizzi P, Friedrich R, Fuentes-Prior P, Richter K, Bock PE, Bode W. 2006. Fibrinogen substrate recognition by staphylocoagulase.(pro)thrombin complexes. *J Biol Chem* 281: 1179-87

Pasztor L, Ziebandt AK, Nega M, Schlag M, Haase S, et al. 2010. Staphylococcal major autolysin (Atl) is involved in excretion of cytoplasmic proteins. *J Biol Chem* 285: 36794-803

Pene J, Chevalier S, Preisser L, Venereau E, Guilleux MH, et al. 2008. Chronically inflamed human tissues are infiltrated by highly differentiated Th17 lymphocytes. *J Immunol* 180: 7423-30

Pereira DJ, McCarty DM, Muzyczka N. 1997. The adeno-associated virus (AAV) Rep protein acts as both a repressor and an activator to regulate AAV transcription during a productive infection. *J Virol* 71: 1079-88

Periasamy S, Joo HS, Duong AC, Bach THL, Tan VY, et al. 2012. How *Staphylococcus aureus* biofilms develop their characteristic structure. *P Natl Acad Sci USA* 109: 1281-86

Peters BM, Ovchinnikova ES, Krom BP, Schlecht LM, Zhou H, et al. 2012. *Staphylococcus aureus* adherence to Candida albicans hyphae is mediated by the hyphal adhesin Als3p. *Microbiology* 158: 2975-86

Petit-Frere C, Dugas B, Braquet P, Mencia-Huerta JM. 1993. Interleukin-9 potentiates the interleukin-4-induced IgE and IgG1 release from murine B lymphocytes. *Immunology* 79: 146-51

Pomposelli JJ, Baxter JK, 3rd, Babineau TJ, Pomfret EA, Driscoll DF, et al. 1998. Early postoperative glucose control predicts nosocomial infection rate in diabetic patients. *JPEN J Parenter Enteral Nutr* 22: 77-81

Proctor RA, van Langevelde P, Kristjansson M, Maslow JN, Arbeit RD. 1995. Persistent and relapsing infections associated with small-colony variants of *Staphylococcus aureus*. *Clin Infect Dis* 20: 95-102

Purcell AW, McCluskey J, Rossjohn J. 2007. More than one reason to rethink the use of peptides in vaccine design. *Nat Rev Drug Discov* 6: 404-14

Rauch S, DeDent AC, Kim HK, Bubeck Wardenburg J, Missiakas DM, Schneewind O. 2012. Abscess formation and alpha-hemolysin induced toxicity in a mouse model of *Staphylococcus aureus* peritoneal infection. *Infect Immun* 80: 3721-32

Rivera AM, Boucher HW. 2011. Current concepts in antimicrobial therapy against select gram-positive organisms: methicillin-resistant *Staphylococcus aureus*, penicillin-resistant pneumococci, and vancomycin-resistant enterococci. *Mayo Clin Proc* 86: 1230-43

Rupp ME, Holley HP, Jr., Lutz J, Dicpinigaitis PV, Woods CW, et al. 2007. Phase II, randomized, multicenter, double-blind, placebo-controlled trial of a polyclonal anti-*Staphylococcus aureus* capsular polysaccharide immune globulin in treatment of *Staphylococcus aureus* bacteremia. *Antimicrob Agents Chemother* 51: 4249-54

Rybniker J, Nowag A, Janicki H, Demant K, Hartmann P, Buning H. 2012. Incorporation of antigens into viral capsids augments immunogenicity of adeno-associated virus vector-based vaccines. *J Virol* 86: 13800-4

Sasaki S, Nishikawa S, Miura T, Mizuki M, Yamada K, et al. 2000. Interleukin-4 and interleukin-10 are involved in host resistance to *Staphylococcus aureus* infection through regulation of gamma interferon. *Infect Immun* 68: 2424-30

Sause WE, Buckley PT, Strohl WR, Lynch AS, Torres VJ. 2016. Antibody-Based Biologics and Their Promise to Combat *Staphylococcus aureus* Infections. *Trends Pharmacol Sci* 37: 231-41

Sendi P, Proctor RA. 2009. *Staphylococcus aureus* as an intracellular pathogen: the role of small colony variants. *Trends Microbiol* 17: 54-8

Sendi P, Rohrbach M, Graber P, Frei R, Ochsner PE, Zimmerli W. 2006. *Staphylococcus aureus* small colony variants in prosthetic joint infection. *Clin Infect Dis* 43: 961-7

Sesardic D. 1993. Synthetic peptide vaccines. *J Med Microbiol* 39: 241-2

Sharon J, Rynkiewicz MJ, Lu Z, Yang CY. 2014. Discovery of protective B-cell epitopes for development of antimicrobial vaccines and antibody therapeutics. *Immunology* 142: 1-23

Sinha B, Francois P, Que YA, Hussain M, Heilmann C, et al. 2000. Heterologously expressed *Staphylococcus aureus* fibronectin-binding proteins are sufficient for invasion of host cells. *Infect Immun* 68: 6871-8

Smith RP, Baltch AL, Ritz WJ, Michelsen PB, Bopp LH. 2010. IFN-gamma enhances killing of methicillin-resistant *Staphylococcus aureus* by human monocytes more effectively than GM-CSF in the presence of daptomycin and other antibiotics. *Cytokine* 51: 274-7

Snapper CM, Paul WE. 1987. Interferon-gamma and B cell stimulatory factor-1 reciprocally regulate Ig isotype production. *Science* 236: 944-7

Sompolinsky D, Samra Z, Karakawa WW, Vann WF, Schneerson R, Malik Z. 1985. Encapsulation and capsular types in isolates of *Staphylococcus aureus* from different sources and relationship to phage types. *J Clin Microbiol* 22: 828-34

Song F, Fux R, Provacia LB, Volz A, Eickmann M, et al. 2013. Middle East respiratory syndrome coronavirus spike protein delivered by modified vaccinia virus Ankara efficiently induces virus-neutralizing antibodies. *J Virol* 87: 11950-4

Spellberg B, Ibrahim AS, Yeaman MR, Lin L, Fu Y, et al. 2008. The antifungal vaccine derived from the recombinant N terminus of Als3p protects mice against the bacterium *Staphylococcus aureus*. *Infect Immun* 76: 4574-80

Stevens TL, Bossie A, Sanders VM, Fernandez-Botran R, Coffman RL, et al. 1988. Regulation of antibody isotype secretion by subsets of antigen-specific helper T cells. *Nature* 334: 255-8

Stickl H, Hochstein-Mintzel V, Mayr A, Huber HC, Schafer H, Holzner A. 1974. [MVA vaccination against smallpox: clinical tests with an attenuated live vaccinia virus strain (MVA) (author's transl)]. *Dtsch Med Wochenschr* 99: 2386-92

Stranger-Jones YK, Bae T, Schneewind O. 2006. Vaccine assembly from surface proteins of *Staphylococcus aureus*. *Proc Natl Acad Sci U S A* 103: 16942-7

Sutter G, Moss B. 1992. Nonreplicating vaccinia vector efficiently expresses recombinant genes. *Proc Natl Acad Sci U S A* 89: 10847-51

Sutter G, Wyatt LS, Foley PL, Bennink JR, Moss B. 1994. A recombinant vector derived from the host range-restricted and highly attenuated MVA strain of vaccinia virus stimulates protective immunity in mice to influenza virus. *Vaccine* 12: 1032-40

Tang DC, DeVit M, Johnston SA. 1992. Genetic immunization is a simple method for eliciting an immune response. *Nature* 356: 152-4

Tenover FC, McDougal LK, Goering RV, Killgore G, Projan SJ, et al. 2006. Characterization of a strain of community-associated methicillin-resistant *Staphylococcus aureus* widely disseminated in the United States. *J Clin Microbiol* 44: 108-18

Tenover FC, Weigel LM, Appelbaum PC, McDougal LK, Chaitram J, et al. 2004. Vancomycin-resistant *S. aureus* isolate from a patient in Pennsylvania. *Antimicrob Agents Chemother* 48: 275-80

Timmerman P, Puijk WC, Meloen RH. 2007. Functional reconstruction and synthetic mimicry of a conformational epitope using CLIPS technology. *J Mol Recognit* 20: 283-99

Tiwari HK, Sen MR. 2006. Emergence of vancomycin resistant *Staphylococcus aureus* (VRSA) from a tertiary care hospital from northern part of India. *BMC Infect Dis* 6: 156

Tsubakishita S, Kuwahara-Arai K, Sasaki T, Hiramatsu K. 2010. Origin and molecular evolution of the determinant of methicillin resistance in staphylococci. *Antimicrob Agents Chemother* 54: 4352-9

Vahedi G, A CP, Hand TW, Laurence A, Kanno Y, et al. 2013. Helper T-cell identity and evolution of differential transcriptomes and epigenomes. *Immunol Rev* 252: 24-40

van Kessel KP, Bestebroer J, van Strijp JA. 2014. Neutrophil-Mediated Phagocytosis of *Staphylococcus aureus*. *Front Immunol* 5: 467

Varma TK, Lin CY, Toliver-Kinsky TE, Sherwood ER. 2002. Endotoxin-induced gamma interferon production: contributing cell types and key regulatory factors. *Clin Diagn Lab Immunol* 9: 530-43

Verkaik NJ, van Wamel WJ, van Belkum A. 2011. Immunotherapeutic approaches against *Staphylococcus aureus*. *Immunotherapy* 3: 1063-73

Vernachio JH, Bayer AS, Ames B, Bryant D, Prater BD, et al. 2006. Human immunoglobulin G recognizing fibrinogen-binding surface proteins is protective against both *Staphylococcus aureus* and *Staphylococcus epidermidis* infections in vivo. *Antimicrob Agents Chemother* 50: 511-8

Volz A, Sutter G. 2013. Protective efficacy of Modified Vaccinia virus Ankara in preclinical studies. *Vaccine* 31: 4235-40

von Eiff C, Heilmann C, Proctor RA, Woltz C, Peters G, Gotz F. 1997. A site-directed *Staphylococcus aureus* hemB mutant is a small-colony variant which persists intracellularly. *J Bacteriol* 179: 4706-12

Walev I, Martin E, Jonas D, Mohamadzadeh M, Muller-Klieser W, et al. 1993. Staphylococcal alpha-toxin kills human keratinocytes by permeabilizing the plasma membrane for monovalent ions. *Infect Immun* 61: 4972-9

Wang XY, Huang ZX, Chen YG, Lu X, Zhu P, et al. 2015. A Multiple Antigenic Peptide Mimicking Peptidoglycan Induced T Cell Responses to Protect Mice from Systemic Infection with *Staphylococcus aureus*. *PLoS One* 10: e0136888

Warrington KH, Jr., Gorbatyuk OS, Harrison JK, Opie SR, Zolotukhin S, Muzyczka N. 2004. Adeno-associated virus type 2 VP2 capsid protein is nonessential and can tolerate large peptide insertions at its N terminus. *J Virol* 78: 6595-609

Weems JJ, Jr., Steinberg JP, Filler S, Baddley JW, Corey GR, et al. 2006. Phase II, randomized, double-blind, multicenter study comparing the safety and pharmacokinetics of tefibazumab to placebo for treatment of *Staphylococcus aureus* bacteremia. *Antimicrob Agents Chemother* 50: 2751-5

Weigel LM, Clewell DB, Gill SR, Clark NC, McDougal LK, et al. 2003. Genetic analysis of a high-level vancomycin-resistant isolate of *Staphylococcus aureus*. *Science* 302: 1569-71

Weinrick B, Dunman PM, McAleese F, Murphy E, Projan SJ, et al. 2004. Effect of mild acid on gene expression in *Staphylococcus aureus*. *J Bacteriol* 186: 8407-23

Weisman LE, Thackray HM, Garcia-Prats JA, Nesin M, Schneider JH, et al. 2009. Phase 1/2 double-blind, placebo-controlled, dose escalation, safety, and pharmacokinetic study of pagibaximab (BSYX-A110), an antistaphylococcal monoclonal antibody for the prevention of staphylococcal bloodstream infections, in very-low-birth-weight neonates. *Antimicrob Agents Chemother* 53: 2879-86

Weisman LE, Thackray HM, Steinhorn RH, Walsh WF, Lassiter HA, et al. 2011. A randomized studyof a monoclonal antibody (pagibaximab) to prevent staphylococcal sepsis. *Pediatrics* 128: 271-9

Woodford N, Johnson AP. 1994. Glycopeptide resistance in gram-positive bacteria: from black and white to shades of grey. *J Med Microbiol* 40: 375-8

Xiao X, Li J, Samulski RJ. 1998. Production of high-titer recombinant adeno-associated virus vectors in the absence of helper adenovirus. *J Virol* 72: 2224-32

Yamaguchi M, Ikeda R, Nishimura M, Kawamoto S. 2010. Localization by scanning immunoelectron microscopy of triosephosphate isomerase, the molecules responsible for contact-mediated killing of *Cryptococcus*, on the surface of *Staphylococcus*. *Microbiol Immunol* 54: 368-70

Yang CK, Ewis HE, Zhang X, Lu CD, Hu HJ, et al. 2011. Nonclassical protein secretion by Bacillus subtilis in the stationary phase is not due to cell lysis. *J Bacteriol* 193: 5607-15

Yang HJ, Zhang JY, Wei C, Yang LY, Zuo QF, et al. 2016. Immunisation With Immunodominant Linear B Cell Epitopes Vaccine of Manganese Transport Protein C Confers Protection against *Staphylococcus aureus* Infection. *PLoS One* 11: e0149638

Zhao Z, Sun HQ, Wei SS, Li B, Feng Q, et al. 2015. Multiple B-cell epitope vaccine induces a *Staphylococcus* enterotoxin B-specific IgG1 protective response against MRSA infection. *Sci Rep* 5: 12371

Zhou X, Zolotukhin I, Im DS, Muzyczka N. 1999. Biochemical characterization of adeno-associated virus rep68 DNA helicase and ATPase activities. *J Virol* 73: 1580-90